CONFERENCE PROCEEDINGS No. 27

CONFERENCE PROCEEDINGS No. 27

AGARD

ADVISORY GROUP FOR AEROSPACE RESEARCH & DEVELOPMENT

7 RUE ANCELLE 92 NEUILLY SUR SEINE FRANCE

Integration of Propulsion Systems in Airframes

★

SEPTEMBER 1967

NORTH ATLANTIC TREATY ORGANIZATION

AGARD Conference Proceedings No. 27

NORTH ATLANTIC TREATY ORGANIZATION

ADVISORY GROUP FOR AEROSPACE RESEARCH AND DEVELOPMENT

(ORGANISATION DU TRAITE DE L'ATLANTIQUE NORD)

INTEGRATION OF PROPULSION SYSTEMS IN AIRFRAMES

Papers presented at the 31st Meeting of the AGARD Flight Mechanics Panel,
held in Göttingen, Germany, 13-15 September 1967

INTRODUCTION

The AGARD Flight Mechanics Panel is interested in the wide aspects of the integration of the various disciplines into a final system as seen by aircraft designers, developers and operators in addition to detailed developments in the areas of stability and control, handling qualities, simulation system methods, flight test and instrumentation.

The Technical-Session of the 31st Panel Meeting in Göttingen, Germany thus made a contribution to the problems of engine-airframe-integration considering both conventional and VTOL-aircrafts.

In Session I and II different topical integration effects of engine thrust, propulsive jet, engine control, nacelle interference and intake design of conventional aircrafts were considered. Of the five papers only the first is largely based on flight tests, while in the others results of analog computer-studies or windtunnel-tests are discussed.

The four papers of Session III and IV discuss two important integration problems of VTOL-Aircraft: i.e., the problems of optimal lateral control and generally the overall design of VTOL control systems, and the problem of hot-gas-ingestion.

Both subjects greatly affect handling qualities and mission performance of modern high performance VTOL-Aircraft design. They are presented as results of simulators studies, windtunnel tests and of detailed flight tests programs.

CLEM C. WEISSMAN
Member of the FMP
Department of the Navy
Office of the Chief of Naval Operations
Washington, D.C.

INTRODUCTION

La commission de la Mécanique des Fluides de l'AGARD s'intéresse non seulement aux larges aspects du problème de l'intégration des différentes disciplines dans un ensemble, tel que le voient les constructeurs, les réalisateurs et les utilisateurs d'avions, mais aussi aux progrès détaillés réalisés dans les domaines suivants: qualités de vol, qualités de maniabilité, méthodes de simulation des systèmes, essais en vol, instrumentation.

La Session Technique de la 31ème Réunion de la Commission tenue à Göttingen, Allemagne, a donc apporté une contribution aux problèmes de l'intégration moteur-cellule que posent les avions du type classique et VTOL.

Les Sessions I et II ont été consacrées aux différents effets d'intégration d'intérêt courant produits par la poussée du moteur, le jet propulsif, la commande du moteur, l'interaction des nacelles et la conception des prises d'air, en ce qui concerne les avions classiques. Des cinq communications présentées, seule la première se base en grande partie sur les résultats d'essais en vol; les quatre autres examinent les résultats d'études sur calculateur analogique ou d'essais en soufflerie.

Les quatre mémoires présentés aux Sessions III et IV, traitent de deux problèmes d'intégration importants posés par les avions VTOL, à savoir: la question du contrôle latéral optimum, et de façon générale, de la conception d'ensemble des systèmes de contrôle des avions VTOL, et la question de l'ingestion des gaz chauds.

Ces deux questions ont une influence importante sur les qualités de maniabilité et les performances de mission des avions VTOL modernes à performances elevées. Elles sont présentées sous forme de résultats d'études sur simulateur, d'essais en soufflerie et d'essais en vol.

CONTENTS

The influence of flight speed on the thrust calibration of a jet engine

by

J.P.K.Vleghert

Scientific Officer
Flight Test Department
National Aerospace Laboratory (NLR)
Amsterdam, Holland

Summary

Engine gross thrust is generally obtained from the pressures over the jet nozzle and its flow area, using a calibration factor derived from test bed comparison of weighed- and calculated (Pearson) thrust, which is extrapolated for flight conditions.

Flight test results show that the static pressure measured in the jet nozzle plane with a NLR-developed nozzle spider is considerably above the value expected from one-dimensional flow and is influenced by flight speed, especially at low nozzle pressure ratio,

Assuming an elliptic static pressure distribution over the jet nozzle diameter the flow- and hence thrust reduction relative to one-dimensional conditions can be calculated. This factor bears close resemblance to the calibration factor obtained on the testbed. As it can be determined in flight, possible discrepancies between test bed- and flight conditions will be shown up. A possible source of discrepancies is the absence- in most cases-of secundary flow outside the nozzle under test bed conditions.

Notations.

A	Area
CPR	Central Pressure Ratio
EPR	Engine Pressure Ratio
JPT	Jet Pipe Temperature
M	Mach number
N	Engine speed
NPR	Nozzle Pressure Ratio
p	Static pressure
P	total pressure
Q	engine massflow
RNI	Reynolds Number Index
RPM	Revolutions Per Minute
RPR	Ram Pressure Ratio
T	total temperature
V	flight speed
X_G	gross thrust
γ	specific heat ratio
Φ	gross thrust parameter
φ_1	weighed/theoretical thrust
φ_2	subcritical massflow ratio (fig.4)
φ_3	effective/geometric flow area

Index

1	ambient conditions
2	engine inlet conditions
j	jet pipe conditions
n	nozzle conditions
*	non-dimensional parameter
eff	effective value

1 Introduction.

Jet engine thrust may be determined, using either of the following three methods or a combination of these

a) by weighing
b) from nozzle conditions
c) from engine parameters.

a) The first method is direct, but only practical on an engine test bed.

b) The second method is semi-direct in that calibration of the nozzle is required, using method a). The nozzle method can be used irrespective of the type of engine in front of the nozzle. It is mostly preferred for the determination of gross thrust, where it requires only pressure measurements. The calibration of a certain nozzly type does not alter with individual specimen, but it can depend to some extend on outside flow conditions, as will be shown in this report. For the determination of net thrust the massflow must be known, requiring additional measurement of total temperature in the jet pipe.

c) Thrust determination from engine parameters is indirect. Usually the general engine characteristics are available, determined for the engine type with a number of engines using method a). For good accuracy, however, a correction should be applied for the individual engine. This mostly occurs on basis of extrapolation of calibration results obtained for the individual engine under a limited range of conditions. Discrepancies may occur under circumstances different from those of the calibration and in some cases due to engine deterioration. Some of these discrepancies may cause a shift in one engine parameter relative to another. The most sensitive indication, however, is total pressure in the jet pipe, which is in fact a nozzle parameter.

The engine parameters depend directly on the nozzle characteristics and can therefore also be influenced by outside flow conditions, as has been discussed under b). The nozzle conditions therefore offer a more direct method of thrust determination except for the case of the massflow, which is closely related to (low pressure) compressor RPM.

In practice jet engine net thrust is usually determined from total pressure in the jet pipe for gross thrust and massflow from compressor RPM for ramdrag. In some cases it may be difficult to obtain an accurate effective value for the total pressure in the jet pipe (uneven pressure distribution directly behind highly loaded turbine, short jet pipe, mixer, etc.). In that case it might be preferrable to use engine conditions throughout, to reduce systematic errors due to pressure pattern variation with,

however, the risk of introducing errors due to the effects discussed above.

In this report a method is given to signal systematic deviations. This method has been flight tested in subsonic flight at fairly low value of the pressure ratio over the nozzle, using NLR's Fokker S-14 jet trainer with measuring equipment developed at NLR (fig.1, 2 and 3).

2 Gross thrust determination.

2.1 Nozzle pressure method.

Jet engine gross thrust X_G is determined by the total pressure in the jet pipe P_j, the nozzle throat flow area A_n and the ambient pressure p_1 as follows:

$$X_G = Q.V_n + A_n\ (p_n - p)$$

$$\text{or}\quad X_G/A_n\ p_1 = \varphi_1 \left\{ f(\gamma)\ \text{NPR} - 1 \right\} \qquad \text{(assuming } \gamma = c_p/c_v = 4/3\text{)}$$

$$= \varphi_1\ (1{,}259\ \text{NPR} - 1)$$

for Nozzle Pressure Ratio $\text{NPR} = P_j/p_1 \geqslant 1{,}85$

$$\text{and}\quad X_G/A_n\ p_1 = \varphi_1\ 2\gamma/(\gamma-1) \left\{ \text{NPR}\ \exp\ (\gamma-1)\gamma \qquad -1 \right\}$$

$$= \varphi_1\ 8{,}00 \qquad (\text{NPR}^{0,25} - 1)$$

for $\text{NPR} \leqslant 1{,}85$

$$X_G/A_n\ p_1 = X_G^{*} = 1{,}333\ \varphi_1 \text{ for NPR} = 1{,}85$$

The above equation is based on the flow model of Pearson, i.e. one-dimensional isentropic expansion in the converging nozzle to a uniform throat Mach number of $M_n \leqslant 1{,}00$ at $\text{NPR} \leqslant 1{,}85$ and - for supercritical NPR - further free expansion to ambient pressure with constant impulse. The thrust calibration factor φ_1 allows partly for friction losses and partly for other deviations from the theoretical flow model. It is found by calibration on an engine test bed as a function of NPR.

In practice the flow through the nozzle has distinctly curved streamlines, which result in the pressure distribution in the nozzle throat plane not being uniform, as is implicated by the Pearson flow model. The static pressure along the centerline of the

nozzle will be higher than along the circumference, resulting in a lower local Mach Number, and also lower local massflow. Therefore the effective flowarea will be lower than the geometric nozzle throat area, which partly explains the fact that the calibration factor φ_1 is always lower than unity. Other factors are boundary layer displacement thickness and friction losses.

At high NPR the Pearson flow model is conservative as it assumes supersonic expansion with constant momentum which is only true for the flow at the circumference of the jet. The inside flow expands more nearly isentropic, giving rise to a slightly larger thrust than according to the Pearson model. This is accounted for by a post-exit thrust correction coefficient.

The static pressure distribution - and therefore the nozzle massflow - will be influenced by internal and external nozzle configuration and by flight speed. Usually this influence is not determined as both static engine test bed and high altitude simulating facilities normally do not have representative flow outside the nozzle. Therefore it can be expected that flight test results with a specific aeroplane type may give results which differ slightly from the test bench data. As it is practically impossible to weigh engine thrust in flight another method must be used to determine the calibration factor φ_1 (see 2.3).

2.2 Engine parameter method.

Jet engine gross thrust may also be determined from flight conditions and - for fixed nozzle engines - one engine parameter, preferably RPM.

Rolls-Royce gives: $(X_G/A\ p_o + 1)/R_{O1} = f(N/\sqrt{T_1})$

re-written in the symbols of this report as

$$(X_G/A_n\ p_1+1)/RPR = \Phi = f(N/\sqrt{T_1}) = f(N^*)$$

This relation is unique for supercritical NPR, because in this case the non-dimensional massflow $Q^* = Q\sqrt{T_j}/P_j$ is constant, causing the engine to work along a fixed line in the compressor characteristics (the working line). At subcritical NPR, however, the relation becomes a function of the Ram Pressure Ratio RPR ($=P_2/p_1$). Lowering RPR at constant N^* (on the test bench by increasing static back pressure, in flight by lowering flight speed and slightly decreasing RPM to compensate for the lower stagnation temperature) in first instance lowers NPR and therefore Q^*, which in turn increases the angle of attack and therefore the pressure ratio of the compressor (a centrifugal compressor, although the mechanism is different, exhibits the same effect). This partly compensates for the lowered NPR, in fact the Engine Pressure Ratio EPR = P_j/P_2 = NPR/RPR increases. As massflow decreases progressively with decreasing NPR (see fig.4b)

the influence of flight speed (or RPR) on engine thrust at constant N^* will increase at lower engine setting.

The engine characteristics are determined on a test bench versus RPR, but without representative outside airflow, which leaves room for slight variations in characteristics due to the secundary effect of outside air flow on the nozzle flow as discussed in the previous chapter. Under cruising conditions NPR will generally be well above critical for a straight jet or a normal bypass engine, minimizing any secondary effect on nozzle flow. In take-off or climb, however, - and on a high-bypass engine may be even in cruise - this effect can be noticeable.

When EPR is measured directly in flight for the particular aeroplane type under test, any deviation from brochure data will be noticed. This is not the case for the engine parameter Φ in the Rolls-Royce brochure, therefore engine calibration should be executed with instrumentation to determine the representative total pressure P_j in the jet pipe.

2.3 Approximation of the nozzle calibration coefficient in flight test.

An earlier NGTE (National Gas Turbine Establishment) report (1) indicated from flight measurements in an Avon-Canberra with a fixed rake across the nozzle, that the static pressure in the nozzle plane is distributed elliptically. On this basis it was considered adequate to measure only the central static pressure and - assuming elliptic distribution - to calculate the effective massflow through the nozzle as a function of NPR and the ratio of central static overpressure Δp_c to total jet pipe pressure P_j. The ratio of this effective massflow to the value indicated by one-dimensional flow at the same NPR is given as the factor φ_3 in fig.4.

This factor φ_3 should approximate the factor φ_1 from the gross thrust equation except for the effect of friction losses in the jet pipe. Due to some direct thrust loss and the displacement effect of the boundary layer, resulting in a slightly lower flow area, the experimental factor φ_1 should be somewhat lower than the calculated φ_3. The latter factor, based on measured NPR and $\Delta p_c/P_j$, should, however, provide a good basis for extrapolation of φ_1 for flight test results, including effects from outside flow.

This method was chosen from a number of alternative methods discussed in lit.2 because it can be used with a fairly simple pick-up (described in 3.2.1) which does not influence the flow outside the nozzle. The flowmodel assumed, i.e. elliptical distribution of static pressure over the nozzle throat plane, will not be correct if the nozzle is not rotation-symmetric as occurs, for instance, when it is cut off at an angle.

3 Test procedure.

3.1 Basic aims.

Primarily it was desired to obtain information as to what extend nozzle flow is influenced by engine - and flight conditions. Nozzle massflow is assumed - according to 2.3 - to be characterized by the nozzle pressure ratio and the central pressure ratio. Both values have been measured over the range of conditions possible in a normal ground test and a flight test programme has been set up to cover the widest airspeed range possible for a number of constant values of the nozzle pressure ratio. This necessitates flying under unsteady conditions, as a medium value of the NPR at low airspeed implicates a high engine setting, and therefore a thrust surplus, which must be used either to climb or to accelerate, while the reverse is the case at high airspeed.

The aeroplane available was NLR's Fokker S-14 jet trainer equipped with a Rolls-Royce Nene engine with centrifugal compressor. The engine is situated behind the side-by-side pilots station, it has a plenum chamber intake fed by two channels from a single pitot intake in the nose of the aeroplane (see fig.1). Maximum speed is about M 0,80; maximum altitude is limited to about 40 000 ft due to the absence of a pressurized cabin.

Also an important goal was to verify if indeed the nozzle flow factor φ_3 according to 2.3 is an approximation of the factor φ_1 obtained by a thrust calibration. For this it was necessary to measure static thrust directly. As no suitable engine test bed was available, it was decided to perform these tests on the aeroplane itself in the open air (see 3.2 for the instrumentation).

A third objective was to determine if the engine data at high altitude shows any difference relative to the brochure, in which no correction for high altitude performance is incorporated.

It was not realized until after analysis of the test results that the influence of nozzle conditions on the engine characteristics is more important for the thrust determination than that on massflow alone. As a result this influence could only be determined for a limited range of engine conditions.

3.2 Instrumentation.

3.2.1 Ground tests.

For the ground tests the engine has been equipped with means to determine intake pressure, total jet pipe pressure and the central static pressure in the nozzle plane. Ambient pressure and temperature have been obtained with normal meteorological instruments.

For the intake pressure the plenum chamber has been equipped with three static pressure pick-ups situated at approximately 120°

intervals just off the inside wall at about the compressor station (see fig.5). As the flow area is rather large at this station the error due to measuring static pressure instead of total intake pressure is small, it was in fact neglected.

For measuring the central static pressure the nozzle has been equipped with an internal swept-forward three-legged spider carrying a static pressure tube with measuring orifices centrally located in the nozzle throat plane (see fig.3). As the gas flow in the nozzle is accelerating from approximately M 0,5 to unity over the length of the static tube it is expected that the static pressure at the measuring orifices is not disturbed by the upstream mounting of the static tube to the three spider legs. This configuration achieves no obstruction in the - often supersonic - flow outside the nozzle and due to the relatively low jet pipe Mach number the thrust loss will be small (calculated to about 10 lbs).

Total pressure in the jet pipe is measured by four pitots in the forward part of the 21 feet long jet pipe, distributed equally along the circumference at 0.73 radius. As the ground tests proved this inadequate, a second set of four pitots has been incorporated in one of the legs of the throat spider. They were radially distributed along the leg so as to probe equal flow areas plus a central pitot. Each tube was connected via a restriction to the internal volume of that leg to effect a single sampled mean total pressure tapping.

Static thrust was measured with the aeroplane in the open, parked on strain gauge equipped pads. These pads are supported by ballbearing mounted rollers on a bottom plate, allowing free movement in the sensitive direction (fig.2). For the strain gauge pods and indicating instrumentation a standard aircraft weighing kit has been used successfully.

Further ground test instrumentation included the normal aircraft tachometer and JPT-indicator, while also a fuel flow meter was installed. Each pressure pickup has been connected to a separate instrument for the ground tests in order to evaluate the quality of the recordings as to fluctuations in time and variation with station.

3.2.2 Flight test.

For flight tests the same pressure pickups have been used as for the ground tests, except that similar pick-ups were manifolded to a single instrument to save space in the photopanel recorder. The fuel flowmeter was deleted as it was not airworthy. JPT-indication could be switched over from the cockpit-instrumentation to the photopanel. Furthermore a normal aircraft altimeter and airspeed indicator have been added, together with a total temperature probe.

All the flight test instrumentation as schematically given in fig.5 has been connected to a pitot-static boom on the nose of the

aeroplane separate from the cockpit-instrumentation to minimize lag by keeping the instrument volume in each static line as small as possible. An additional advantage was that the PEC correction of the nose boom was lower.

4 Test results.

4.1 Ground tests.

First of all a ground run was done with instruments connected to each pick-up separately to see if the indication was steady. It appeared necessary to insert a slight restriction in the pitot tubes. With this restriction a slow engine acceleration and deceleration was executed (respectively 200 and 50 RPM/sec) with no noticeable lag in the total pressure indication (max. difference 0,5 °/o).

Next a series of static thrust measurements has been executed with the aeroplane in the open, parked on the strain gauge equipped pads described in 3.2.1. Engine RPM was stabilized for one minute before photopanel readings were taken during a further minute. Thrust readings were obtained over a range from 1000 - 4000 lbs by electrically balancing the strain gauge cells. Readings at the left and right main wheels agreed within 50 lbs, readings at increasing successive thrust settings agreed with those at decreasing thrust within 20 lbs.

From the test results the Rolls-Royce parameter $\Phi = (X_G/269\ p_o+1)/R_{01}$ was calculated, reduced to a ram pressure ratio of 1.00 and compared with the engine brochure. Agreement was generally within 50 lbs, measured thrust being slightly higher at low RPM and slightly lower at high RPM.

Secondly the factor $X_G/A_n p_1$ was calculated, compensating for the slight variation of nozzle area with JPT due to metal expansion (fig.6). Comparing this value with the theoretical value from Pearson at the same NPR yields the calibration factor φ_1.

The results using the four jet pipe pitots were unsatisfactory, probably due to the measuring station being too close to the highly loaded single stage turbine. The spider pitots situated at the end of the 21 ft long jet pipe gave much better results. The measured factors φ_1 and φ_3 based on P_{j2} generally fall within $\pm$ 1 °/o on separate lines given in fig.4, indicating good measuring accuracy. The difference of 2 - 3 °/o between the two coefficients can be explained by friction losses and boundary layer displacement. This gives confidence in the extrapolation of φ_1 to higher values of NPR, based on measured values of φ_3.

Further ground tests showed the manifolded value of similar pressure pick-ups to be the same as the mean value of the separate instrument readings, making it possible to conduct the flight tests with single pressure instruments. In this configuration of the instrumentation the system lag was measured for the different pressure

parameters. The results showed time constants varying between 0,1 and 0,3 seconds. After the flight tests the static thrust measurement was repeated with results agreeing with the pre-flight tests.

4.2 Flight tests.

As many of the tests had to be done under unsteady conditions, the way of testing was varied in order to duplicate the measurements under different conditions, i.e. a high value of NPR was measured both in level, accelerated flight (constant static pressure, increasing total pressure) and in steady climb (both static and total pressure decreasing). The end results did not show differences due to the way of measuring. This was confirmed by the fact that lag corrections, calculated for a typical case using experimentally determined time constants, amounted to a maximum of 0,2 °/o of the measured value - in this case p_i - which is negligeably small.

In fig.7 the central pressure ratio $\Delta p_c/P_{j2}$ has been plotted against RPR for a number of values of NPR. The relationship can very well be approximated by a straight line for each value of NPR.

The result has been summarized in fig.8 which gives a cross-plot of CPR vs NPR of the extreme values of RPR obtained in the tests.

With fig.4 the flight range of values of φ_3 are determined from the measured values of NPR and CPR. At the lower engine settings this graph shows a reduction in φ_3 of about 2 °/o with increasing flight speed. At the normally used higher settings the variation is negligible and shows justification of a linear extrapolation of the factor φ_1 determined from static thrust measurements.

5 Conclusions.

1) The results of the static thrust measurements agree with the Rolls-Royce Nene brochure within 1-2 °/o of max thrust.

2) There is good agreement between the thrust calibration factor φ_1 determined from weighed thrust and the factor φ_3 calculated from total- and central static pressure in the nozzle. The difference of 2-3 °/o is of the right order to be caused by boundary layer displacement and friction losses.

3) Flight test results show that at normal engine settings a straight extrapolation of the factor φ_1 to higher nozzle pressure ratioes is justified. At low engine settings and high flight speeds a massflow reduction of about 2 °/o is indicated.

'6 Acknowledgement.

The author wishes to acknowledge the valuable discussions with members from the National Gas Turbine Establishment, the Royal Aircraft Establishment and Rolls-Royce which preceded and largely determined the test programme.

References.

1) Holl, R. e.a. — Some flight thrust measurements on an Avon-Canberra installation CP 518 June '55.

2) - — Definitions of jet engine thrust. Rep.C.P..-190 BARC May '54 JRAeS '55

3) Rose, R. Dee, F.W. — Test bed calibration of an Avon RA 28 comparing several methods TN Aero 2861, Dec. '62.

4) Vleghert, J.P.K. — Bepaling van stuwkracht van straalmotoren. NLR V.1922. 1964.

FIG. 1 STATIC THRUST DETERMINATION ON FOKKER S – 14 JET TRAINER

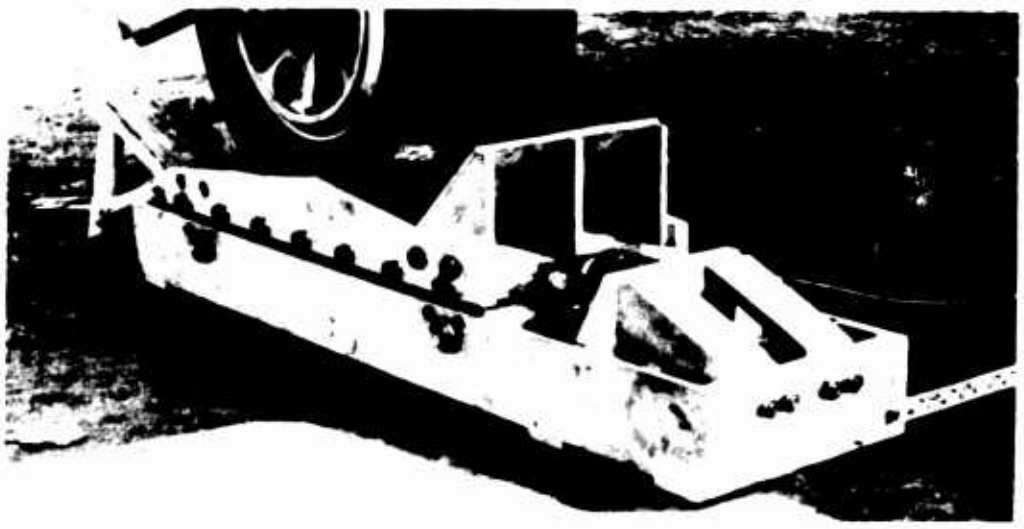

FIG. 2 CLOSE – UP OF THRUST MEASURING PAD UNDER MAIN WHEEL

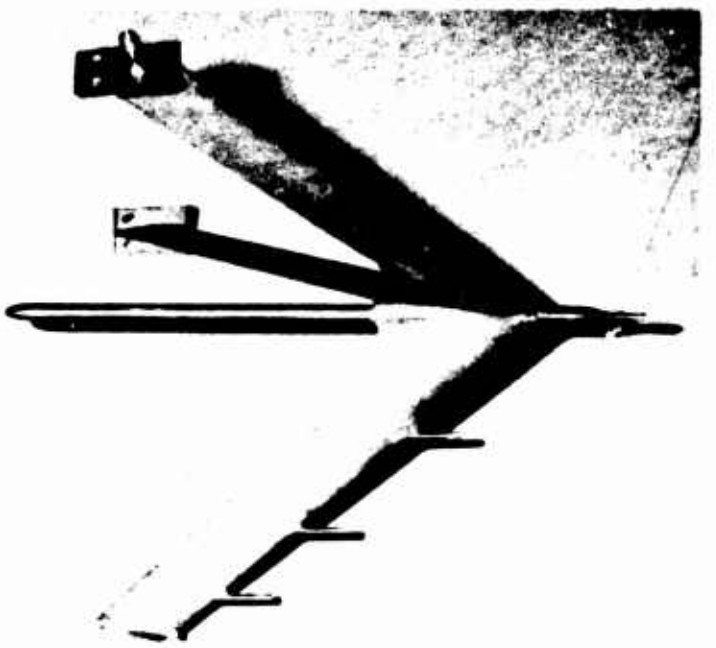

FIG. 3a JET NOZZLE SPIDER WITH STATIC – AND TOTAL PRESSURE TAPPINGS

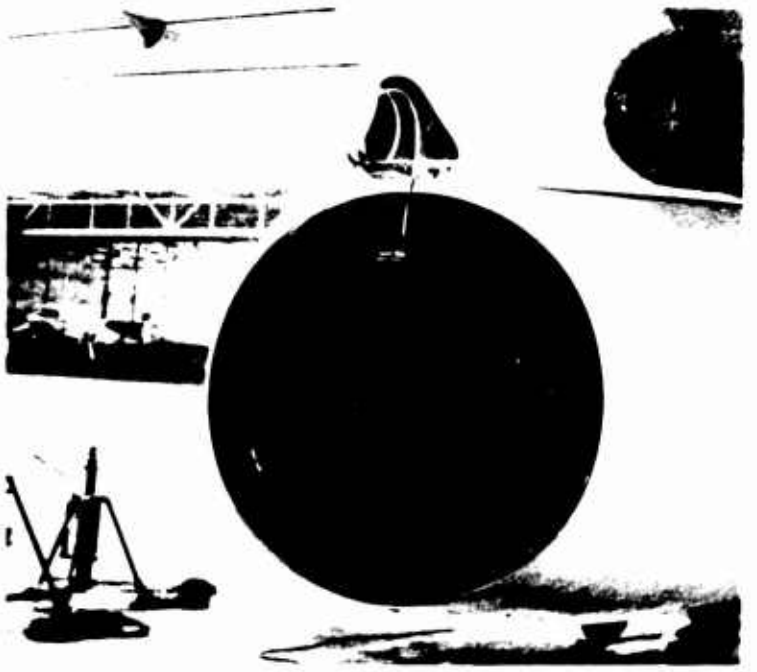

FIG. 3b INSTALLATION OF JET NOZZLE SPIDER

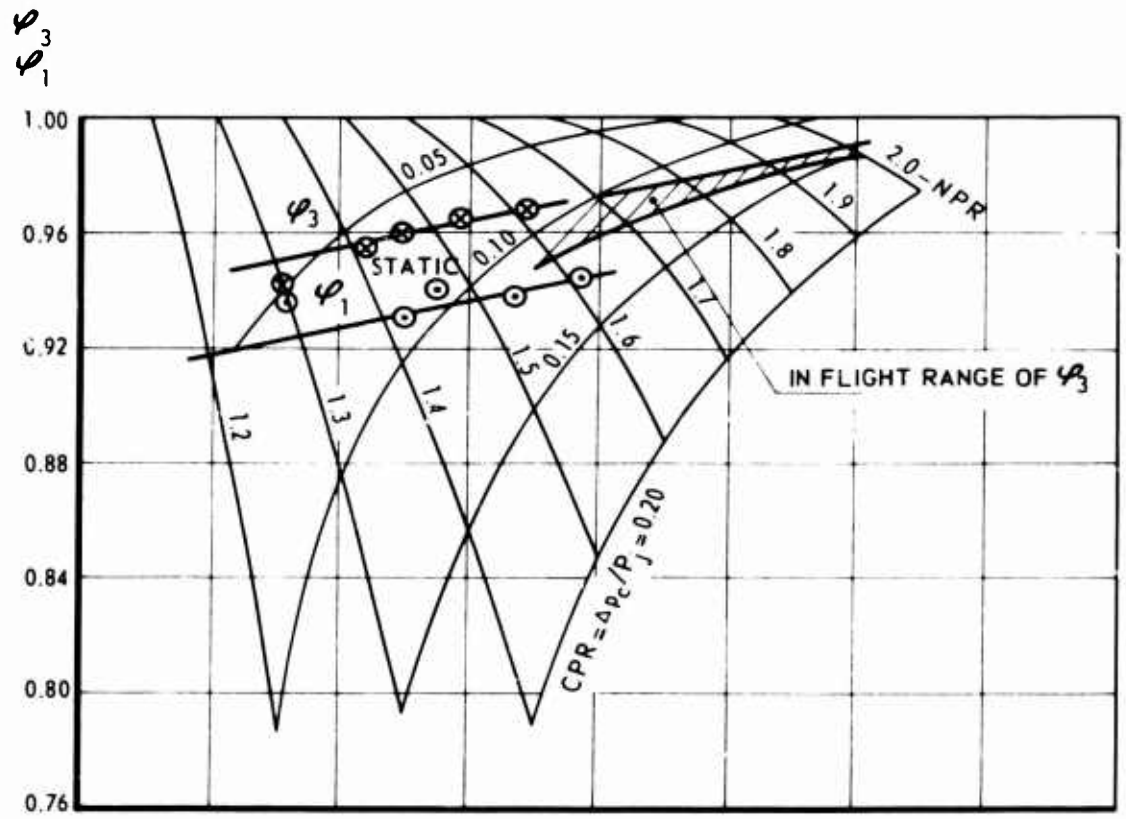

FIG. 4 CALIBRATION – AND CORRECTION FACTORS

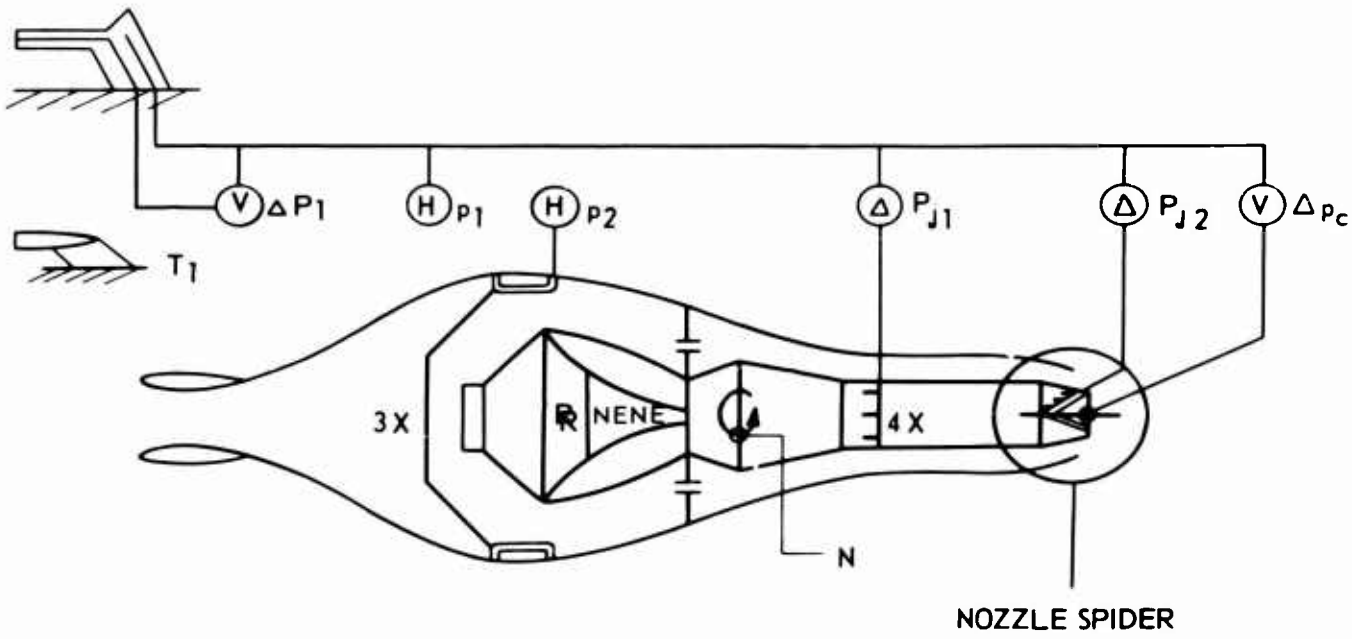

FIG. 5 SCHEMATIC DRAWING OF FLIGHT TEST INSTRUMENTATION

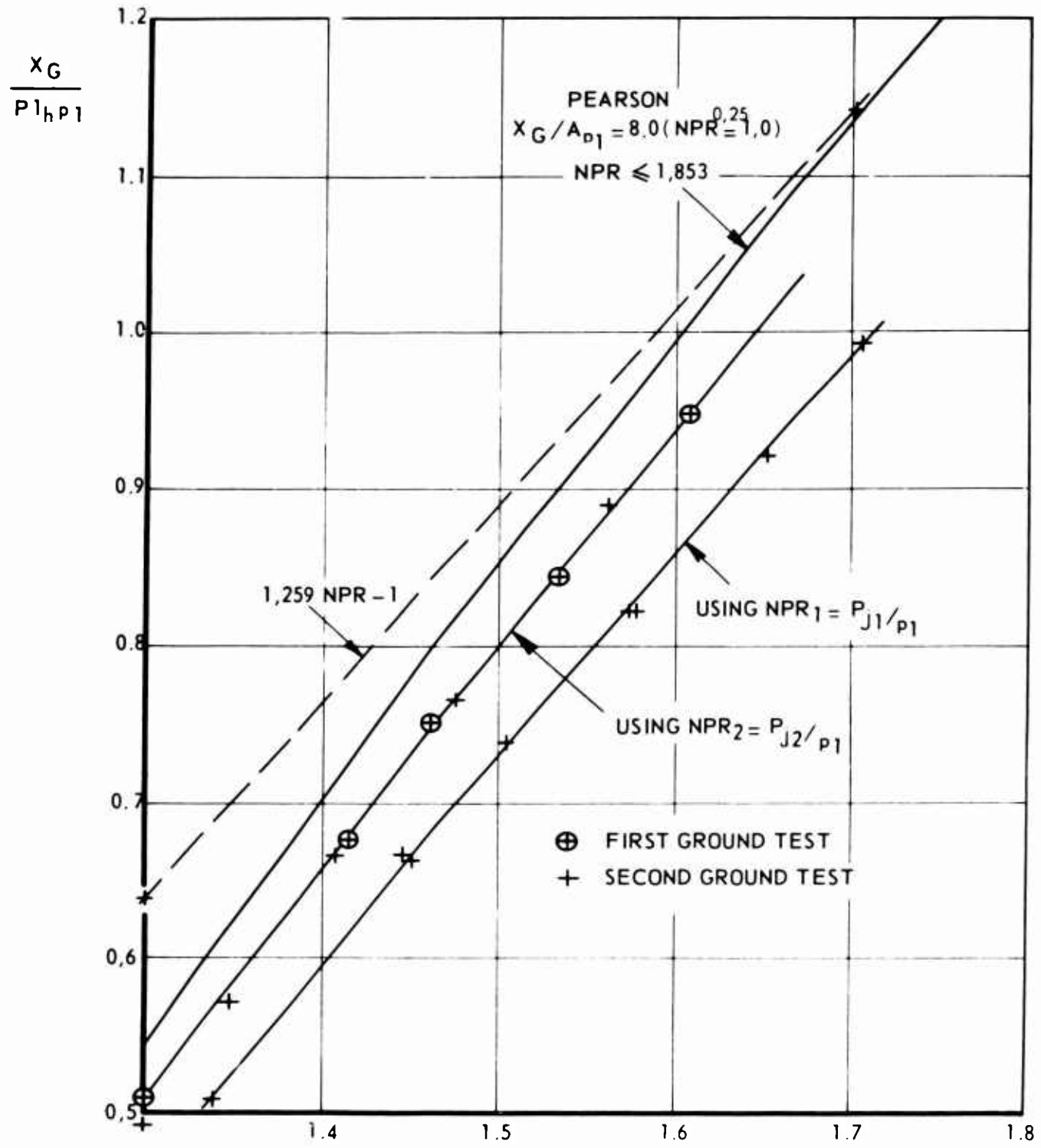

FIG. 6 COMPARISON OF MEASURED STATIC THRUST WITH PEARSON VALUE

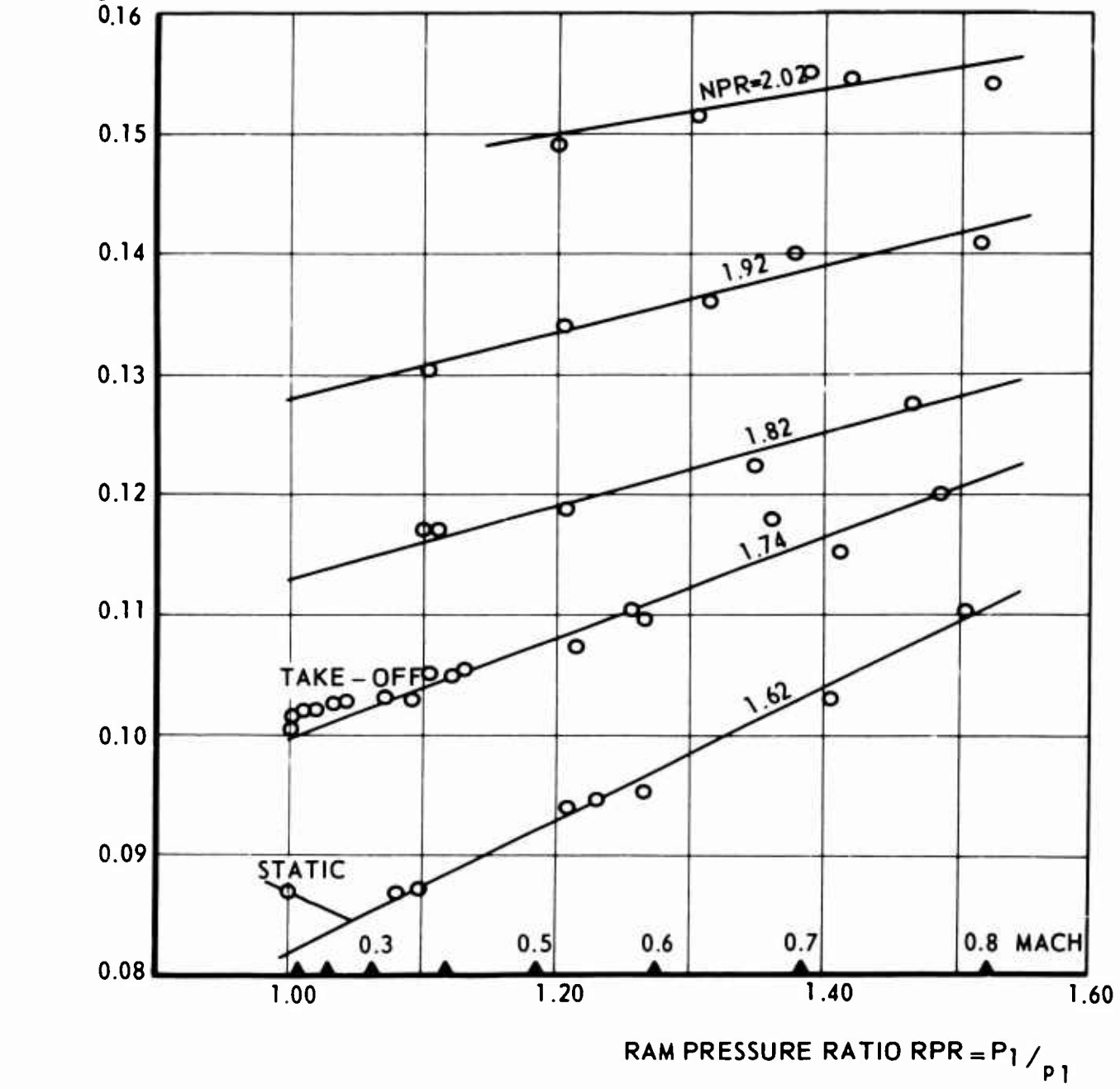

FIG. 7 INFLUENCE OF FLIGHT SPEED ON CENTRAL PRESSURE RATIO

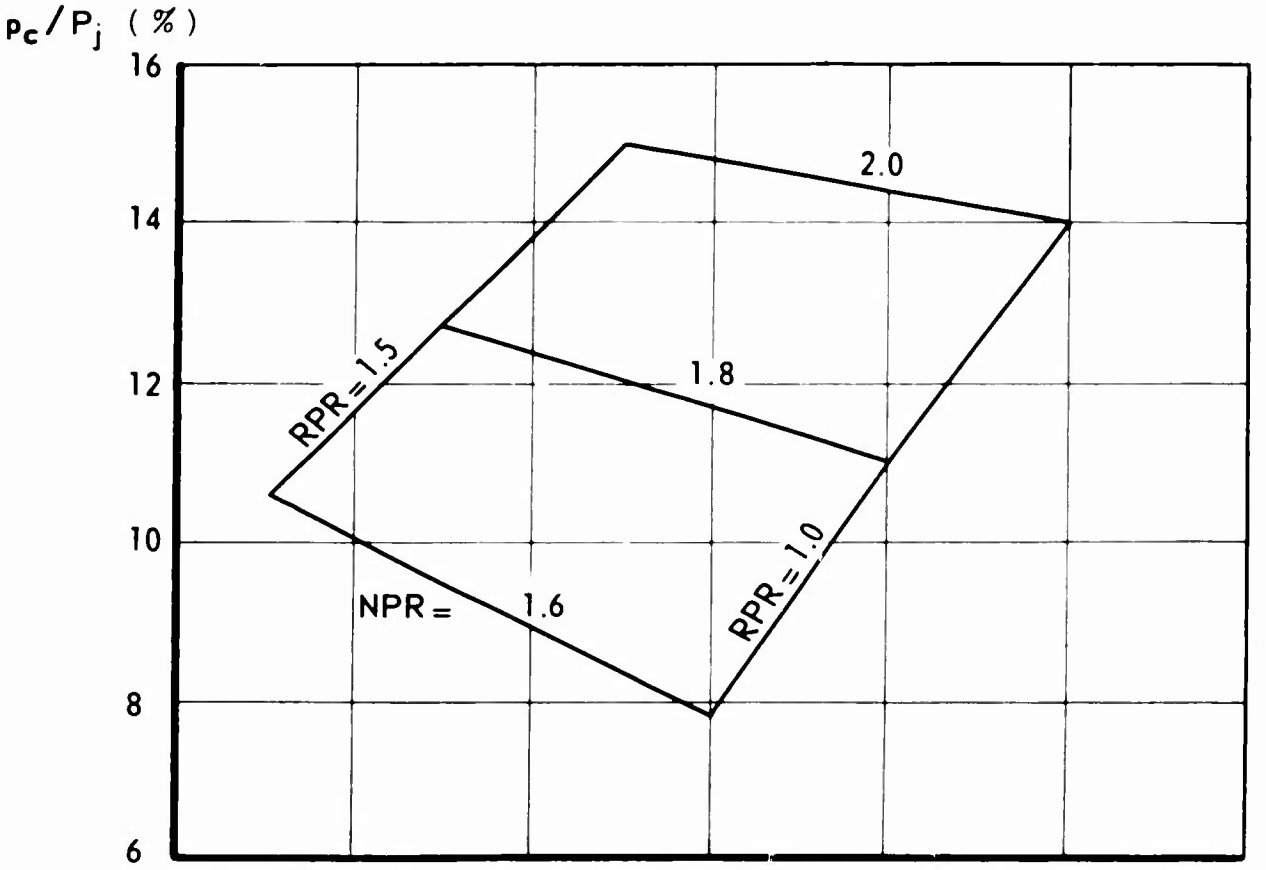

FIG. 8 CENTRAL PRESSURE RATIO AS A FUNCTION OF NOZZLE PRESSURE RATIO AND FLIGHT SPEED

" JET INFLUENCE ON V/STOL-AIRCRAFT IN THE TRANSITIONAL AND HIGH SPEED FLIGHT REGIME "

G. Krenz, Dipl. - Ing., Germany
Chief of Project Aerodynamics Department
of Vereinigte Flugtechnische Werke, Bremen

J. Barche, Dr. - Ing., Germany
Chief of Aerodynamics Department
of Vereinigte Flugtechnische Werke, Bremen

SUMMARY

This paper summarizes some results of VFW investigations related to aerodynamic problems of V/STOL aircrafts.

The results are based on windtunnel tests for a fighter type aircraft in a range from zero forward speed up to sonic velocity.

Special attention has been paid on the change of aerodynamic forces and moments during transition and in STOL with ground interference. In addition tests up to transonic speed are discussed.

Finally a possible theoretical approach on jet influence on wings by means of a simple jet model will be shortly discussed.

NOTATION

b	wing span
$\bar{c}$	mean aerodynamic wing cord
c_D	drag coefficient
c_L	lift coefficient
h	height above ground
L	aerodynamic lift
l	rolling moment
M_∞	mainstream Mach number
m	pitching moment
N	normal force
n	yawing moment
P_∞	ambient static pressure
P_T	total pressure
P_T/P_∞	nozzle pressure ratio
s	wing half span
T	total installed static thrust
T_N	normal thrust component
v_∞	mainstream velocity
v_i	efflux velocity
$(v_\infty /v_j)e$	effective velocity-ratio
W	aircraft weight
$\Delta L, \Delta D, \Delta m$	increments in lift, drag and pitching moments due to jet influence
ΔL_o	lift increment at zero mainstream speed due to jet influence
α	angle of attack, deg
β	angle of sideslip, deg
η_H	horizontal tail setting angle
ρ_∞	mainstream air density
ρ_j	efflux density
σ	angle between thrust vector and fuselage datum

JET INFLUENCE ON V/STOL-AIRCRAFT IN THE TRANSITIONAL AND HIGH SPEED FLIGHT REGIME

Günter Krenz and Jürgen Barche

1. INTRODUCTION

It is well-known by a number of published papers [1-6] that in contrary to conventional airplanes V/STOL aircrafts are strongly influenced by engine jets and intake flow conditions. This is mainly due to the fact that in low speed flight the engine's thrust must be used to lift the aircraft. Thus the powerful jets are inclined up to 90^{o} relative to the mainstream and induce secondary forces and moments on the wing and tailplane which are of the same order of magnitude as the aerodynamic loads. In addition the big massflow ratio causes intake forces in the low speed range which are normally not to be expected from conventional aircraft.

The jet and intake .nduced forces and moments depend in a different manner on the aircraft's flight Mach number. Therefore a separation into typical flight phases might be useful for a better understanding of the problems.

Such an outline is shown in Figure 1 which summarizes the characteristic phases for V/STOL aircrafts and main parameters in the flight range from zero forward speed up to sonic velocity.

As indicated in the left row a division into hovering, transition, STOL and wing supported flight seems to be reasonable. The second row shows the main parameters whilst in the third row that forces and moments are indicated, which are mainly influenced. In the right line the resultant main additional forces and moments are sketched.

For VTOL the main parameters are the clearance of the aircraft relative to the ground. This influence is normally restricted to normal force as well as pitching and rolling moments.

During transition the ground influence completely disappears, but additional parameters arise such as the ratio between mainstream and jet exit velocity or the attidude of the aircraft relative to the free stream.

For a STOL aircraft the problems are more complex, because all mentioned parameters including ground effects are more or less significant

In aerodynamic flight the main interference between jet and aircraft is on longitudinal motion only.

Regarding the discussed Mach number range, it is obvious that jet influence is especially remarkable for transition. Nevertheless in this paper a few hovering results and some high speed tests are dealt with, because little information has been available in this flight ranye up to now.

The considerations are done for a fighter type aircraft. Model configurations corresponding to the results are symbolized in the diagram. The results are obtained on 1:10 models with sonic jets in German low speed wind tunnels and in the transonic tunnel of the ARA in Bedford/England as well as on VFW-test rigs.

2. JET INFLUENCE ON PARTICULAR FLIGHT PHASES

2.1 Hovering

As it is wellknown the interaction between ground jets leads in principle to two different flow configurations resulting in different reactions on the aircraft [2]. These two configurations are indicated in Figure 2a.

On the left side jet induced normal forces and pitching moments are shown for a VTOL type whose nozzle configuration produces the so-called fountain effect. The fountain increases the pressure between the nozzles thus giving a positive lift force for small ground clearances.

The moments strongly depend on the nozzle configuration especially with reference to the wing. That means that positive as well as negative moments normally can arise.

On the right side test on a close cluster of jets configuration are plotted. This configuration cannot produce a fountain. The curves are approximately valid also for a single nozzle configuration having the same thrust. No positive lift force can be obtained in this case because the sucking action of the wall jet induces negative pressures on the lower side of the wing. These forces are increased by decreasing the ground distance.

A comparison of ground effect measurements done by VFW and NASA [5] shows figure 2 b. In this diagram were also drawn the distances of the jet exits of the different models. The nozzlearrangementexplains the arise or the absence of the fountain - effects.

The measured moments are of the same order of magnitude as in the above mentioned case. Because there is no aerodynamic rudder efficiency in hovering flight, the stabilization of the aircraft must be realized by a bleed nozzle system or by thrust modulation.

A detailed description of model- and testing technique is given in AGARD paper 26 of the Fluid Dynamic Panel.

As it can be seen from the tested configurations the influence of the ground is restricted to a clearance of roughly a wing span. The remaining lift loss is due to the suction of the free jets and therefore mainly a function of the nozzle efficiency. [3]

2.2 Transition

Swivelling the jet nozzles the increased forward speed leads to an increased jet inrerference even for smaller nozzles angles. A general explanation of this feature will be given in Figure 3.

To counterbalance the weight of the aircraft during transition the total normal forces N as a sum of lift L, normal thrust component T_N and jet ind' ced lift loss Δ L must equalize the weight W. In the diagram a typical variation of that forces is plotted against Mach number for constant angle of attack and variable swivelling angle. The hatched curve shows the resulting lift loss if the total normal force equalizes the weight.

It can be seen from that figure that with increasing aerodynamic lift and therefore reduced normal thrust component the jet induced lift loss firstly grows up and having reached a well-defined maximum decreases to a small value at the end of transition.

As a thumbrule it may be noted that normally the maximum lies between half and three quarters of the aircrafts minimum speed for aerodynamic flight and may reach the order of 0.1 up to 0.4 of the aircraft weight.

Connected with that lift losses considerable changes in pitching, yawing, and rolling moments are to be expected, which result from wing and especially from jet tail-interferences.

It is obvious that these features are highly important for the aircraft's handling during transition. A more detailed discussion therefore seems to be necessary.

2.2.1 Longitudinal motion

Figure 4a shows the influence of the main parameters on forces and moments in longitudinal motion of an aircraft type as symbolized in the diagrams.

On the left side the lift loss-thrust ratio is plotted against the effective velocity ratio with nozzle angle and angle of attack as parameters.

Generally the increase of these three parameters strongly increases the lift losses.

Besides this the configuration i. e. especially the disposition of jet exits relative to the wing has a big influence as can be seen comparing the curves marked by the different symbols. To reduce lift losses jet exit must be kept away from the wing as far as possible [2,4].

Furthermore nozzle shape will influence the jet effects. Generally it can be stated: As more as the jet decays as stronger the jet influences are to be observed [3]. On the other hand nozzles with strong jet decay are recommended to reduce the noise level and the ground erosion. This demand is therefore in contrary to the development of nozzles with small jet induction.

On the right side of Figure 4 a the additional moments based on thrust and mean aerodynamic wing cord are plotted against effective velocity ratio. The additional nose up moments depend on the same parameters and in the same manner as the lift losses. Thus an increased angle of attack, swivelling angle and velocity ratio increase the moment.

In comparison with the lift losses, however, which are mainly due to jet interference on the wing, the arising additional pitching moments are chiefly depending on the tailplane contribution, which varies strongly with the height of the tail relative to the jets [1,2].

It is highly important to notice that growing nose up moments are combined with an increased angle of attack.

Comparing correlated changes in lift and moments for a fixed velocity ratio and jet direction of the symbolized types of aircraft it follows that jet influence decreases aircraft stability. On the other hand for a fixed attitude of the aircraft a positive zero pitching moment-shift arises, with increasing nozzle swivelling angle and decreasing velocity ratio.

That shift not demonstrated in the diagrams, leads to the typical positive elevator setting for such an aircraft during transition.

Figure 4b shows the lift losses and the changing of the moments measured with the VFW-model compared with NASA-measurements[4]. The lift- and moment characteristics have the same tendencies, but its values are strongly diverging.

Summarizing all the effects the following essential consequences for jet influence on longitudinal motion during transition can be drawn.

1. Tilting the nozzles in more vertical position produces a normal thrust component; a great part, however, will be lossed by strong jet induced lift losses.

2. Jet influence results in a positive zero pitching moment-shift and in additional destabilizing effects during landing transition. The jet induced destabilization must be compensated by high static stability and by means of artificial stabilizing systems such as bleed air or thrust modulation. In order to compensate zero pitching moment-shift together with decreased stability the horizontal tail setting angle normally must be enlarged to positive values during landing transition[7]. This feature is demonstrated in Figure 5 where nose up moments are increased to a maximum with decreasing transition speed. Certainly an unconventional behaviour of VTOL aircraft design.

   In addition due to destabilizing character attention must be paid on the swivelling procedure in order to prevent abrupt moment changes.

3. In addition to jet interference on lift and pitching moment jet influence on drag is shown in Figure 6, where drag polars with and without jets are compared. For o fixed angle of attack lift as well as drag decreases but generally the lift - drag ratio becomes worse. This is mainly due to remarkable changes of the lift distribution by jet induction in the mid wing thus giving higher induced drag.

   Comparison of the two diagrams shows that the influence decreases with increasing velocity ratio and decreasing swivelling angle.

2.2.2 Lateral motion

Jet influences on lateral motion are mainly characterized by changes in the yawing and rolling moments due to intake and exit flow, as sketched in Figure 7. In this figure the basic configuration - i. e. the aircraft without intake and exit flow - and the additional moments are plotted against forward speed for a fixed incidence, angle of yaw and nozzle position. It can easily be seen that jet influence decreases the yawing and increases the rolling moments, thus stabilizing in yaw and destabilizing in roll.

The intake flow on the other hand more or less reduces the weather cock stability. The destabilizing intake moment for a fixed yaw angle being roughly a linear function of the flight Mach number equalizes the stabilizing parabolic yawing moment at a certain speed. From hovering up to this limiting speed the aircraft becomes unstable with respect to yaw motions. This is of course a normal problem for each V/STOL aircraft, however, it must be solved in order to use the aircraft's capability.

The limiting speed which is marked by the line B in Figure 7 mainly depends on aircraft configuration and mass flow ratio. The unstable speed range is larger for fuselage front intakes than for side or wing intakes.

In any case stabilizing in roll, worsened by jet influence as seen in Figure 7, must be efficient in the speed range of unstable yawing moments. In practice no serious problems will occur, because of the support of bleed air.

A much more delicate problem are the additional rolling moments beyond the boundary B in Figure 7 which need rather big efforts in bleed system design in order to avoid significant handling limitations.

As mentioned above the discussed intake and exit flow interferences are valid for constant incidence, angle of yaw, and nozzle position. It may be noticed, however, that an increase of these parameters increases the moments with the same tendencies as they are given for an aircraft without jets.

2.3 STOL

Much more complicate as during transition the jet effects are to predict for the STOL phase of an aircraft. This is because the ground acts as a new and highly effective parameter, which is illustrated in Figure 8.

In this figure lift and pitching moment due to ground interference on jet influenced airframe are plotted against the relative ground clearance for given incidence, nozzle position and velocity ratio. On the left part of the figure, which is valid for zero incidence, the typical tendency of ground effect is to be noticed. That means that extremely small distances cause suction forces, whilst additional lift forces are measured for higher clearances and in general it can be stated, that in about a wing span distance the ground effect completely disappears [5].

In a similar manner the additional pitching moments are nose down for small clearances and change to small positive values in about a half span distance. These effects are normally increased by an increased nozzle angle, the velocity ratio, however, is not of strong importance for that case of zero angle of incidence as can be seen in Figure 8.

As a typical example it may be assumed that a rolling aircraft has a relative ground clearance of 0.4. For a nozzle swivelling angle of 30° and a velocity ratio of about 0.13 this leads to a positive ground induced moment of about 0.03 T, marked by the point P_O.

On the right hand side of Figure 8 the same curves are shown with the only exception, that they are valid for an angle of attack of 15°.

The incidence increases the additional lift and moments which in addition are more sensitive with respect to jet direction and velocity ratio.

But again for the example mentioned above even for 15° incidence the moment remains rather unchanged as can be seen comparing P_{15} and P_o.

Starting from that point, for fixed velocity ratio, nozzle angle and incidence the hatched lines illustrate the changes in lift and moment as they are to be expected during take-off. That means, that together with decreasing induced lift the pitching moment tends from negative to positive values in a rather smooth progress.

This is in principle valid also for higher speed ratios. In this case the slopes are stronger, however.

Much more effective than velocity ratio the jet direction seems to be. From Figure 8 it can be seen that a 60° nozzle angle gives worse results than a 30° nozzle swivelling angle. This leads to the assumption that for STOL the nozzle angle should be as low as possible.

A point of particular interest is the rudder effectiveness with respect to ground influence.

Test results for the symbolized configurations indicate that no significant changes could be measured apart of a small increase for positive incidence. This can be derived comparing the curves for zero and negative horizontal tail setting angle in Figure 8.

One can notice that ground influence producing a nose down pitching moment is slightly decreased for negative setting angle.

That means, uninfluenced rudder efficiency used to get nose up moments according to negative tail setting is supported by decreased nose down moments due to ground interference. In summary no severe trim and stability problems are to be expected for STOL when using small jet deflections.

2.4 Jet interference in high speed flight

In section 2.2 it has been demonstrated that a lot of interference problems are connected with the transition phase of jet supported V/STOL aircraft. New problems might be expected in high-speed and especially in transonic flight due to compressibility effects of the free stream velocity, in particular if the jet nozzles are fitted near the center of gravity on both sides of a fuselage. On the other hand it is wellknown

that the interference of a jet in a nearly parallel stream is in a first order proportional to the difference of the jet exit and the free stream velocity. Thus the difference in high speeds is smaller than in low speed flight.

From our experience it appears that sonic jet pressure ratio is the main parameter in transonic flight.

A typical test result is shown in figure 9 where for Mach number 0.90 and three nozzle pressure ratios the lift coefficient is plotted against incidence and pitching moment coefficient. From this example it can be stated that for small incidences neither the lift nor the pitching moment slope are remarkably changed within the measured pressure range from one up to four. The main influence seems to be a shift in zero pitching moment and zero lift angle. The stability of the aircraft is only effected at higher incidences i.e. load factors which normally cannot be used. It may be noticed, however, that these incidences where stability will be influenced by jet interference are somewhat smaller at smaller Mach numbers.

Nevertheless as it is known from low speed tests the zero pitching moment and zero lift angle shifts seem to be the main feature of the problem.

It therefore will be of general interest to compare these low and high speed values. This has been done in Figure 10, where zero pitching moment and zero lift angle are plotted against the reciprocal effective speed ratio. For critical nozzle exit pressure the figure covers a Mach number range from zero up to one.

The correlation of the results is rather good. The result can therefore be used as a guide for jet influence in transonic flight if low speed tests are available.

The small values compared with low speed results prove once more that even for side mounted nozzles the problems of jet interferences are to be solved in the transition phase and not in the transonic flight region.

This is valid for lateral stability too, where normally the jet influences can be completely neglected.

3. THEORETICAL APPROACH

The importance of jet induced forces and moments on V/STOL aircraft design asks for a theoretical approach. Because of the complex problem no complete theory can be expected at this moment but even some guide lines could be helpful for the project engineer.

Recently an attempt was done by Williams and Wood [2] who established the "vortex-sheet theory", which can be called a "far-field-theory" of a single jet, based on Woolers small perturbation approach.

Another possible theoretical approach, using near field effects will be shortly described: It is wellknown that a jet induces a velocity field, as indicated in Figure 11. On a wing the additional normal and tangential velocity components will be induced which are proportional to the exit velocity v_j. The tangential components are to be understood as change in local dynamic pressure whilst the normal components give an additional circulation decreasing the sectional lift coefficient.

Thus in total a change both in sectional lift slope and magnitude and in addition a shift of the aerodynamic center should be expected.

To calculate these effects some empirical knowledge of the induced velocities normal to the jet boundary is necessary, which can be obtained from test results. Replacing the jet boundary by an arbitrary surface distribution of singularities which give the actual normal velocities on the boundary a potential-theoretical model can thus be established, in order to calculate the complete induced velocity field. From these calculations it appears, that the most important effects are generated in the vicinity of the nozzle. Therefore in most cases an approximation of the jet by a model jet of only some diameter's length seems to be sufficient. On the other hand that means that the jet history far downstream has no significant importance on a wing, provided that the speed ratio v_∞/v_j is small enough to ensure that no big deflections in the neighbourhood of the nozzle will occur.

As indicated in Figure 11 three different regions of jet effects can be defined in principle. In region I which covers the hovering phase the influence of the free streem velocity is extremely small. This means that the jet induced tangential components are big compared with the free stream velocity. Thus non-linear effects or strong changes in the lift coefficient slope are to be observed.

In region II the tangential components as well as the curvature of the jet path can be neglected in first order calculations. This simply means that only the normal components of the jet inductions are important, giving a linear function between L/T and $(v_\infty/v_j)_e$.

On the other hand this effect can be interpreted as a negative camber of the wing or as a simple α .- shift for constant lift slope. By means of the model described above this region can be easily calculated using the lifting surface theory.

The third region may be understood as a speed range where the jet deflection must be considered. This region can also be calculated by means of the lifting surface theory, but a more detailed knowledge about the jet inductions should be demanded. That means that the jet may no longer be compared with a submerged jet and should be better replaced by a vortex sheet as proposed by Williams and others [2,8]

Fortunately for most jet supported V/STOL aircraft transition will be finished at the end of region II.

A comparison of theoretical calculations done in 1964 with new experimental results is shown in Figure 11 for the symbolized wing-body combination. The agreement is quite good, although the interaction between the six jets was neglected. It therefore seems useful to continue on this theory which is described in more detail in an unpublished VFW work but will be published in the near future.

REFERENCES

1. Williams, J. Wood, M.N. — Aerodynamic Interference Effects with Jet Lift Schemes on V/STOL Aircraft at Forward Speeds. AGARDograph 103, Part 2, 1965.

2. Williams, J. Wood, M.N — Aerodynamic Interference Effects with Jet-Lift V/STOL Aircraft under Static and Forward-Speed Conditions. Zeitschrift für Flugwissenschaften, Juli 67.

3. Kuhn, R.E. — NASA Research on the Aerodynamics of Jet VTOL Engine Installations. AGARDograph 103, Part 2, 1965.

4. Vogler, R.D. — Interference Effects Of Single And Multiple Round Or Slotted Jets On A VTOL Model In Transition. NASA TN D-2380, 1064.

5. Vogler, R.D. — Ground Effects On Single-And Multiple-Jet VTOL Models At Transition Speeds Over Stationary And Moving Ground Planes. NASA TN D-3213, 1966.

6. Otis, J.H.Jr. — Induced Interference Effects On A Four-Jet VTOL Configuration With Various Wing Planforms In The Transition Speed Range. NASA TN D-1400, 1962.

7. Chinn, H.W. — Results Of Flight Tests On The Short SC 1 VTOL Research Aircraft With Particular Reference To Handling Qualities In The Hover And Transition. AGARD Report 527, 1966.

8.	Wooler, P.T.	On The Flow Past A Circular Jet Exhausting At Right Angles From A Flat Plate Or Wing. Journal Of The Royal Aeronautical Society, March, 1967.
9.	Barche, J.	Strahlprobleme bei Kurz- und Senkrechtstartern. WGLR, 10. Sitzung des Ausschusses "Aerodynamik" am 8. Dezember 1966.
10.	FW-Bericht 25-62	Sekundäre Kräfte und -Momente an VTOL-Flugzeugen im bodennahen Schwebeflug.

PHASES		PARAMETER	MAIN INFLUENCE	SYMBOL
1.	VTOL $M_\infty = 0$	GROUND CLEARANCE NOZZLE POSITION JET DIRECTION	THRUST LIFT MOMENTS (TEMPERATURE)	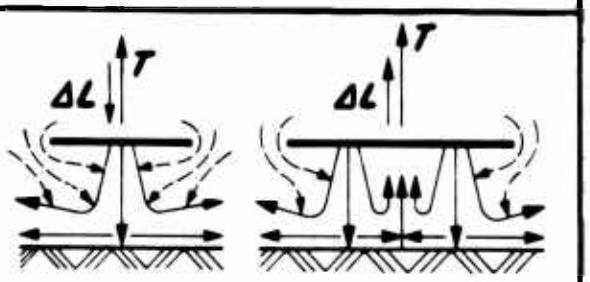
2.	2.1 TRANSITION $M_\infty \to 0$ 2.2 STOL $M_\infty \to 0$	NOZZLE POSITION JET DIRECTION VELOCITY RATIO INCIDENCE, YAW GROUND CLEARANCE	LIFT, SIDEFORCE PITCHING YAWING } MOMENTS ROLLING	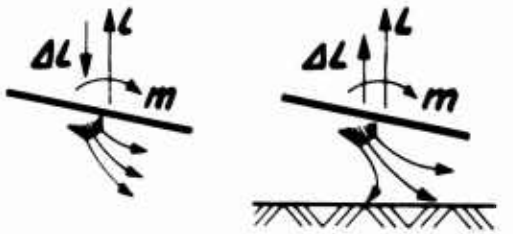
3.	AERODYN. FLIGHT $M_\infty \leq 1$	VELOCITY RATIO INCIDENCE, YAW	LIFT PITCHING MOMENT DRAG	

Fig. 1 Jet problems survey

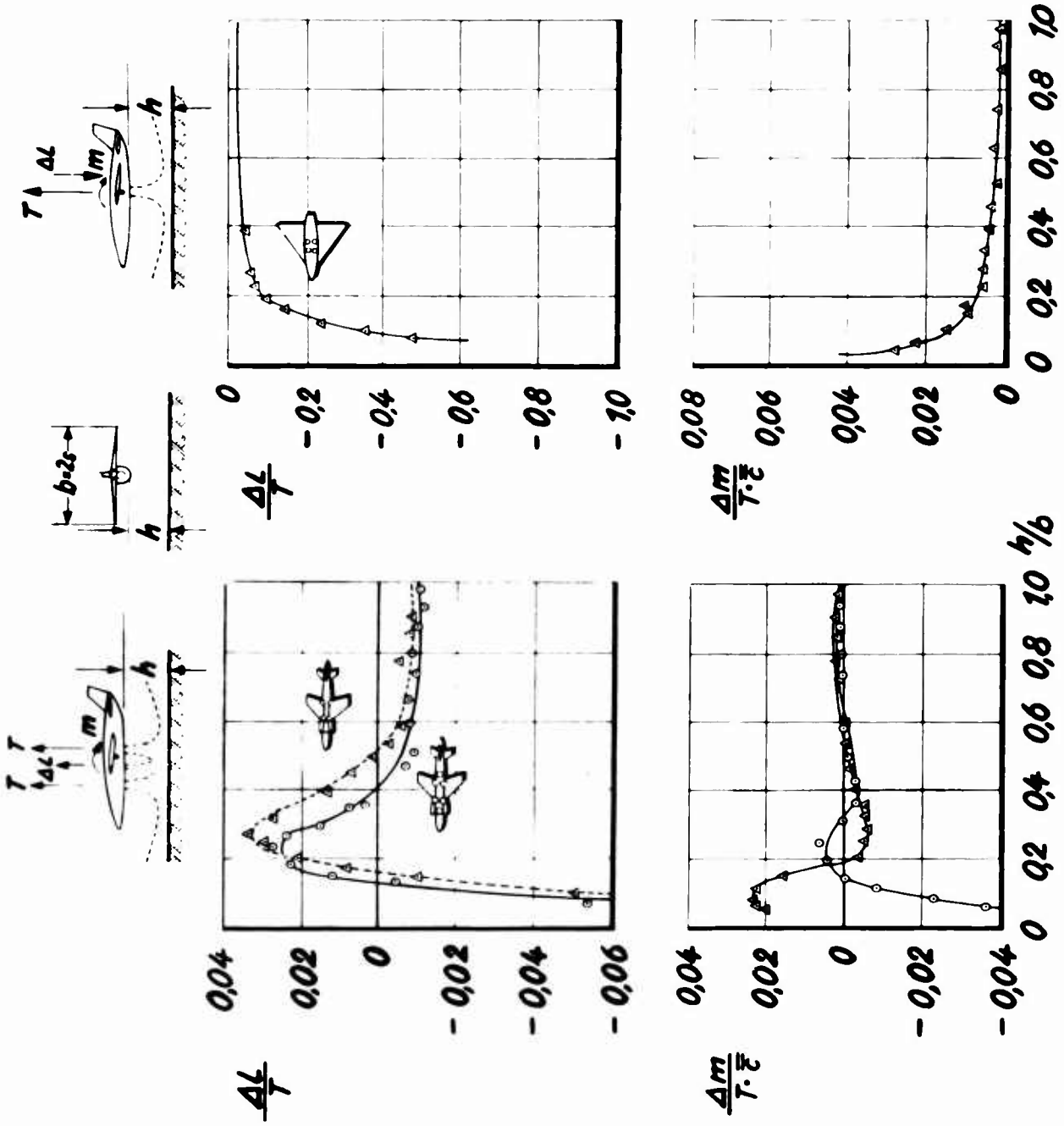

Fig.2(a) VTOL ground influence

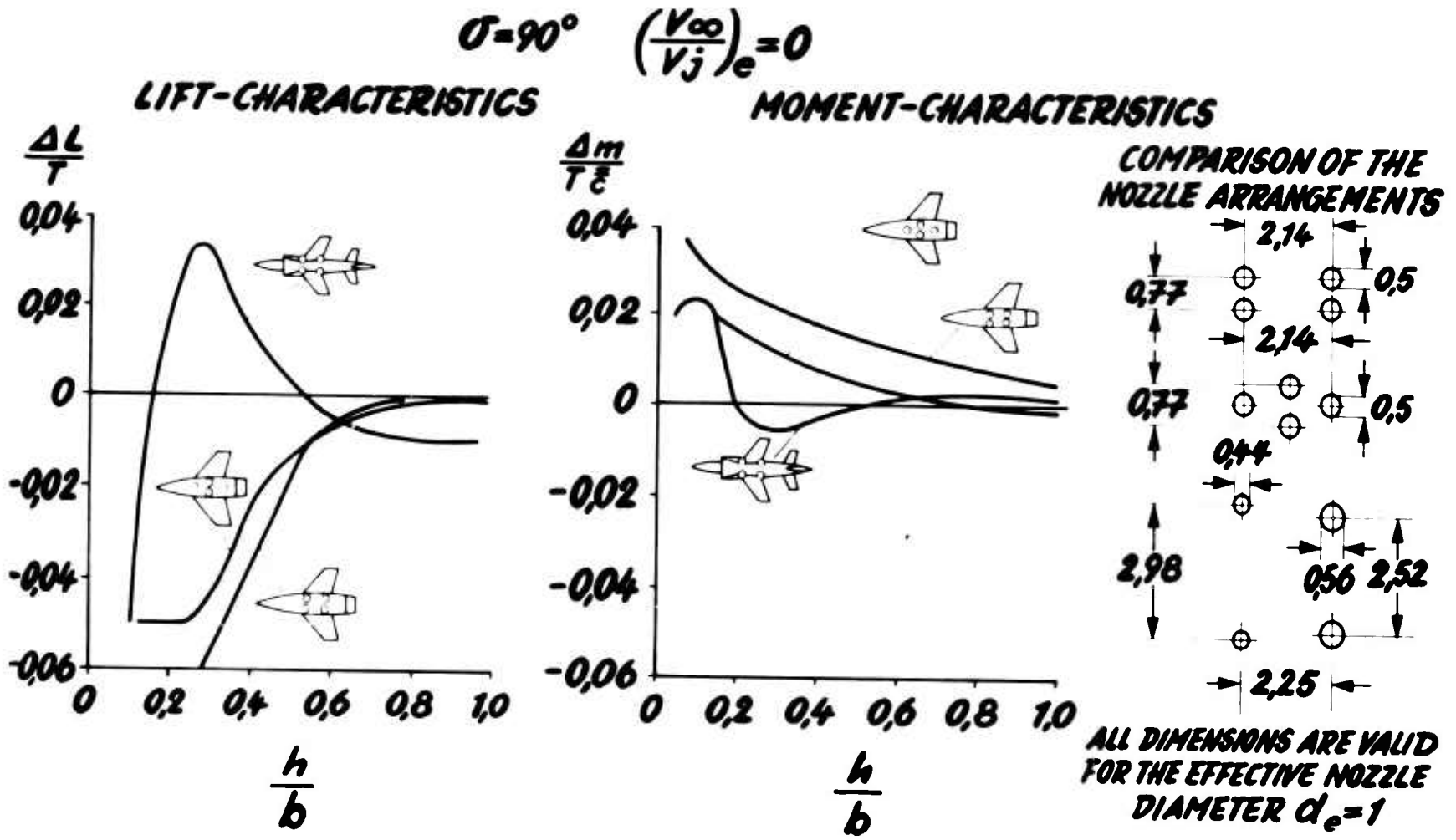

Fig.2(b) VTOL ground influence

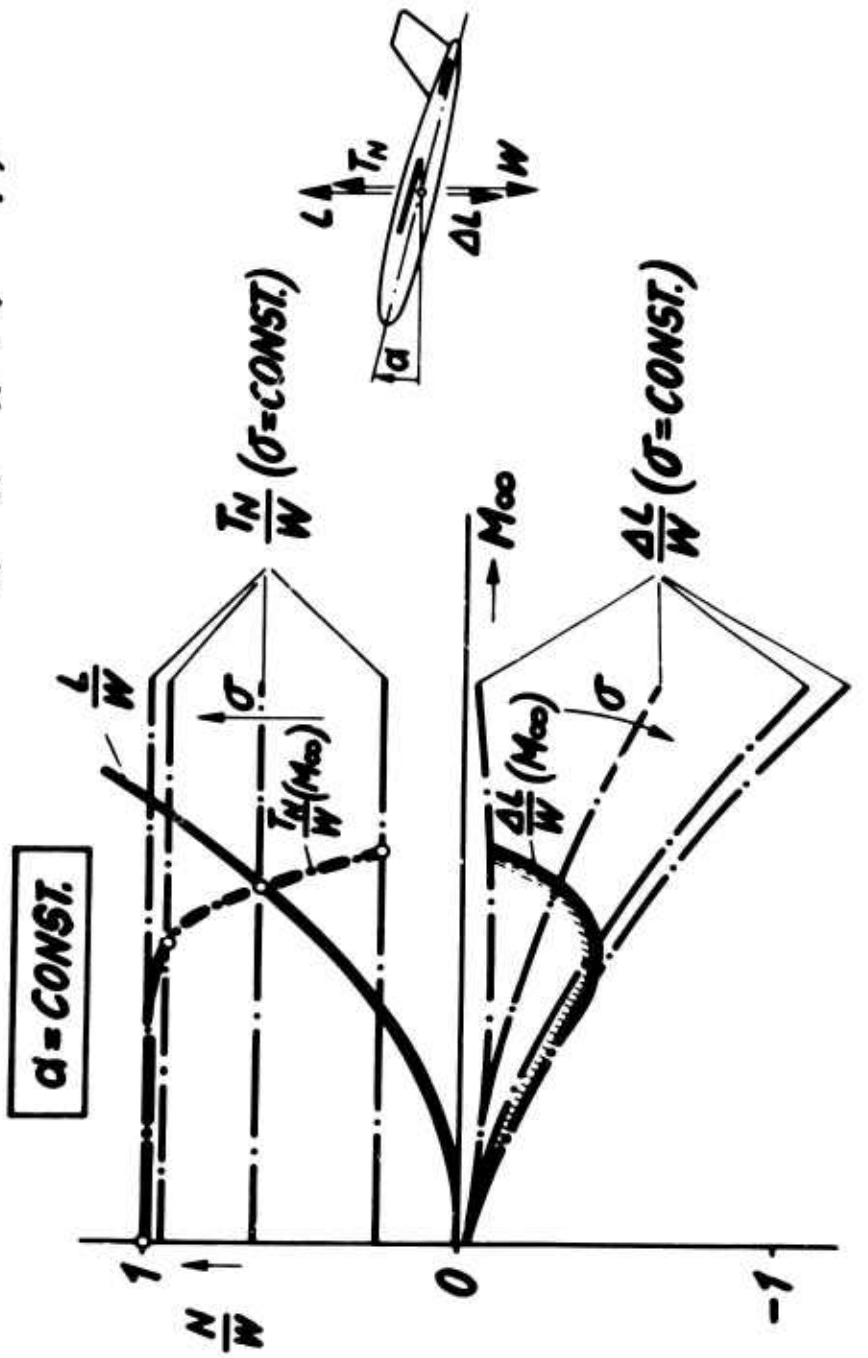

Fig.3 Transition vertical forces

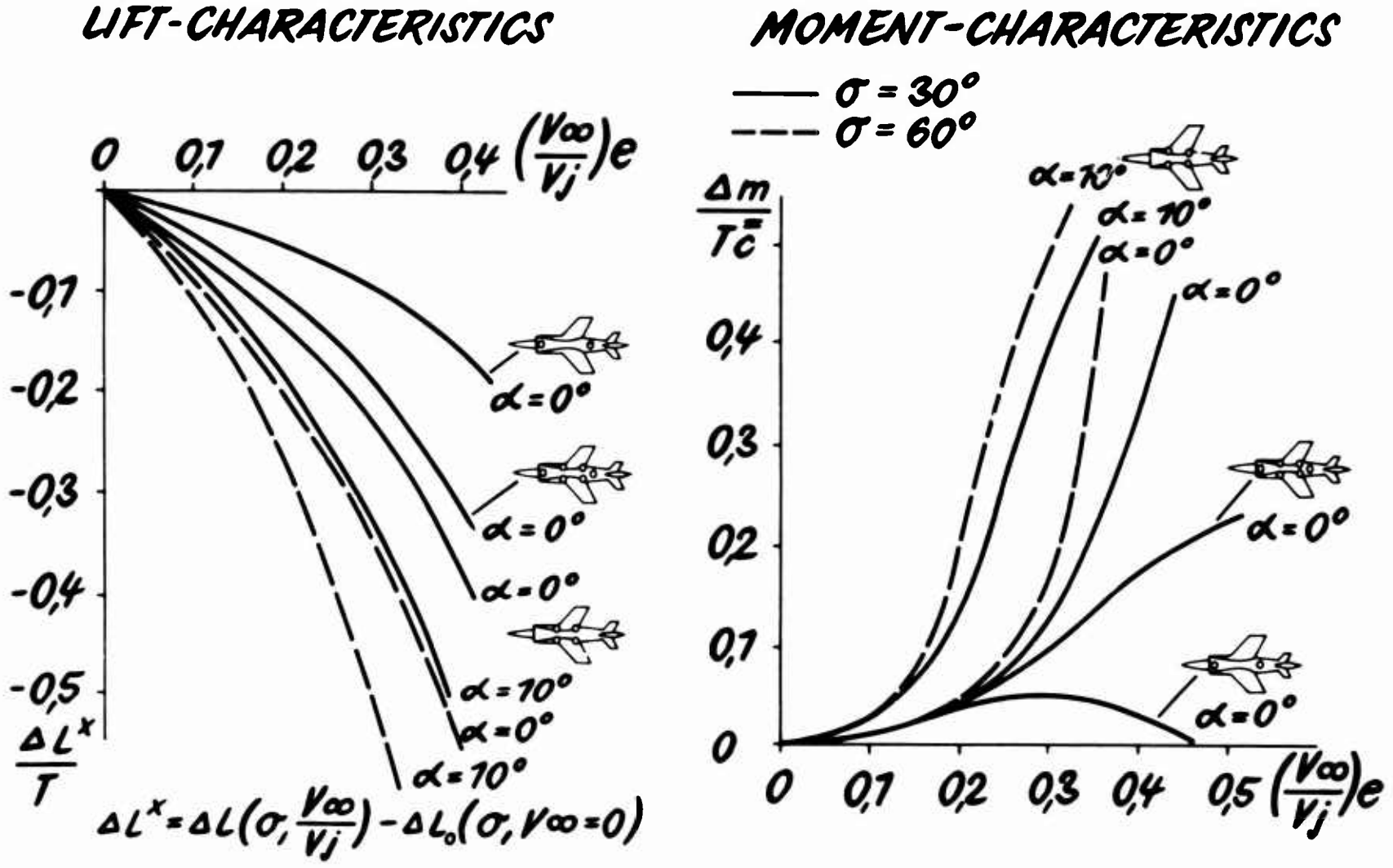

Fig.4(a) Effect of jet angle nozzle disposition and incidence

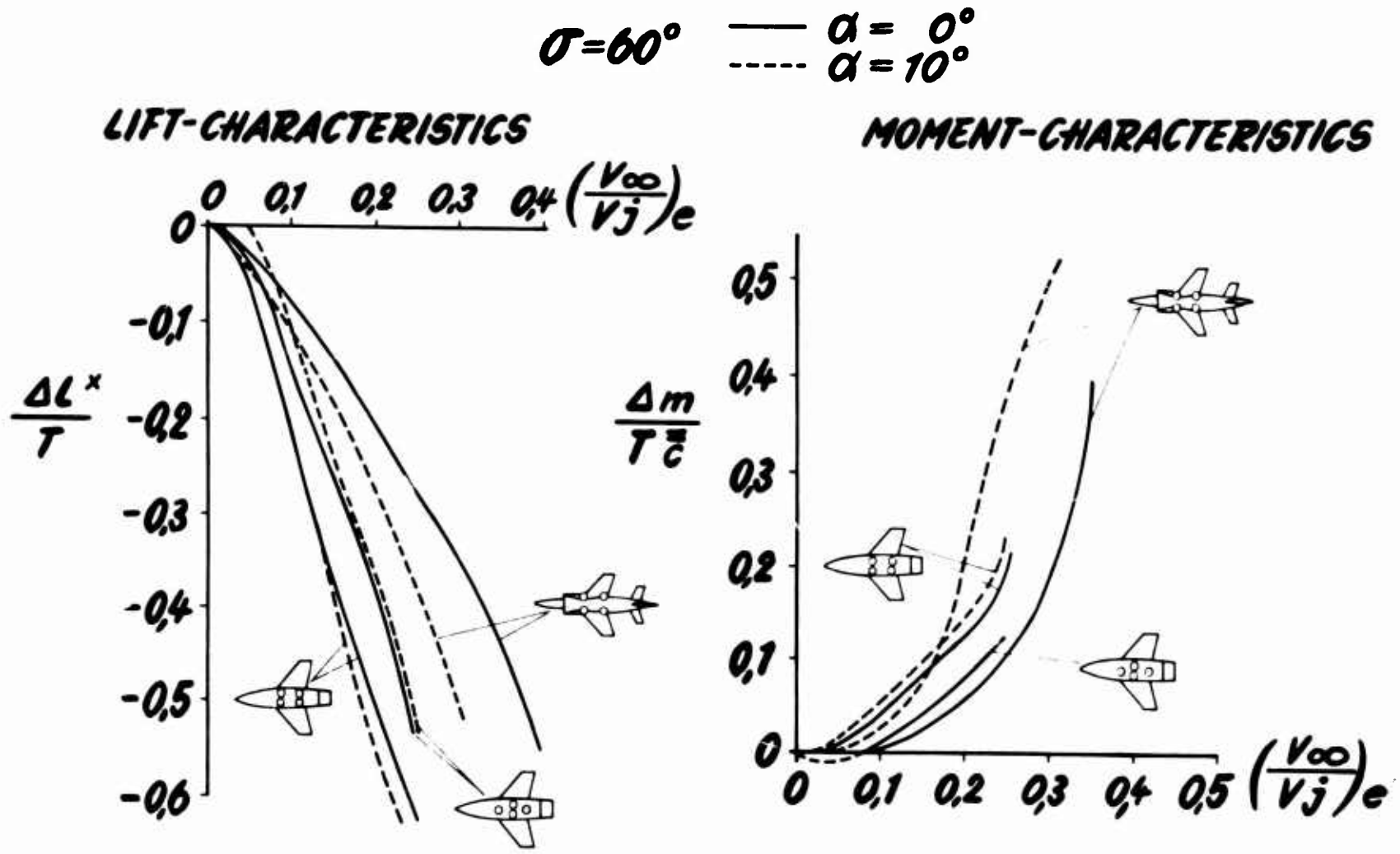

Fig.4(b) Effect of jet angle nozzle disposition and incidence

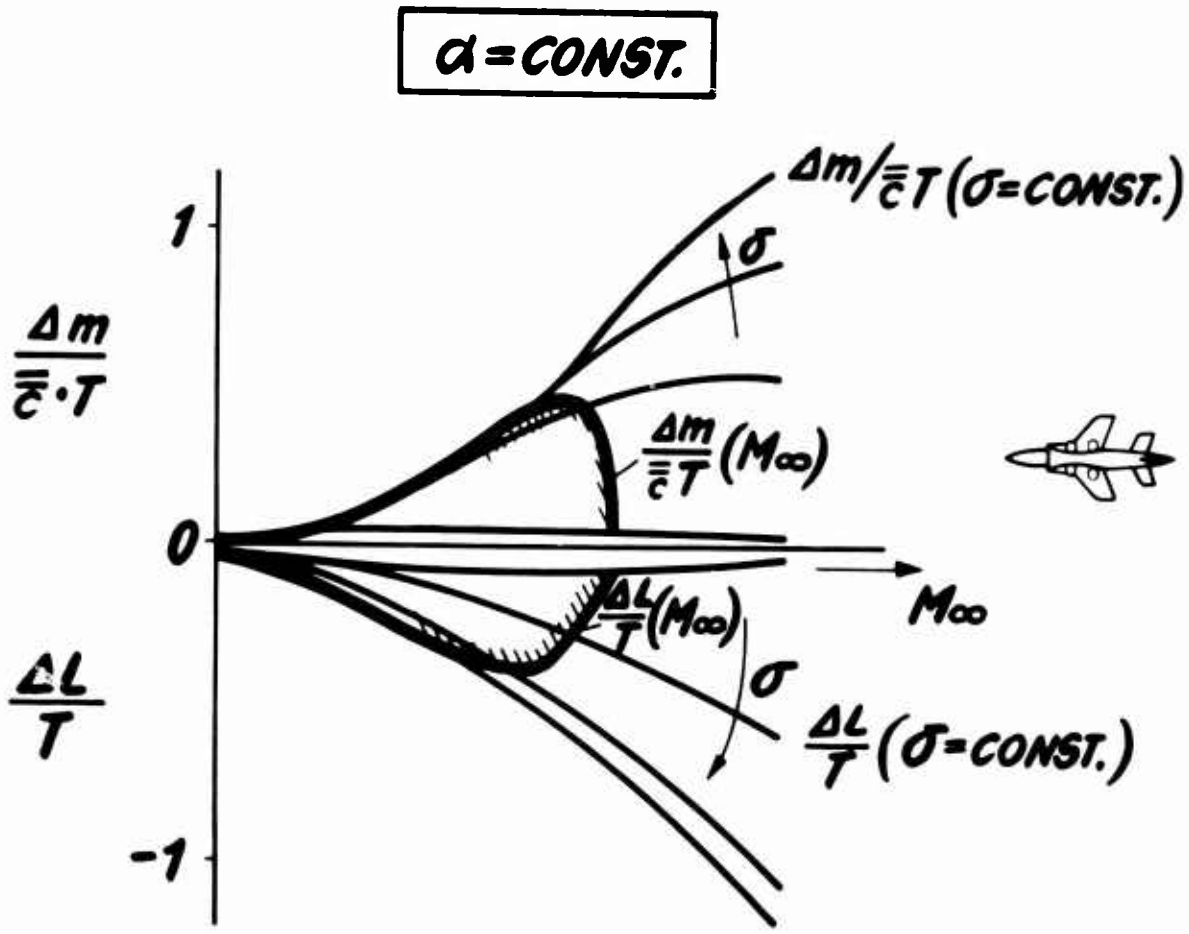

Fig.5 Jet induced lift and pitching moments during transition

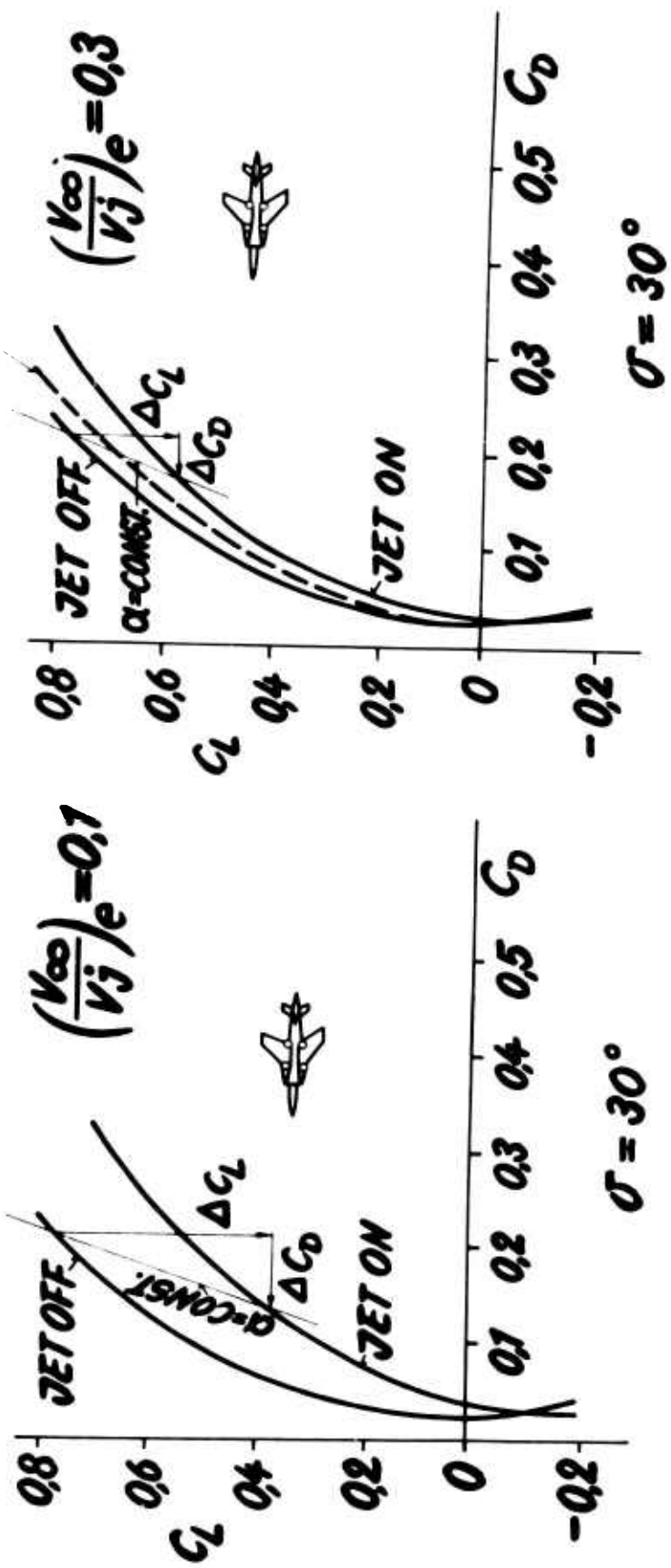

Fig.6 Jet influence on lift drag ratio

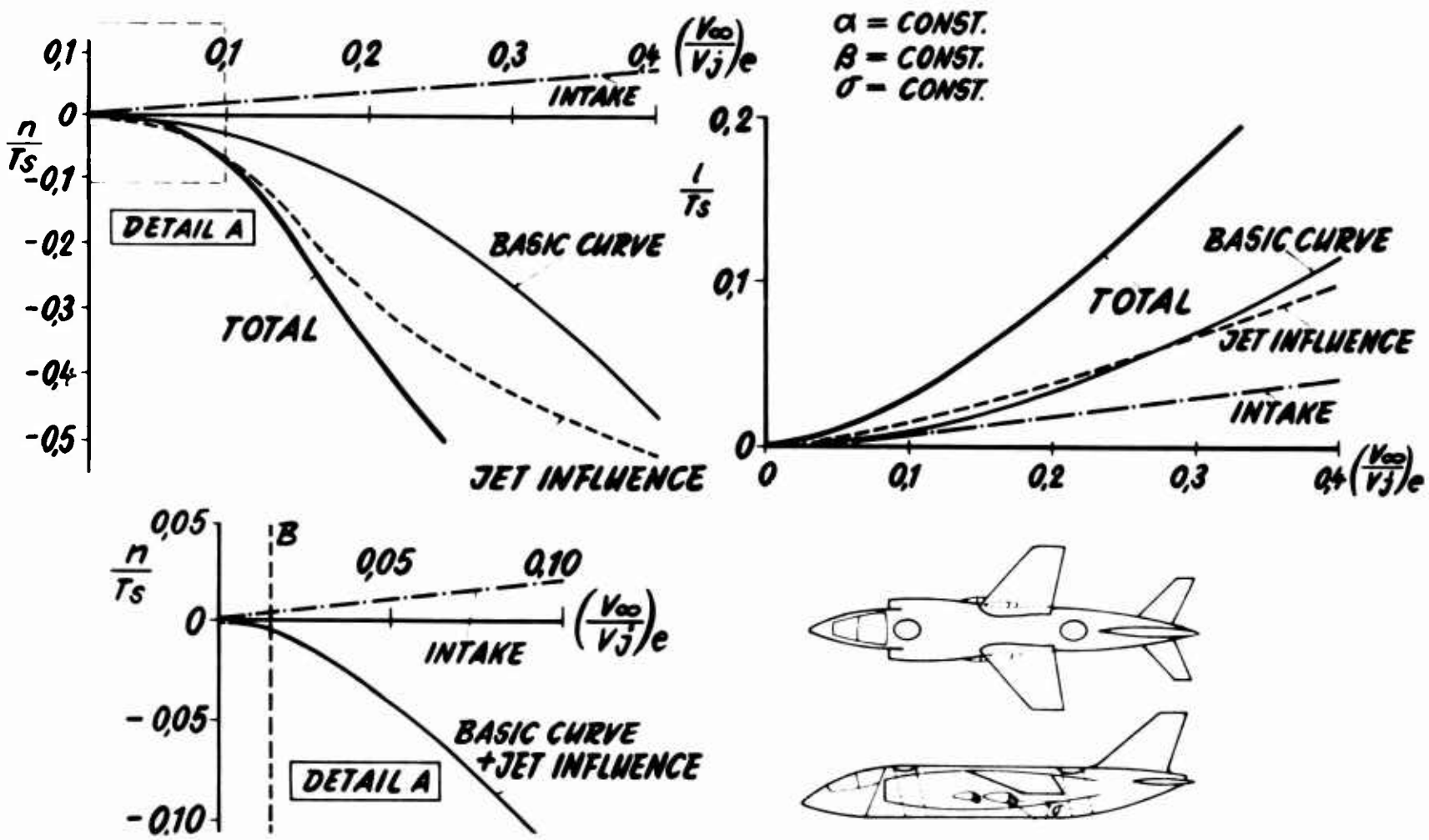

Fig.7 Intake- and jet influence on lateral motion

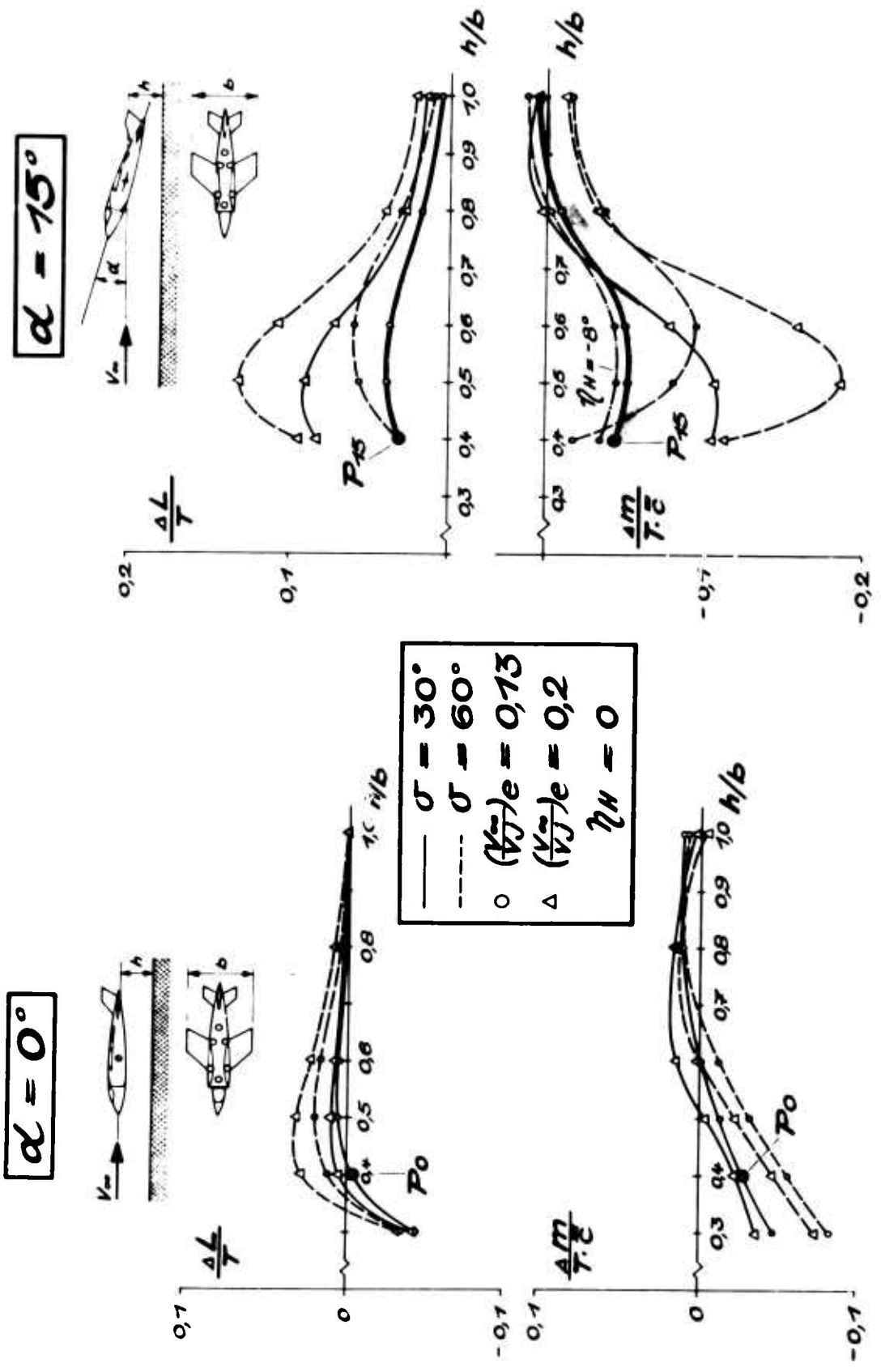

Fig.8 Ground influence on STOL

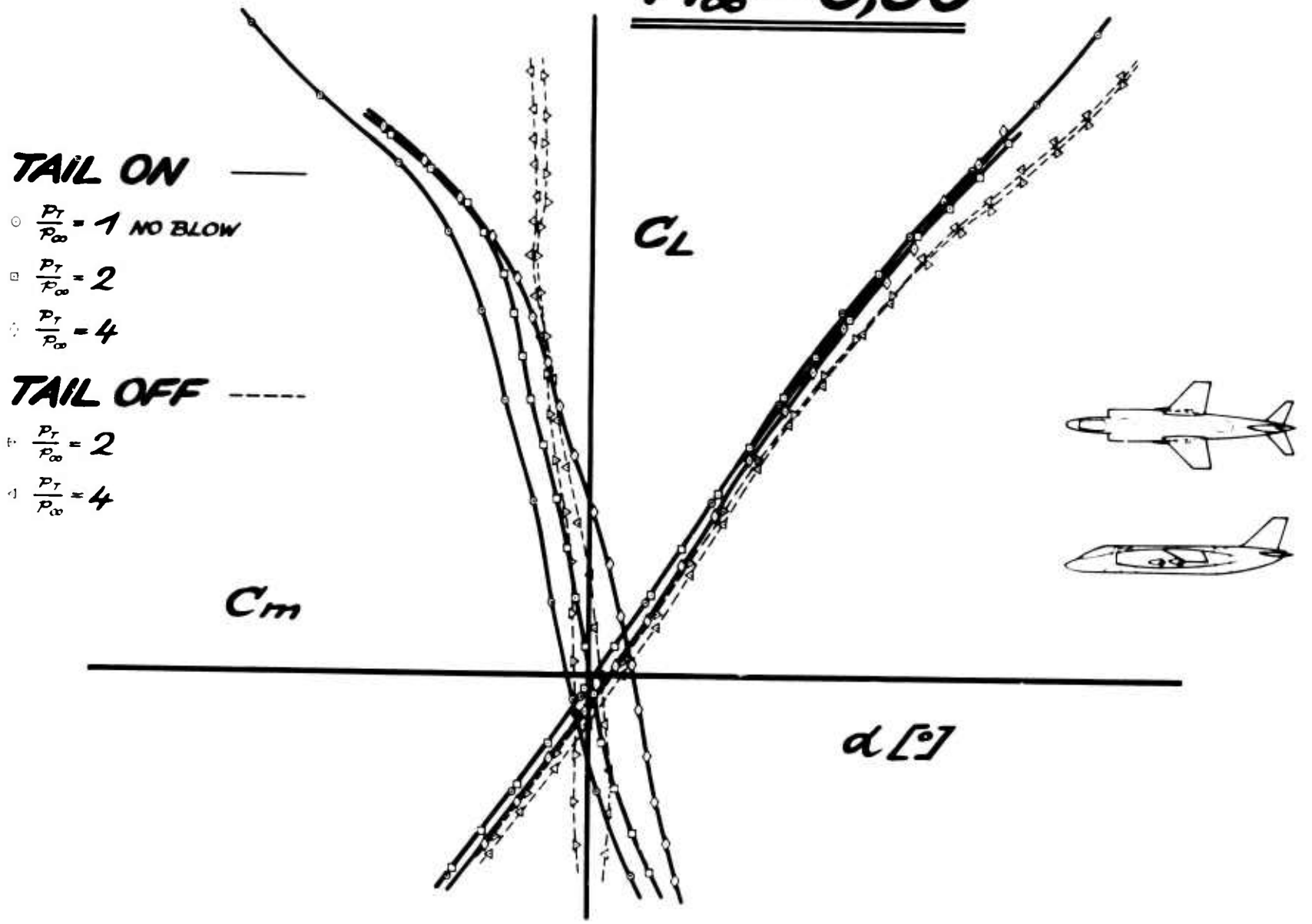

Fig.9 Influence of jet pressure ratio on lift- and moment-coefficients at transonic speed

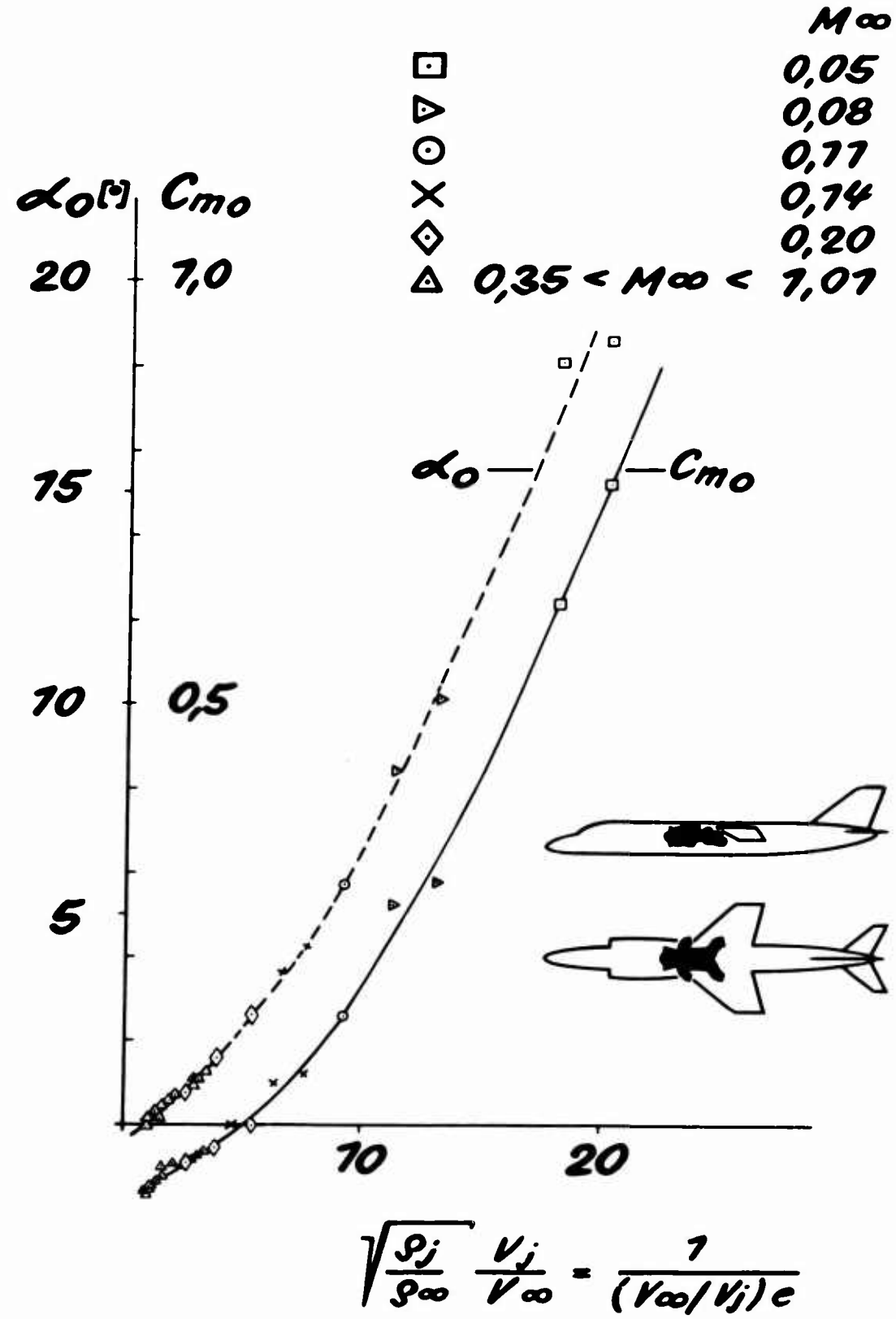

Fig. 10 Effect of speed ratio on zero lift angle and zero moment

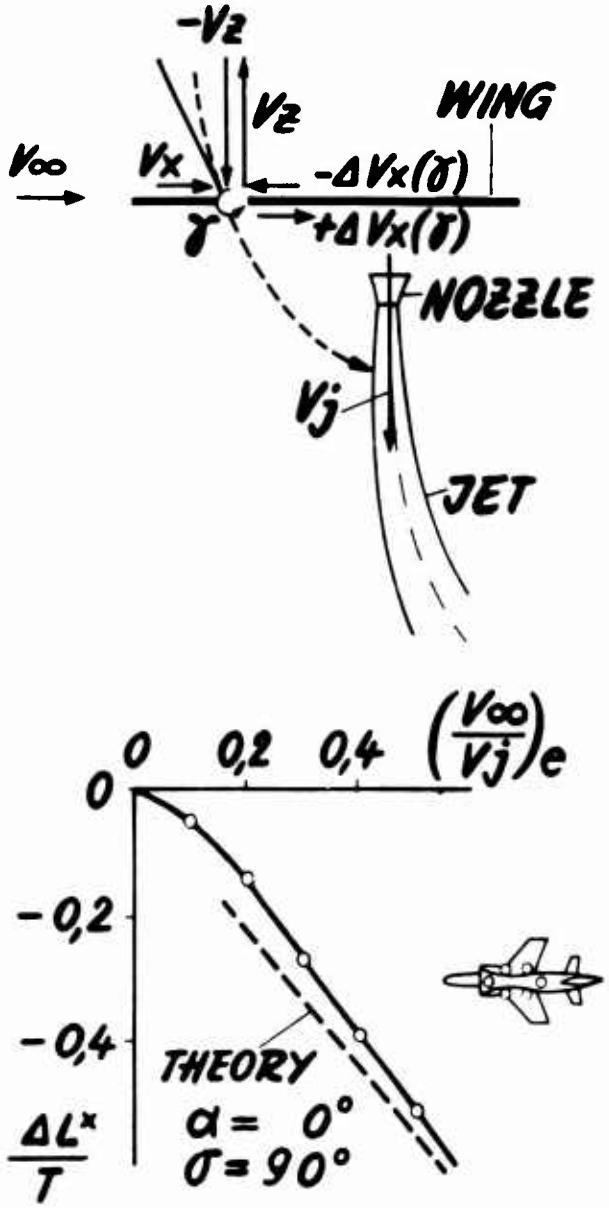

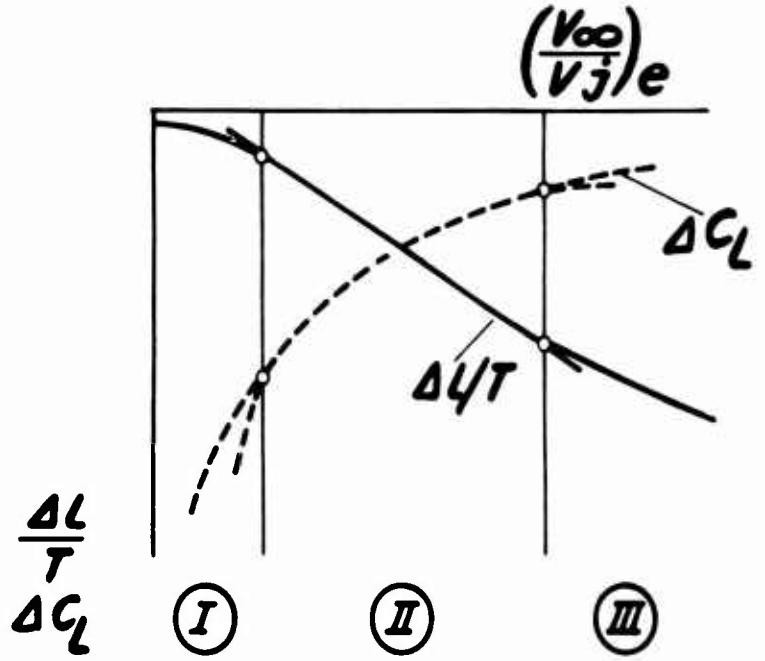

REGION	$(V_\infty/V_j)_e$	JET DEFLECTION
I	$\ll 1$	NO
II	< 1	SMALL
III	< 1	STRONG

Fig. 11 Jet influence on wings, theoretical concept

Some Studies into Improvements in Automatic Throttle Control

by N. H. Hughes M.A.

Blind Landing Experimental Unit

Royal Aircraft Establishment Bedford

Summary

The characteristics of automatic throttle control systems are described with particular reference to speed holding, height holding on the glidepath and throttle activity. The deficiencies of existing systems are examined and a modified form of control is presented which shows promise of avoiding most of these deficiencies.

Some Studies Into Improvements In Automatic Throttle Control

1 INTRODUCTION

Automatic throttle control systems (auto-throttles) are being installed in an increasing number of civil and military aircraft and are in passenger service with Trident and V.C.10. Although auto-throttle has been considered for other phases of flight, it is primarily used during approach and landing. In these critical phases, there is increasing pressure on pilots in fitting-in with ever tightening air traffic control procedures, and auto-throttle assists by relieving the pilot of the workload of speed control. In addition it contributes to safety by improving speed holding on the approach, thereby reducing the risk of stalling the aircraft and enabling better height holding to be achieved on the glidepath. During automatic landing, precise throttle control is particularly important in achieving accurate control of the touchdown point, and with supersonic transport (S.S.T.), and future aircraft which can be speed-unstable on the approach, auto-throttle is probably vital to make the aircraft flyable in turbulent conditions.

An auto-throttle can be made to work by applying throttle proportional to airspeed error. However, to take out initial condition errors at engagement and to compensate for long-term changes in flight path, it is universal practice to include an additional throttle demand from the integral of airspeed error, a term which has to be made weak, and therefore slow, to satisfy stability considerations. Finally, to compensate for shorter term changes in flight path, a throttle demand from pitch attitude is included. Such a system is shown in Fig. 1.

Such auto-throttle systems, which will be described in the remainder of the report as conventional auto-throttles, work well in still air conditions or in the presence of steady wind shear. However, in turbulent conditions, the direct airspeed input to the throttle causes it to follow the fluctuations due to gusts, producing excessive throttle activity. Much of the throttle movement which occurs is regarded by the pilots as unnecessary and is due to small short-term gusts which the pilot neglects when controlling manually. This throttle movement causes unnecessary wear and tear on the engines and produces a variation in amplitude and frequency of engine noise which appears to be much more worrying to passengers and people on the ground than a steady engine note. The throttle activity may also affect the performance of the pilot or autopilot in holding height on the glidepath, particularly in the case of propeller driven aircraft where slipstream can account for a large proportion of lift or in any case where the engines are mounted above or below the centre of gravity. Also, in multi-engined aircraft with widely separated engines, variation in engine response can produce significant yawing moments when the throttles are active, thereby disturbing azimuth performance.

With a conventional auto-throttle, therefore, there is a clash between the need to keep the airspeed gain high to provide good airspeed

holding in wind shear or large gusts and the desire to reduce the gain to minimise the throttle activity in continuous turbulence. The turbulence inputs to the system extend over a very wide frequency band and any attempt to introduce sufficient filtering on the airspeed signal to produce worthwhile smoothing, results in a serious degradation in closed-loop stability of the overall speed control system.

Just as smoothing on the airspeed signal introduces stability problems, the use of a jet engine at low power setting can cause instability because the engine response becomes very slow, and this virtually precludes use of conventional auto-throttle with existing engines for steep approach paths such as are being considered for noise abatement. Such basic problems of engine response can only be solved by modifications to engine design, including possibly the use of nozzle control to provide direct control of thrust regardless of basic power setting. However, there is scope for considerable improvement in the performance of auto-throttles, when used with engines at normal power settings, by modifying the control system. This paper describes how, starting from a re-definition of the performance requirements for an auto-throttle, it is possible to design a system which shows promise of avoiding most of the disadvantages of conventional systems.

2 AUTO-THROTTLE DESIGN CRITERIA

The problems with existing auto-throttle systems are not so much what they do in terms of airspeed holding but criticisms of the way they do it - particularly the throttle activity already referred to. In considering possible modifications to auto-throttle control, therefore, the aim was to try to reduce the throttle activity without prejudice to the performance of the system. In establishing the kind of throttle behaviour which would be acceptable, discussions were held with pilots and handling experts and the following desirable criteria were defined.

An auto-throttle, under conditions of average turbulence, should neglect small amplitude short period gusts but maintain average airspeed error near zero. Under conditions of large sustained gusts or extreme wind shear, however, the auto-throttle should react quickly to contain the airspeed error within safe bounds. Also, because of the greater threat to safety of speed loss, both because of the danger of stalling or approaching a zero rate of climb speed and because an engine is generally more sluggish to accelerate than to lose thrust, it is desirable that the auto-throttle should respond more rapidly to a speed loss than to a speed gain.

Although we have described the qualitative characteristics which we would like to be shown by an auto-throttle system, we have not yet defined a quantitative performance criterion on which the acceptability of a modified system may be judged. To do this it is necessary first to study the behaviour of the existing type of auto-throttle more closely. However, even before doing this we have to examine the characteristics of the plant we are controlling - namely the engine.

For the purposes of this paper, we will assume that we are controlling a jet engine. Often, for the purposes of stability analysis, this is regarded as a simple lag and has the response to a series of throttle movements shown in figure 2. In practice, however, for many engines this is an over-simplification, and we have chosen to represent the engine in a more complex manner so that its response is as shown in figure 3. When the throttle is opened, thrust is determined by the turbine speed (R.P.M.), and both rise together as though the engine were a simple lag. When the throttle is closed, thrust follows the throttle but R.P.M. decay with the same lag as applied to the acceleration. If the throttle is opened again before the R.P.M. have decayed to the steady state value, thrust follows the throttle to the value dictated by the present R.P.M., and then continues to rise from that point with the simple lag. The characteristics simulated have been deduced as a simplification of the characteristics of a common engine in present day service, and thrust has been scaled to suit an S.S.T. Although these characteristics may be regarded as rather extreme in comparison with the most modern designs, they are sufficient to illustrate the major effects that engine response characteristics can have on auto-throttle performance.

To return to the problems of specifying auto-throttle performance, we will first look at the behaviour of the conventional auto-throttle system when subjected to various disturbances. All the results we will present were obtained from an analogue simulation of an S.S.T. on the approach to land, flying on the glide path under autopilot control. Figure 4 shows the performance of the system in responding to step head and tail gusts with the linear and non-linear engines described above. In both cases the responses are well damped, but it can be seen that the non-linear engine's sluggish acceleration slows down the response to a tail gust slightly in comparison with a head gust. In terms of known specifications for auto-throttle performance, based on damping and settling time, either of these systems is satisfactory. However, use of random horizontal turbulence as a disturbance brings to light several interesting features of the system. Figure 5 shows the behaviour of the conventional auto-throttle with a linear engine simulation. The first striking thing is that the airspeed fluctuations do not seem to be reduced by the use of auto-throttle, the r.m.s. airspeed error being the same as the r.m.s. gust velocity. Although close inspection shows that the auto-throttle does alter the low frequency structure of the airspeed fluctuations, it does not affect the majority of the high frequency fluctuations. One therefore observes that under turbulent conditions, such as frequently occur on the approach to land, an auto-throttle is certainly not able to act as a short-term speed control. In fact, the indications are that if it were required for the auto-throttle to make a significant reduction in the airspeed fluctuations due to turbulence, the system gain and bandwidth would have to be increased a great deal. Of course, such a form of control would be extremely jerky and uncomfortable and would not be acceptable. As it is, it can be seen that the conventional auto-throttle produces a lot of engine activity in turbulent conditions,

even though this activity results in negligible reduction in airspeed error.

Having disposed of airspeed holding as a usable criterion for evaluating auto-throttle performance, one must look elsewhere. For assessing safety in the approach and landing, it is considered that the accuracy of height holding on the glidepath is the prime parameter, and for the remainder of the study it has been assumed that the acceptability of auto-throttle system, from a performance point of view, can be judged by observing the effect it has on height in turbulent conditions. Under the test conditions considered, the conventional auto-throttle with linear engine produced an r.m.s. height error of about 2.3ft (0.7m), whereas with the non-linear engine (Fig. 6) the r.m.s. height error increased to about 4.4 ft (1.4m). Close inspection of the records also shows that the non-linear engine, with its slow acceleration, allows larger height losses to occur than height gains. Although the differing engine characteristics cause significant and readily detectable differences in height holding on the glidepath, the speed holding appears unaffected, confirming the superiority of height holding as a criterion for comparing performance in these conditions. Because of its significant effect on performance, it is clear that accurate engine dynamic response data is required if a fully satisfactory auto-throttle design is to be achieved. However, practically the only data available from aero engine manufacturers is in the form of slam acceleration and deceleration time histories and steady state relationships between R.P.M. and thrust. This leaves many questions unanswered particularly about the dynamic response relationships between small throttle movements and thrust at various operating points over the usable power range. Although more insight into engine operation may be obtained by simulating the complete non-linear fuel control system, much more information on the dynamic response of the engine is needed if a fully satisfactory auto-throttle design is to be achieved.

In an attempt to avoid under-estimating the effects of engine response, the possibly pessimistic non-linear engine model described above was used for the remainder of the study.

3 DEVELOPMENT OF A MODIFIED AUTO-THROTTLE SYSTEM

Before considering additions to the conventional form of automatic throttle control, it is worth demonstrating what would happen with simpler control. The simplest form would be no control at all, which would certainly satisfy the requirement for minimum throttle activity under average conditions. However, as we have considered an S.S.T. aircraft, which is speed unstable, we obtain the obviously unacceptable result shown in figure 7 - the classical divergence.

A form of control which might enable long term control of the mean airspeed to be obtained, without introducing much throttle activity, would be to apply throttle as a function of the integral of airspeed

error only. This results in the instability shown in figure 8 and we conclude, therefore, that a direct speed term is necessary to provide satisfactory closed-loop operation. Unfortunately, if airspeed is used as the direct control term, this contains noise which extends right through the frequency band needed for ensuring closed-loop stability and as was stated in the introduction, little useful filtering of the airspeed signal can be achieved without upsetting stability.

A way of obtaining satisfactory closed-loop stability without introducing noise, is to replace the direct throttle control term by groundspeed, obtained by integrating the output of a fore-and-aft accelerometer, retaining integral of airspeed as a long-term monitor. Figure 9 shows the performance obtained from this system. It is stable, and throttle and R.P.M. activity is slight but height holding on the glidepath is seriously affected, the r.m.s. error increasing to 6.6 ft. (2.2m) in comparison with 4.3 ft. (1.4m) for the standard system. This results because the system tolerates large low frequency airspeed errors which would have been removed by the direct throttle control in the conventional system, and these low frequency airspeed errors significantly disturb the flight path.

Between the extreme cases so far considered, where the direct control is either all inertial or all airspeed, there is a wide range of possible complementary filtered systems in which the direct term is groundspeed at high frequencies and airspeed at low frequencies. A limited study of complementary filtered systems was made and it was found that very little of the airspeed term could be replaced by inertial information before height holding began to suffer, a smoothing time constant of as little as 1 second causing a noticeable degradation in performance. Figure 10 shows the performance of such a system and it can be seen that very little reduction in throttle activity is achieved.

The above linear auto-throttle systems were studied to establish to what extent the throttle activity could be reduced by inertial and complementary filtered schemes, without penalty on height holding on the glidepath, and it was concluded that little advantage could be obtained. Also, no account had been taken of the desire outlined in section 2 to provide preferential treatment for the effects of large gusts and speed losses. After some experimentation, the non-linear scheme, shown in simplified block diagram form in figure 11, was devised. It enables throttle activity to be reduced under average conditions, but provides height holding only slightly inferior to that obtained with the conventional auto-throttle in conditions of heavy turbulence. The system operates as follows:-

Under all conditions, long term monitoring of the airspeed is maintained by commanding throttle from integral of airspeed error. Provided airspeed error is less than some threshold value, the direct throttle control is from groundspeed, but when airspeed error exceeds the threshold, the direct term is replaced by complementary filtered airspeed. The comparator, which makes the change-over from groundspeed to complementary

filtered airspeed control, is made asymmetrical, operating for speed losses greater than 5 ft/sec (1.65 m/s) and for speed gains greater than 10 ft/sec (3.3 m/s). This ratio of limits was found to eliminate the large height losses previously referred to when the non-linear engine model was used. Although we state above that complementary filtering of the airspeed signal was only slightly effective in reducing throttle activity it was considered worth incorporating to reduce the tendency for the system to respond unnecessarily to large "spiky" gusts of short duration.

The performance of the system in moderate turbulence (3.5 ft/sec {1.2 m/s} r.m.s.) is shown in figure 12. In these conditions, the comparator thresholds are only occasionally exceeded and the system behaves very similarly to the pure ground speed control system considered previously, having a very low level of throttle and R.P.M. activity. Figure 13 shows the behaviour of the system in high turbulence conditions (6.5 ft/sec {2.1 m/s} r.m.s.). The characteristic behaviour of the system of ignoring small gusts and responding only to the large ones is clearly seen. This characteristic enables the system to show reduced throttle activity in comparison with the conventional system even under these turbulent conditions, and R.P.M. variation is reduced by 2:1 which should show a worth-while reduction in noise perceived by passengers. In spite of these advantages, the r.m.s. height holding on the glidepath does not suffer, a figure of 4.4 ft (1.5m) r.m.s. being obtained in comparison with the 4.3 ft (1.4m) yielded by the conventional system.

No mention has been made so far of the authority limitation of auto-throttle systems or their behaviour in the presence of extreme gusts. Both conventional and the modified auto-throttles will have similar response to gusts which are large in comparison with the comparator threshold in the modified system. At present, auto-throttles operate with a speed gain of about $\frac{1}{150}$ 'g' per ft. $\left\{\frac{1}{50}\text{ 'g' per m/s}\right\}$ and are limited in authority to between $\pm$ 0.1 and $\pm$ 0.2 'g'. Hence gusts of greater than 15 to 30 ft/sec (5 to 10 m/s) will cause the auto-throttle to saturate. It is believed that in certain rare weather conditions, gusts which appear effectively as steps of 60 ft/sec could occur, and even if there were no authority limitation, simulation tests suggest that these would cause height losses of 50 to 100 ft on the approach, depending on the engine response characteristics and airspeed filtering used. Much worse results will occur when the authority is limited.

In the studies described here, no attempt has been made to take advantage of reduced throttle activity in average conditions in possibly allowing increased auto-throttle gain and authority to be used to counteract the effects of such extreme gusts, and there is clearly scope for further investigation in this area. However, design of a system to cope effectively with such extreme conditions cannot be regarded solely as an auto-throttle design problem and must be a complete system design

including auto-throttle, autopilot and, if necessary, the aircraft itself and its lift control system. Such a study was outside the scope of this report. However, the reduction in throttle activity and satisfactory performance predicted in conditions of average and heavy random turbulence is regarded as sufficiently encouraging to justify flight test of the modified auto-throttle system and this is planned for the near future.

Whereas use of auto-throttle has so far been restricted to the limited periods of approach and landing where it is required for safety reasons, throttle and engine activity have so far precluded its use for extended periods in cruise, climb and descent. However, provided that the predicted improvements are realized in flight the modified system should allow much wider use of auto-throttle without causing annoyance to pilots and passengers and without penalty to engine life or reliability.

4 CONCLUSIONS

The deficiencies of existing auto-throttle systems have been examined with particular regard to throttle activity in turbulence. It has also been shown that airspeed holding is a poor criterion for judging the performance of auto-throttles in general. It is proposed that the effect of the auto-throttle on height holding should be used as a performance criterion and it has been shown that it is possible to develop a modified auto-throttle system which shows considerably reduced throttle activity in turbulence without predjudice to autopilot height holding on the glidepath. Although a detailed application of the techniques proposed would clearly have to be worked out to suit a particular airframe-engine combination, it is believed that the principles should be generally applicable.

The study has shown that the engine dynamic response characteristics can have a large effect on the performance of the overall autopilot and auto-throttle system and it is clear that more detailed information is required from aero engine manufacturers if an auto-throttle design is to be achieved which provides satisfactory aircraft performance, behaviour acceptable to pilots and passengers and which interferes least with efficient operation of the engines.

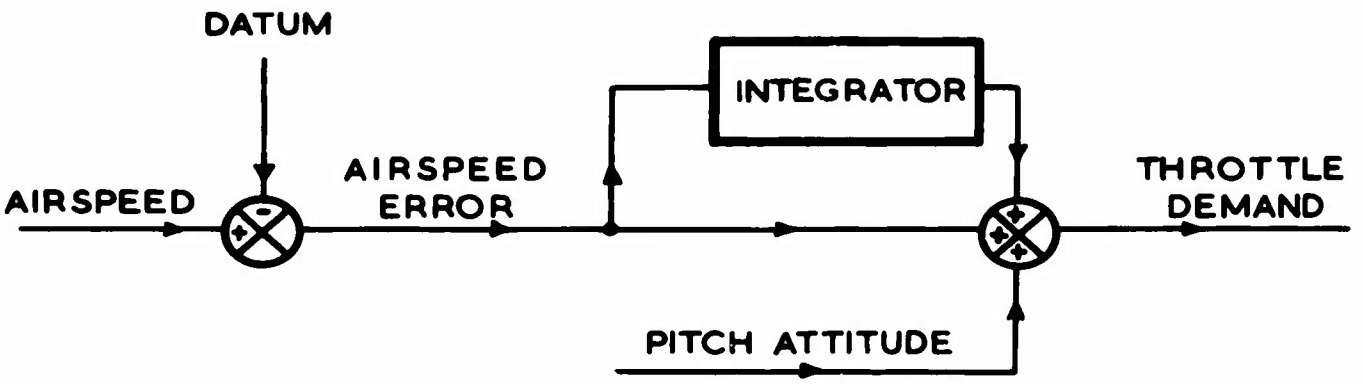

FIG. 1. CONVENTIONAL AUTO-THROTTLE

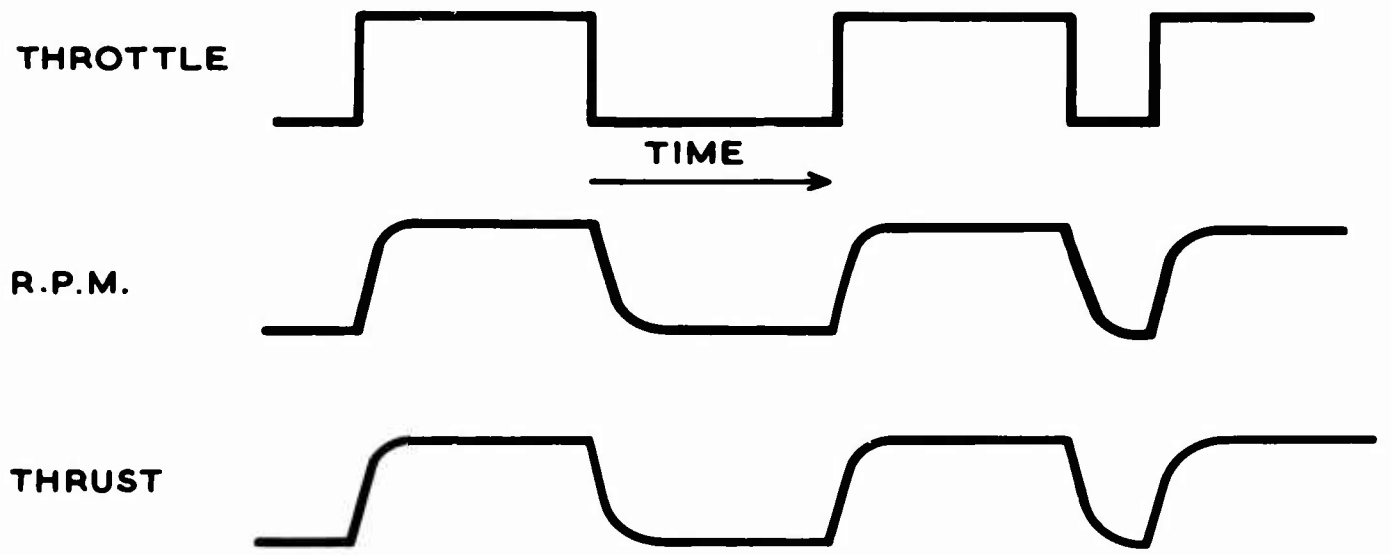

FIG. 2. JET ENGINE RESPONSE
LINEAR MODEL

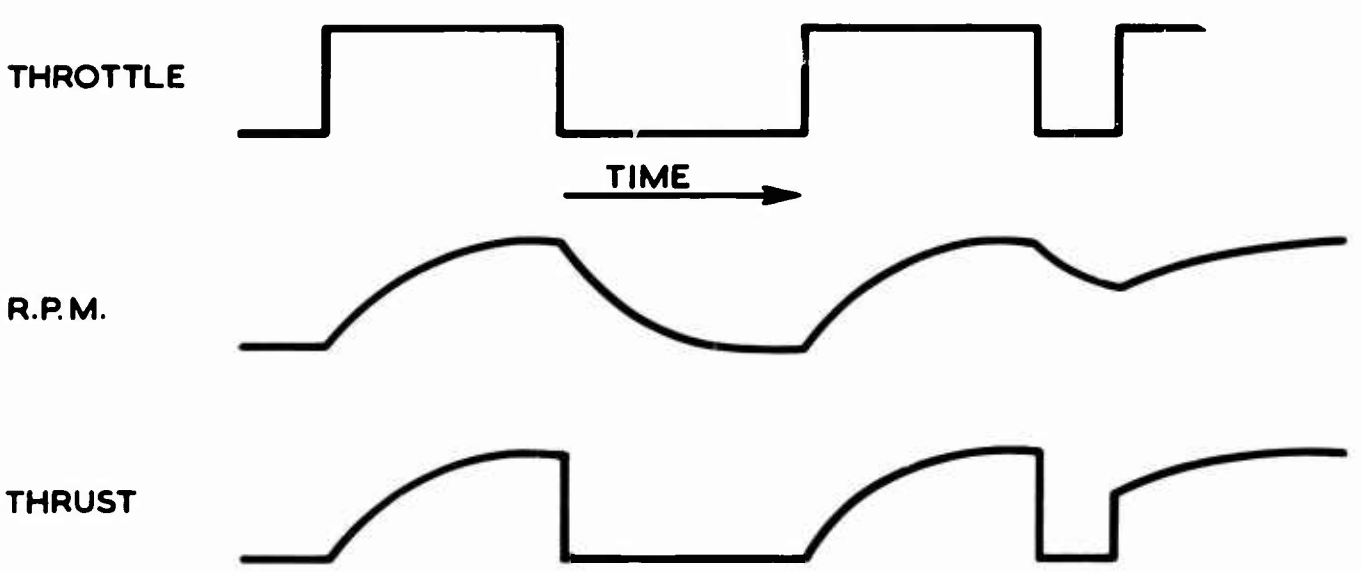

FIG. 3. JET ENGINE RESPONSE
NON - LINEAR MODEL

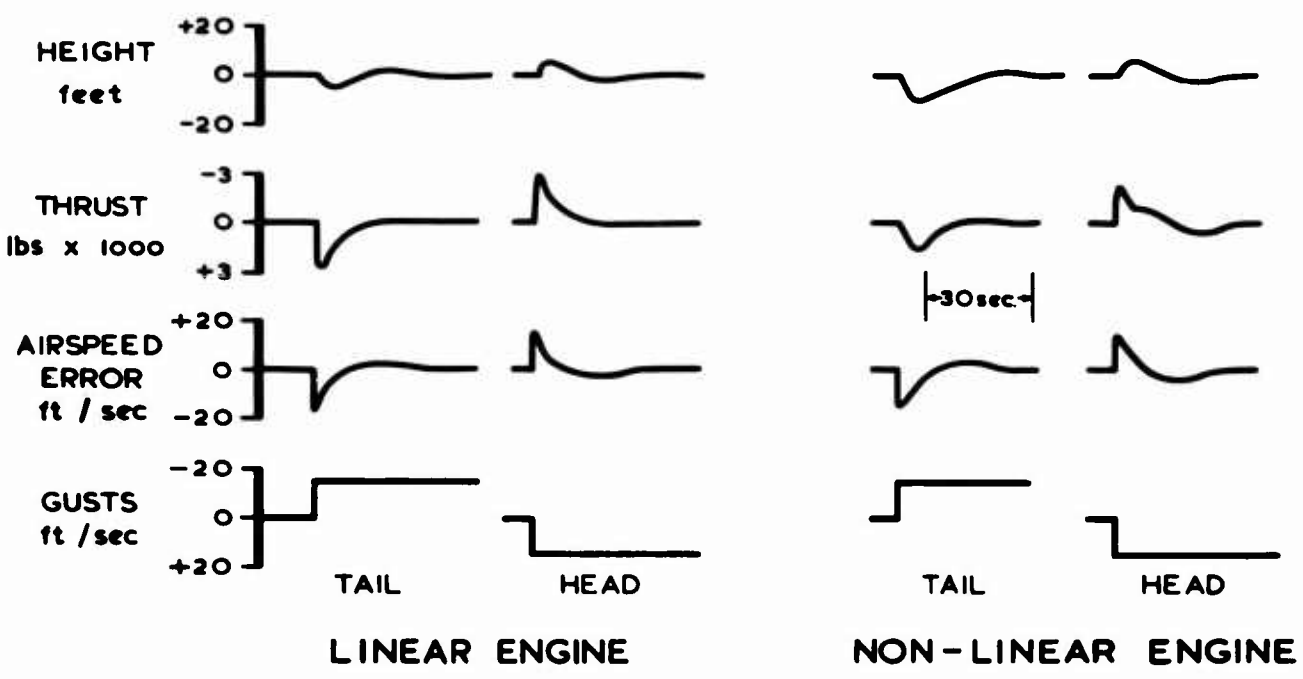

FIG. 4. RESPONSE OF CONVENTIONAL AUTO - THROTTLE
TO STEP HORIZONTAL GUSTS

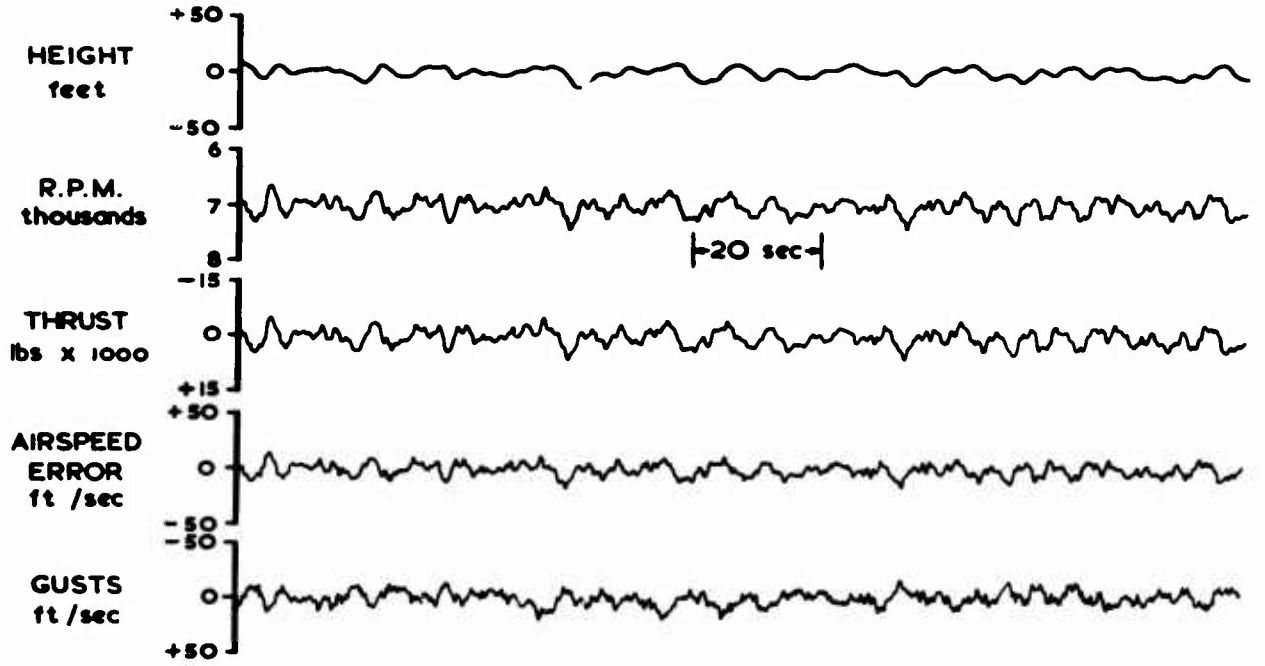

FIG.5. PERFORMANCE OF CONVENTIONAL AUTO-THROTTLE IN TURBULENCE LINEAR ENGINE

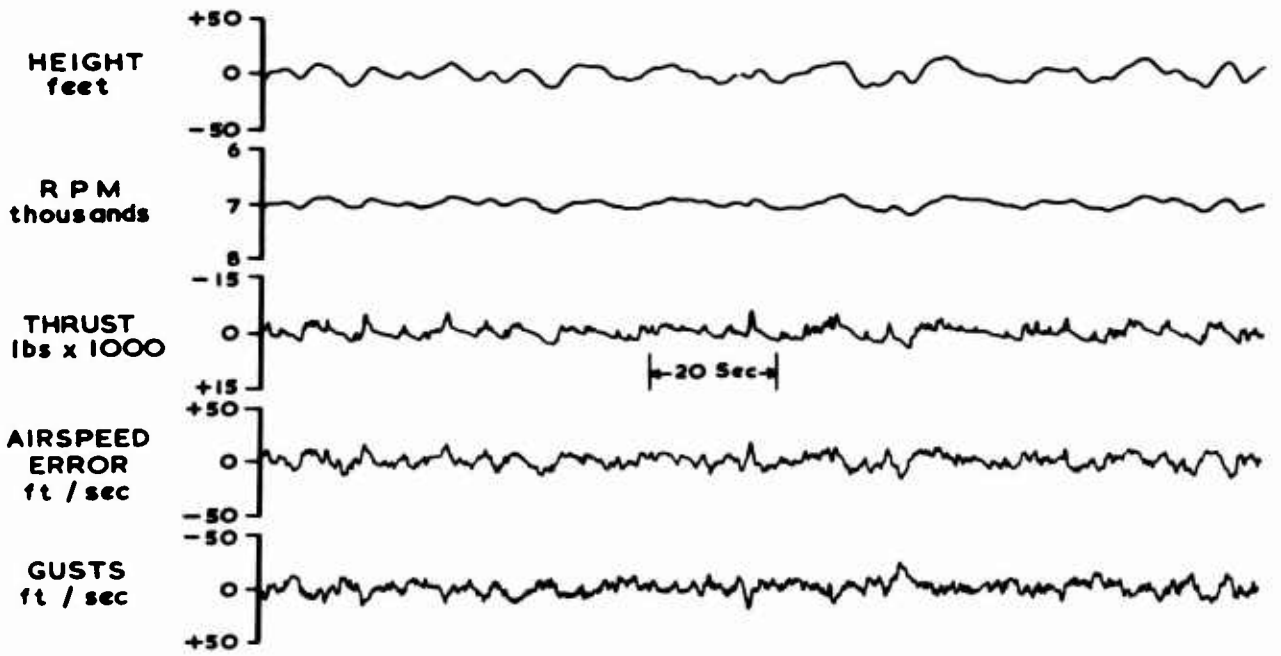

FIG.6. PERFORMANCE OF CONVENTIONAL AUTO-THROTTLE IN TURBULENCE NON-LINEAR ENGINE

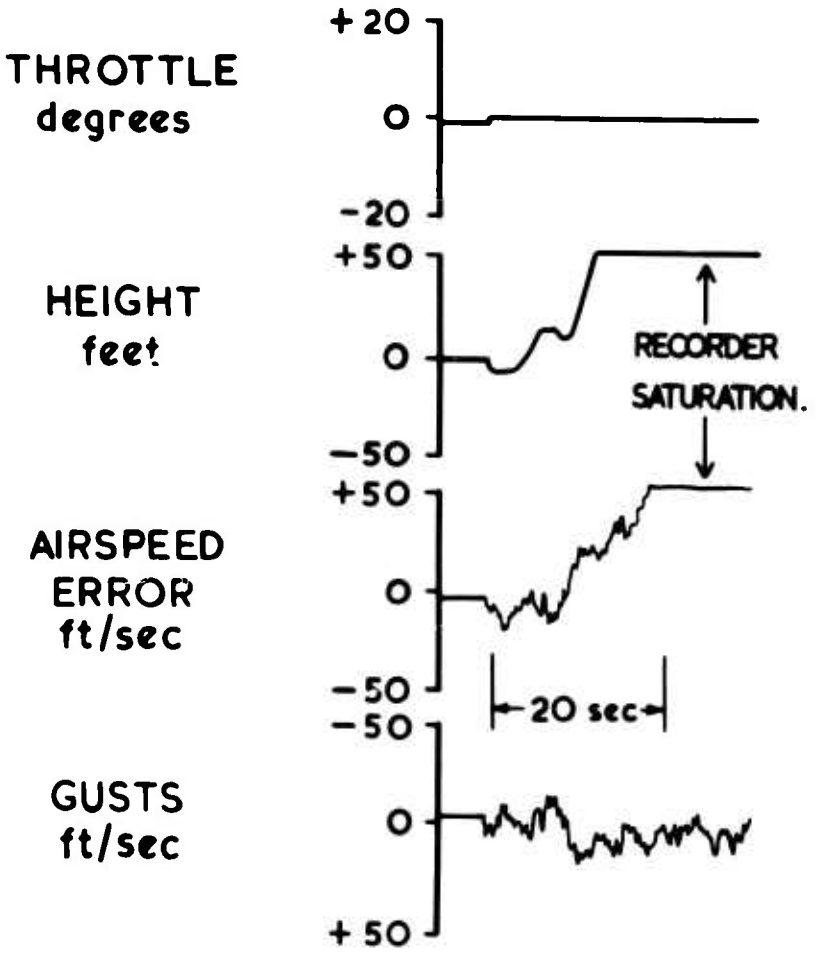

FIG.7. FIXED THROTTLE

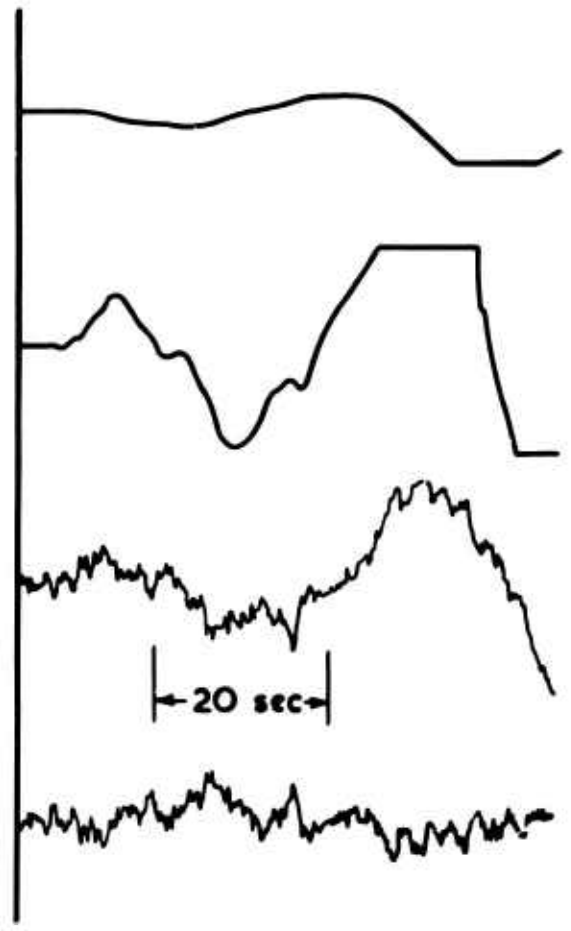

FIG.8. INTEGRAL CONTROL

PERFORMANCE WITH SIMPLIFIED AUTO-THROTTLE

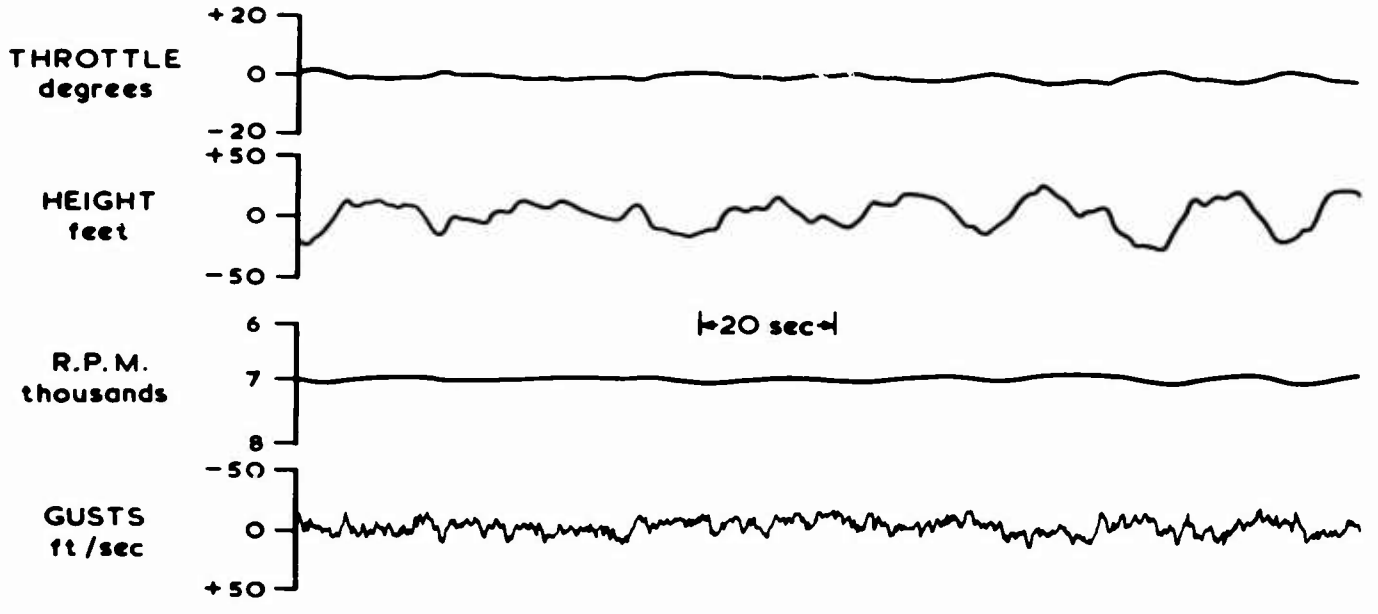

FIG. 9. AUTO-THROTTLE PERFORMANCE
INERTIAL CONTROL

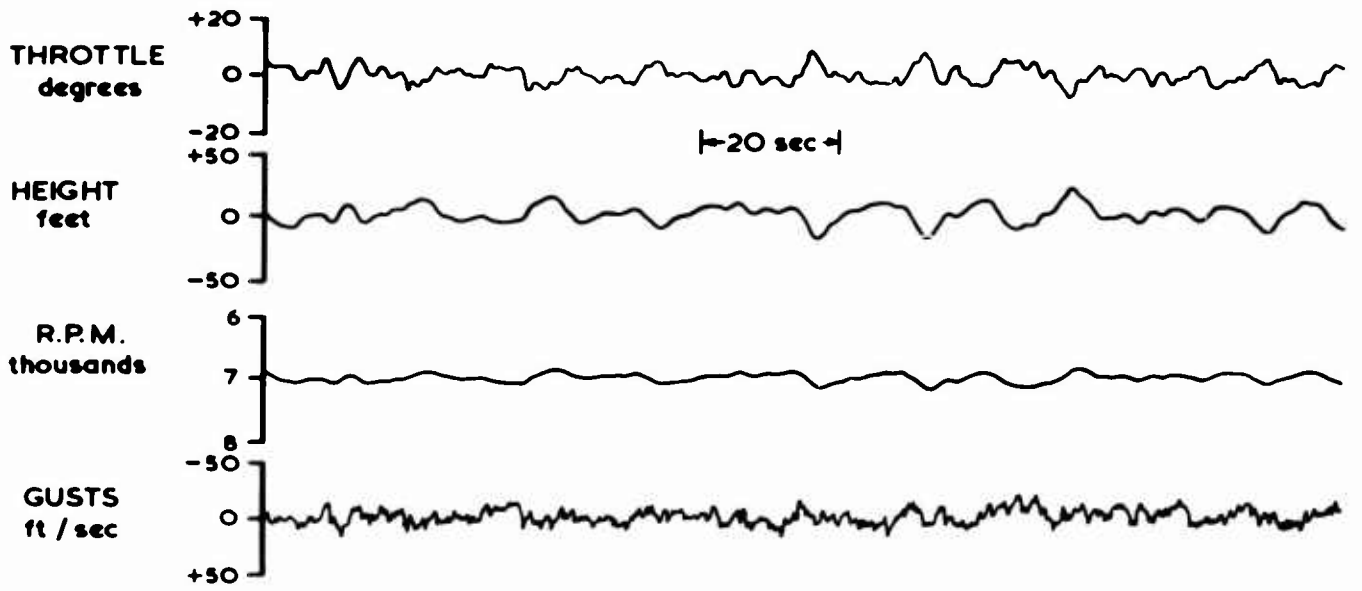

FIG. 10. AUTO - THROTTLE PERFORMANCE
COMPLEMENTARY FILTERED AIRSPEED AND GROUNDSPEED SYSTEM

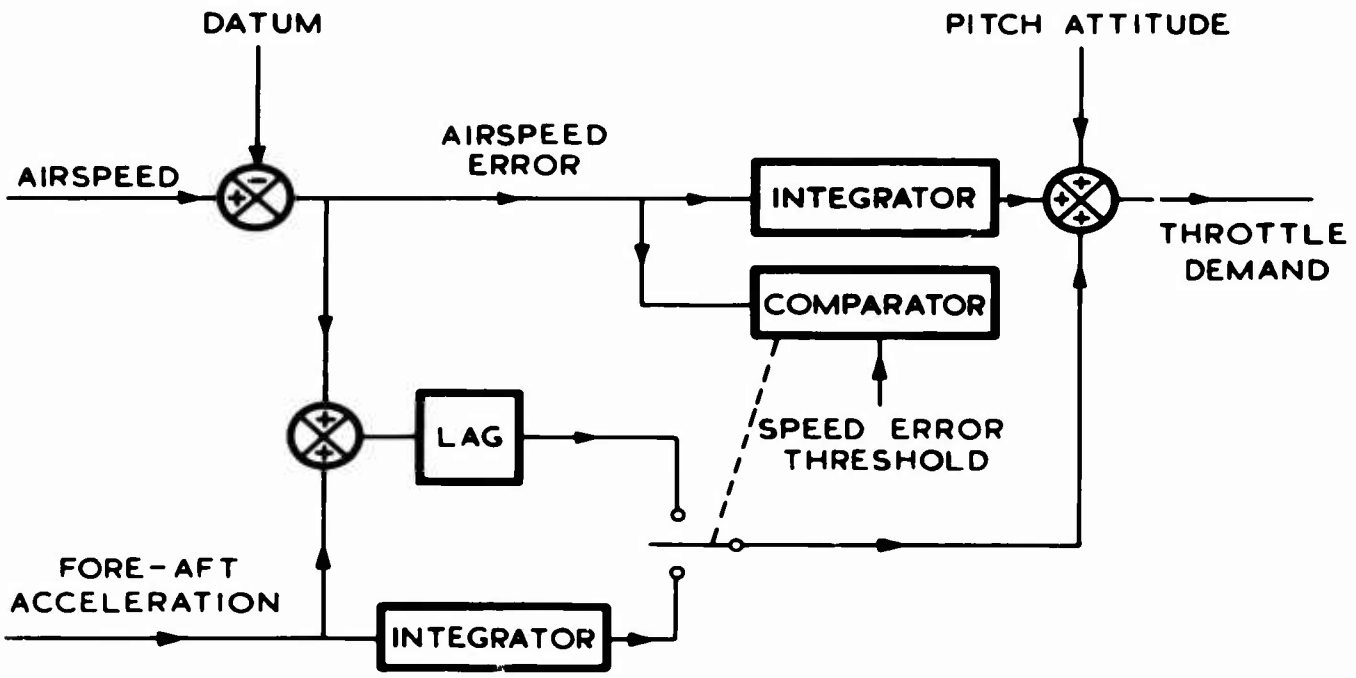

FIG.11. MODIFIED AUTO-THROTTLE

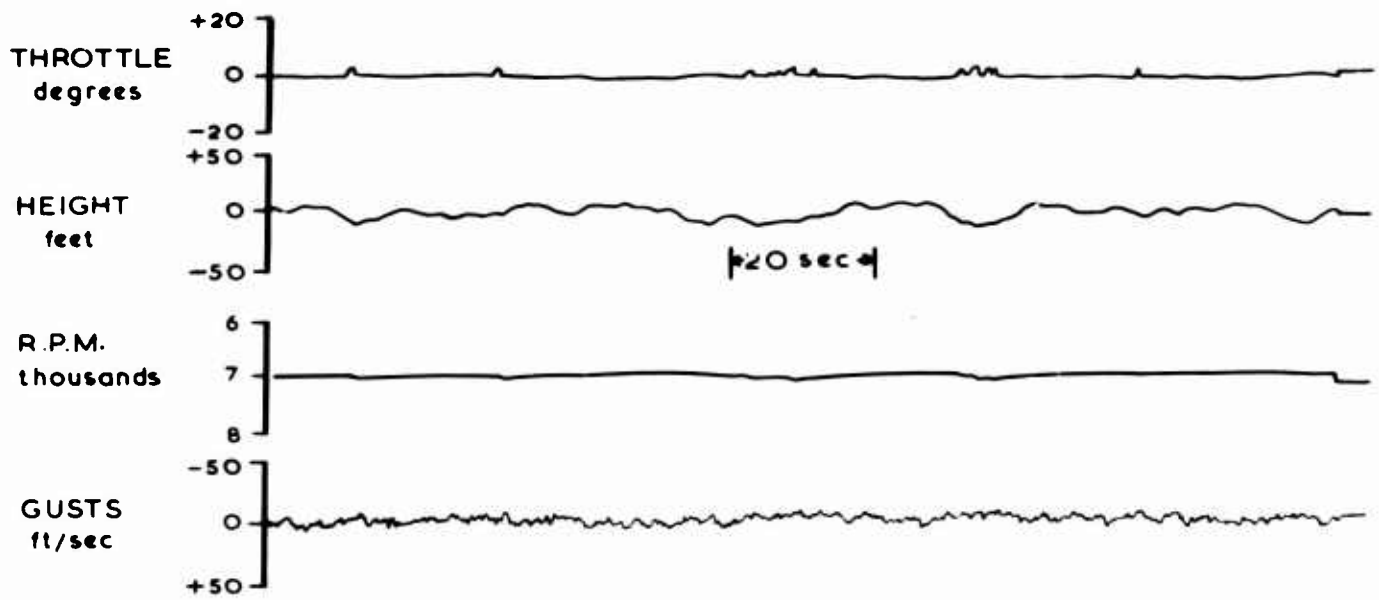

FIG.12. AUTO-THROTTLE PERFORMANCE
MODIFIED SYSTEM 3·25 ft/sec R.M.S. TURBULENCE

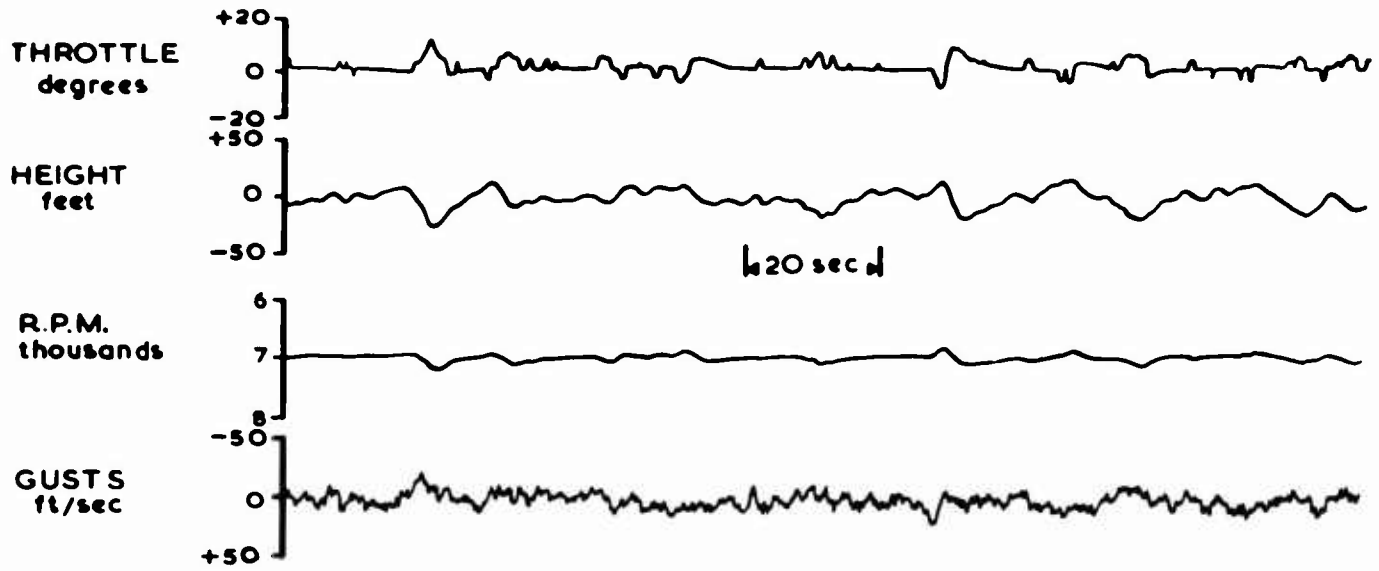

FIG. 13. AUTO-THROTTLE PERFORMANCE
MODIFIED SYSTEM 6·5 ft/sec R.M.S. TURBULENCE

ENGINE AIRFRAME INTEGRATION PROBLEMS PECULIAR TO AIRCRAFT CONFIGURATIONS WITH NACELLES MOUNTED ABOVE THE WING

by

G. Löbert and J. Thomas

Vereinigte Flugtechnische Werke, München

ENGINE AIRFRAME INTEGRATION PROBLEMS PECULIAR TO AIRCRAFT CONFIGURATIONS WITH NACELLES MOUNTED ABOVE THE WING

G. Löbert and J. Thomas

1. INTRODUCTION

From the beginning of the introduction of jet propulsion for transport aircraft it was found practical to accommodate the engines in isolated nacelles mounted close to the wing or fuselage. Since structural considerations dictated relatively short pylon lengths a problem of aerodynamic interference arose.

From the aerodynamic point of view, the practical engine locations may be divided into three groups. These are the location of the engines at the rear fuselage, below and above the wing. Though the aerodynamic interference problem is only one of the various criteria to be considered when selecting the engine location, this probably was the reason why the engine location above the wing has not been given consideration up to now. Small short-range transport aircraft have to be provided with an extremely high thrust/weight-ratio due to the necessarily short take-off distances and the small number of engines. In the case of low-wing configurations it is, however, no longer possible to mount the relatively large bypass engines below the wing without major structural and aerodynamic drawbacks. A structural disadvantage will result from the large landing gear length while the cut-out in the trailing-edge flaps in the region of the engine jets results in a reduction of the maximum lift coefficient. The location of the engines at the rear fuselage of an aircraft of this size will cause considerable problems of balance and trim due to the unfavorable arrangement of cabin, wing, engines, and tail. The aerodynamics of this configuration differs only slightly from that of an engine arrangement above the wing, because for a reasonable arrangement of the various center of gravity locations the engine air intake generally overlaps the trailing edge of the wing considerably.

There is, therefore, a certain class of low-wing aircraft for which an engine location above the wing is unavoidable. In the present paper we would like to point out and analyze the aerodynamic advantages and disadvantages of this aircraft configuration. We will draw upon the information obtained in this company in a pre-design investigation of the aerodynamics of this engine location. Much of the wind-tunnel testing carried out in this preliminary investigation was done with the model configuration shown in Figure 1.

2. GENERAL AERODYNAMICS OF THE WING-NACELLE-INTERFERENCE

Before giving a detailed analysis of the various aerodynamic consequences of this engine-aircraft-configuration, we should discuss the cause of the nacelle-wing-interference.

Figure 2 shows the distribution of the local Mach number above a NACA 64A016 airfoil section for a free-stream Mach number of 0.65 at two different lift coefficients. Considerable supervelocities occur in a large region above the wing. These are additively superimposed on the supervelocities of the undisturbed air intake and pylon to a first approximation.

The diagram indicates one aerodynamic property of this engine arrangement. Another is seen from the next figure (Fig.3) where the flow around the engine nacelle under the influence of the wing is shown schematically. It can be seen that the nacelle induces vertical as well as horizontal perturbation velocities on the wing. In order to fulfill the boundary condition on the wing surface, a circulation distribution is generated whose induction exactly compensates the vertical component of the perturbation velocities caused by the engine nacelle. The nacelle thus generates, as a result of its flow displacement, a lift, a pitching moment, and a drag force on the neighboring wing. This flow displacement which is caused by the finite thickness of the intake lip and the flow around the intake leading edge resulting from engine throttling, is intensified by the fact that the engine intake lies in a region of increased velocity. Aerodynamically, the intake operates in a more throttled condition than that indicated by the intake velocity ratio V_1/V_∞ .

The circulation distribution on the wing chord locally generates horizontal velocity increments which combine with those of the flow field of the engine nacelle. These two components combine with each other on the wing upper surface, whereas on the lower surface they cancel each other almost completely.

The measured pressure distribution on the wing in the vertical plane of symmetry of the nacelle is plotted in Figures 4 and 5 for the two cases with and without nacelle for different longitudinal and vertical locations of the intake.

In these tests both the engine inlet flow and exhaust jet were simulated whereas the engine pylon was not included. It can be seen that on the upper side of the wing positive pressures are induced in front of the intake and negative pressures below the nacelle, whereas the wing lower side was affected only slightly. Qualitatively, this incremental pressure distribution corresponds to that of the flow between the nacelle and the plane defined by the wing chord. Obviously, only aft engine locations can be considered, because only in this region has the wing a sufficient margin between the local pressure and the minimum pressure on the wing to accommodate the suction peak of the interference pressure distribution.

Figure 5 shows that the magnitude of the aerodynamic interference considerably depends on the vertical location of the nacelle as was to be expected. Since this geometric quantity has an equally large influence on the structural weight the aerodynamicist can use this means of reducing the interference problem only to a limited degree.

Figure 6 shows the measured effect of the intake velocity ratio on the wing pressure distribution. As was to be expected, the suction peak directly below the engine nacelle increases with increasing engine throttling.

Figure 7 is a plot of the interference pressure distribution in the spanwise direction. As a result of the principle of reflection the lateral decay of the engine

disturbance has a similar behaviour to that of the x-components of the flow around the isolated nacelle. At a distance of half a nacelle diameter from the engine plane of symmetry the suction peak has already decreased to 65% of its maximum value, whereas the magnitude of the retarded flow in front of the nacelle has decreased by only 8%.

3. LOW SPEED CHARACTERISTICS

Regarding the low speed characteristics of this configuration the problem of the effect of the engine nacelle on maximum lift, longitudinal stability, and drag will be of particular interest. In the course of the pre-design investigations low speed wind tunnel tests were conducted using a 1/5th scale model of the configuration shown in Figure 1. The effect of the nacelle on lift increases with increasing flap deflection. Whereas with $\delta_F = 0$ practically no change or lift can be detected the addition of the nacelles results in a small decrease of C_L when the flaps are extended. In the linear region of the $C_L(\alpha)$-curve this results from a change in circulation while in the region of maximum lift an additional lift loss is caused by flow separation at the aft end of the wing-pylon-junction. Here, the nacelle creates a particularly adverse pressure gradient, as is shown in Figure 4, to which is added the positive pressure gradient of the engine pylon. Better flow conditions can be achieved by means of a more favourable distribution of pylon thickness and by extending the pylon past the wing trailing edge. The largest loss of $C_{L_{max}}$ is approximately $\Delta C_L \approx 0.1$. This may be considered to be a very good result. A comparable nacelle located below the wing, which would in the present configuration have to be mounted directly below the wing or on a very short pylon, would cause a disturbance of the flow around the wing leading edge and necessitate a cut-out in the trailing edge flaps and would thus result in markedly higher loss of $C_{L_{max}}$. Considering the $C_L(C_m)$-curves for the tail off configuration negative shift of the pitching moment curve for the clean configuration is to be noted. The pressure distribution below the nacelle shows that the local lift changes mutually compensate but generate an additional moment, i.e. a zero moment change which becomes visible here. An inspection of the pressure distributions on the upper surface of the wing (Fig. 4) shows that for this location of the nacelle the induced pressures result in a negative pitching moment with hardly any effect on wing lift. With extended flaps the effect of the engine nacelle at a constant angle of attack is much the same as before. However, since there is in this case, as mentioned previously, a simultaneous loss of lift practically no change in C_{m_0} can be detected. The slight destabilisation near $C_{L_{max}}$ is caused by the small region of separated flow near the wing-pylon-junction. The effect of the engine nacelles on the drag polars is to displace these by nearly a constant amount, i.e. for this engine location there is practically no influence of the nacelles on the induced drag.

If the calculated value for the form drag of both nacelles and pylons is subtracted from the drag of the complete configuration there remains an interference drag ranging between 6 and 10% of the zero-lift drag of the wing-body configuration. The interference drag of 7% for the flaps retracted case is in good agreement with that obtained in transonic tests. The flow conditions in the engine intake during cruising flight are of great importance for the durability of the engines. Intake measurements have shown that throughout the complete flight envelope no total pressure losses occur at the compressor face during normal operation. This favorable characteristic may be attributed to the fact that the flow asymmetry at the intake due to a change in angle of attack is smaller by an order of magnitude than for example, in the case of a conventional engine arrangement in front of the wing. This can be seen from Figure 9.

where the change of the flow direction in a body-fixed system of axes as a result of an angle of attack change is shown.

Stalling

What is the connection between the desired behaviour of the wing and the engine intake conditions during stall? In addition to the usual requirement of a stable pitching moment behaviour and sufficient aileron effectiveness, there is for this engine location the requirement that the intake flow distortions shall not exceed a limit defined by the engine manufacturer. The flow disturbances present when the engines are located above or behind the wing are a consequence of the geometric arrangement of wing and engine: in the stalled condition, the intake moves into the wake of the wing. Since large total pressure losses and flow nonuniformities occur in the wing wake, it is possible that the engine may surge, flame-out, overheat or be severely damaged. The large number of aircraft with intakes above and behind the wing proves that this problem can be solved. The pressure losses occurring in the intake at an angle of attack of 6-7° beyond $C_{L_{max}}$ (Fig.10) are in the same order of magnitude as those of existing aircraft, e.g. the DC 9. It is of utmost importance at which angle of attack the maximum admissible distortion limit will be exceeded. If this angle exceeds the angle of maximum lift sufficiently so that it will not be reached in a dynamic stall then there is no problem of inlet flow distortion. A natural phenomenon helps in this respect: due to the reduction of supervelocity near the wing leading edge (see Figure 4) a limited region of the wing below the nacelle separates at a considerably larger angle of attack than the remaining wing. When the flow separation progresses from the trailing to the leading edge the first disturbance reaches the air intake about 6° beyond the stall angle of attack as is confirmed by Figure 10 which shows the relationship between $C_L(\alpha)$ and $p_{total}(\alpha)$ for the flaps-up configuration. With a further increase of angle of attack the flow disturbance progresses uniformly from the bottom to the top of the air intake. It must be ensured that at all flap deflections no leading edge separation occurs otherwise the margin of about 6° can be reduced considerably. This is of course no great task in the case of transport aircraft with moderately thick wing sections.

4. EFFECTS ON HIGH SPEED FLIGHT CHARACTERISTICS

Critical Mach Number

The aerodynamic problems to be solved when selecting the engine location and when designing the nacelles and pylons have already become evident during the general considerations described in the first section. It is obvious that the critical Mach number of the clean wing can only be achieved if the maximum negative pressure of the integrated configuration does not exceed the maximum suction of the clean wing. This means that engine nacelle and pylon cannot be located in the area of maximum supervelocities of the wing section; consequently the engine nacelles can only be mounted on the rear part of the profile.

Although, strictly speaking, local pressures can only be calculated when the three-dimensional problems of lift and thickness of wing, nacelle, pylon, and fuselage are solved simultaneously, the results of the step by step treatment are already very satisfactory. Thus the engine inlet lip has to be designed for the locally raised

Mach number which corresponds to the cruise condition. Then the pylon design must guarantee that the supervelocities occurring under free-stream conditions do not exceed the still available span to the maximum allowable speed. This requires that the distance between the position of maximum nacelle diameter and the maximum pylon thickness becomes as large as possible. When designing the pylon shape the upper section caused the bigger problems, because of the smaller allowable supervelocities and the various structural and aerodynamic requirements specified by the engine manufacturer. These requirements may prove to be very restrictive in case of a bypass engine with a short duct operating at the critical pressure ratio. The shapes of the intake lip and of the engine pylon, developed on the basis of these considerations, are shown in Figure 11. The corresponding pressure distributions measured for the cruise condition are presented in Figure 11(a). As one may see, the suction on the upper wing surface is everywhere below the maximum value of the clean wing. The suction peak occurring at the pylon exceeds this value by $\Delta C_p = 0.14$ which corresponds to a reduction in the critical Mach number of 0.03. This high negative pressure can be reduced to the wing level by modifying the pylon section. Taking into consideration the static thrust behaviour, the intake had not been designed for Mach 0.80, as would be necessary, but for Mach 0.75. This results in a suction peak built up at the lower side of the intake lip. This suction peak, however, is unobjectionable because of its very small extension in the streamwise direction. Figure 14(a) shows the corresponding aerodynamic drag characteristics of the aircraft. One can see that the addition of the unthrottled bypass nacelle and of the engine pylon leads to a 0.035 reduction in the drag rise Mach number.

The foregoing considerations indicate that an engine nacelle installed above the wing strongly affects the three-dimensional pressure field on the upper wing side. This type of engine location is, however, unsuitable for wings with higher sweep angles, since it is well known that the favourable aerodynamic characteristics of these wings are due to the undiminished sweep of the isobars. While the reduced sweep of the isobars at the wing root can easily be corrected by relatively simple geometrical modifications of the inboard wing, this is no longer possible with a swept wing having an engine nacelle mounted above its upper side.

Tuck-Under

As pointed out in Section 1, an engine nacelle installed above the wing may considerably change the lift and pitching characteristics of the wing. This can result in an influence of the speed stability, since these interference effects become larger with increasing Mach number which is a consequence of the increasing lateral extension of the nacelle displacement effect with increasing Mach number.

As is known the speed stability is proportional to

$$\left.\frac{\partial C_m}{\partial M}\right|_{\substack{n=\text{const.}\\ i_T=\text{const.}}}$$

For the steady level flight condition the following applies

$$C_L = \frac{\text{const.}}{M^2} .$$

Now we obtain

$$\left.\frac{\partial C_m}{\partial M}\right|_{\substack{n=\text{const.}\\ i_T=\text{const.}}} = \left.\frac{\partial C_m}{\partial M}\right|_{C_L=\text{const.}} - 2\,\frac{C_L}{M}\cdot\left.\frac{\partial C_m}{\partial C_L}\right|_M$$

$$= \left.\frac{\partial C_m}{\partial M}\right|_\alpha - \left.\frac{\partial C_L}{\partial M}\right|_\alpha \cdot \left.\frac{\partial C_m}{\partial C_L}\right|_M - 2\,\frac{C_L}{M}\cdot\left.\frac{\partial C_m}{\partial C_L}\right|_M$$

$$= \left.\frac{\partial C_{m_{WB}}}{\partial M}\right|_\alpha + \left.\frac{\partial C_{m_T}}{\partial M}\right|_\alpha - \left.\frac{\partial C_{L_{WB}}}{\partial M}\right|_\alpha \cdot \left.\frac{\partial C_m}{\partial C_L}\right|_M -$$

$$- \left.\frac{\partial C_{L_T}}{\partial M}\right|_\alpha \cdot \left.\frac{\partial C_m}{\partial C_L}\right|_M - 2\,\frac{C_L}{M}\cdot\left.\frac{\partial C_m}{\partial C_L}\right|_M . \qquad (1)$$

In the incompressible flight regime all terms except the last one become zero and Equation (1) now reads

$$\frac{\partial C_m}{\partial v} = -2\,\frac{C_L}{v}\,\frac{\partial C_m}{\partial C_L} . \qquad (2)$$

From Equation (1) we see that the effect of compressibility becomes more and more important with decreasing lift coefficient and static longitudinal stability. The first term of this equation may be written in the following form:

$$\left.\frac{\partial C_{m_{WB}}}{\partial M}\right|_\alpha = \left.\frac{\partial C_{m_{NWB}}}{\partial M}\right|_\alpha + \left.\frac{\partial C_{L_{WB}}}{\partial M}\right|_\alpha \cdot \frac{x_s - x_{NWB}}{\bar{c}} . \qquad (3)$$

At a constant angle of attack the change of pitching moment contribution of the horizontal tail (second term of Equation (1)) is primarily due to a change of the wing downwash caused by a changed lift distribution on the wing. Sign and magnitude of this change of pitching moment depend on the lateral and vertical arrangement between the incremental wing lift distribution and the horizontal tail location. Generally the wing lift which decreases with increasing Mach number at a constant angle of attack results in a reduction of downwash at the horizontal tail thus reducing the speed stability. A nose-up pitching moment can only be generated by a decrease of lift in the outboard wing area or an increase in the inboard region.

With

$$\left.\frac{\partial C_{L_T}}{\partial M}\right|_\alpha = \frac{S_H}{S}\left(-\left.\frac{\partial C_{L_{WB}}}{\partial M}\right|_\alpha \cdot \frac{d\epsilon}{dC_{L_{WB}}} \cdot C_{L_{\alpha_T}} + \left.\frac{\partial C_{L_T}}{\partial M}\right|_{\alpha_T} - \left.\frac{\partial \epsilon}{\partial M}\right|_{C_{L_{WB}}} \cdot C_{L_{\alpha_T}}\right)$$

and

$$\left.\frac{\partial C_{m_T}}{\partial M}\right|_\alpha = -\left.\frac{\partial C_{L_T}}{\partial M}\right|_\alpha \cdot \frac{l_T}{\bar{c}}$$

and Equation (3), Equation (1) reads

$$\left.\frac{\partial C_m}{\partial M}\right|_n = \left.\frac{\partial C_{m_{NWB}}}{\partial M}\right|_\alpha + \left.\frac{\partial C_{L_{WB}}}{\partial M}\right|_\alpha \cdot \frac{C_{L_{\alpha_T}}}{C_{L_{\alpha WB}}} \cdot \frac{S_T}{S} \cdot \left(\frac{l_T}{\bar{c}} + \left.\frac{\partial C_m}{\partial C_L}\right|_M\right) \times$$

$$\times \left[C_{L_{\alpha WB}} \cdot \frac{d\epsilon}{dC_{L_{WB}}} + 1 - \frac{\partial \epsilon}{\partial \alpha}\right] - \left(\left.\frac{\partial C_{L_T}}{\partial M}\right|_{\alpha_T} - C_{L_{\alpha_T}} \left.\frac{\partial \epsilon}{\partial M}\right|_{C_{L_{WB}}}\right) \times$$

$$\times \left(\frac{l_T}{\bar{c}} + \frac{\partial C_m}{\partial C_L}\right) \cdot \frac{S_T}{S} - 2\,\frac{C_L}{M} \left.\frac{\partial C_m}{\partial C_L}\right|_M . \qquad (4)$$

The first term of Equation (4) represents the change of the wing zero lift pitching moment as a function of Mach number. The second term results from the change of the wing lift at a constant angle of attack and consists of two parts which take into account the change of the downwash at the horizontal tail and the incidence adjustment required for sustaining the necessary lift. This change of wing lift as a function of Mach number may be caused either by subcritical compressibility effects or by the formation, amplification, and movement of compression shock waves. Generally, these transonic phenomena result in a loss of wing lift, since they are initiated on the upper wing side. By means of a favourable distribution of thickness and camber, however, it is possible to create similar transonic flow conditions on both sides of the wing without changing the lift coefficient. It should be noted that this second term is proportional to the horizontal tail volume. Therefore the problem of speed stability becomes particularly severe with high-speed short-haul aircraft, since the $C_{L_{max}}$ values and the wing loading, necessary for take-off and landing, require large tail volumes on one side and very small lift coefficients at cruise on the other.

In the case of an airplane with conventional geometry where Mach-dependent lift loss occurs in the inboard wing area, the coefficient of $\partial C_{L_{WB}}/\partial M$ of Equation (4) ranges between 0.5 and 1.0.

In order to get an impression how the fore-and-aft position of the engine nacelle influences the speed stability at sub-critical speeds, we have calculated the lift and the pitching moment of a two-dimensional configuration at Mach 0 and 0.707. This configuration consisted of a flat plate at zero incidence and of a nonlifting two-dimensional body. The results of this simple calculation are shown in Figure 12. As may be seen, the sub-critical lift losses reach their maximum when the maximum diameter of the engine nacelle is located at the wing trailing edge. On the other hand, the destabilizing wing moment reaches its maximum when the maximum engine diameter is located at about 50% wing chord. It is interesting to note how rapidly the influence of the Mach number on the interference effect diminishes when the leading edge of the displacement body moves behind the trailing edge of the flat plate. The curves in Figure 13 are plotted for two different values of the coefficient of $\partial C_{L_{WB}}/\partial M$ for the total moment change caused by compressibility. They indicate that within the sub-critical Mach number range, forward nacelle locations have a stabilizing effect whereas central and rearward positions decrease the speed stability.

Figure 14 shows the pitching moment curves measured for the configuration shown in Figure 1 at $n = 1$, ϵ_T = constant, for the following three configurations: complete

aircraft without nacelles, aircraft with nacelles and original intake lip, and complete aircraft with improved intake lip shape. The individual drag divergence Mach numbers are also shown. The dashed curves indicate the pitching moment variation which would be obtained without compressibility effects. It may be seen that the measured curves initially slowly deviate from the corresponding dashed curves, and then diverge rapidly above the critical Mach number. Whereas the first effect is due to the growing displacement effect of the nacelle, the second corresponds to the well-known speed instability caused by shock-induced loss of wing lift.

These two Mach number regions can also be seen in Figure 14(c) where the lift coefficient at a constant angle of attack is plotted against the Mach number for the three configurations mentioned above. The strong stabilizing effect above Mach 0.8 is due to the loss of lift on the outboard wing. The horizontal tail experiences a further increase in downwash when the lift of the thicker inboard wing area increases again beyond a certain Mach number.

The approximate scale drawn in Figure 14(b) for the horizontal tailplane setting angle is an indication of the small angular changes of downwash and angle of attack which are involved in the problem of speed stability. Thus complete compensation of the undesired natural trim change is possible by means of a proper variation of stabilizer setting with Mach number, amounting to a maximum change of tailplane incidence of 0.9°.

The shock-induced speed instability may be eliminated by creating similar transonic conditions on the lower wing side as those occurring on the upper surface. This may be achieved by a suitable modification of the camber and thickness distribution of the wing. During an attempt to obtain a similar result by mounting a simple two-dimensional displacement body on the wing lower surface, the powerful effect of such a body on wing lift was discovered. In addition to the normal procedure of eliminating tuckunder by a suitable wing design, we investigated the effect of a small blister mounted on the upper surface of the horizontal tail on longitudinal trim.

Figure 15(a) shows a comparison between the pitching moment curves with and without a small horizontal tail blister. The same diagram also shows the lift coefficient based on the blister area acting on the horizontal tail as a function of the Mach number. As may be seen the blister initially increases the stabilizer lift but as soon as the critical Mach number is reached a large downward force is induced on the horizontal tail. The former effect is due to the local change of airfoil camber. The transonic force characteristics of the blister may be explained by the fact that, owing to the increase of entropy in the normal shock located above the blister surface and the increase of the boundary layer thickness, the external flow is displaced in a normal direction downstream of the blister. It can be shown that to a first approximation the following relationship exists between the displacement thickness of the entropy layer downstream of the blister and the transonic wave drag of this body.

$$\partial = \frac{W_B}{K_{PLOC} M_{LOC}^2} \left[1 + (K-1) M_{LOC}^2\right] .$$

This explains the considerable trim change caused by the blister above its critical Mach number.

Clearly the Mach number at which the transonic blister effect starts to become operative may be controlled by the thickness ratio and its intensity by means of the area of the blister. Thus almost any desired variation with Mach number can be generated, i.e. the pitching moment characteristics required for the proper control forces can be achieved without any artificial devices. This is illustrated by the double blister shown in Figure 15(b). This blister was designed such that the smaller, thicker blister becomes operative at Mach 0.65, whereas the larger, slightly thinner blister begins to function at Mach 0.70. The same diagram shows the pitching moment characteristics at $n = 1$, ϵ_T = constant for the complete aircraft with and without this double blister. One can see that by means of this device it is possible to considerably increase the speed stability above that of the aircraft without compressibility effects.

Extensive pressure and force measurements have shown that the blister causes practically no unfavourable side-effects. The influence on zero-lift drag, elevator effectiveness, elevator hinge moment, longitudinal stability and horizontal tail buffeting are either extremely small or of secondary importance. This is best demonstrated by the fact that the boundary layer downstream of a blister designed for Mach 0.65 does not separate even at Mach 0.80. The reason for this behaviour is that with increasing free-stream Mach number the Mach number directly upstream of the normal shock on the blister initially increases, then reaches a maximum value, thereafter decreases slightly and finally approaches a constant value. When taking into consideration that the blister is located within the region of retarded flow immediately upstream of its own entropy layer this behaviour may be understood to a certain extent. The advantages of such a blister with its self-protecting property are obvious.

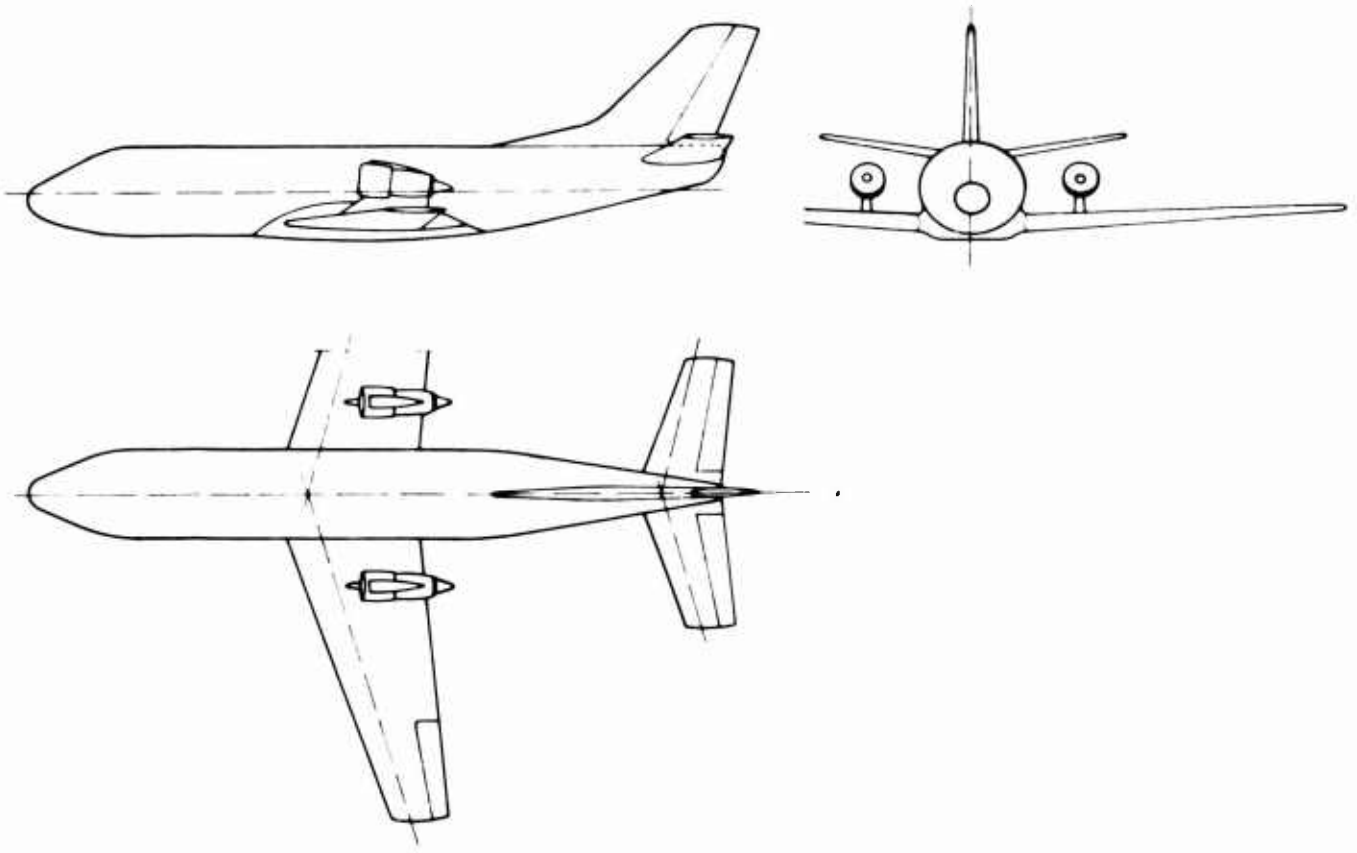

Fig. 1 Configuration tested in low and high speed wind tunnels

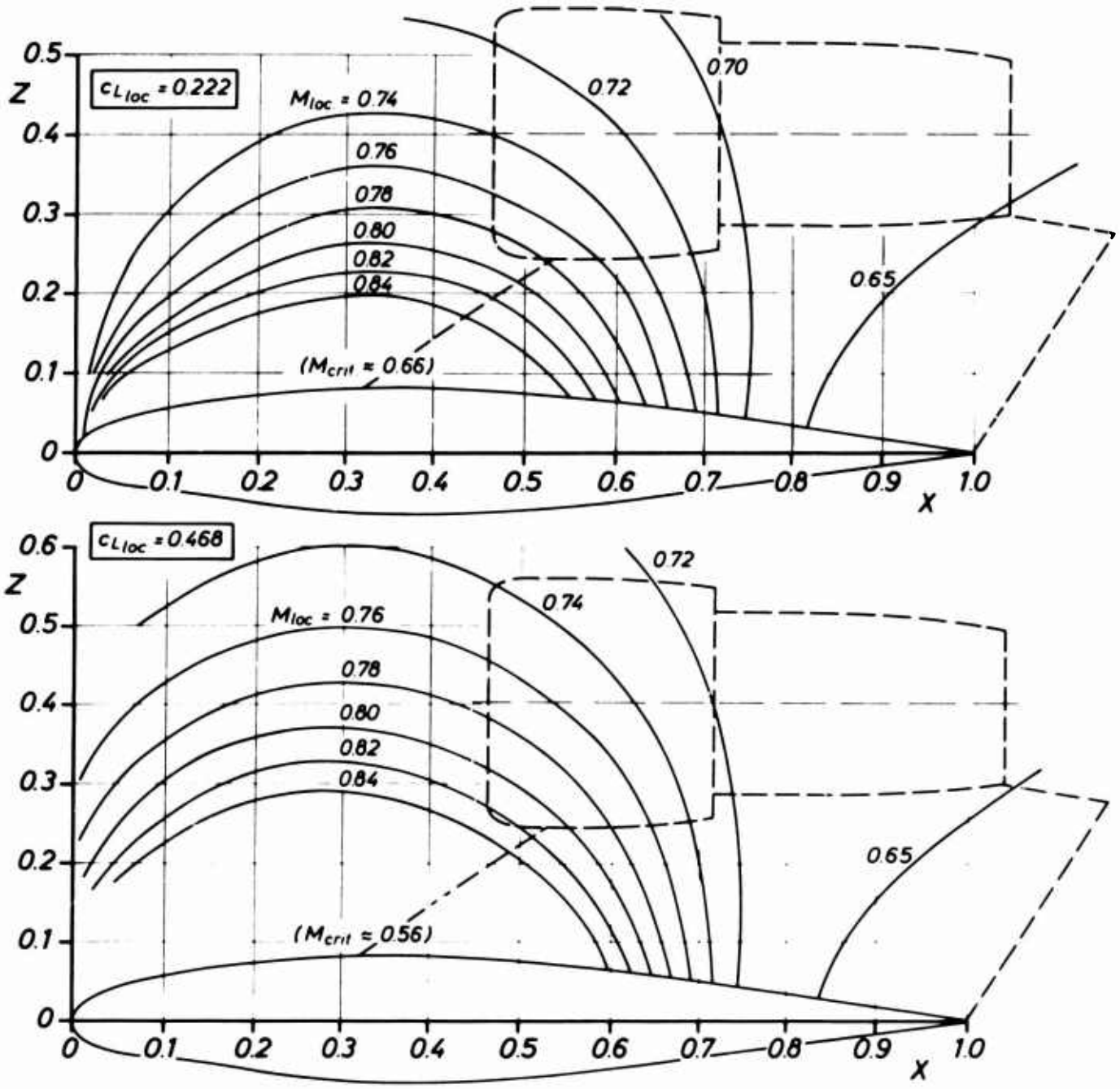

Fig. 2 Local Mach numbers for the clean wing. Wing thickness ratio 15.79%

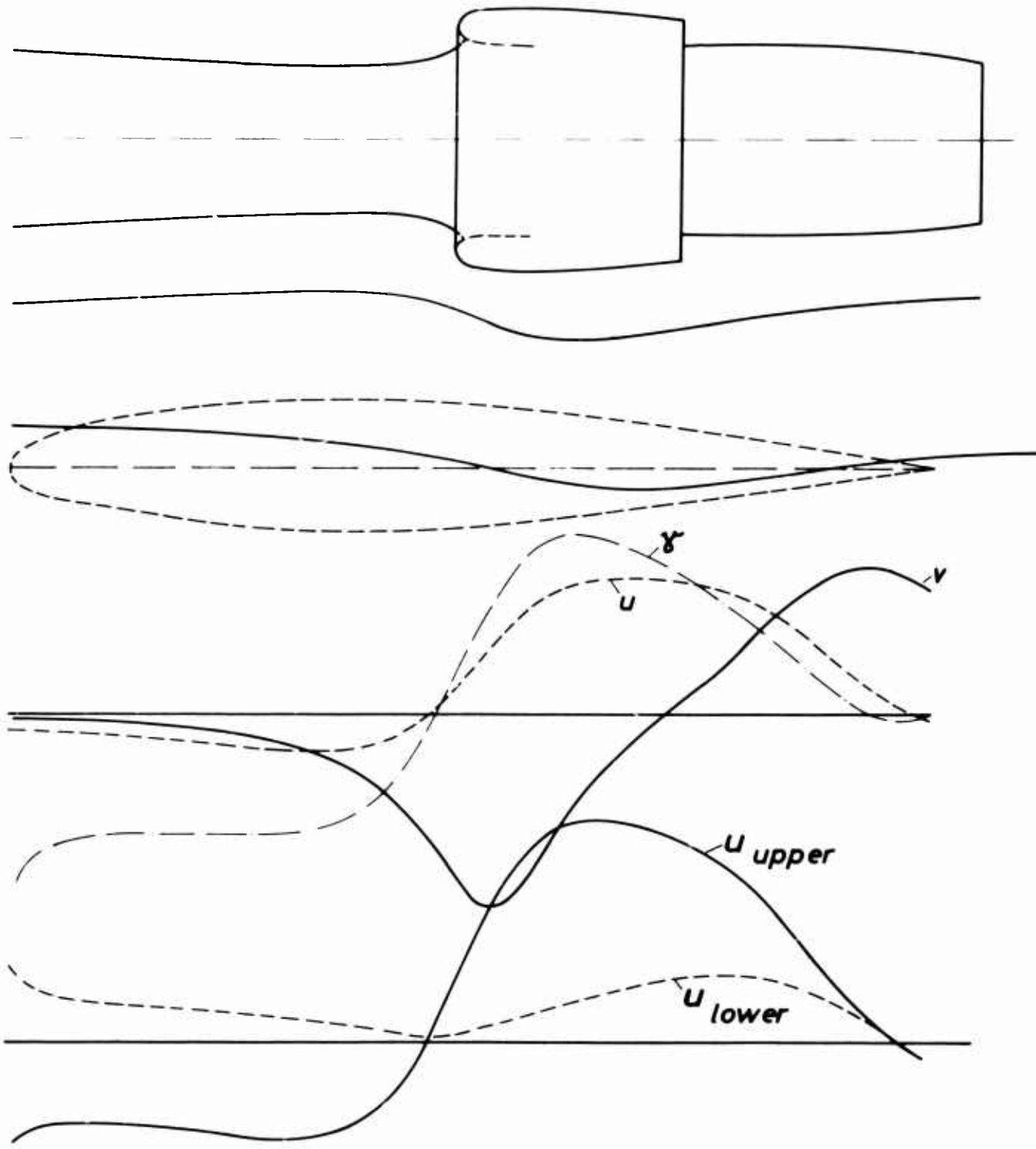

Fig. 3 Schematic representation of nacelle flow pattern and resulting velocity perturbations on the wing

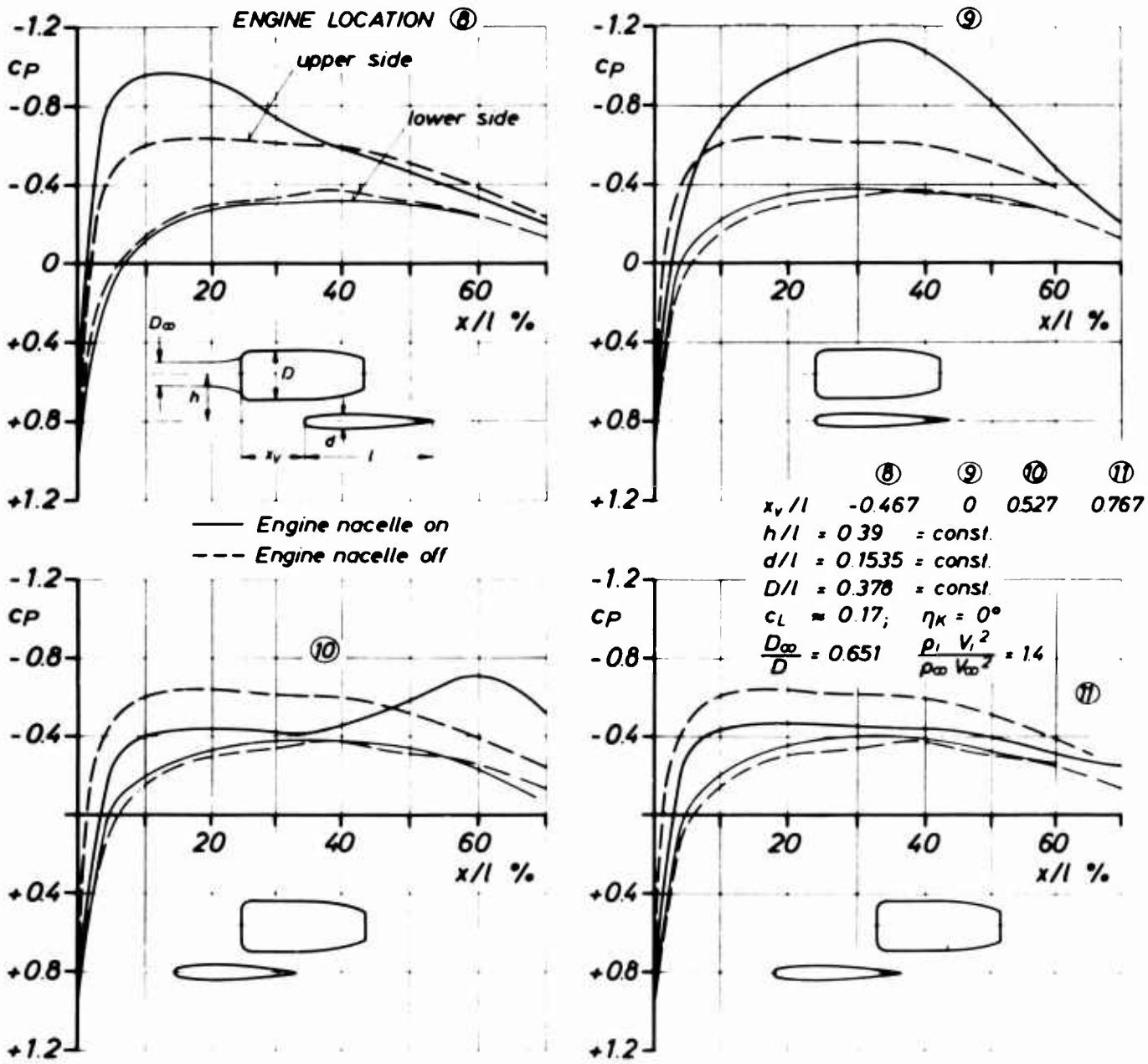

Fig. 4 Influence of the engine location on the wing pressure distribution. Constant h/*l*

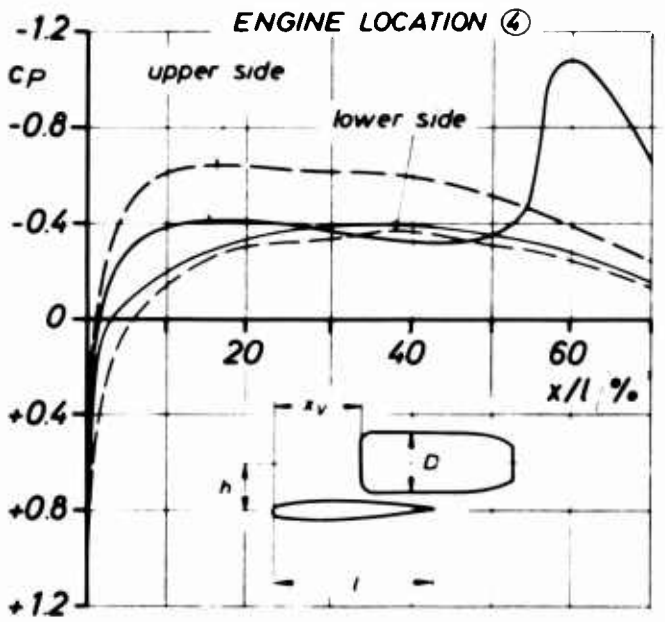

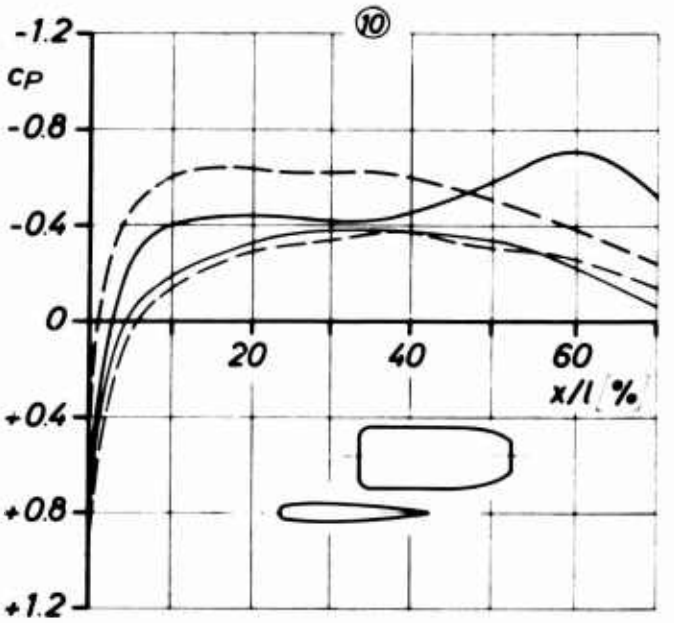

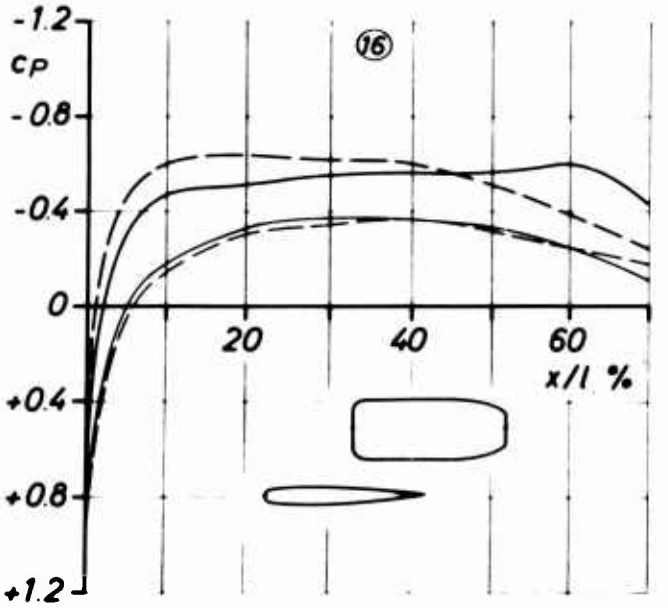

	④	⑩	⑯
h/l	0.32	0.39	0.46

$x_v/l = 0.527 = \text{const.}$
$d/l = 0.1535 = \text{const.}$
$D/l = 0.378 = \text{const.}$

$\alpha_F \approx -0.5°$ $\quad c_L \approx 0.17$
$\eta_K = 0°$ $\quad q_1/q_\infty = 1.4$
$\frac{\bar{v}_2}{v_\infty} = 0.94$ $\quad \frac{D_\infty}{D} = 0.651$

——— Engine nacelle on
— — — Engine nacelle off

Fig. 5 Influence of the engine location on the wing pressure distribution. Constant x_v/l

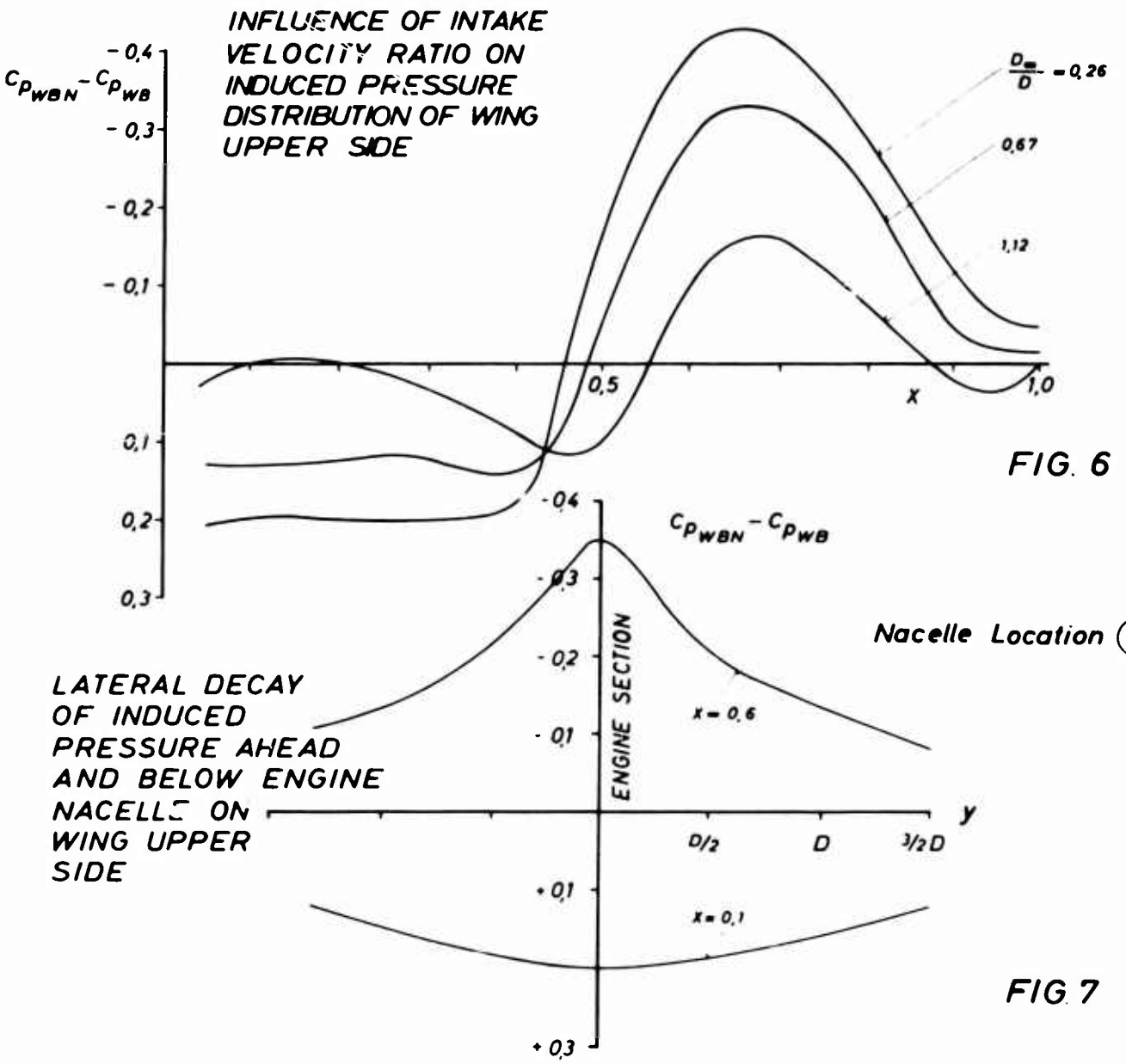

FIG. 6

FIG. 7

Figs. 6 & 7 Influence of engine nacelle on wing upper side

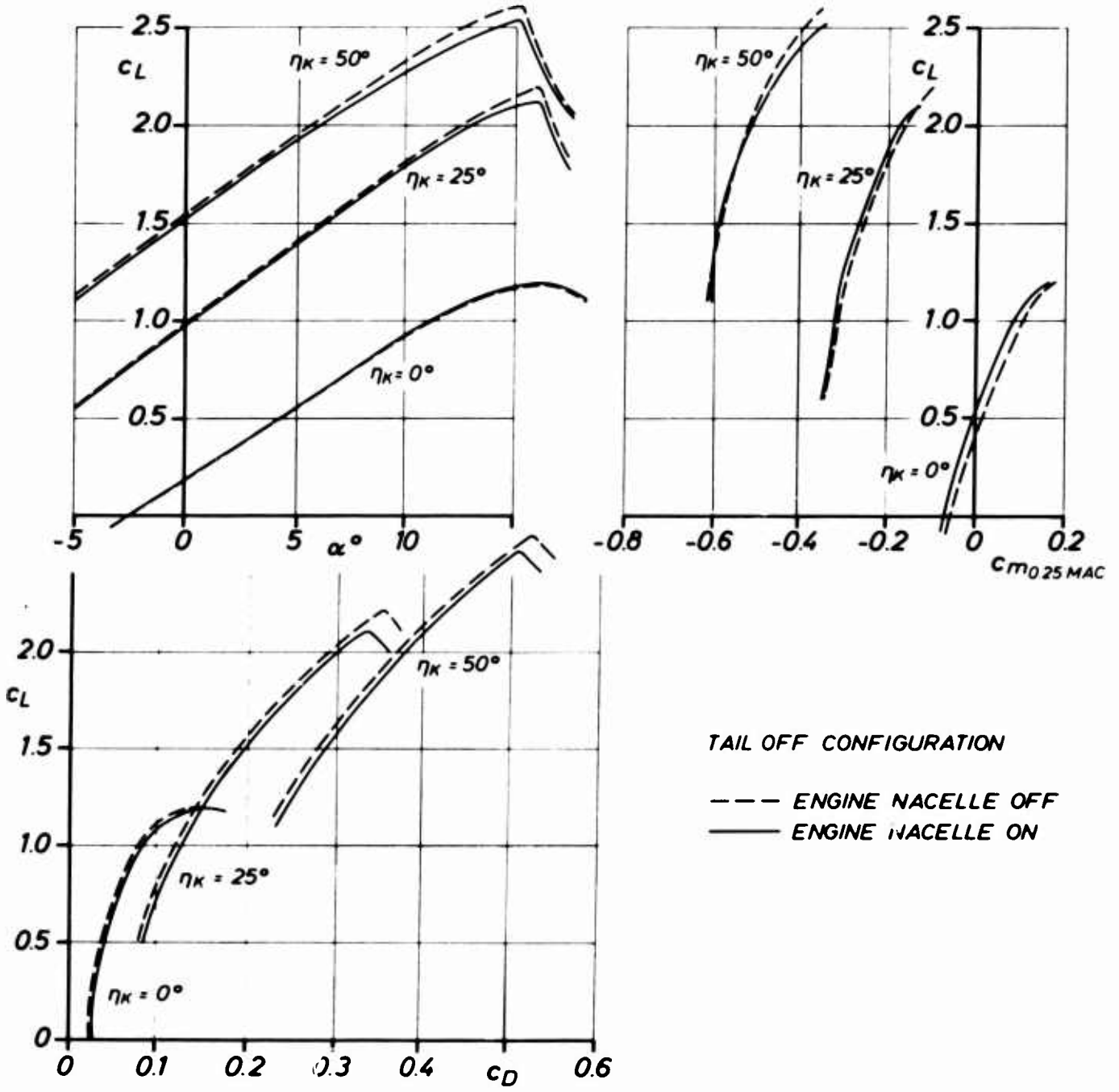

Fig. 8 Lift, drag and pitching moments. Low speed tests; Re = 2.4×10^6, $M_\infty = 0.17$

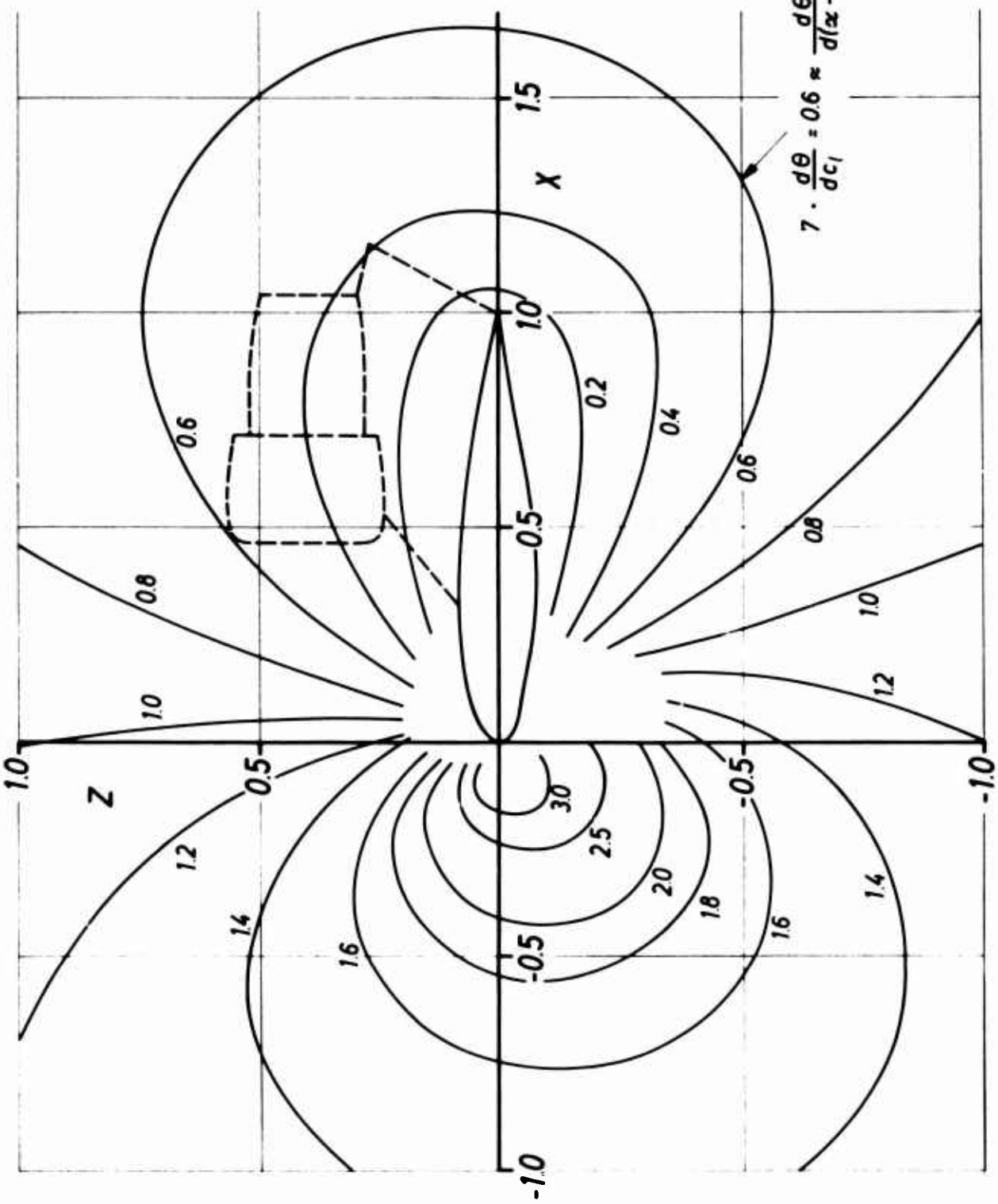

Fig. 9 Change of local flow direction with change in airfoil incidence for a modified NACA 64 A-015.79 airfoil

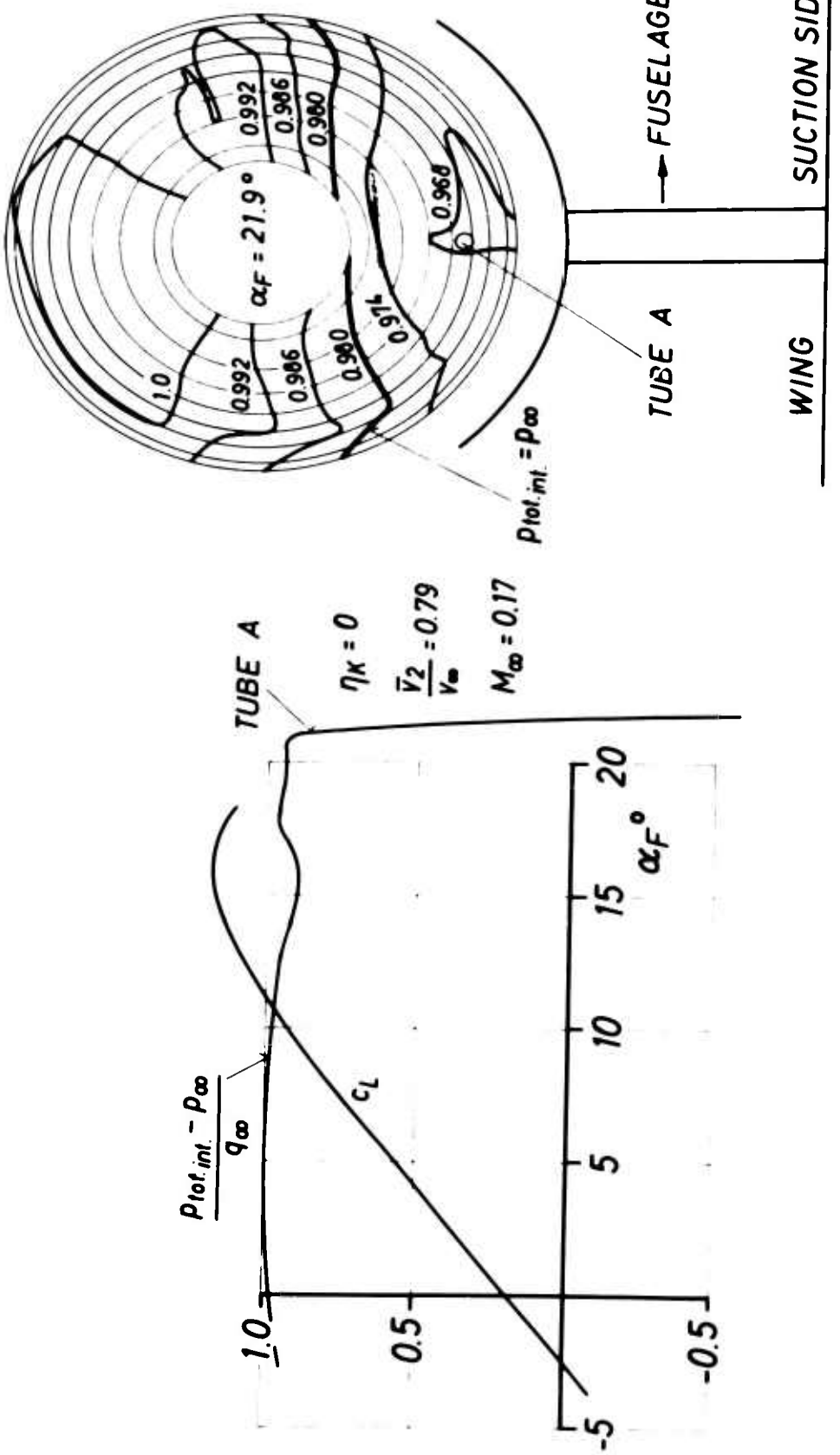

Fig. 10 Wing lift behaviour and total pressure ratios at the compressor face

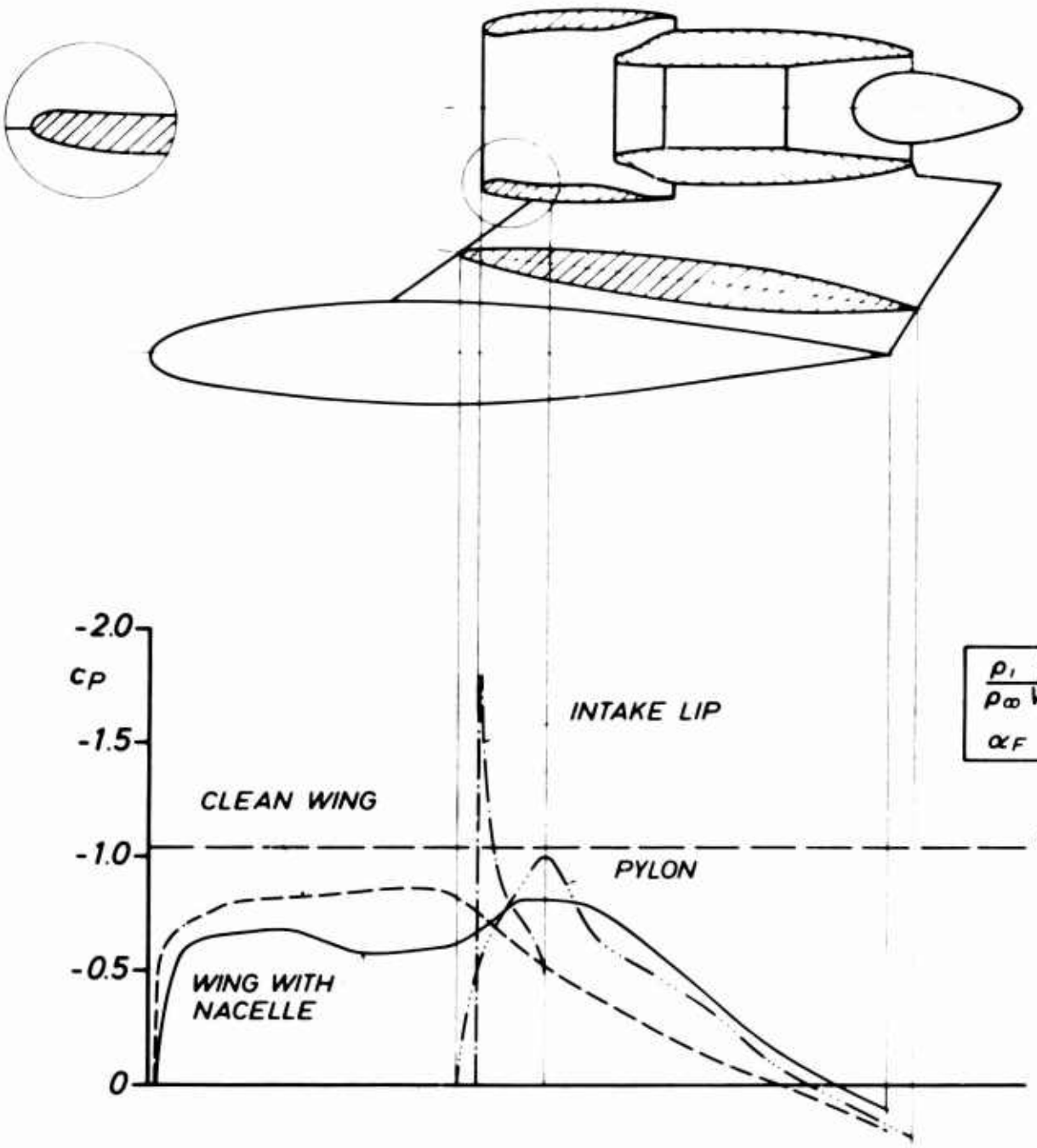

Fig. 11 Pressure distributions on the wing, the pylon and the fan lip at $M_\infty = 0.65$, $C_L = 0.19$

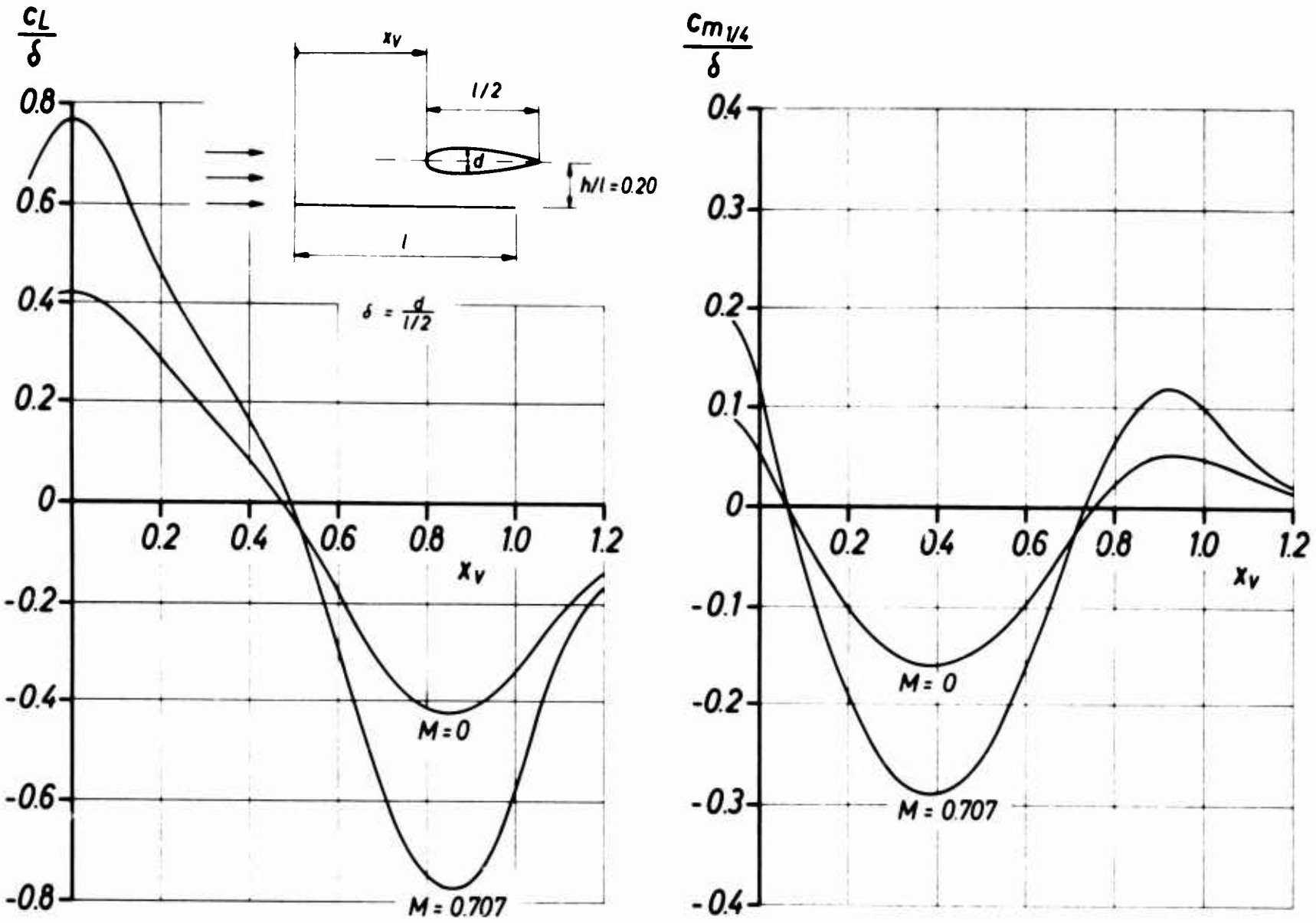

Fig. 12 Lift and pitching moment of a flat plate at zero incidence in the proximity of a two-dimensional body

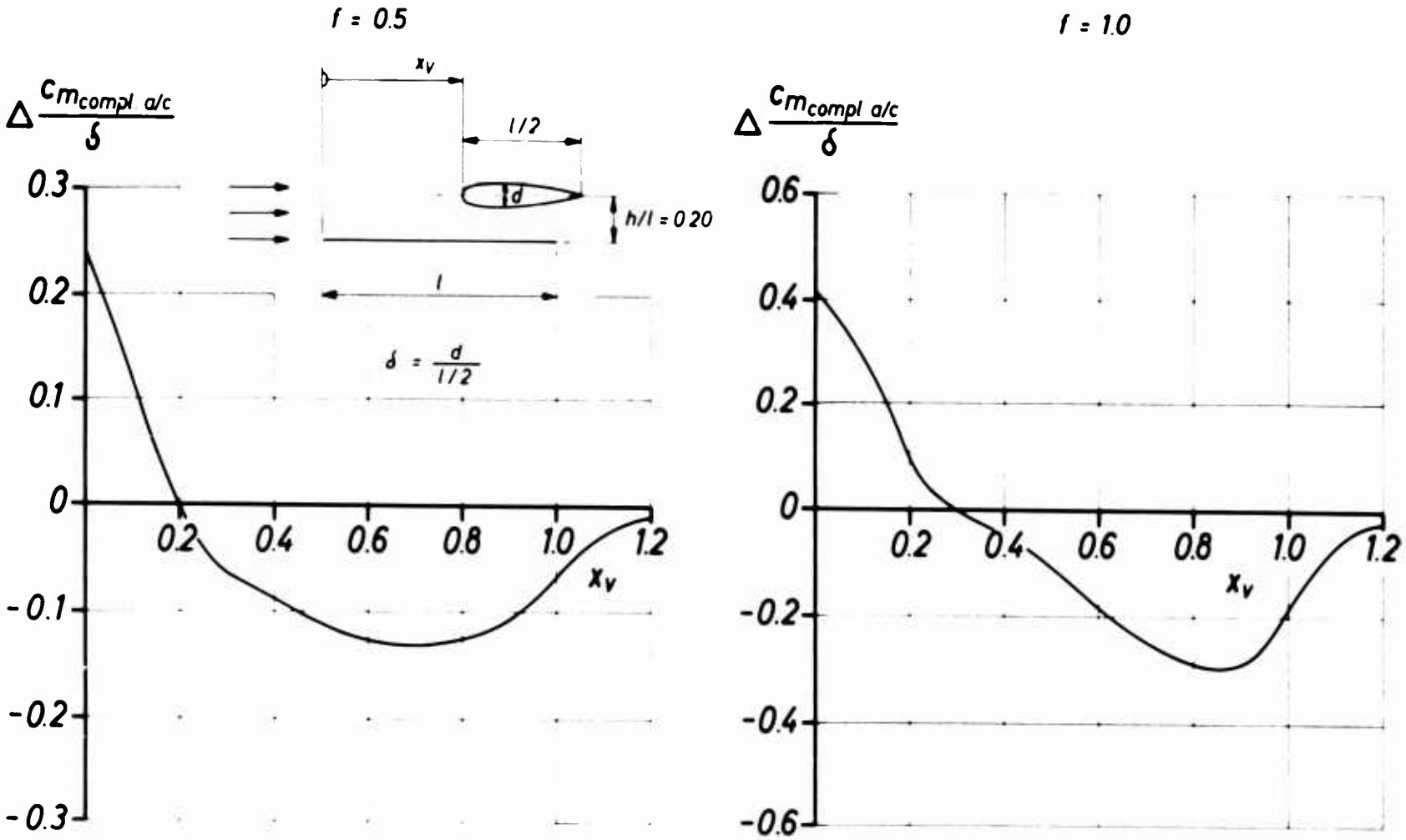

$$c_{m_{1/4\,compl\ a/c}} = c_{m_{1/4}} + f \cdot c_L$$

$$\Delta c_m = c_{m_{M=0707}} - c_{m_{M=0}}$$

Fig. 13 Change of zero-lift pitching moment with Mach number for a two-dimensional wing nacelle configuration including the effect of the horizontal tail

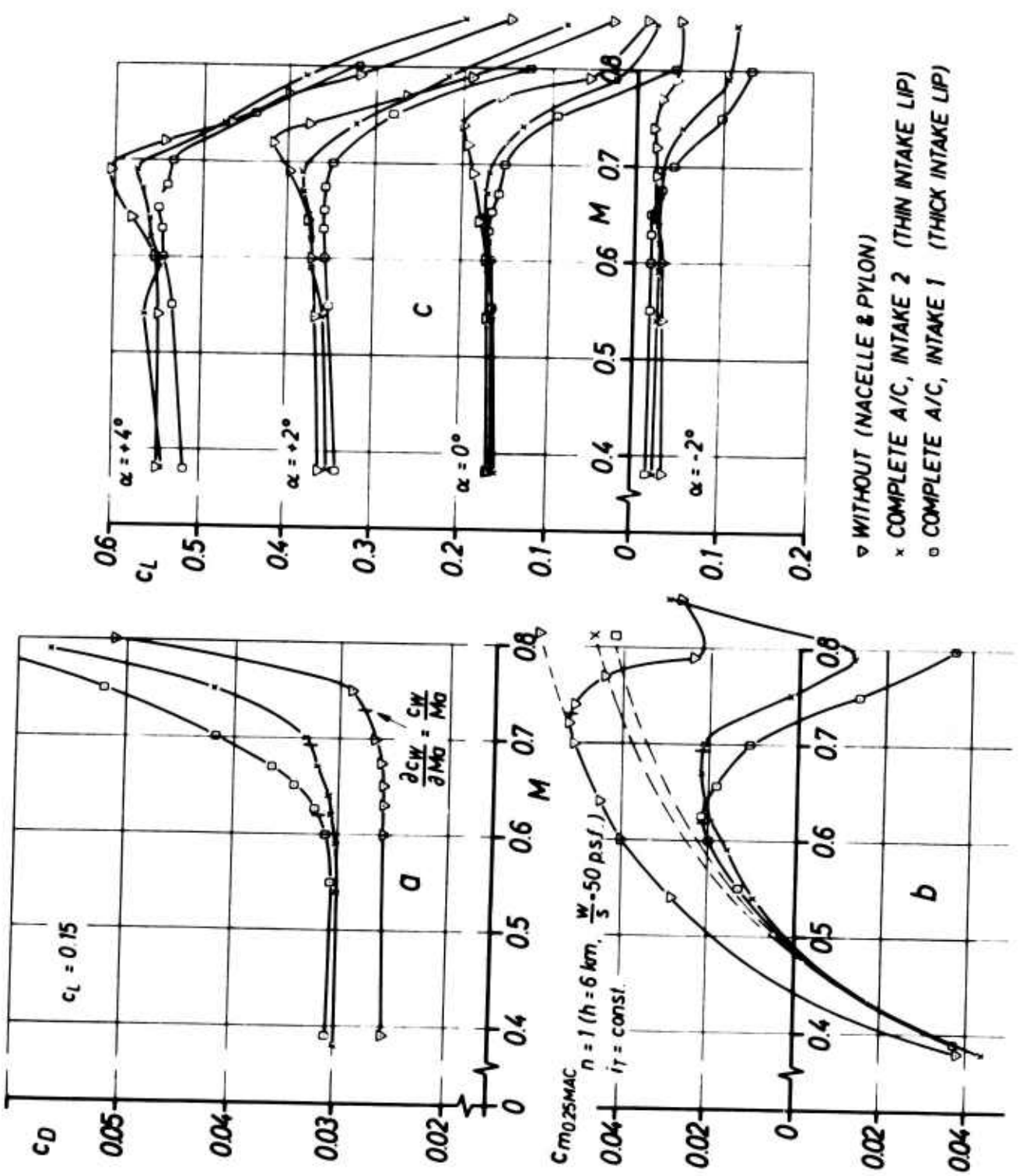

Fig. 14 Drag, pitching moment and lift versus Mach number

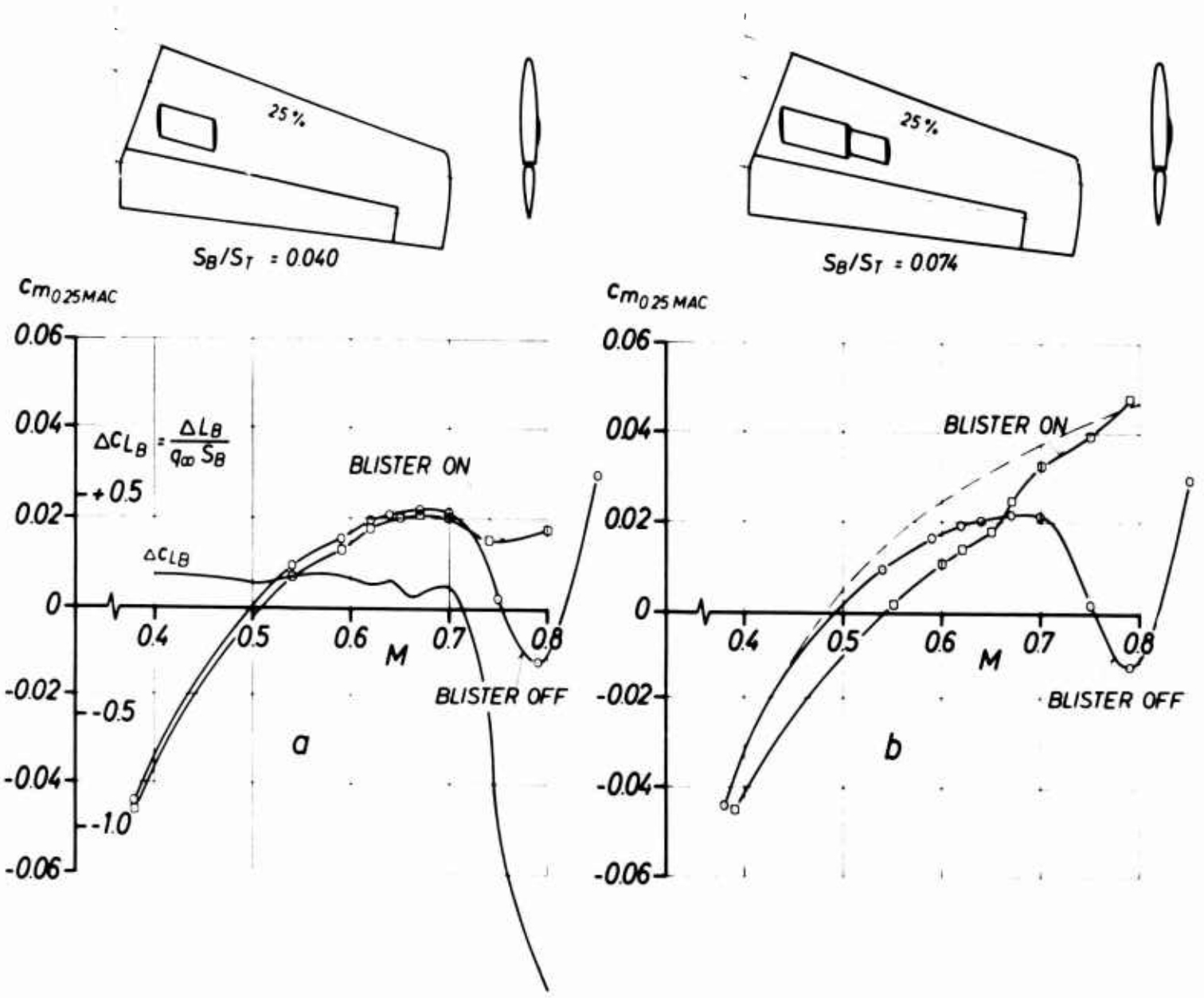

Fig. 15 Effect of blister on pitching moment at $n = 1$ ($h = 6$ km, $W/S = 50$ lb/ft^2) and i_T = constant. (Complete aircraft, engine intake 2)

AIRCRAFT AND PROPULSION OPERATIONAL CONSIDERATIONS RELATED TO INLET DESIGN

by

Frederick T. Rall, Jr

Aeronautical Systems Division,
United States Air Force,
Wright-Patterson Air Force Base, Ohio, USA

SUMMARY

Diagnostic tests of an inlet mounted on the side of a fuselage and under a wing have been conducted in a wind tunnel. Studies of the flow field ahead of the inlet identified an influence on inlet performance. The effects of varying both inlet location and the fuselage geometry were related to inlet pressure recovery, distortion and turbulence. The fuselage boundary layer was subsequently found to be of particular importance to this inlet location.

Full scale engine tests have investigated the effects of inlet turbulence on a turbojet. These tests, conducted in an altitude facility incorporating a choked venturi to provide the desired turbulence, have shown that inlet turbulence reduced the engine stall margin.

Wind tunnel tests of an underwing inlet have shown the effects of inlet unstart on the stability and control characteristics of a supersonic aircraft. The role of the inlet control system was included. The effect of inlet unstart has been found to be a major design parameter in the placement of the propulsion system.

ACKNOWLEDGEMENT

The source material for this paper has yet to be formalized into suitable documents for ready referencing. The author, therefore, acknowledges the work of all the Air Force and Industry engineers, whose efforts have made this paper possible.

I. INTRODUCTION

The integration of airbreathing propulsion systems with specific airframe designs can be broadly classified into the two general categories of Performance and Operational. Under the Performance category would fall such things as inlet pressure recovery, exhaust nozzle drag, and propulsion system weight. Under the Operational category would fall the numerous inlet-engine compatibility problems, the effect of inlet and engine operation on aircraft stability and control, and acoustic fatique problems generated by exhaust noise. Performance sells airplanes. Good operation is the pilot's objective. A successful airplane has both.

In the quest for ever increasing performance capabilities, the propulsion systems and the airframe have become more and more integrated with a continually higher state of tune. Propulsion systems are now located so as to create a favorable interference effect on the aircraft lift-to-drag ratio. Inlet structure is utilized to carry aircraft loads as well as inlet loads. Subsonic diffusers operate at higher duct Mach numbers in order to save some drag and to reduce weight. Compressor operating lines have moved closer to the surge line in order to improve efficiency. Exhaust nozzles are designed to ingest airplane boundary layer air in order to reduce weight. Variable inlet, engine, and nozzle geometries and associated control systems are utilized to maintain high efficiencies across the speed regime.

Performance has been the motivating force behind the trend toward integration and we have accepted as necessary evils the solutions of the operational problems as they arise. We tend to worship the God of Performance continually and pray to the God of Operations only when we are in trouble. To support the belief that a more balanced approach can be achieved by emphasis, this paper deals exclusively with the operational considerations of the airframe-propulsion integration.

The length limitations of this paper, prohibit an extensive review of the operational interface area. Therefore, examples have been selected on the basis of current interest and developments and to illustrate the variety of the inter-relationships. The following sections present examples of the influence of (1) the airframe on the inlet, (2) the inlet on the engine, and (3) the inlet on the airframe.

II EFFECT OF AIRFRAME ON INLET

Much research effort has been expended in investigating the optimum place to locate an inlet on various aircraft configurations. These data have generally shown that placing the inlet under the fuselage or a lifting surface, tends to shield the inlet from adverse effects due to increasing angle of attack. In addition,

locating the inlet in such a position at supersonic speeds offers the advantages of a reduced local Mach number due to the wing leading edge shock which offers the performance advantage of a reduced inlet capture area and, hence, less weight and drag. For an aircraft design which incorporates a high wing and engines located aft in the fuselage, locating the inlet under the wing and next to the fuselage is natural. In order to investigate the effect of an inlet being bounded on two sides, a wind tunnel model was built as shown in Figure 1. The inlet configuration was selected on the basis of low spillage drag at the lower supersonic Mach numbers and the inlet was designed to have the shocks essentially on the inlet lip at 2.2 Mach number. Porous bleed was incorporated on the compression surfaces in order to minimize shock wave-boundary layer interactions.

A splitter plate was located between the fuselage and the inlet in order to prevent the oblique and normal shocks from interacting with the fuselage boundary air. The distance of the splitter plate from the fuselage was selected on the basis of the expected height of the fuselage boundary layer. Aft of the splitter plate leading edge, the flow area was continuously increased underneath the splitter plate to insure that the fuselage boundary layer would pass below. No difficulties were expected from the wing boundary layer because of the relatively short distance between the wing leading edge and the inlet. Flows were designed to remove the boundary layer from the wing surface and the outboard side of the splitter plate and prevented these relatively low energy flows from entering the inlet. A combination sub-inlet and plow was located underneath the splitter and aft of the inlet cowl in order to remove the air from beneath the splitter.

The first series of wind tunnel tests were conducted on the inlet removed from the fuselage. To prevent the bleed-off of pressure around the conical compression surface in the isolated inlet tests, a complete 360° compression surface was installed forward of the inlet cowl station. This circumferential surface replaced the quarter-circle design cone. The tests were run at 0° angle of attack and at the local Mach numbers expected underneath the wing for level flight angle of attack. The inlet and diffuser performance was as predicted, from the theoretical shock pattern and emperical subsonic diffuser losses.

The next step was to measure the flow field provided by the aircraft at the inlet face plane without the inlet and splitter plate installed. The local velocity vectors were measured by conical probes. No boundary layer measurements were attempted. Tests were conducted at Mach numbers up to design and from angles of attack of zero to 16°, the limit on the conical probe calibration. The results of these tests were as expected. The Mach number at the inlet face was quite uniform at all angles of attack tested. The flow, however, showed significant changes in angularity. At 0° angle of

attack, the flow was essentially in the free stream direction. As the angle was increased beyond 6°, the flow showed increasing components in the upward and outboard direction. This flow angularity appeared to originate from the cross flow around the fuselage and from the span wise flow associated with the highly swept wing leading edge. The magnitude of the flow direction change was less than that of the angle of attack and, therefore, the wing provided the desired shielding from the full free stream angularity.

The fuselage, wing, and inlet were next tested together. The results are presented in Figure 2 in terms of inlet total pressure recovery, compressor face total pressure distortion, and turbulence. The total pressure distortion parameter, D, is an area-weighted factor which basically considers circumferential total pressure variations. The turbulence, or noise, was measured by a dynamic pickup at the simulated compressor face. This pickup had a relatively flat frequency response up to approximately 200 cycles per second.

The results of this test were quite disappointing. The inlet pressure recovery was expected to continually increase with angle of attack because of the reduced Mach number aft of the wing leading edge shock. The data showed the maximum recovery occurred at the lowest angle of attack tested. In addition, the steady state distortion and turbulence increased with angle of attack so rapidly that engine stalls could be predicted.

In order to investigate the reasons for the relatively poor inlet performance at the higher angles of attack, additional wind tunnel tests were prescribed. A series of five total pressure rakes were added to the fuselage immediately ahead of the splitter plate. The data from these rakes are presented in the form of constant total pressure profiles around the fuselage as shown in Figure 3. At α-5°, the fuselage boundary layer height agrees well with the predictions. As the angle was increased, however, the boundary layer height began to bulge significantly and the splitter plate distance from the fuselage was no longer sufficient to capture all of the fuselage boundary layer. These data were measured both with and without the inlet and splitter plate on the model in order to determine the effect of the inlet on this boundary layer characteristic. There was no significant difference in the results.

The bulging of the boundary layer was diagnosed to be caused by the increase in pressure underneath the wing as angle of attack was increased, plus the increasing vertical component of the free stream velocity at the higher angles. These two forces tended to squeeze the fuselage boundary layer. Since the boundary layer was constrained by the fuselage and wing surface, it relieved itself by locally bulging beyord its normal height.

The measured inlet performance could then be explained by the fuselage boundary layer coming over the splitter plate leading edge. This relatively low energy air interacted with the inlet shock waves, causing some of the low energy air to spill into the inlet and adversely effecting the inlet performance at the higher angles of attack. In order to test this theory, the inlet was moved outboard so as to place the leading edge of the splitter just outboard of the bulged fuselage boundary layer. The splitter was also changed from a vertical orientation to one parallel to the fuselage. (Figure 4) The splitter orientation was changed in order to increase the distance between the splitter and the inlet, and thus further decrease the possibility of splitter plate boundary layer air entering the inlet. This change was also consistent with eliminating the vortex on the outboard side of the splitter plate. This vortex, generated by the lower leading edge corner of the splitter, had been noted during oil flow tests. It was believed to be caused by the cross-flow around the fuselage which caused a lifting vortex. Changing the splitter orientation was expected to change the loading on the splitter plate and thus cause the corner vortex to pass under the splitter.

The test results of this configuration change are shown in Figure 4. The inlet pressure recovery, distortion, and turbulence were all greatly improved and the inlet was now operating as expected. These results indicated that the fuselage boundary layer air was responsible for the previous poor inlet performance.

To further test these conclusions, the inlet and splitter were moved back to their original location and a fence was added along the bottom of the fuselage as shown in Figure 5. This fence was designed to deflect the fuselage cross flow outward and downward, and thus shield the boundary layer along the fuselage side from the cross flow at the higher angles of attack. The pressure recovery and total pressure distortions of this configuration are compared to those of the original inlet in Figure 5. These data show the fence to be quite effective in improving the inlet performance. The effectiveness of the fences further substantiates the boundary layer bulging theory.

The overall conclusion from these tests is that locating an inlet under a wing and next to a fuselage can be accomplished quite successfully but that careful attention must be paid to the fuselage boundary layer.

III EFFECT OF INLET ON ENGINE

As noted in the previous section, inlets can deliver quite turbulent flow to the engine face. In order to investigate what effect this turbulence had on the operating characteristics of a turbojet engine, a ground test was conducted on an actual engine. The test was run in an altitude test cell with the basic test setup and in-

strumentation as shown in Figure 6. The test arrangement consisted of an airflow metering venturi with a translating centerbody which allowed the throat area to be varied. This variation in geometry produced varying shock wave systems and, because of the shock wave boundary layer interactions, produced varying intensities of turbulence at the compressor face.

Steady state total and static pressures at the compressor face were measured by four 5-probe pitot-static rakes arranged 90° apart. Dynamic total pressures at the compressor face were measured by four 2-probe rakes located 90° apart and in between the steady state pitot-static rakes. The dynamic pressure instrumentation provided valid data up to about 200 cycles per second.

A typical waveform generated in this test is shown in Figure 7 along with the spectral distribution. The amplitude of the pressure fluctuation was found to be distributed in an essentially Guassian manner about the steady state pressure level. This property permitted the wave amplitude to be defined on a probabilistic basis since the standard deviation, σ, is equal to the root mean square, RMS. The definition of turbulence which was arbitrarily selected is as follows:

$$T = \text{Turbulence} = 6 \times \text{RMS}\left(\frac{\Delta P}{P_{t_2}}\right) \times 100\% = 6\sigma$$

With this definition, turbulence is the ratio of the 99.7% probable amplitude range to the steady state total pressure level.

Each of the eight dynamic total pressure pickups at the compressor face were individually analyzed and showed that the turbulence varied in value over the face of the compressor. Figure 8a shows the turbulence variation across the face of the compressor for a particular setting of the turbulence generator at a simulated Mach number of 2.2, and a fixed engine speed and centerbody position. In order to describe the turbulence at the compressor face with one number, an arithmetic-average of the turbulence of each of the eight dynamic pressure measurements was utilized.

In addition to generating turbulence, the test set-up also created some steady-state total pressure distortions at the compressor face. Figure 8b shows the distortion profile for the same test conditions as the turbulence profile in Figure 8a. All of the steady state total pressure distortions were found to be generally a one per revolution circumferential pattern with a large radial component. The engine had been previously tested to determine the effects of distortion on engine operation at $M_o = 2.2$. These data showed that the distortions generated in the present series of tests had practically no affect on the engine operation, including stall margin. Thus, the results of the turbulence tests can be directly attributed to turbulence and not to any effect of distortion.

The results of the testing showed that turbulence reduces the engine stall margin by decreasing the pressure rise across the compressor required to induce stall. Engine stalls were induced in each of the following manners:

1. Instantaneous stalls - The turbulence level was increased by continuously moving the centerbody until stall occurred or by setting the centerbody and increasing airflow until stall occurred.

2. Steady-State Stalls - The turbulence level was set and the engine was operated at steady state conditions until a stall occurred.

3. Fuel Pulse Stalls - A turbulence level was set which was not sufficient to cause "Steady-State Stalls". A fuel pulse was then injected into the combustor until the compressor would stall.

4. Afterburner Light-Off Stalls - A turbulence level was set and the afterburner lit off. Depending on conditions, stall would or would not result.

The Instantaneous Stalls were quite enlightening since the value of turbulence at which the engine would stall varied significantly. Six instantaneous stalls were obtained at M_o = 2.2 and 100% RPM. The turbulence levels at these stall conditions varied from 11.5% to 22%. This wide range of turbulence levels for stalls suggested that the occurance of stall might be probabilistic rather than deterministic. For this reason these stalls were analyzed on a probability basis and the results are shown in Figure 9. These data show that as turbulence amplitude was increased that the probability of stall increased. The solid line on Figure 9 describes a Gaussian distribution and tends to support the probabilistic nature of the stalls resulting from turbulence.

The steady-state stalls occurred after setting the conditions and waiting some time period which would vary from several seconds up to eight minutes. Nine stalls of this type were encountered at M_o = 2.2 and 100% engine speed. These stalls again tend to support the probabilistic nature of the turbulence-stall phenomena.

The fuel pulse stalls were used to measure the compressor stall margin, defined at a constant corrected engine speed. Figure 10 presents the results of these tests in terms of the stall margin as a function of the average turbulence level. The zero turbulence intersection was evaluated with screens in front of the engine to remove the turbulence as well as in previous engine tests. The zero margin intersection was based on the 50% probability of stall from Figure 9. The data at intermediate turbulence levels were scattered about the line drawn. A definite decrease in stall margin is apparent as turbulence is increased.

Additional tests were conducted in which the engine stall margin was increased by such things as increasing exhaust nozzle area which lowers the compressor operating line. In each case the engine tolerance to turbulence was increased. Thus, turbulence effects are similar to other mechanisms for causing engine stall, in that they all respond favorably to increased stall margin.

More instrumentation was required in these tests to have determined the physical process involved in the turbulence induced stalls. In particular, higher frequency response instrumentation would have provided more insight into the possibility of high energy levels occuring at frequencies greater than 200 cycles per second. Additional instrumentation would have provided a better definition of the spatial variation of turbulence which may well be of significance. Additional tests with increased instrumentation will be required to understand this stall phenomena. It is to be expected that such tests will lead to a better understanding of the stall mechanism and a more deterministic approach to the influence of turbulence.

The overall conclusion from these tests is that turbulence decreased the compressor stall margin and, hence, should be considered in future inlet and engine design.

IV EFFECT OF INLET ON AIRFRAME

As the maximum Mach number of airbreathing aircraft has increased, the amount of air handled by the inlet relative to the amount of air handled by the aircraft wing has also increased. This has given rise to increasing concern of the possible adverse effect of propulsion system operation on the stability and control characteristics of the aircraft. Of particular concern was the impact of internal compression inlets, which under some failure conditions, could forcefully expel the internal shock waves forward of the inlet cowl (inlet unstart) and could cause significant change in the aircraft's flow field. This concern led to an investigation of the effects of an inlet unstart on the aircraft shown in Figure 11. This aircraft had two independent internal compression inlets located underneath and within the flow field of the wing. The inlets were located just forward of the center of gravity close to the centerline of the aircraft. This location tended to minimize the forces and moments caused by an inlet unstart and by unsymmetrical thrust. Bypass doors, located on top of the wing just forward of the two vertical tails spilled excess inlet air between the tail surfaces, as shown in Figure 12.

In order to investigate the effects of inlet unstart on the aircraft stability and control, wind tunnel tests were conducted on an aircraft force model. The model incorporated variable inlet geometry and simulated the bypass geometries and flow conditions. The bypass air was provided by an independent source of high pressure air

brought into the model. This air supply was separately and independently controlled. The model also contained pressure instrumentation on the inlet ramps and cowl, the body, and on the vertical tails. Since the external inputs of an unstarted inlet and deflected bypass doors were expected to be mutually independent, they were measured separately. The tests were conducted at a Mach number of 3.0.

The incremental yawing moment coefficient resulting from an unstarted left hand inlet is shown relative to the percentage of the design inlet capture area ratio in Figure 13. The data points were obtained by varying the left hand inlet contraction ratio and inlet airflow. These data have been corrected to zero duct exit thrust differential between the left and right hand ducts while the right hand inlet remained started. Only stable inlet operating points were included since the six component force balance had a natural frequency close to the inlet buzz frequency. This caused the force measurements to be unreliable during unstable inlet operation.

The vertical lines in Figure 13 identify the maximum unstarted capture area ratios for various inlet contraction ratios. The force measurements, together with the inlet ramp and cowl pressure data, showed that the high pressure air behind the expelled shock wave acted on the external ramps of the inlet causing a significant yawing moment. The pressures on the outboard cowl produced a yawing moment opposite to that of the inlet ramps but the cowl moment was relatively small in comparison. Integration of the ramp and cowl pressures agreed well with the force balance measurements.

The data of Figure 13 suggested that the incremental yawing moment could be reduced by increasing the inlet throat height. This increase in throat height would allow the expelled terminal shock wave to stabilize closer to the inlet cowl, thus reducing the inlet ramp area which is being acted upon by the high pressures. The inlet control system would automatically increase the inlet throat height after an inlet unstart in order to restart the inlet. The length of time that the aircraft would be exposed to this incremental yawing moment would be dependent upon the inlet control system and the maximum rate of movement of the inlet throat. To insure that inlet back pressure would not be limiting the flow through the inlet during the restart cycle, the inlet bypass doors were to be opened automatically shortly after the inlet unstarted.

Unstarting the left hand inlet also resulted in a relatively large left wing down rolling moment. This resulted from the low energy inlet spillage air destroying some of the lift on the left wing. The larger the amount of air spilled around the inlet, the larger the incremental rolling moment. Thus increasing inlet throat height would also reduce this input as well as the yawing moment input.

The effects of bypass door operation were also obtained by both force measurements and static pressure surveys. During these tests, the right hand bypass doors were maintained closed while the left hand doors were opened varying amounts. The pressure data showed a high static pressure existed on the body over the doors when the left hand bypass doors were opened at Mach 3.0. This pressure decreased in magnitude aft of the doors. These pressures, in conjunction with the gross thrust of the bypass air, caused a positive pitching moment input. The pressure distributions on the left hand vertical tail showed that the left hand bypass air expanded around the tail. This lowered the outboard tail pressures and produced a negative side force on the tail. The right hand vertical tail was unaffected. The force measurements obtaining incremental yawing and pitching moment coefficients, as a function of left hand bypass door opening, are shown in Figure 14.

The net effect of an inlet unstart and bypass door opening was to produce a yawing couple, a rolling moment, and a positive pitching moment. The forces which cause these moments are shown schematically in Figure 15.

The input forces during inlet buzz had to be estimated because the force model was unreliable under this condition. Observance of static pressure taps on the inlet ramps during buzz established the maximum upstream movement of the terminal shock pattern. The assumption was made that a normal shock existed at this most forward station for a given period of time during the buzz cycle. The static pressure behind the normal shock could then be calculated and was assumed to act on all of the exposed ramp surface aft of the shock. Previous experience showed this to be conservative because the shock pattern on the ramps during unstart consists of a series of lambda shocks generated by boundary layer separation rather than the simple normal shock which was assumed.

A digital computer simulation of the aircraft response to these aerodynamic moments and forces was conducted next. Many assumptions were necessary in this simulation. In each case, the assumptions were made which would give the largest airplane response:

a. The right hand inlet would always remain started independent of the airplane response.

b. The left hand engines would continue to produce thrust at a level consistent with the inlet pressure recovery during the unstart-restart cycle. (It is to be noted that the asymmetrical thrust would result in a yawing moment opposite to that caused by the inlet unstart and bypass door opening. Thus the asymmetrical thrust produced a "favorable" yawing moment for this aircraft configuration.)

c. The lightest airplane weight was selected.

The inputs were scheduled as a function of time consistent with the automatic inlet control operation. The results of this simulation are shown in Figure 16. When the left hand inlet unstarted and the bypass doors opened, the resulting yawing moment manifested itself as a sizeable side slip angle. The side slip angle, in conjunction with the incremental rolling moment, caused the bank angle. The side load factor at the center of gravity reach 0.8g.

Additional simulation runs were conducted with the stability augmentation system on. This significantly reduced the airplane response. Additional various modifications to the automatic inlet control system were investigated which also reduced the aircraft response.

In view of the lack of pilot input in the digital simulation, the airplane simulator was modified to simulate an inlet unstart and the pilot was incorporated into the loop. The results of this showed that the pilot input occasionally was out of phase with the aircraft response and accordingly could aggravate the aircraft motions. These simulator tests depended upon the pilot response to instrument readings. The pilot's ability to control the aircraft was expected to improve in flight because of the additional cues of sight and acceleration. None the less, modifications were made to reduce the inputs from the inlet and to improve the stability. These changes made the airplane satisfactory on the simulator.

Flight testing has demonstrated that inlet unstart can be safely accomplished. In general, the airplane response is significantly less than predicted by the conservative analysis. Three interesting conditions which had not previously been expected, have been observed during flight tests.

First - The acceleration on the pilot during the unstart, is such that he creates an input into the control column when he is thrown forward with a force of about 0.2g.

Second - The aircraft flexibility is such that the pilot side force accelerations and buffeting are much higher than expected during inlet buzz.

Third - The stability augmentation system sensors are located near the inlet and receive an oscillating input from inlet buzz forces. This induces a small oscillation input from the stability augmentation system which had not been previously expected.

INLET WIND TUNNEL MODEL CONFIGURATION

FIGURE 1

INLET PERFORMANCE

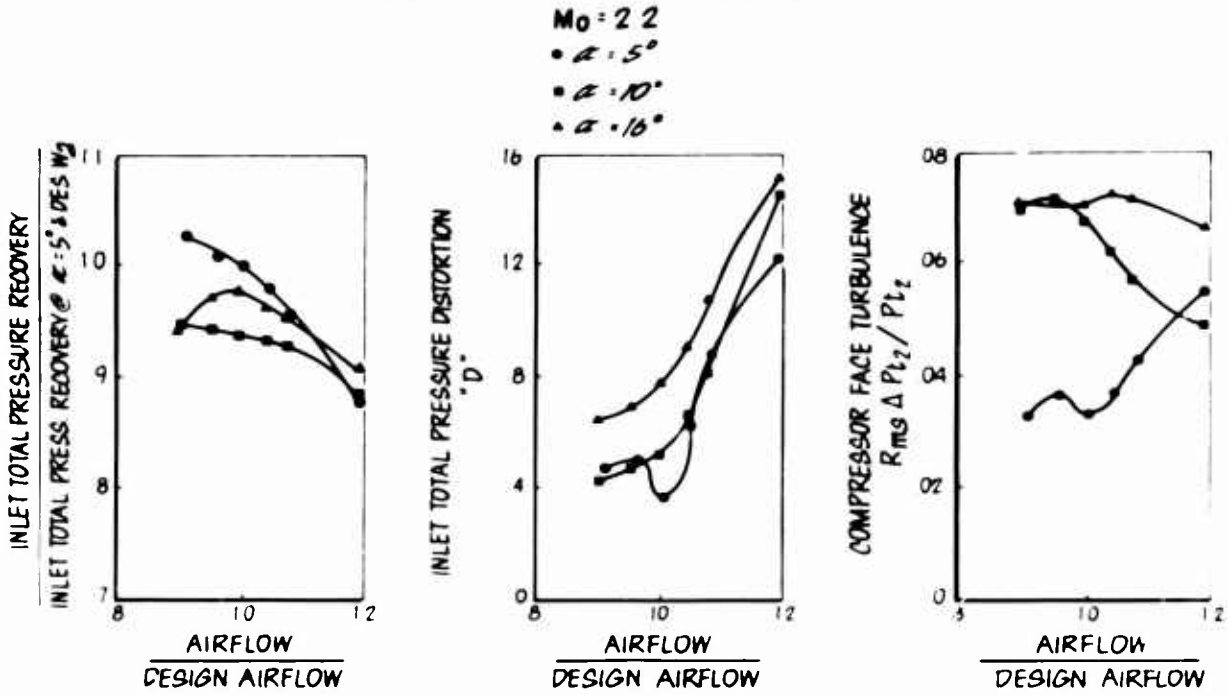

FIGURE 2

FUSELAGE BOUNDARY LAYER SURVEY

$M_0 = 2.2$

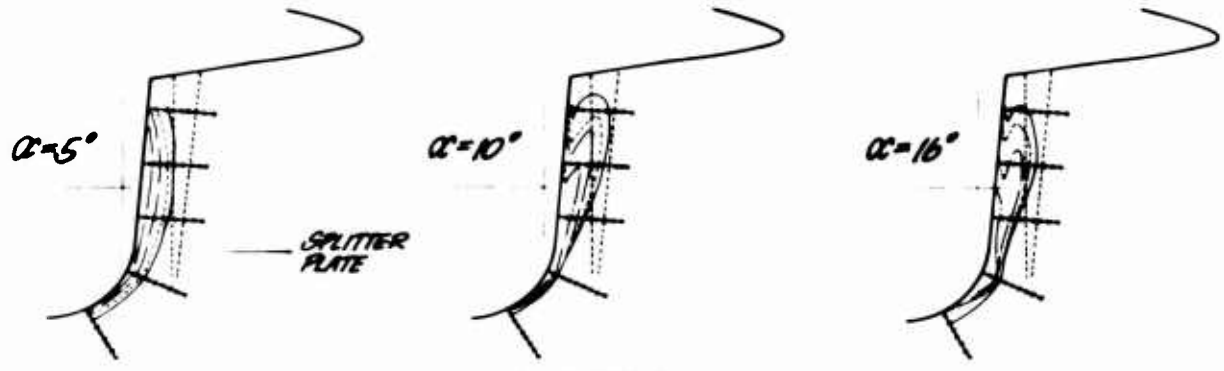

FIGURE 3

INLET MOVED OUTBOARD

$M_0 = 2.2$

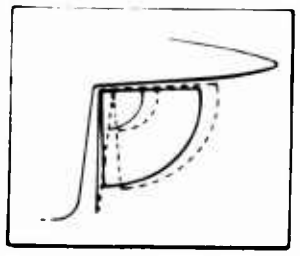

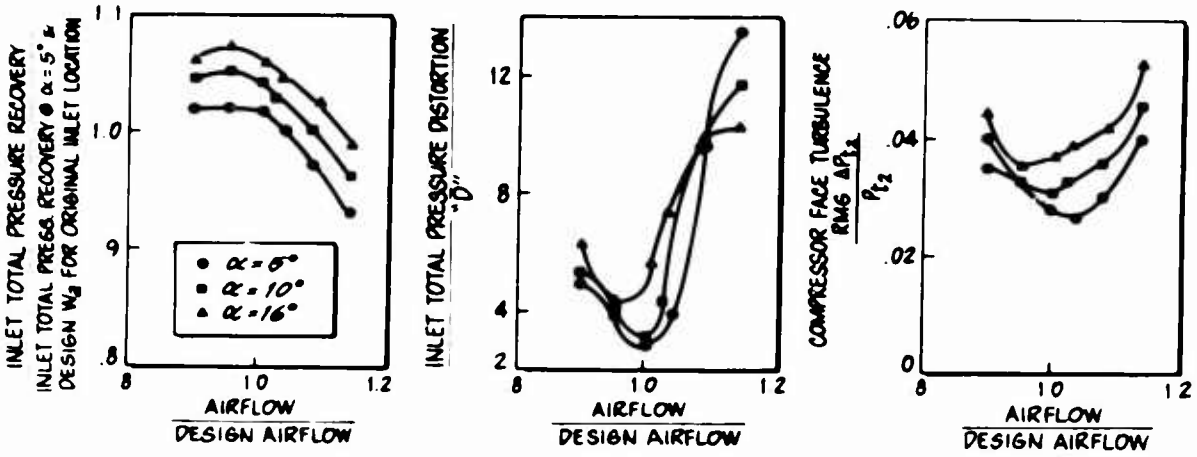

FIGURE 4

EFFECT OF FUSELAGE FENCE

$M_0 = 2.2$

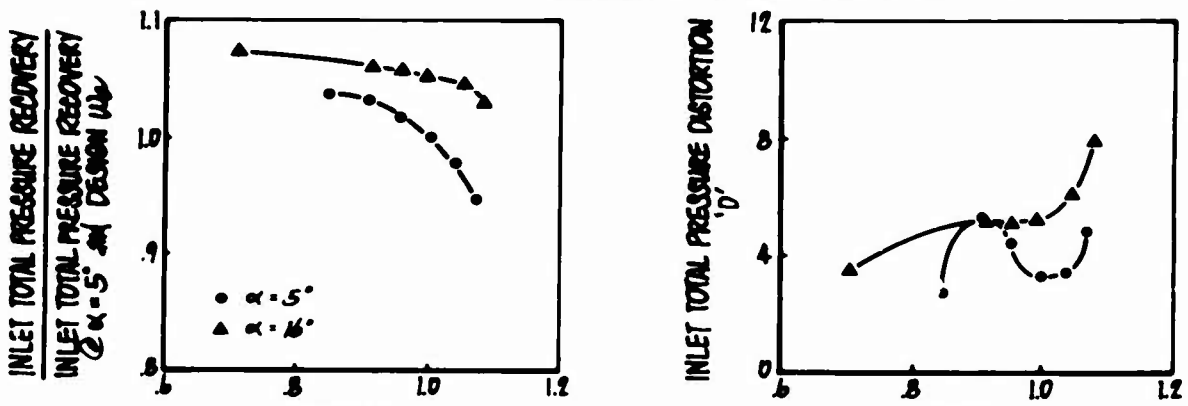

FIGURE 5

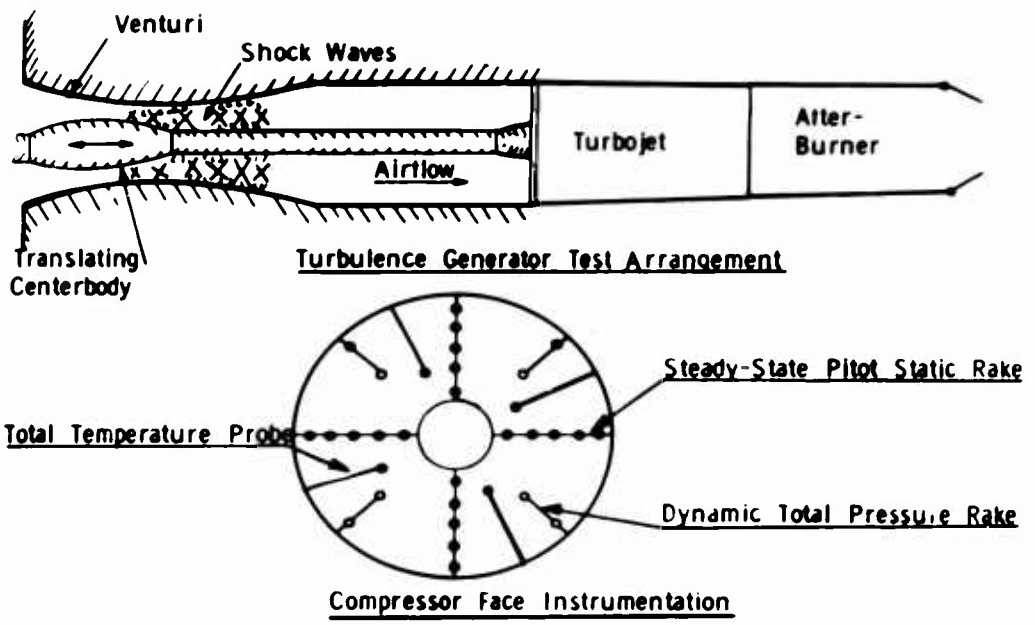

FIGURE 6

TURBULENCE CHARACTERISTICS

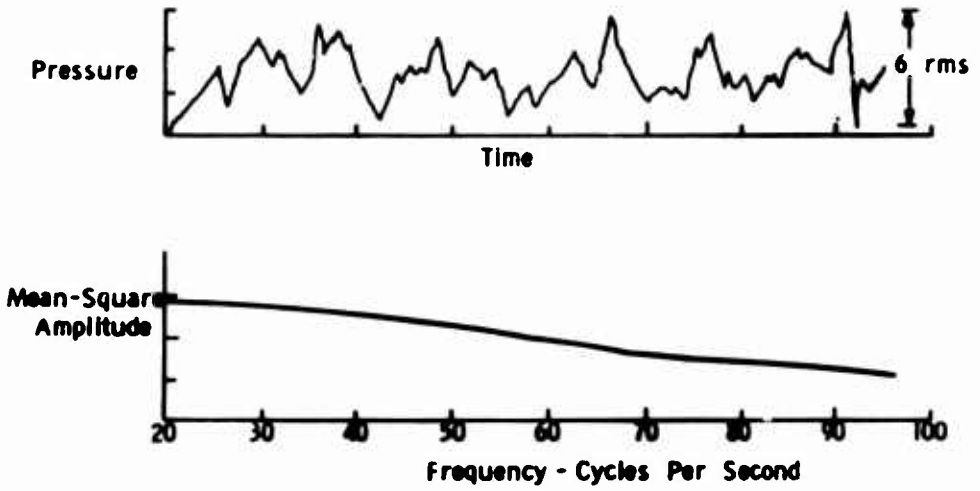

FIGURE 7

Turbulence and Distortion Profiles
Mo= 2.2
Fixed Centerbody Position & Engine Speed

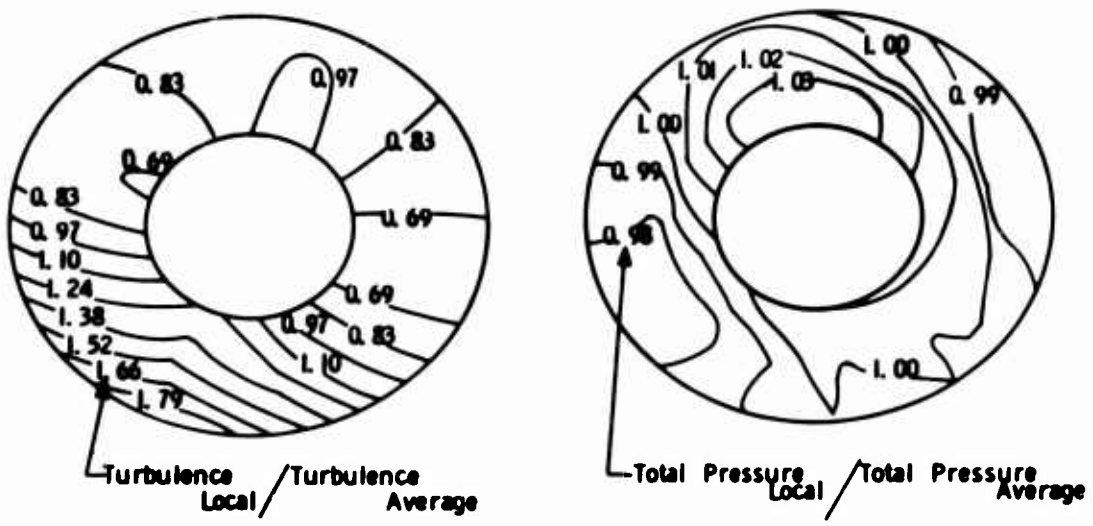

a. Turbulence

b. Distortion

FIGURE 8

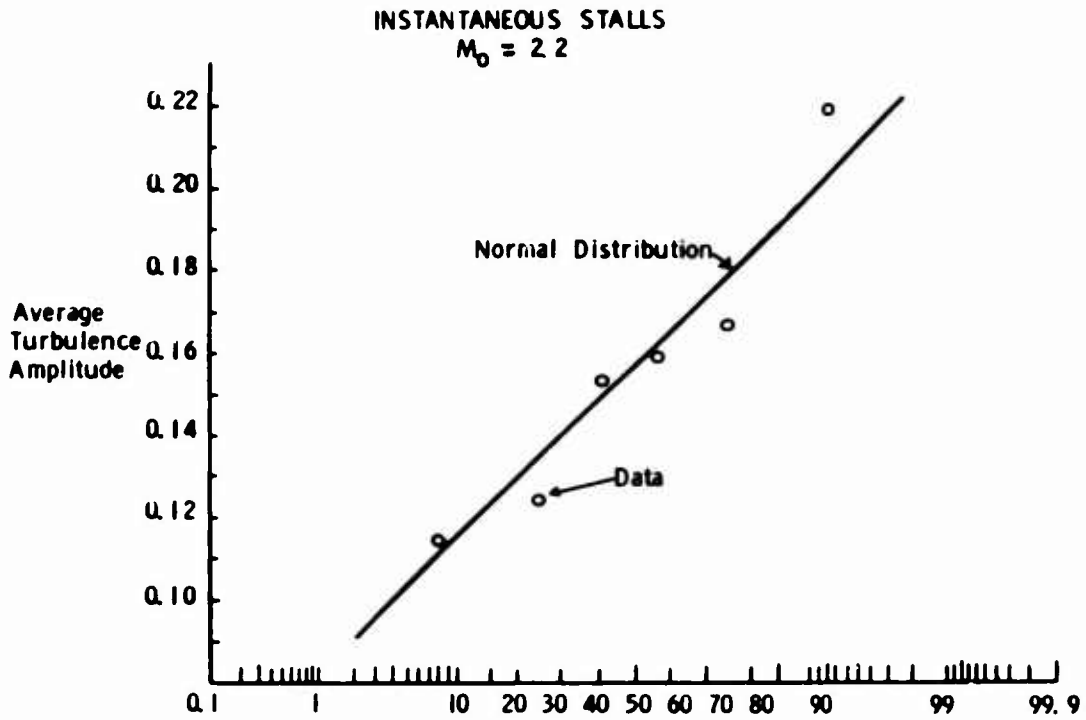

FIGURE 9

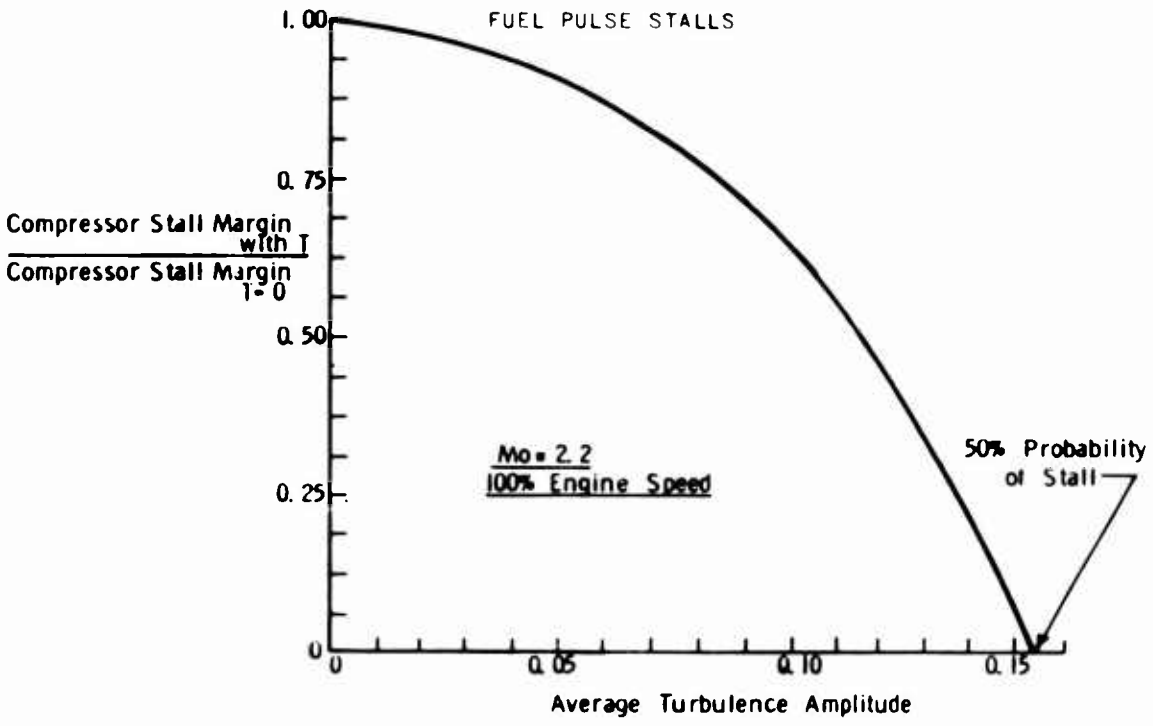

FIGURE 10

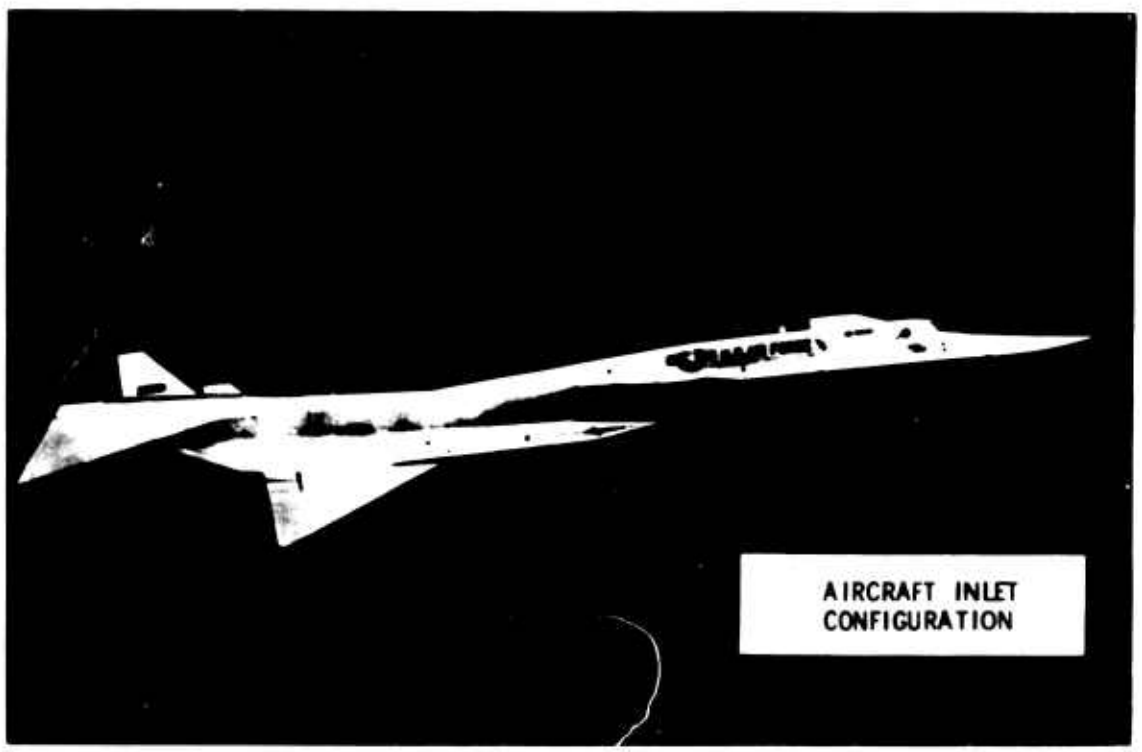

FIGURE 11

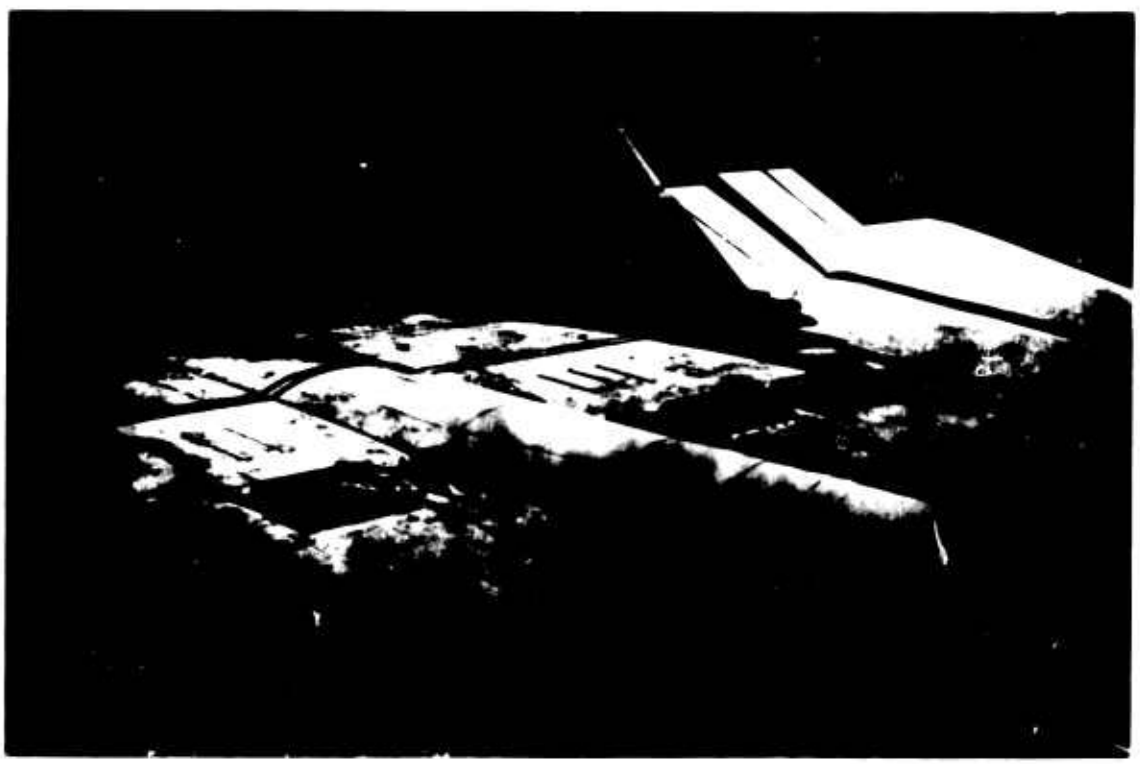

FIGURE 12

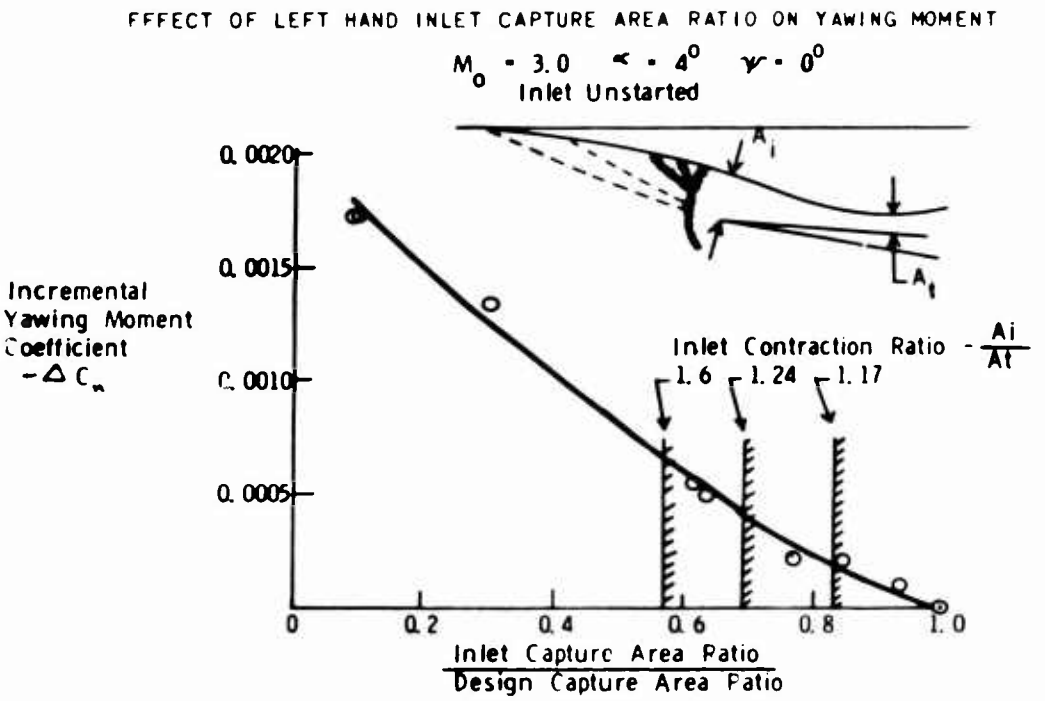

FIGURE 13

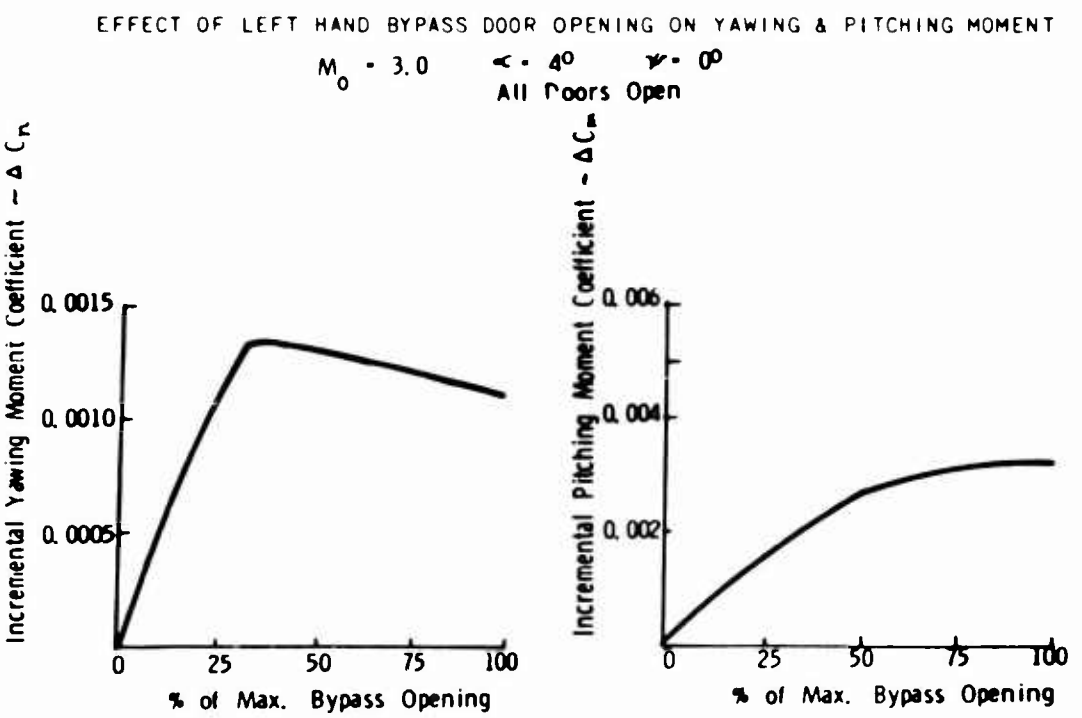

FIGURE 14

MAJOR FORCES FROM INLET UNSTART AND BYPASS OPERATION

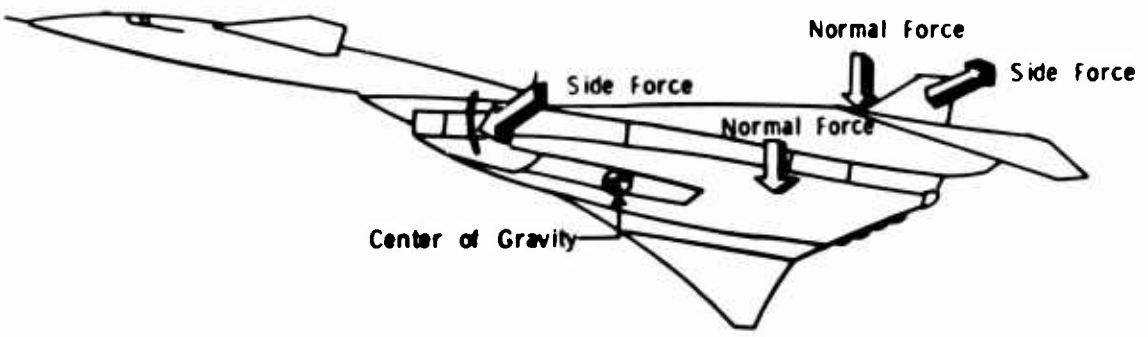

Inlet Spillage Causes

- Yaw
- Roll

Bypass Operation Causes

- Yaw
- Pitch

FIGURE 15

ESTIMATED AIRCRAFT RESPONSE DURING LEFT HAND INLET UNSTART

M_0 = 3.0 Light Weight, No Stability Augmentation System, No Pilot Control

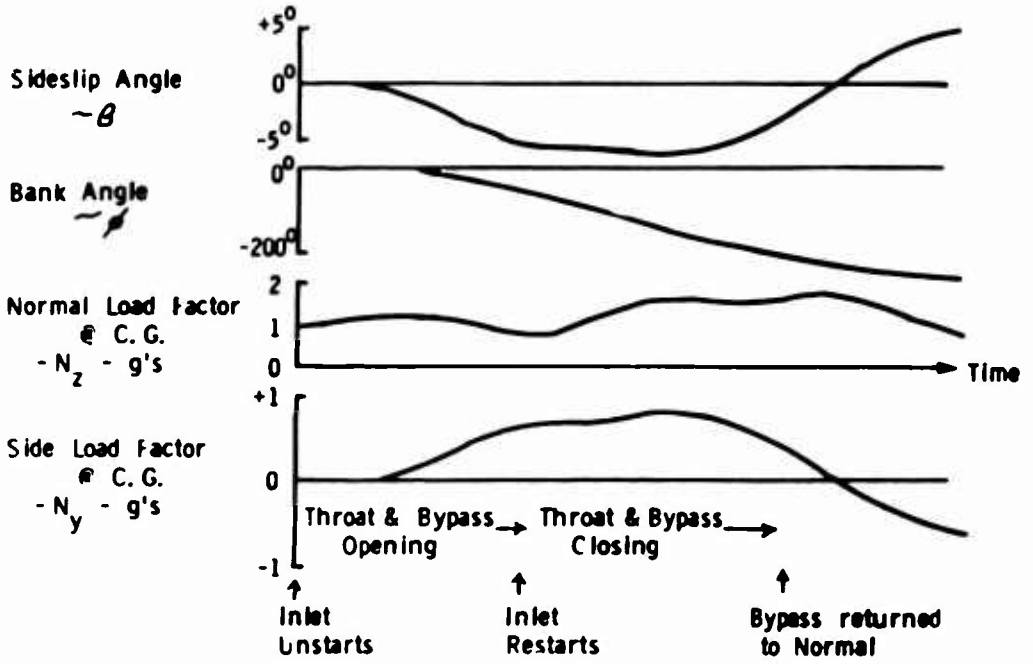

FIGURE 16

A DISCUSSION OF THE USE OF THRUST FOR CONTROL OF VTOL AIRCRAFT

By Seth B. Anderson,
Ames Research Center
Moffett Field, Calif., U.S.A.

SUMMARY

The use of engine thrust to control VTOL aircraft in hover has been examined to point out the importance of certain items that affect handling qualities. Information is based on the results of NASA-Ames Research Center tests using the piloted six-degree-of-freedom motion simulator and the X-14A variable stability and control aircraft. The discussion includes consideration of the use of thrust vectoring and thrust modulation. The results indicate that thrust vectoring to produce lateral translation can be used satisfactorily, reducing roll angular acceleration requirements. When thrust modulation is used for control, control lags must be minimized to avoid oscillatory tendencies.

A DISCUSSION OF THE USE OF THRUST FOR CONTROL OF VTOL AIRCRAFT

By Seth B. Anderson*

1. INTRODUCTION

Control of VTOL aircraft in hover and low-speed flight has been an important item in pacing the development of this type of aircraft. The required reaction forces for attitude control during hover have commonly been achieved by the use of engine compressor bleed air. This method, used on early jet lift VTOL aircraft such as the Shorts SC-1, Bell X-14A, and Lockheed XV-4, has been successful whenever a sufficient quantity of bleed air was available. More recently, particularly for larger VTOL aircraft such as the EWR VJ-101 and Dornier DO-31, engine thrust has been used directly for control. This method has the obvious advantages of improved efficiency and lighter weight, but when it is used, certain items should be considered carefully to insure satisfactory handling qualities. Handling qualities are affected by:

Thrust vectoring authority
Thrust response (engine time constant)
Excess thrust for maneuvering
Gyroscopic coupling
Engine failure
Cross coupling
Ingestion and recirculation of exhaust gases

The first three items are basic to any configuration, while the last four depend on the configuration, and although important, will not be discussed in detail in this paper.

The purpose of this paper is to present some information, recently obtained by NASA, on the use of engine thrust for control of VTOL aircraft. Information is based primarily on the results of NASA-Ames Research Center tests using the piloted six-degree-of-freedom motion simulator and the X-14A variable stability and control aircraft.

2. RESULTS AND DISCUSSION

Thrust modulation and thrust vectoring are used in the following ways for control of VTOL aircraft: Roll and pitch moments as well as height can be controlled by thrust modulation while translation and yaw can be controlled by thrust vectoring. Because the requirements for controlling roll are generally demanding, the discussion has been

---

*Chief, Flight and Systems Simulation Branch, Ames Research Center, NASA, Moffett Field, California 94035.

oriented toward the roll axis. It should be recognized that the research thus far covers only the hover mode and further research studies should include the transition area.

2.1 Simulator Study of Thrust Vectoring

The proper use of thrust vectoring is important since angular acceleration control power may be reduced if, instead of tilting the aircraft, the pilot uses thrust for translation. A translational control has obvious advantages for large aircraft for which large amounts of roll inertia severely limit the angular response. The amount of translational acceleration desired must be defined as well as the method of controlling it. Preliminary information on a direct translational control system has been reported (1) and the method of control is shown schematically in Fig. 1. The control which employed a movable vane in the engine exhaust was investigated in two phases. Tests were first made in the Ames piloted multiaxis motion simulator (Fig. 2) and then in flight in the X-14A jet lift VTOL aircraft. The simulator tests sought answers to two questions: (1) how to control a lateral thrust vectoring vane from the cockpit (i.e., by a thumb controller or by stick deflection), and (2) how much to deflect the vane for satisfactory maneuvering. Answers to these questions were needed to expedite the flight test program.

2.1.1 Effect of type of controller.- Three methods of operating a controller were studied: (1) vane deflection commanded by the stick, (2) vane deflection proportional to bank angle, and (3) vane deflection by a thumb controller mounted on top of the stick. In the first method the vane was geared directly to the stick so lateral acceleration, A_y, was proportional to stick deflection. When pilots evaluated this method of control by a series of lateral quick stops and reversals, phasing problems between roll attitude and side acceleration occurred regardless of the gains. This control method could not be made satisfactory with a rate-damped system, and with an attitude command system the pilot did not have precise control during a roll reversal when side velocity was momentarily opposite to that normally associated with a given bank angle. In the second method, with side acceleration proportional to bank angle and an optimized rate-damped system, the control method was found to be satisfactory when the side acceleration for a given bank angle φ was increased by a factor of 1.5

$$A_y = 1.5(g \sin \varphi)$$

For the third method two types of thumb controller action, on-off (bang-bang) and proportional, were studied. The proportional thumb controller was preferred because of the pilot's desire to modulate side acceleration for "fine" control.

2.1.2 Effect of amount of side acceleration available.- The pilot rating of maximum amounts of side acceleration, for both the proportional

and on-off thumb controller, are presented in Fig. 3. The preferred range was 0.08 to 0.13 g, depending somewhat on the type of controller used. The minimum for adequate maneuvering was 0.08 g while values greater than 0.13 g were uncomfortable for the pilot. As expected, the on-off controller was less satisfactory at the higher g values because the pilot tended to induce an oscillation (PIO) laterally as a result of the side force against his arm.

2.1.3 Effect of type of controller and maximum roll control power.- When the results from the simulator study of the various methods of control (Fig. 4) are compared with the conventional (vane inoperative) roll-to-translate method of control, two points are evident: (1) The vane improved (lower number) pilot rating; (2) programming the vane as a function of bank angle was not as desirable as actuating the vane by a thumb controller on top of the stick. The method of coupling side acceleration with bank angle had the obvious benefit of requiring smaller angular displacement and, hence, lower maximum angular acceleration ($\ddot{\varphi}$) to achieve a given side acceleration. When high values of $\ddot{\varphi}$ were used, however, the system was too sensitive and was rated slightly less desirable than the conventional system. The separate thumb controller was clearly easier to use for maneuvering sideways at the lower values of $\ddot{\varphi}$ and the pilot needed only a small amount of $\ddot{\varphi}$ to correct for inadvertent upsets. The pilot desired attitude stabilization in roll which would eliminate for all practical purposes any need for additional angular roll control ($\ddot{\varphi}$).

2.2 Flight Study of Thrust Vectoring

The flight evaluation of the side acceleration vane was made using the X-14A jet lift VTOL aircraft shown in Fig. 5. The close-up shows the vane control surface, complete with outrigger airfoils needed to improve effectiveness and reduce longitudinal cross coupling. The variable stability and control features of the X-14A permitted a systematic study to be made of the effect of variations in roll control power (angular acceleration) and sideward acceleration without the distraction of any cross-coupling effects such as roll due to vane deflection. A satisfactory value of roll damping was used for these tests. The evaluation maneuver consisted of a lateral translation of about two wing spans (approximately 70 ft) as well as flying around an obstacle course. These tests were made out of ground effect in calm air since only maneuvering aspects were to be evaluated. The proportional thumb controller method of regulating the vane, evaluated in the simulator studies, was essentially unchanged for the flight program.

2.2.1 Effect of side acceleration values.- The first series of flight tests were conducted to determine the amount of side acceleration desired for wings-level lateral offset maneuvers. The results (Fig. 6) indicate that A_y of the order of 0.03 g is acceptable and 0.10 g is satisfactory. In terms of the amount of time required to move sideward one wing span (33 ft), the foregoing A_y values correspond to approximately 13 and 7 sec, respectively. When low values of A_y were used,

the response was too sluggish and too much lead time was required to maneuver precisely. Higher values of A_y (greater than 0.10 g) were desired when moving forward as well as sideways. In flat turns, however, at 20 knots forward speed, the maximum side force capability of the vane (0.15 g) was insufficient to offset the centrifugal force, and the pilot preferred to add bank angle. At the high A_y values, there was, of course, an appreciable thrust decrement and a consequent loss of altitude. This demanded adaptation since the pilot no longer could use bank attitude as a reference for height adjustment.

2.2.2 Effect of reductions in roll control power.- Data in Fig. 7 show how pilot rating changed as roll control power, $\ddot{\Phi}$, was varied. The flight results confirm the simulator tests in that less maximum angular acceleration was needed to obtain a satisfactory pilot rating when the vane was used to reposition the aircraft laterally. It should be recognized that in this case the pilot was not evaluating control power in the usual sense; roll control was used only to keep the wings level. As angular acceleration was reduced for the conventional (roll to translate) method of control, the airplane became too sluggish and the pilot used full control to speed up the repositioning. Consequently, pilot rating deteriorated because no control margin was available for correcting trim or upsets.

Several additional observations can be made from the data in Fig. 7 relative to the use of thrust for translational control. First, it was not possible to define the minimum $\ddot{\Phi}$ needed for maneuvering out of ground effect with the thrust vectoring (vane) system tested because additional roll control power was needed to fly in ground effect disturbances during takeoff and landing since the pilot could not select lower control power values ($\ddot{\Phi}$) in flight. It would be expected that lower values of $\ddot{\Phi}$ than those shown would be entirely satisfactory for the thrust vectoring control out of ground effect. With the rate stabilization available for the X-14A tests, the pilot had a combined task of translation and roll stabilization. If attitude stabilization were used, some very minimal angular acceleration would be required to allow the pilot to adjust bank angle for conditions such as touchdown on a non-level surface. A second point is that when a rate-damped SAS was used for landing and takeoff of the X-14A, roll control power could not be reduced below approximately 0.6 rad/sec^2 regardless of the type of control method used. In other words the disturbances due to ground effect cause attitude upsets that were not alleviated by the vane control method alone. For this reason, as well as to reduce roll disturbances introduced inadvertently by the pilot, attitude stabilization would be required with the vane control system. Finally, the difference between the lowest value of control power acceptable (0.6 rad/sec^2) and the value where the curves intersect (0.9 rad/sec^2) is an indication of the minimum amount of control power needed for conventional (roll to translate) maneuvering. Thus, 0.6 rad/sec^2 needed for ground-induced upsets and disturbances plus 0.3 rad/sec^2 required for minimum maneuvering, a total value of 0.9 rad/sec^2, represents the minimum total control power

required to operate the X-14A aircraft with a rate-damped stabilization system. More than 0.9 rad/sec^2 is needed, of course, for more rapid maneuvering and for gusty air.

2.2.3 Effect of vane response.- Another factor to be considered in evaluating the thrust vectoring method is the time constant (response) of the control system. The system used had a first-order time constant of approximately 0.2 second. Although systematic tests were not conducted to evaluate their effects, larger time constants would probably degrade pilot opinion. In recent NASA Langley tests (2) to investigate height control requirements time constants greater than 0.5 second presented little problem during hovering (away from the ground); however, during landing the pilot had to alter his technique (to reduce overcontrolling) to allow a safe touchdown. It follows that, if precise sidewards maneuvering is needed (for operation in close quarters), low control system time constants are needed for the thrust vectoring system.

2.2.4 Use of vectored thrust for larger aircraft.- One can only speculate at this time from the limited testing on the X-14A how acceptable a lateral acceleration vane would be for larger aircraft. Other than the obvious advantage of easing the angular acceleration roll problem for high-inertia aircraft, it would appear logical that when hovering larger span aircraft near the ground, the pilot might prefer to use vectored thrust because he would have less tendency to strike a wing tip. To check this hypothesis the wing span of the X-14A was doubled, as shown in Fig. 8, by installing lightweight tubes and wing tips of orange-colored styrofoam spheres.

Three pilots then evaluated the thrust vectoring control as well as the conventional roll-to-translate method for the extended span aircraft in air taxi, quick reversals, and obstacle course maneuvers. Other than a barely perceptible tendency to hover at a higher altitude, none of the pilots preferred to use thrust vectoring for fear of hitting a wing tip in operational-type maneuvers. Apparently this simulation of size was too crude to result in meaningful conclusions. Although the tests generally showed no serious limitations to the use of the vane control, it was apparent that this type of control would be used more for air taxi type maneuvers (slow, relatively short distances). For quicker repositioning, the pilot would prefer to re-aline the aircraft in a flat turn. The flat turn maneuver requires training because the side forces are not natural. Further research should be conducted with the vane control in slow speed flight; however, as noted previously, attitude stabilization is needed to unburden the pilot and thereby allow a more accurate assessment of the vane control method.

2.3 Thrust Modulation

A slowly responding turbojet engine will require the pilot to lead the output to compensate for the sluggish behavior. Little information is available to aid in defining tolerable levels of engine

time-constant for VTOL thrust modulation. Engine time-constant is of particular importance when larger thrust engines, such as the deflected cruise type, are used for control in hover and when fan thrust is controlled by varying fan rpm. There are two areas of primary interest to consider when thrust modulation is used for controlling VTOL aircraft: (1) the effect of thrust time constant on control requirements, and (2) the effect of reducing total lift when a control moment is applied. The following discussion primarily concerns the effect of time constant.

2.3.1 Effect of lag on control requirements.- Current control specifications (3) for VTOL aircraft are expressed in terms of an attitude change after a given time following a control input. It is shown in Fig. 9 that as control lag is increased, the moment needed to produce a given attitude increases, depending on the time increment. Since the attitude change for the roll axis is taken after 0.5 sec, it is apparent that even a low value of control lag (0.2 sec) doubles the required moment. The attitude change for the yaw and pitch axes is taken after 1 sec so the effect of lag on moment requirement is less severe.

2.3.2 Types of control lags tested.- There are two primary control lags of interest when engine thrust is used as part of the control system. These are the first-order and second-order lags whose characteristics are shown in generalized form in Fig. 10. The shape of the first-order-type curve is typical of large turbojet engines. In this case, the thrust response is dominated primarily by large rotary inertia. The initial response depends on the addition of fuel and the increase in exhaust temperature. The final steady-state thrust value is reached with no overshoot. The second-order system is typical of small lift engines with high thrust-to-weight ratios and lift fans.

The primary variables selected for the study on the piloted six-degree-of-freedom motion simulator were the time to reach 63 percent of the final steady-state value and the percent initial overshoot. Such nonlinear effects as actuator rate-limiting and control system inertia which affect control power requirements were not included in this simplified program.

2.3.3 Effect of first-order lag in roll control.- It was of interest to examine how different types of control systems were affected by first-order lags, since a more sophisticated control system might be more tolerant of poor thrust response. All the control systems used optimum values of control sensitivity and damping. Zero lag was maintained about the pitch and yaw axes. Results are shown in Fig. 11 for unstabilized (acceleration), rate-damped, and attitude command systems. A number of observations can be made from these results: (1) At zero time lag only the control systems with stabilization feedback loops were rated satisfactory, (2) lags could reach approximately 0.2 sec before stabilized systems were rated unsatisfactory, and (3) the more sophisticated (attitude command) system suffered more with the larger control lags. This poorer behavior is believed to be due in part to the fact

that the response of the attitude stabilization system also contains a similar value of lag. For all types of control systems the pilots complained about the feeling of reduced damping and the tendency toward pilot-induced oscillations (PIO). As lag was increased, precise quick stops and reversals became more difficult and eventually even steady hovering became impossible. It can be shown in a closed-loop stability analysis that as loop gain is held constant and lag is increased, both frequency and damping are reduced and instability eventually results. In the simulator tests increasing the damping ratio of the attitude stabilization to the order of 1.5 reduced the oscillatory behavior, but with this high value of damping a sluggish response resulted in spite of the large control power used (2.0 rad/sec^2).

2.3.4 Effect of lag with increased control sensitivity.- Increasing control power to maintain the same bank angle after 1 second did little to improve the situation. As shown in Fig. 12, pilot rating still deteriorated as the PIO tendency remained. A nonlinear type of control system could possibly reduce the PIO tendency; however, tests to determine this effect were not conducted.

2.3.5 Comparison of first- and second-order lag systems.- The overall thrust response of lift engines is inherently more rapid than that of larger turbojet engines. However, depending on the degree of sophistication of the fuel control, there may be some overshoot of the steady-state value. Because the initial thrust response may not be rapid if the overshoot is reasonably low, the stability and piloting characteristics of a second-order system might be expected to be no better than that of a first-order system. The simulator results shown in Fig. 13 bear this out; the pilot again complained about PIO tendencies. There is essentially no difference in pilot rating between the two systems when the second-order system has a 3.5-percent overshoot which corresponds to a damping ratio of 0.7. The fact remains that with the type of characteristics shown, control with thrust-modulated lift engines should still be adequate since pilot rating is satisfactory below a response time of approximately 0.2 sec, well within the time response capability of current lift engines.

2.3.6 Effect of overshoot with second-order lag.- An additional consideration in the thrust modulation characteristics of some types of lift engines and also lift fans when used for control is the amount of tolerable overshoot. The results in Fig. 14 indicate that pilot rating deteriorates as overshoot percentage increases. These results were obtained with an attitude stabilized control system using a constant value of roll control lag of approximately 0.12 sec (to 63 percent). These larger values of overshoot are obviously undesirable and could be avoided by proper design of the fuel control system. In the case of lift fans, lead terms could be introduced with an electronic control to improve lag and reduce overshoot.

2.3.7 Thrust margin required for maneuvering.- When thrust modulation is used for attitude control for pitch or roll, a loss in altitude may occur unless sufficient excess thrust is available. Factors which affect the amount of excess thrust required to maintain altitude for a commanded change in roll attitude include the moment of inertia in roll, I_x, the distance between the engines and the roll axis, d, the weight of the aircraft, W, and the geometric distribution and excess thrust of the lift engines.

Tests were conducted on the piloted six-degree-of-freedom motion simulator to evaluate excess thrust requirements during moderately brisk lateral sidestep maneuvers. The results of the simulator studies are presented in Fig. 15, in terms of the usual pilot rating boundaries. Shown in the satisfactory region is the VJ-101 aircraft. It is shown that the amount of excess thrust required to achieve a satisfactory pilot rating increases rapidly as the parameter I_x/dW increases beyond 0.1. At the larger values of I_x/dW the pilot complained about the inability to maintain altitude during even mild roll reversals. Further studies need to be carried out on this problem to include pitch-roll coupling and the effect during transition.

3. CONCLUSIONS

The use of engine thrust to control VTOL aircraft has been examined to point out the importance of certain items that affect handling qualities. The following conclusions have been drawn from piloted simulator and flight tests related to the use of engine thrust for control by vectoring and modulation:

1. Limited flight tests showed no serious limitations to the use of a vane in the engine exhaust to vector thrust for sideways translation.

2. When using thrust vectoring directly to translate sideways the pilots preferred a separate proportional type controller mounted on top of the stick rather than direct gearing to the stick or programming the vane as a function of bank angle.

3. Values of lateral acceleration of the order of 0.10 g were satisfactory for normal sideways maneuvering. Values larger than 0.15 g are desired for moving forward and sideways.

4. Compared to the conventional roll-to-translate method, using the vane reduced roll control power requirements. It was necessary to provide only enough roll control power to adjust for wings leveling. Attitude stabilization in roll was needed to use the vane control method effectively.

5. When thrust modulation was used for control, simulator tests showed that control lags below 0.2 sec were satisfactory for stabilized

hover control systems. For the type of system used the attitude command system deteriorated more rapidly with increasing control lag than did the rate-damped system.

6. There was essentially no difference between pilot rating of first- and second-order lag systems, provided the initial overshoots for the second-order system were small.

7. Despite increases in control power to maintain a constant bank angle after 1 sec, pilot rating still deteriorated as control lag was increased.

8. Regardless of the type of control system used, the pilots complained about poor damping and PIO tendencies as control lag was increased.

4. REFERENCES

1. Anderson, Seth B.: Considerations for Revision of V/STOL Handling Qualities Criteria. NASA SP-116, 1966, p. 229.

2. Kelly, James R.; Garren, John F., Jr.; and Deal, Berry L.: "Flight Investigation of V/STOL Height-Control Requirements for Hovering and Low-Speed Flight Under Visual Conditions." NASA TN D-3977, 1967.

3. Recommendations for V/STOL Handling Qualities, AGARD Rep. 408, Oct. 1962.

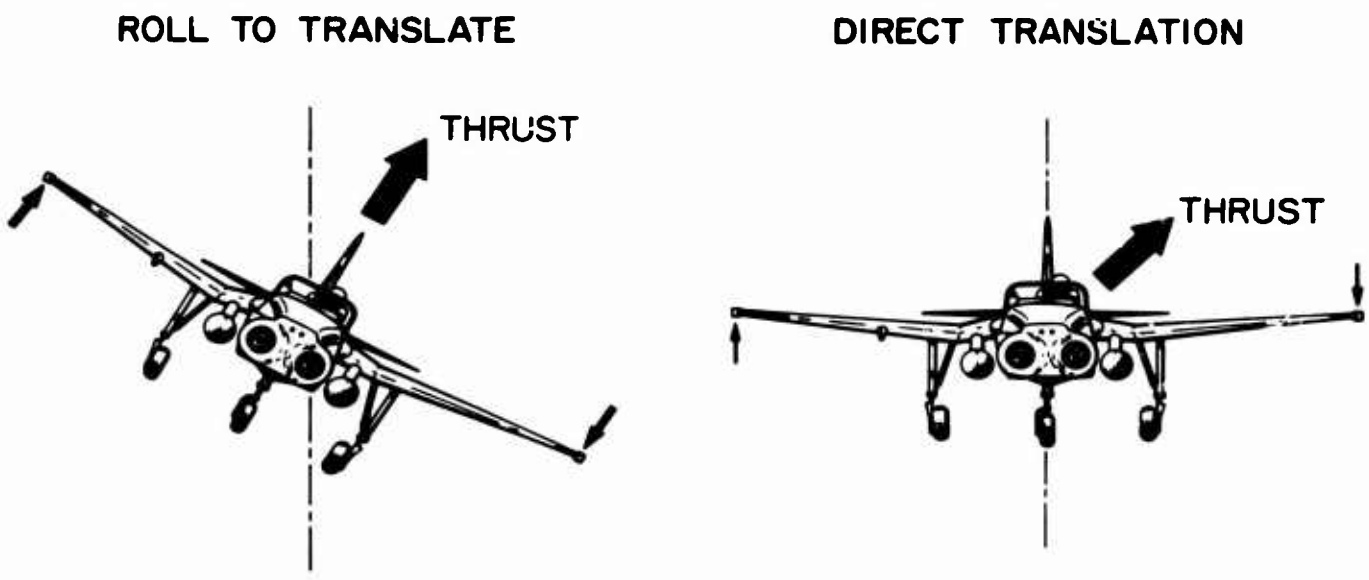

Fig. 1 Translational control methods

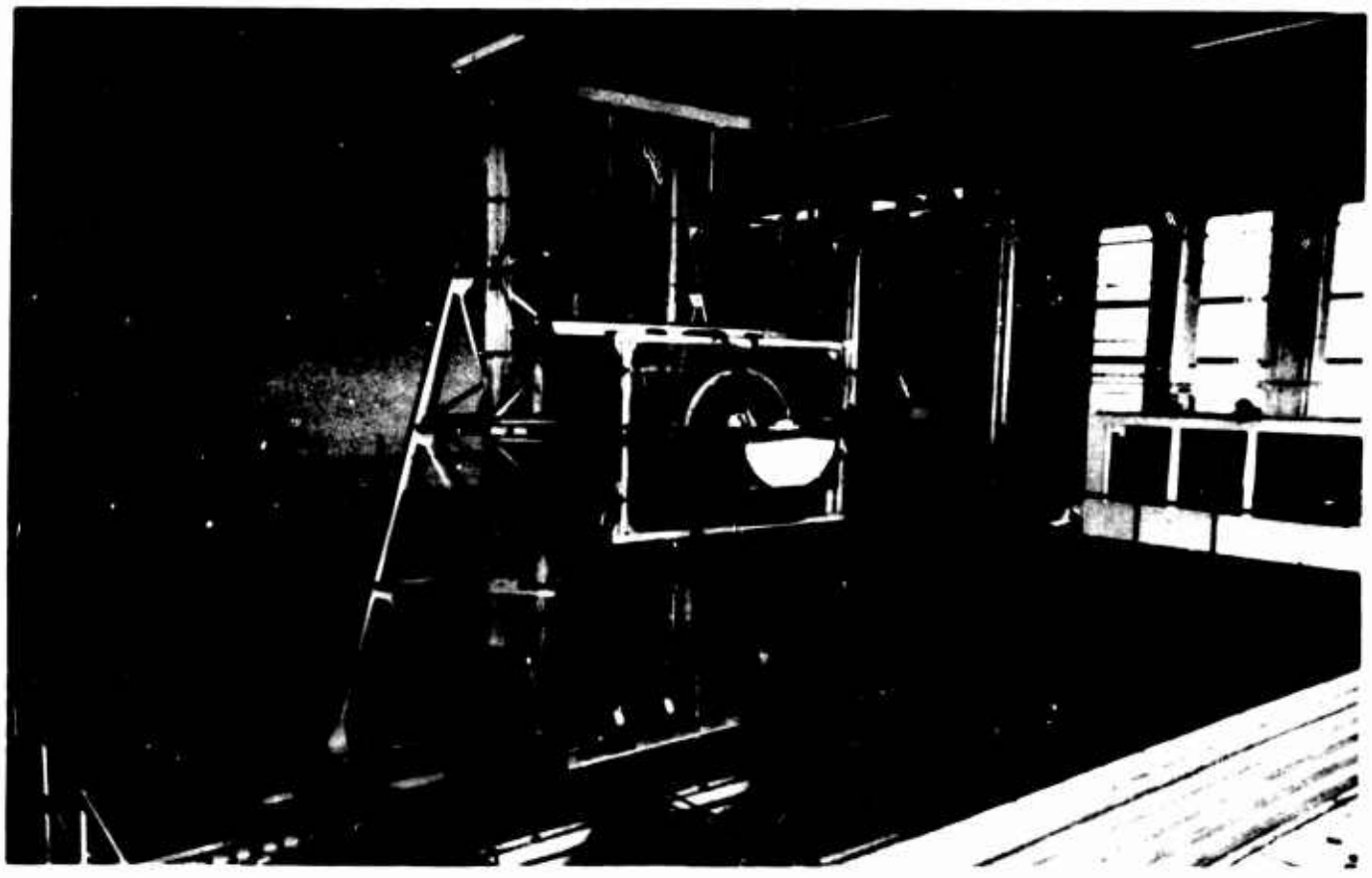

Fig. 2 Six-degree-of-freedom-motion simulator

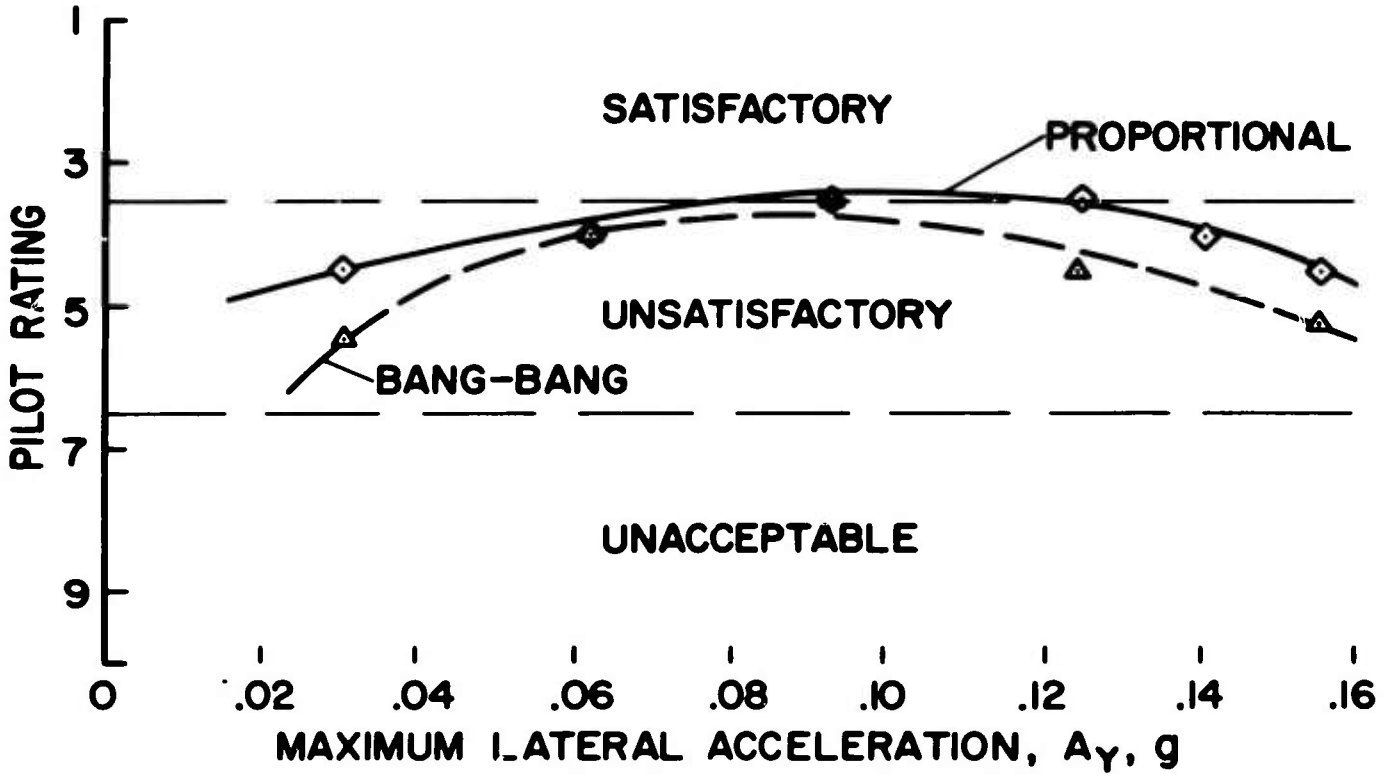

Fig. 3 Effect of lateral acceleration on pilot rating for two types of thumb controllers; six-degree simulator

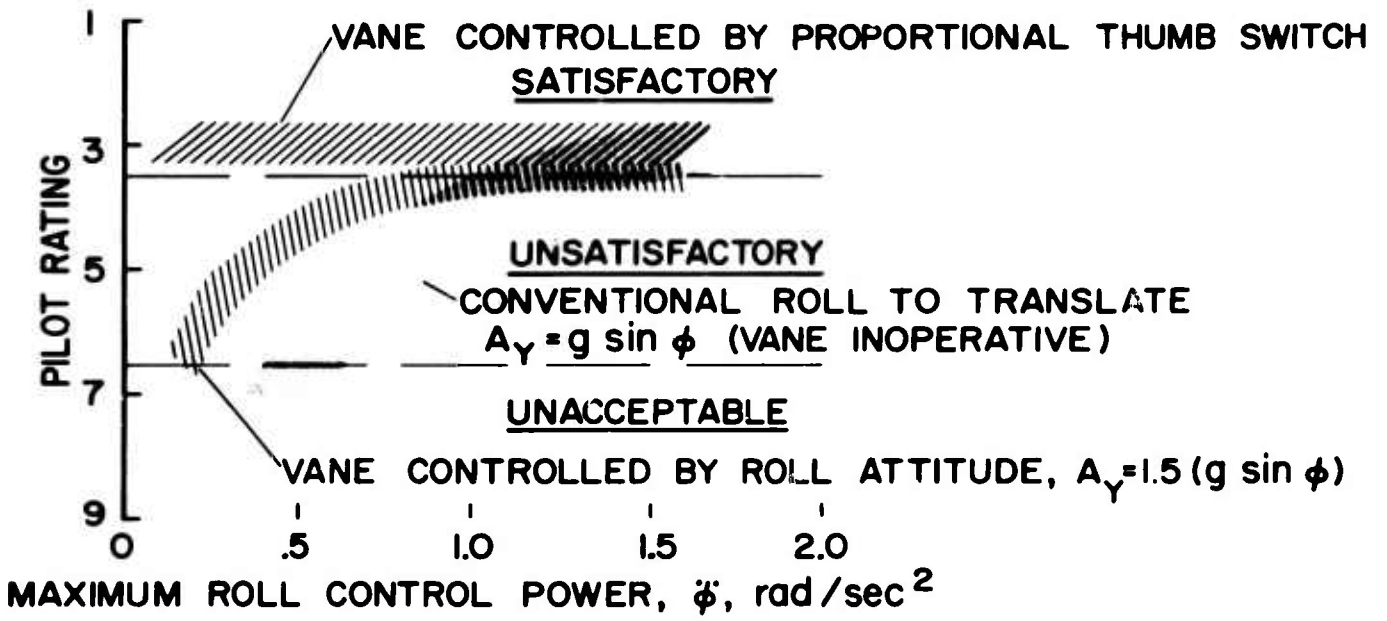

Fig. 4 Effect of various lateral control methods on pilot rating; six-degree simulator

Fig. 5 X-14A VTOL aircraft equipped with lateral acceleration vane

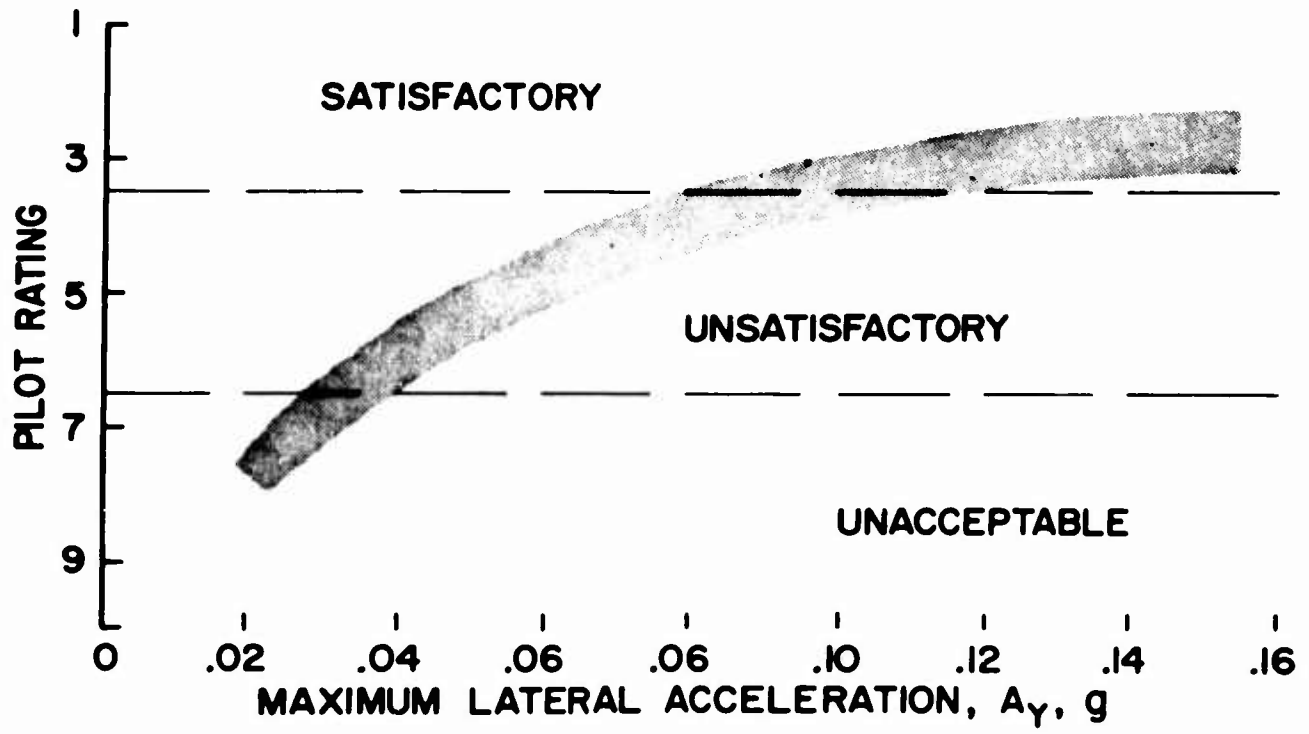

Fig. 6 Effect of lateral acceleration on pilot rating, X-14A

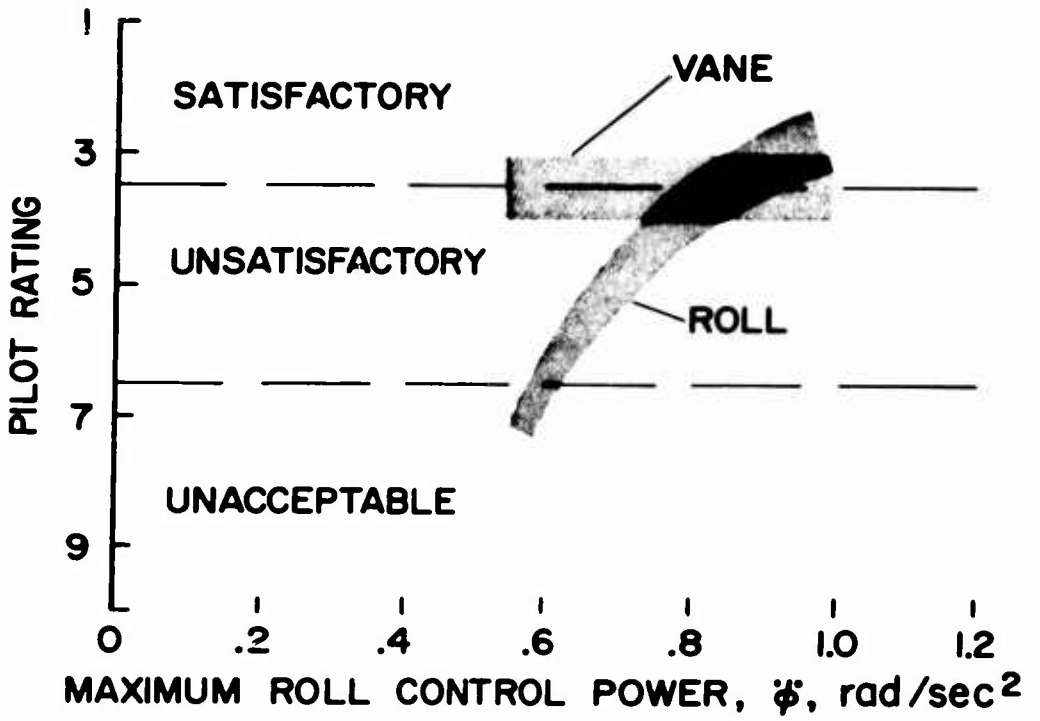

Fig. 7 Comparison of vane and conventional roll control methods for lateral maneuvering, X-14A

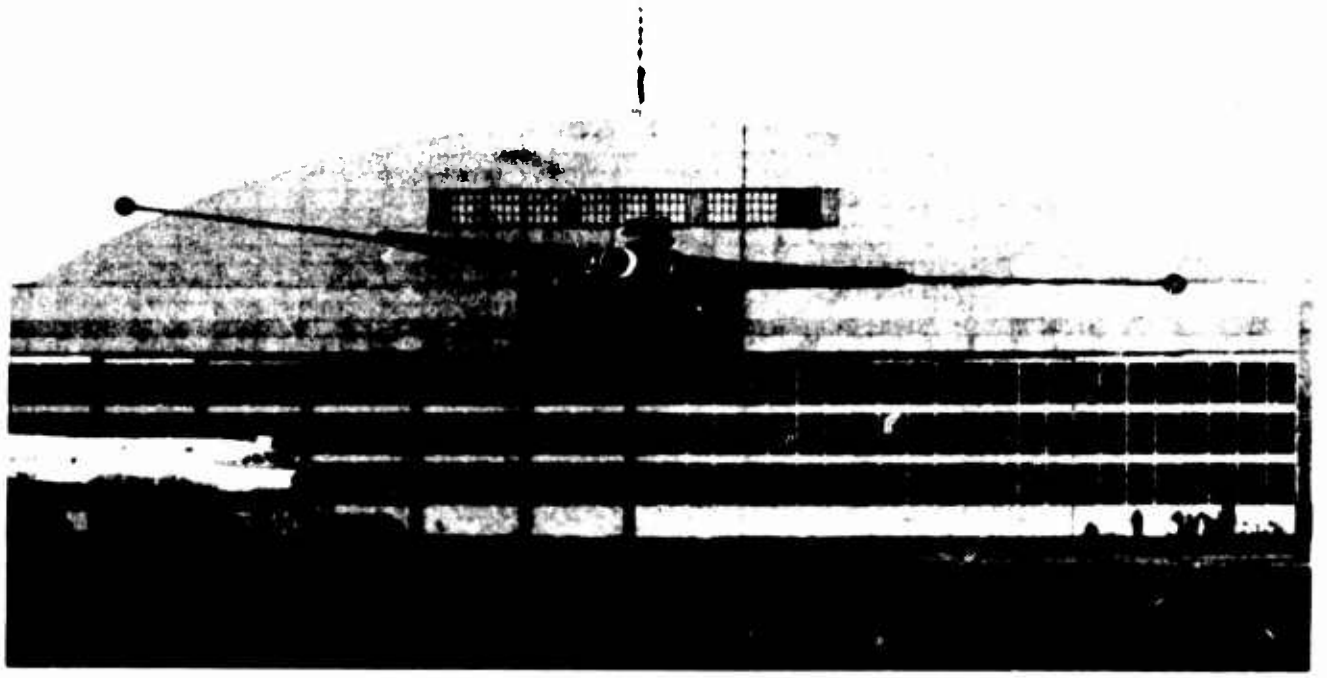

Fig. 8 X-14A VTOL aircraft with wing tip extensions

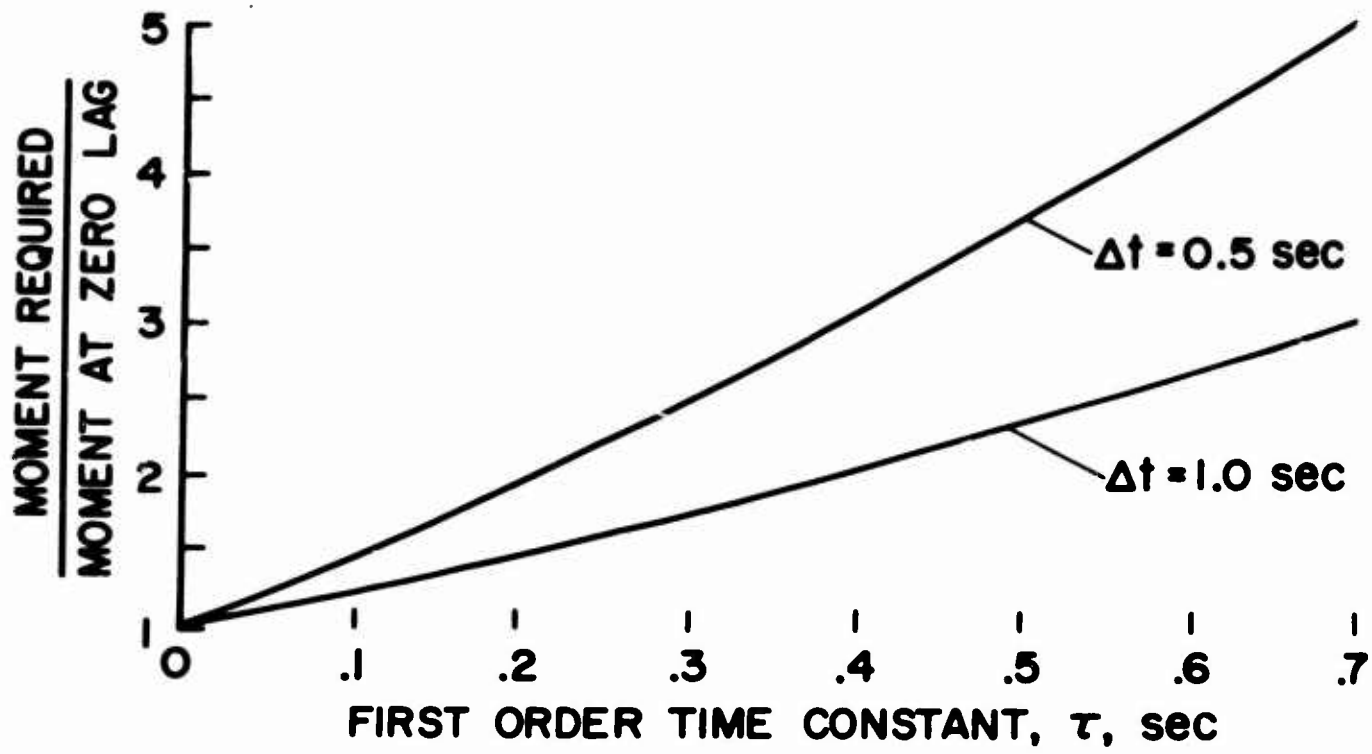

Fig. 9 Effect of time constant on moment required for attitude change

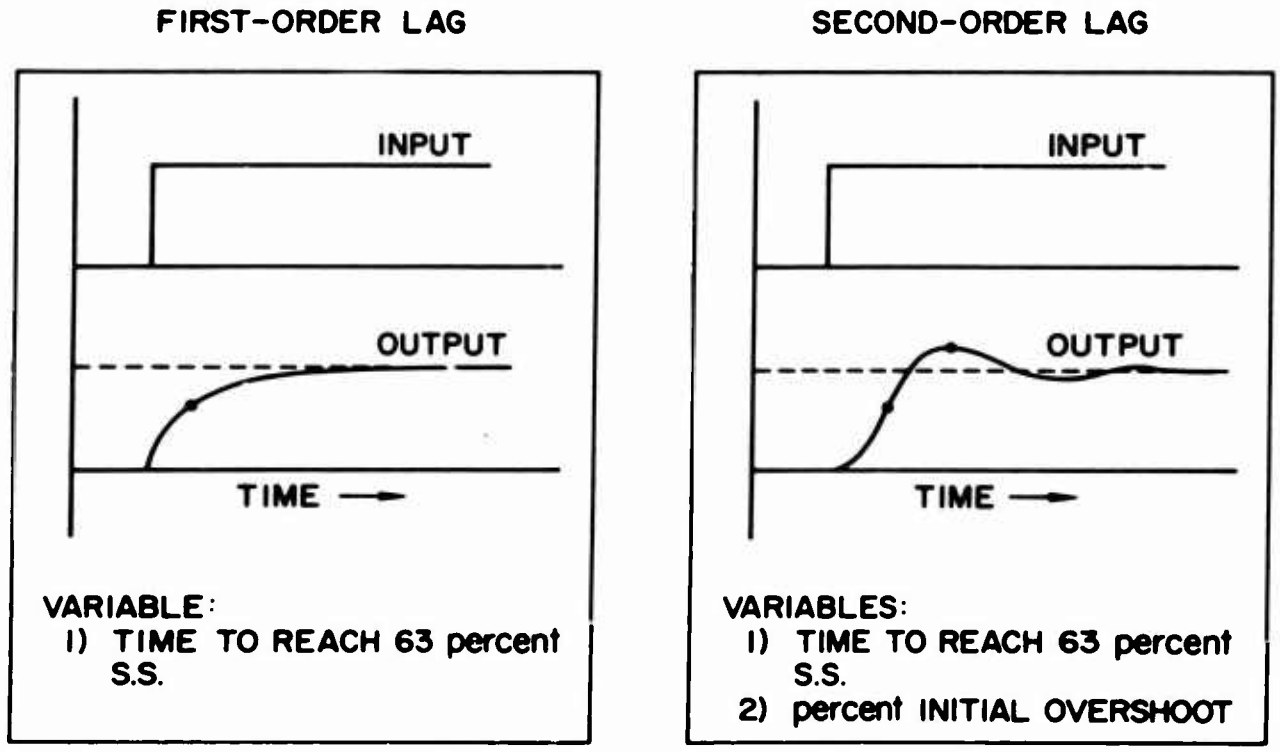

Fig. 10 Types of control lag tested

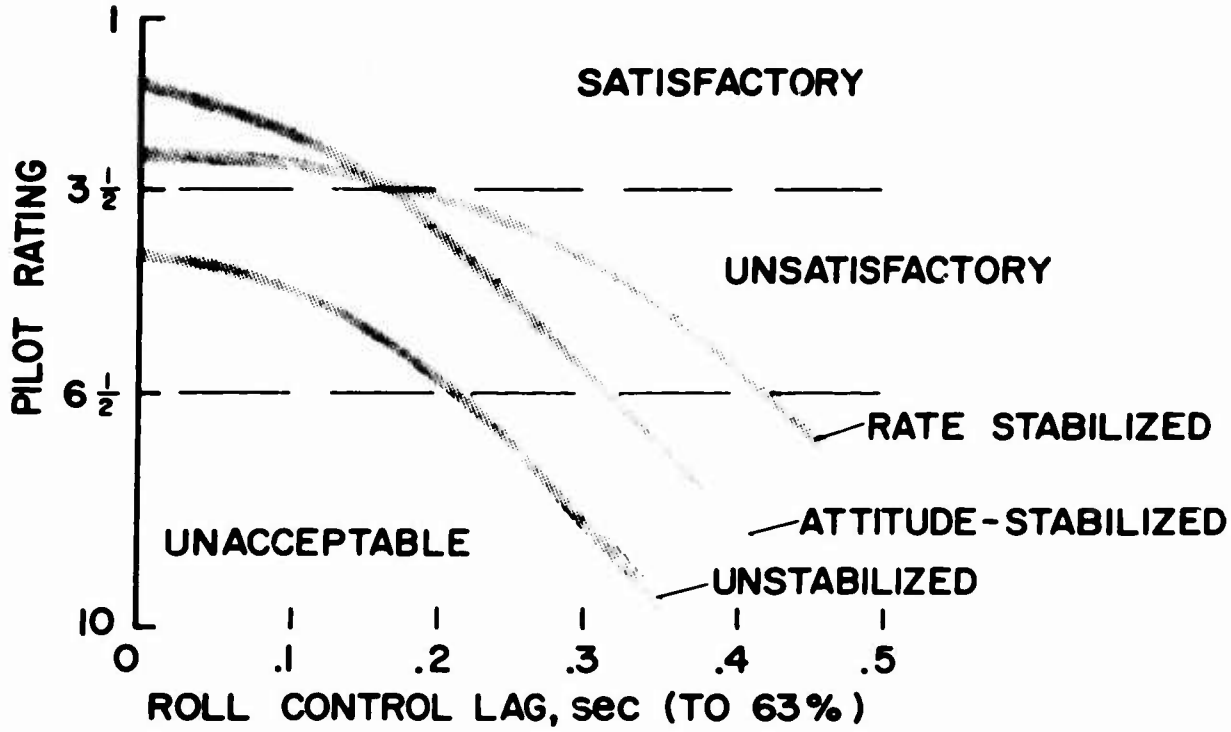

Fig. 11 Effect of first-order lag in roll control, six-degree simulator

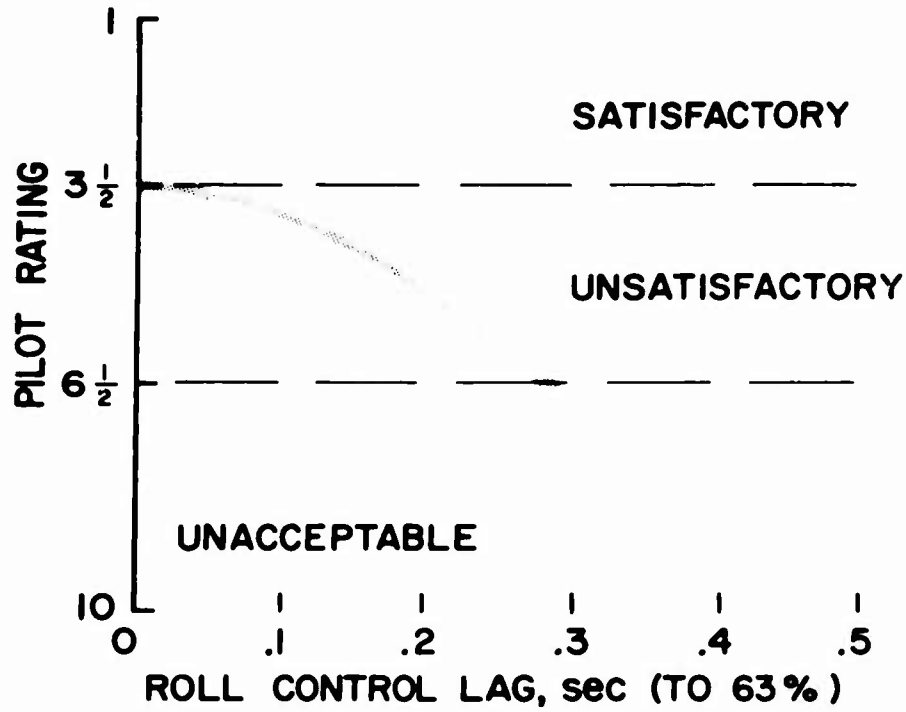

Fig. 12 Effect of lag on pilot rating (bank angle after 1 sec kept constant); six-degree simulator

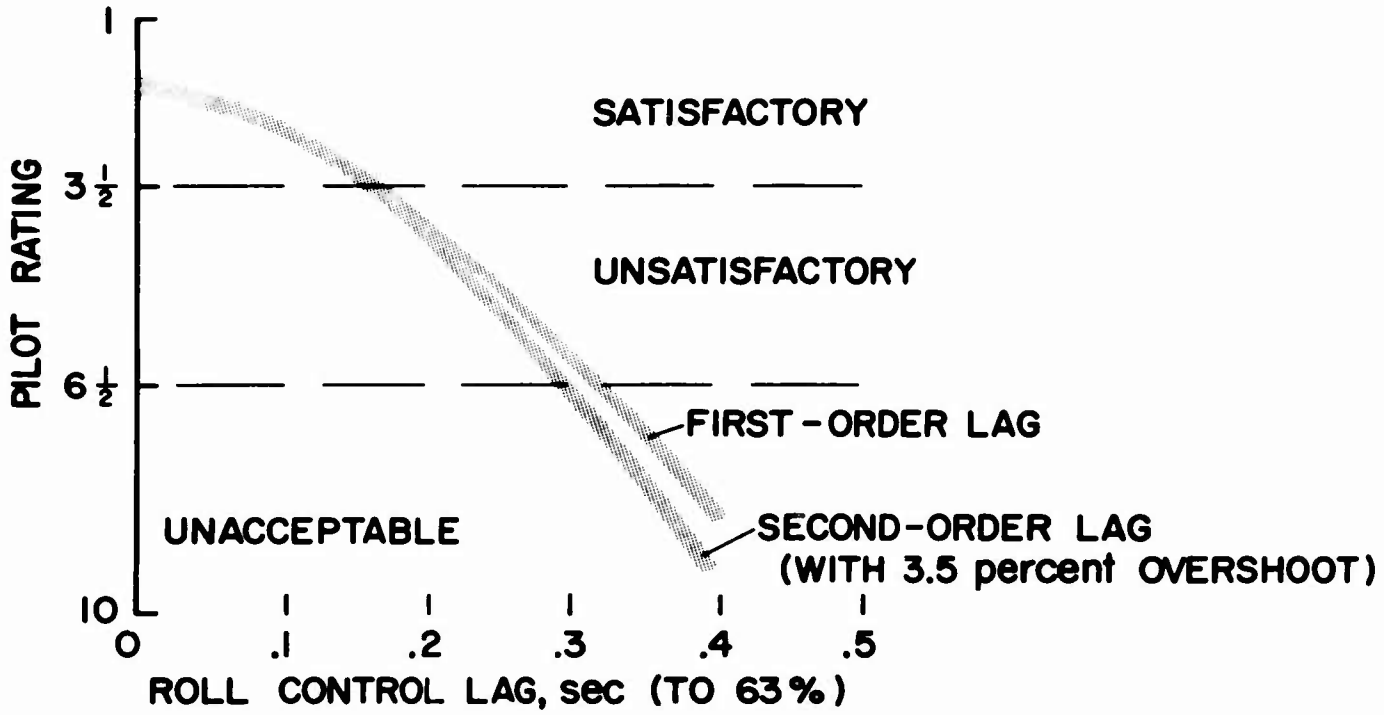

Fig. 13 Comparison of first- and second-order lag effects on roll control for an attitude-stabilized system; six-degree simulator

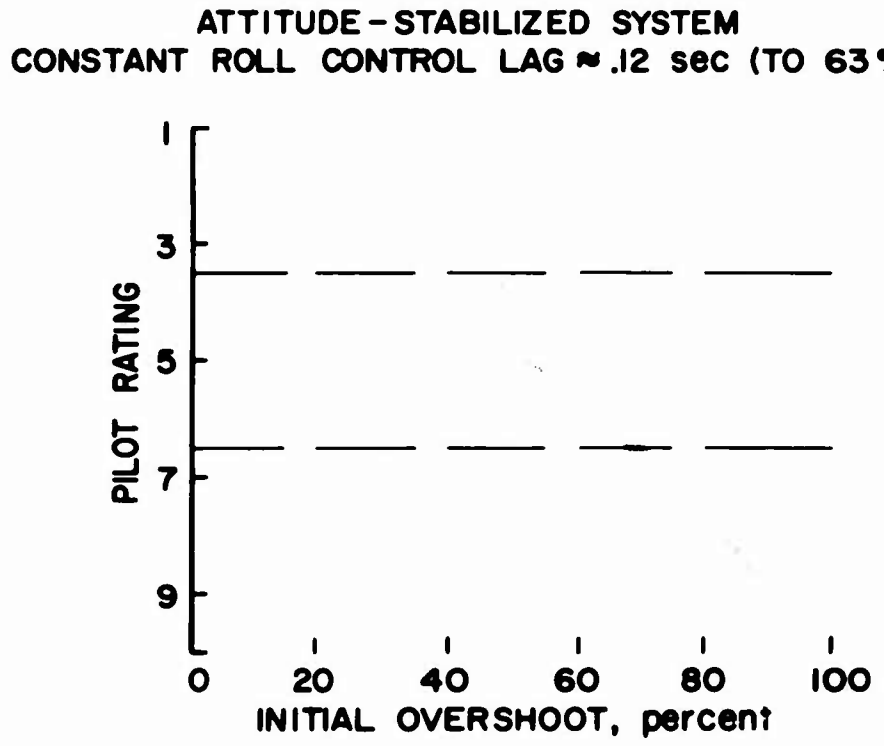

Fig. 14 Effect of overshoot with second-order control lag; six-degree simulator

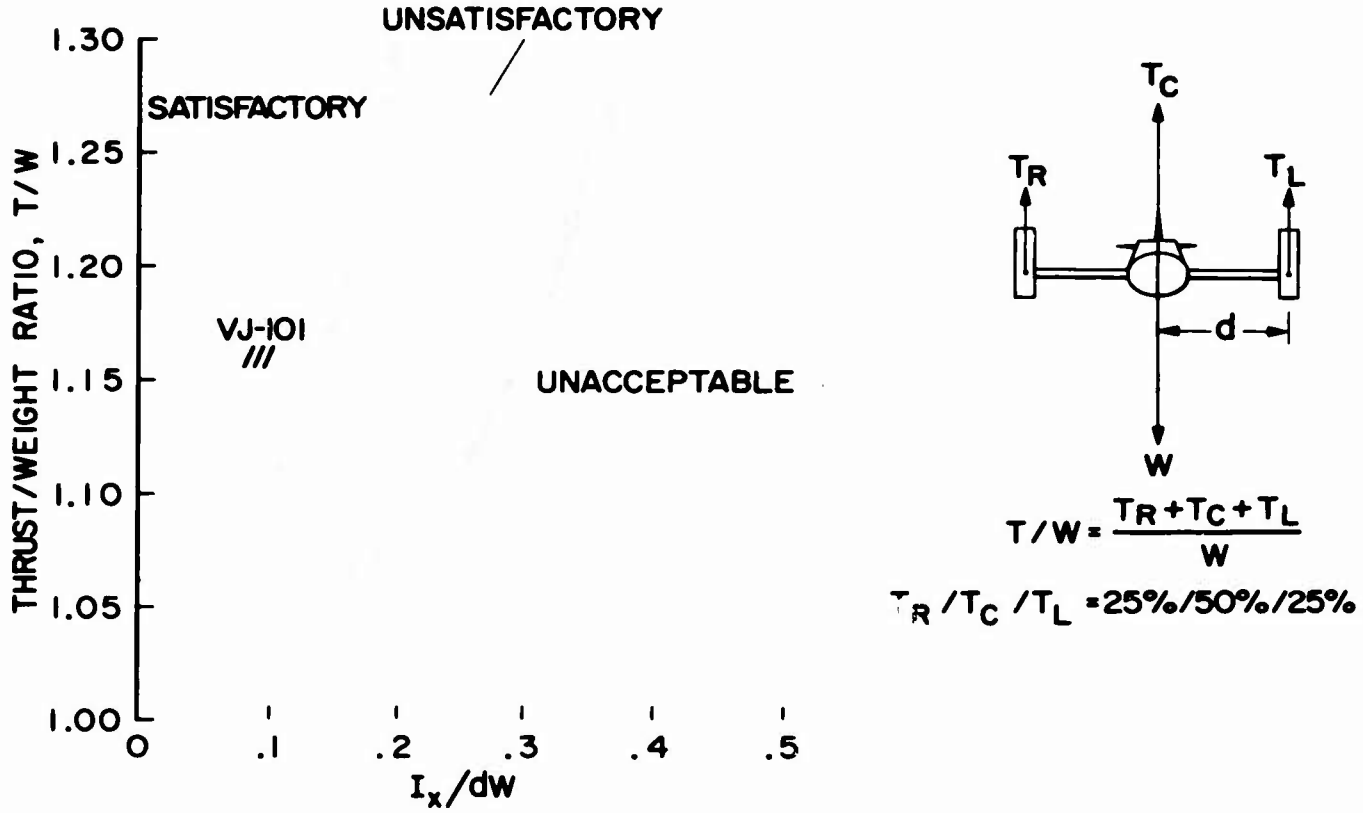

Fig. 15 Effect of thrust requirements in roll

REACTION CONTROL SYSTEM PRELIMINARY DESIGN CONSIDERATIONS FOR A JET-LIFT RESEARCH AIRCRAFT

D. L. Hirsch, Member of Technical Management

W. W. Stark, Engineering Specialist

W. B. Morris, Engineering Specialist

NORTHROP NORAIR
A Division of Northrop Corporation
3901 W. Broadway
Hawthorne, California 90250

ABSTRACT

The preliminary design of a jet-lift aircraft reaction control system has been completed. The aircraft mission is one of terminal area flight control research; the research will involve variation of flight control parameters in hover and transition. The design work was sponsored by NASA-Langley Research Center under a study contract.

Results of the study are presented describing the vehicle arrangement, the low-speed control power requirements, the reaction control system design philosophy, and the preliminary design details of the reaction control hardware.

The aircraft employs a vertical side-by-side compacted arrangement of lift engines and two horizontal lift/cruise engines. An engine compressor bleed air system provides reaction control. Maximum single axis control power levels were established on the basis of summed elements for trim, maneuver, and recovery from a single engine failure. The all-axis simultaneous control power requirement established at 60 percent of the single axis maximums was normally the critical requirement. An engine compressor bleed rate variable up to 10 percent was available to meet all these demands.

Important design requirements were: 1) minimum cross-coupling between attitude control and lift forces, 2) near constant control sensitivity, and 3) low system weight. A system employing swiveling and differential discharge area nozzles offered the most satisfactory design solution.

NOMENCLATURE

W	aircraft weight	lbs.
I	aircraft moment of inertia about a principal axis	slug-ft^2
M	moment applied about an aircraft principal or body axis	ft-lb
C.P.	control power $\sim \frac{M}{I}$	rad/sec^2
SAS	stability augmenter system	
VSS	variable stability system	
T/W	thrust to weight ratio	
L/W	lift to weight ratio	
c.g.	aircraft center of gravity	
VFR	visual flight rules	
IFR	instrument flight rules	
NASA	The National Aeronautics and Space Administration	

MISSION DESCRIPTION AND GENERAL REQUIREMENTS

The technology associated with handling qualities and flight operations in the terminal flight area is in urgent need of research for V/STOL aircraft. Vehicle response requirements, stability augmenter requirements, landing aids, cockpit displays, piloting problems, and operating procedures lack definition for low speed, all weather operation. A design study has been completed under the sponsorship of the NASA which establishes a vehicle and control system configuration for gathering flight data on these problem areas pertinent to fighter-type aircraft. The mission of the vehicle, then, is to obtain the research data through flight tests.

Because it is complicated and time-consuming, the most demanding maneuver in the terminal area is considered to be the final instrument approach to a small VTOL site under low ceiling and visibility conditions; the time (fuel consumed) in the approach can be critical in jet-lift vehicles. Other operations which may play a dominant role in subsystem selection include entrance into the landing traffic pattern, acceleration to wing-borne flight, and deceleration to thrust-borne flight Air traffic control requirements and terrain and obstacle clearance will place certain constraints on the operation that must be considered in any investigation. Because of pilot control workload, there is added concern where configurations have lift engines; the engines and associated subsystems (doors, etc.) must be started, adjusted, and checked. The impact of these variables on operations is also a mission objective.

To meet the mission requirements, it was necessary that the aircraft be capable of high hover endurance and utilize a mixed propulsion system comprised of lift-only plus horizontally mounted lift-cruise engines. With this general propulsion definition, numerous trade studies were conducted to size the aircraft and finalize the general aircraft design requirements. Some requirements of particular importance to the control system design which were specified at the study outset include: (1) developed hardware components available off-the-shelf in 1968 to 1969 with current technology were to be used in the design approach; (2) a bleed or bleed derivative (i.e., bleed-burn) reaction control system was to be used because the superior time response characteristics of a bleed system allows simulation of most other control methods; (3) a variable stability system (VSS) operable through transition was necessary to encompass the range of control variables; (4) control system actuation had to be compatible with the high response requirements of the VSS, and (5) the aircraft had to be capable of recovering and maintaining altitude and attitude after failure of any single engine during hovering and transition flight.

VEHICLE DESCRIPTION

General Arrangement

Figures 1 and 2 depict the aircraft configuration as it evolved from the mission requirements. The inboard view is descriptive of engine and equipment arrangement and volume devoted to control ducting. Salient aircraft features include the compact vertical side-by-side arrangement of YJ85-GE-19 lift engines and the over-wing location of two YJ85-GE-19 lift/cruise engines. A minimum moment arm from the aircraft c.g. to the most remote lift engine was sought to minimize the pitching moment induced

by an emergency engine out condition. The closest engine spacing for this purpose would have necessitated placement of two engines through the wing-box, with fuel tankage at the extremities of the engine installation; however, such a structural compromise was ultimately avoided because the longest moment arm was to the forward lift engines, and the aft lift engine location was traded with fuel location without exceeding the same arm. Vehicle pitch/yaw inertia at a single weight remained virtually unchanged by the trade. Aside from the engine out consideration, the clustering of the engines close to the c.g., with the fuel tanks fore and aft of the engines, produced favorable pitch/yaw moment of inertia changes during flight. Consumption of fuel during a single flight results in a decreasing power setting with less available bleed air, a decreasing pitch and yaw moment of inertia, and therefore a fairly constant level of available control power.

The wing with its high aspect ratio was the derivative of a design approach representing the forward position of a variable sweep wing. In addition to favorable drag characteristics, the high aspect ratio wing provided a reaction control roll moment arm advantage.

The lift exhaust system of the lift/cruise engine is ducted back from the nacelles through the fuselage near the vehicle center. Rolling moments induced by engine failure, and possible hot gas reingestion in ground effects are minimized by the arrangement.

Selected Engine Characteristics

The Rolls Royce RB 162-81 and the General Electric YJ85-GE-19 lift engines were examined as candidates for research mission suitability. Among many other criteria the lift engines were compared on the basis of installed thrust rating, T/W ratio, specific fuel consumption, thrust vectoring capability, operating restrictions and unit costs. To meet flight control needs, the installations were compared on the basis of control thrust to lift thrust ratio, operation with off-design bleed rates, and ducting installation difficulties. The research mission required engine out safety and long operating periods at high power settings with large bleed air extraction. Although the Rolls Royce engine represents the best T/W technology that would be available in developed hardware, the YJ85-GE-19 showed the higher mission suitability.

The thrust rating of the YJ85-GE-19 lift engine at sea-level, and an ambient temperature of 80 °F, is 3,015 pounds with a bare engine thrust-to-weight ratio of 7.2 (Reference 8). Installed thrust is 2,320 pounds when maximum bleed air is extracted for control purposes and a vectoring exhaust nozzle is attached. The YJ85-GE-19 engine is completely flexible in bleed operation, with no restrictions on variations in bleed rate up to the maximum of 10 percent of compressor airflow. This allows the selection of either a variable or constant bleed system for attitude control. Static installed performance at the maximum 10 percent bleed rate with installation losses noted are shown in Table 3.

Thrust diverter valves were necessary elements of the lift/cruise engine installation. Hardware availability of the valves constrained the selection to a single lift/cruise candidate: the YJ85-GE-19 engine. Bleed air was available from the lift/cruise engine manifolding for either lift engine start or flight control; a portion of the air was also available for cabin and equipment conditioning. The engine characteristics for the installed lift/cruise application are a part of Table 3.

Lift capability of the propulsion-control system as a function of engine speed is shown in Figure 3. An important point is that lift is essentially unaffected in the 8 to 10 percent bleed range utilized by the control system. These data include control-system losses, but assume full utilization of the control thrust as lift.

Control Design Objectives

In addition to providing the required control power, objectives sought in the control system design were: (1) the least complex system compatible with performance; (2) very low cross-coupling effects between an applied control moment, lift, and other control axes; (3) minimum mechanical interconnect between individual axis systems; (4) constant control sensitivity with control movement; and (5) minimum system weight.

Various means of augmenting compressor bleed air thrust and the use of a separate self-contained system using rocket-fueled reaction jets were investigated (Reference 7). Augmentation systems investigated were bleed-burn at the nozzles, a separate bleed-burn turbine driving a compressor, wing-tip fans for roll control, and a separate gas generator. All these augmentation systems are feasible and capable of boosting compressor bleed air thrust by factors of 1.20 to 1.50. However, augmentation systems are relatively complex, have higher overall system weight, and are more costly than an unaugmented bleed system since they are not available as off-the-shelf hardware in the necessary sizes.

All factors indicated that an unaugmented bleed system using reaction jets was best suited to this V/STOL design, if a match between control power and lift and the mission requirements could be obtained. Although both variable and constant bleed techniques were system candidates, the mission requirements of extended VTOL testing with probable high control power demands indicated the desirability of a constant bleed system with the engine exhaust sized for limit exhaust gas temperature at the maximum bleed rate. The bleed-rate range would have to be held to the minimum compatible with desired system operation to limit adverse effects on engine stall margin. Compressor stall margins of turbo-jet engines are reduced when bleed rates are rapidly decreased; individual engines vary considerably in sensitivity to this change. The YJ85-GE-19 engine is relatively insensitive to bleed-rate changes with no operational restrictions although high performance lift engines designed specifically for constant bleed operation generally do restrict bleed-rate variations.

CONTROL REQUIREMENTS

Control Power Requirements

The Northrop study defined a set of pitch, roll, and yaw axis control power requirements that would provide ample research mission capability. To define desired control power levels, advantage was taken of current research findings from flight (VJ101 aircraft and hover-rig) and simulator efforts. References 4 through 6 recount recent analysis of control power usage for jet-lift aircraft which provided input to the investigation. Many other general handling quality and variable stability requirements were examined including stick forces, stick sensitivity, trim rates, static and dynamic properties of the vehicle-control system combination, stability derivative simulation range, and basic airframe damping. All these considerations influenced the mechanization of the control actuation arrangement, but the major influences on reaction system, size and weight were the control power requirements. The control power requirements, therefore, are singled out for review.

AGARD 408 and 408A (Reference 1) criteria were available and in general, their handling quality recommendations were considered as preliminary requirements for the aircraft. However, a preliminary investigation by NASA prior to the contractor study had already revealed a need to employ modified single axis nominal control power requirements and simultaneous requirements to meet research objectives. The NASA modifications were multiples of the AGARD nominal requirements and therefore based essentially on aircraft weight and moments of inertia. The Northrop study of this area produced a set of control power requirements tailored specifically for the vehicle.

The study findings result in requirements which are configuration dependent for all contributions to total control power except that necessary to maneuver the vehicle. For the research mission, engine-out safety under IFR conditions is stressed. Contributions to the total single axis control power are summed from the following input elements:

1. Trim-Longitudinal control power must be available to trim all static moments through transition; lateral and directional control power must be available to trim in a 35 knot sidewind or 15 degrees sideslip, whichever is greater. Sufficient full scale and wind tunnel data were available on similar vehicle arrangements to estimate the low speed trim requirements for the chosen configuration. Longitudinally, the greatest trim demand placed on the reaction control occurs at hover, and is the result of an interference moment in ground effect. Expressed as control power, it is the order of 0.5 rad/sec^2. Similarly, the greatest lateral trim requirement occurs at hover in the 35 knot sidewind, the aerodynamic and power effects amount to a control power demand of approximately 0.75 rad/sec^2.

2. Gyro-coupling-The vertical arrangement of lift engines gives rise to gyroscopic pitch-roll cross-coupling during maneuvering flight. The effects of the horizontally mounted engines were small enough to be neglected. An estimate of the control power necessary to offset this effect made necessary an analysis of the reference data rotational rates encountered during maneuvering flight at hover. Under VFR conditions a 10 deg/sec rate was essentially the maximum attained in the tests. This gives rise to a maximum control power demand of 0.03 rad/sec^2 in the pitch axis and 0.17 rad/sec^2 in the roll axis.

3. Engine Failure-Control power must be available to balance and recover from the most critical engine failure. Simulator research involving engine failures during low speed IFR flight (Reference 5) have indicated control power levels satisfactory for recovery from such an emergency upset. Necessary control power is a function of the control dynamics and effective vehicle damping. For this specific aircraft, it is approximately 1.5 times the static imbalance caused by engine failure. This amounts to 0.2 rad/sec^2 in pitch and 0.27 rad/sec^2 in roll.

4. Maneuver-Control power must be available for maneuver based on control usage under VFR conditions. By comparison to the sum of configuration dependent power elements, the task-dependent maneuvering elements are small. Analysis of the referenced tests and data reveal maneuvers conducted under VFR conditions rather than IFR conditions to be the most demanding on control power. As the mode of control is regressed from attitude (proportional to stick position) through rate to acceleration, control

demands increase. Because the research aircraft employs a dual redundant rate-damping stability augmenter which engages in event of VSS failure, the control demands attributable to a rate command control system were applied. Maximum encountered control power levels which cover more than 99 percent of all maneuvers under these conditions were as follows: pitch axis- 0.3 rad/sec^2; roll axis- 0.5 rad/sec^2; yaw axis- 0.2 rad/sec^2. The analysis of control power usage distribution in reference 4 produced a definition that has been adopted in this work. Because the maximum value of control power in the usage distribution is difficult to define, the control power value sufficient to cover at least 99 percent of the usage for a maneuver is established.

Rules for summation of the control power elements to establish a minimum installed level per individual axis by all three approaches are defined in Table 1. This table also compares the criteria for simultaneous all-axes availability of control power. Simultaneous control power is the initial acceleration available about each axis with full cockpit control displacements simultaneously in pitch, roll, and yaw. The contractor conducted study recommendations for simultaneous control power availability are dominated by considerations of imbalance due to potential failure; in the case of this aircraft, the critical consideration is failure of the engine most remotely located from the c.g. The total simultaneous required control power represents the sum of control power both on axes affected and unaffected by the failure. It allows for recovery of the engine failure while the vehicle is trimmed at the edge of its operating envelope. These recommendations are also numerically compared with AGARD 408 and NASA recommendations in Figure 4.

Following the presentation of study findings, the final decision of NASA was to employ its previously derived criteria as design guides for this vehicle. The study did, however, reveal differences between maneuvering and configuration dependent control power requirements. Because the compact jet-lift vehicle has relatively low trim requirements, the methods result in similar individual axis nominal control power recommendations. For moderate and low disk-loaded vehicles with large trim requirements, an inappropriate or dangerous level of design control power could result from a lack of consideration of the difference between maneuvering and configuration dependent elements.

Performance-Control Requirements

Because available control bleed air is a function of engine power setting which varies with lift, the control power requirements were specified in connection with desired hover performance in and out of ground effect. The single axis and simultaneous requirements must be met for all engines operating and one engine inoperative at all flyable weight conditions of the aircraft. Because of reduced power settings, the lightest weight condition is the most critical; it also sizes the ducting system and maximum reaction nozzle areas. The lowest weight design point is equal to 1.09 times the empty weight; this L/W factor includes a fuel margin of 5 percent of the empty weight and a 4 percent allowance for lift interference out of ground effect. Interference lift effects due to induced flow by the jet exhausts were estimated from model and full-scale tests (Reference 9) to be 15 percent in ground effect and 4 percent in free air. Critical combined lift performance and control requirements were a lift-to-design weight ratio of 1.20 in free air with all engines operating and a L/W of 1.09 with one engine inoperative. Control power requirements which had to be met at these lift performances were 80 percent pitch and 50 percent of nominal roll and yaw levels with all engines operating, and 20 percent of nominal pitch and yaw levels and 50 percent of nominal roll levels with one engine out. These conditions are tabulated in Table 2.

REACTION CONTROL SYSTEM DESIGN

Ducting System

Pitch and roll system ducting are interconnected to insure control availability about either axis in case of failure of any engine. Due to the numerous turns and restricted turn radius, the flow areas of the ducts were selected for a flow Mach number of 0.3 to limit system pressure losses. Duct diameters of 8.5 in. for pitch and 4.0 in. for roll resulted in a maximum pressure drop of 20 percent from the engine exhaust port to the nozzle on maximum control demand of a single axis. For the simultaneous control flow rates, pressure drops are in the order of 10 to 15 percent. A layout of the ducting system is shown in Figure 5.

Because weight was a major consideration, various duct, bellows and flange materials and mixes of materials were investigated: stainless steel, titanium, plastic and composite materials were those considered. Recent developments in the field of electron beam welding allowed the consideration of a joined steel and titanium system. The potential advantage was reduction in the weight of the ducting and, particularly, the joints. However, titanium bellows are not well enough developed to give assurance that they could be available in the required time frame. Also, the cost and time required to tool up for this type of production is not warranted for a prototype research airplane, and the approach was abandoned in favor of more conventional materials. The design choice was 321 stainless steel. Regardless of the duct and joint material, the weight of the insulation and radiant foil necessary for airframe, equipment and personnel protection will remain essentially constant.

The ducting is subjected to thermal shock, an internal pressure of approximately 70 psi with surge pressures, airplane bending loads and differential expansion. Ducting five inches and under can be assembled with bellows and "V" type clamps. However, as duct diameters increase, the strength requirements at the joints are such that bolted flanges are necessary. If the internal pressure were the only load seen by the ducting, the steel skin gauges would only have to be in the order of 0.002 inches. Handling, tension, compression and bending loads forced the skin gauges to 0.03 - 0.05 inches.

One main duct runs fore and aft in the fuselage, with branches out to the wing tips. The bleed air leaves the engine at about 475 °F, and insulation at selected locations is provided to protect equipment, structure and personnel. The main duct is supplied by all the engines, provides bleed air for in-flight start of the lift engines from the cruise engines and is the source for cabin and equipment conditioned air.

In order to start the lift-only engines using bleed air from the cruise engines, it is necessary that the roll and pitch control nozzles be closed during start-up. An alternate approach could utilize a separate duct for start with valving in the ducting to divert compressor air as required. The latter approach, requiring valving adequate for the 8.5" main duct is heavy, and was not considered seriously. The design approach requires only a single duct with actuators at each of the roll and pitch nozzles to close the nozzles during duct pressurization and lift engine start-up. The actuators, incorporated in the mechanism at the nozzles, add only six lbs. to the overall system weight and provide the added advantage of permitting the pilot to select sensitivity of the nozzles relative to control movement for the full range of stick movement.

Reaction Nozzles

Pitch control, variable-area nozzles are located at the extremities of the longitudinal axis. The pitch nozzles exhaust downward only, with differential nozzle reaction thrust generating the required control moment. Yaw control moment is obtained by rotating the pitch nozzles differentially until the desired yaw moment is obtained. Reaction nozzles located at the wing tips and capable of exhausting either up or down provide roll control. An up-down roll system was necessary to reduce duct diameters for compatibility with wing thickness. Reaction system weight was also reduced by this approach. The nozzle discharge areas are rectangular to provide a linear thrust change with movement of the control. The nozzle designs are shown in Figure 6.

Nozzle area schedules are shown in Figure 7. Areas of both pitch nozzels increase when they are rotated for yaw control beyond 40 degrees up to a maximum of 54 degrees. This limits the amount of rotation necessary to obtain the maximum required yaw moment and still retain null (zero control) areas small enough to achieve maximum roll moments without forcing a reduction in pitch nozzle areas. Similarly, null areas of the roll nozzles were sized to allow maximum pitch control with no change in roll nozzle areas. The total nozzle area with all nozzles at their respective null positions is 23.3 sq. -in. which results in an almost constant bleed rate of 8.0 percent in the engine speed range between 92 and 99 percent rpm. The maximum effective total nozzle area of 32.0 sq. -in. results in a bleed rate of 10 percent, the nominal bleed rate limit of the YJ85-GE-19 engine.

The nozzle schedules allow the attainment of 56 percent of the maximum pitch control requirement and 36 percent of the roll requirement with no control cross-coupling or lift change and no change in the bleed rate. Each roll nozzle is scheduled to open an additional 2.2 sq.-in. after the opposite nozzle closes before it starts to discharge in the opposite direction. This allows the attainment of 50 percent of the available roll control with minimum cross coupling into the pitch axis and lift, and presents no problem in the mechanical design of nozzle area-control systems.

The reaction jet nozzle design provides acceptable bleed air discharge coefficients when the nozzle is full open, and a good seal when the nozzle is shut. The nozzle is intended to be of welded construction from 4130 type chrome-moly steel with a thermal expansion coefficient of approximately 6.3×10^{-6}. Designing the nozzle gate of a material with a higher thermal coefficient (19-9 corrosion resistant steel with a thermal coefficient of 8.5 or 9×10^{-6}) insures that binding or sticking will not occur due to thermal shock. The flanged sealing surfaces are coated with teflon to reduce the leakage rate and to minimize rubbing friction in case the nozzle or gate distorts under load. The width of the flange was selected so that the rate of leakage of compressor air when the nozzles were closed would be a minimum. The nozzle gate design results in a low inertia, low friction load for the actuation system. Good first order frequency response is indicated. The variable stability and stability augmentation actuators sum pilot commands through the same control system to the nozzle. Control output under all conditions is assured by the capability of any one of the nozzles to provide limited capability even if the opposing nozzle is jammed.

Necessary redundancies, insulation and allowance for unpredictable stresses result in a fairly heavy system design. The ducting, bellows, nozzles, flanges, valving, etc. add a total system weight of approximately 500 pounds or 3.6 percent to the empty weight of the airplane.

CONTROL SYSTEM PERFORMANCE

Control Power Available

As shown by Figure 8. the available simultaneous control power met the requirements for all hover conditions. The simultaneous requirements with all engines operating and the aircraft at minimum flight weight proved the more critical due to the reduction in bleed air and available control-air specific thrust at the low engine power setting (N 91.2% rpm) required for hover. When the engine most remotely located from the c.g. (forward lift engine) is inoperative, engine power required for hover increases to about 93 percent rpm. No problem is indicated in meeting the engine-out simultaneous control requirements. A satisfactory match between required and available control power was possible by allowing the bleed rate to vary from approximately 8 percent to the maximum of 10 percent. The single axis control power requirements can also be met continuously from maximum power to the low power setting required for hover at light weight. Figure 8 also shows that a L/W ratio of 1.24 is obtainable with all engines operating and 1.10 with the forward lift engine out, which more than meets the lift performance requirements. Although not shown by the figure. an added requirement of a minimum L/W ratio of 1.20 in free air with control powers of 80 percent pitch and 50 percent roll and yaw applied was also met.

Control Cross-Coupling

Control cross-coupling arises from two sources. Because of engine rotational inertia, the application of a control moment about one attitude axis results in a moment about another axis. Secondly, improper design in the physical arrangement of the reaction jets could introduce unacceptable moments about other than the commanded axis. or changes in total lift that might be troublesome from a handling qualities point of view. Because a rate-damping SAS is basic to the control design, no mechanical interconnects between control axes are included to offset the engine gyroscopic effects. This section will deal only with the effects of reaction jet arrangement.

The application of a pitching moment induces no roll or yaw moment. and results in insignificant lift changes because total system lift (engine plus control thrust) remains essentially constant. The down-down pitch reaction jets do produce control moments about a varying center of percussion rather than the aircraft c.g., but this effect was found small enough to neglect.

The roll nozzles are slightly aft of the center of pitch rotation. Therefore. any change in the net lift of the roll nozzles induces a small pitching moment. The induced pitching moment and lift resulting from the application of a roll moment are shown in Figure 9. No pitch or lift changes are induced for roll control applications up to 50 percent of the maximum available; changes of only 300 lb. in lift and 700 lb.-ft. in pitching moment result from a maximum applied roll moment. The application of a yaw moment induces no roll moment because the line-of-reaction of the pitch-yaw nozzles intersects the roll axis. No change in pitch or side force is developed by the application of a yaw moment in the absence of a pitch control moment. A small lift loss due to the angularity of the pitch-yaw nozzle to the vertical does result. but it is equal to only 300 lb. for a maximum yaw moment. When a yaw moment is applied simultaneously with a pitch moment. side forces and a difference in commanded pitch moment result. varying in magnitude with the amount of pitch moment. With a maximum simultaneous control application. a 12 percent difference in commanded moment. a side force of 500 lb. and a lift loss of 200 lb. occur. The induced pitching moment. although small, may result in the need for a pitch-yaw nozzle differential interconnect. The side force results in an incremental translational acceleration of only 0.03 g which is not significant from a handling qualities viewpoint.

REFERENCES

1. V/STOL Working Group, "Recommendations for V/STOL Handling Qualities," AGARD 408 and 408A (Oct. 1962).

2. "Airplane Specification for Northrop N-309 NASA V/STOL Jet Operations Research Airplane," NASA CR-66417, Northrop Norair NOR-67-8, Vol. I (July 1967).

3. "Substantiating Technical Data," NASA CR-66419, Northrop Norair NOR-67-8, Vol. III (July 1967).

4. Schaeffler, J., Alscher, H., Steinmetz, G., VFW, Germany and Sinacori, J.B., Northrop Norair, "Control Power Usage for Typical Flight Maneuvering in Hover from a Systematic Analysis of Flight Test Data of the VJ-101 Aircraft and a Hover-Rig," AIAA Paper # 66-816 (Oct. 1966).

5. Hirsch, D.L., Sinacori, J.B., Gallagher, J.T. and O'Donnell, F.B., "The Status of Flight Control Research and Development," Northrop Norair, NOR-64-292 (Nov. 1964).

6. Sinacori, J.B., "V/STOL Ground Based Simulation Techniques," Northrop Norair, NOR 67-85 (May 1967).

7. "Lift Engine Installation Technology," Continental Aviation and Engineering Corp. (June 1965).

8. "YJ85-GE-19 Engine Model Specification No. E1129," General Electric Corp. (1 Nov. 1966).

9. Lavi, R., "Parametric Investigation of VTOL Hot Gas Ingestion and Induced Jet Effects in Ground Proximity," Northrop Norair, NOR-67-32 (Feb. 1967).

TABLE 1

ATTITUDE CONTROL POWER (C.P.) REQUIREMENTS
(COMBINED AERO & REACTION; HOVER AND TRANSITION)

		AGARD 408	NASA	Norair
Pitch (Total)		Nominal minimum is a function of W&I.	1.5 X AGARD 408	Minimum installed C.P. ①·②·③·④ or ③·⑤ whichever is greater
Maneuver	(a) Normal maneuvering			C.P. for 99% usage (jet-lift a/c with rate damped systems) under VFR conditions ①
	(b) Gyroscopic effects	Gyro effects shall consume no more than 20% of nominal C.P. levels for maneuver rates	Same as AGARD 408	C.P. for 99% VFR maneuver roll rates to offset pitch changes (commanded by gyro) ②
Trim (Total)		C.P. to trim in transition not to exceed 80% of the nominal level	Same as AGARD 408	C.P. needed to offset trim change in ground effect or transition (beyond the trim capability of δ_H) whichever is greater ③
Emergency	(a) Engine out trim	C.P. to balance critical engine failure not to exceed 50% of the nominal level	C.P. remaining after balance of critical engine failure must be at least 20% of that available before failure (at worst c.g.)	C.P. equal to that for static balance of critical engine failure ④
	(b) Engine out recovery	C.P. available for recovery shall be at least 1.25x the engine out moment		C.P. equal to 1.5 x critical engine out moment, or sum of ①·④, whichever is greater ⑤
	(c) SAS failure	50% of the nominal C.P. must be left in the recovery direction at hover following single failure	No effect from single failure, dual redundancy required	No effect from single failure, dual redundancy required
SAS Authority Limits		Implied 50% authority limit		50% of ①·②·③
Roll (Total)		Nominal minimum is a function of W&I	2.0 X AGARD 408	Minimum installed C.P. ⑥·⑦·⑧·⑨ or ⑧·⑩, whichever is greater
Maneuver	(a) Normal maneuvering			C.P. for 99% usage under VFR conditions (jet lift a/c with rate damped systems) ⑥
	(b) Gyroscopic effects	Balancing gyro effects at demonstration rates shall consume no more than 20% of nominal C.P.	Same as AGARD 408	C.P. for 99% VFR maneuver pitch rates to offset roll changes (commanded by gyro) ⑦
Trim	(a) Sideslip balance	Trim for a 35 kt sidewind or ±15 β (whichever is greater) shall consume no more than 50% of nominal C.P.	Same as AGARD 408	C.P. to trim 35 kts sidewind or ±15 β whichever is greater at $\beta = 0°$ (beyond the trim capability of δ_a) ⑧
Emergency	(a) Engine out trim	C.P. to balance critical engine failure not to exceed 50% of nominal	C.P. remaining after balance of critical engine failure must be at least 50% of that available before failure	C.P. equal to that for static balance of critical engine failure ⑨
	(b) Engine out recovery	C.P. for recovery shall be at least 2.0 X engine out moment		C.P. equal to 1.5 X critical engine out roll moment, or sum of ⑥·⑨ whichever is greater ⑩
	(c) SAS failure	Reduction in damping allowable with single failure	No effect from single failure, dual redundancy required	No effect from single failure, dual redundancy required
SAS Authority Limits				50% of ⑥·⑦·⑧
Yaw (Total)		Nominal minimum is a function of W&I	1.5 X AGARD 408	Minimum installed C.P. ⑪·⑫·⑬
Maneuver	(a) Normal maneuvering			C.P. for 99% usage under VFR conditions (jet lift a/c with rate damped systems) ⑪
	(b) Gyroscopic effects	Balancing gyro effects at demonstration rates shall consume no more than 20% of nominal C.P.	Same as AGARD	⑫
Trim	(a) Sideslip balance			C.P. to balance 35 kts sidewind or ±15 β whichever is greater at $\beta = 0$ (beyond trim capability of δ_R)
Emergency	(a) Engine out trim (transition)	Implied that yaw reaction control should be necessary for engine out trim (use aero control only)	C.P. remaining after balance of critical engine failure must be at least 20% of that available before failure	C.P. equal to that for static balance of critical engine failure ⑬
	(b) SAS failure	Reduction in damping allowable with single failure	No effect from single failure, dual redundancy required	No effect from single failure, dual redundancy required
SAS Authority				
Simultaneous		100% of the individual nominal C.P. levels available all axes simultaneously	60% of nominal C.P. level must remain on each axis with full cockpit control displacements (implied 100% on critical axis with 50% remaining on other axes)	Following single engine failure, total simultaneous C.P. = C.P. on failed axis + C.P. on unaffected axes or where C.P. on failed axis = 1.5X failure trim, and C.P. on unaffected axis = Trim + gyro effect + 1/2 normal maneuver

TABLE 2

NASA V/STOL RESEARCH AIRCRAFT
REQUIRED CONTROL MOMENTS

Design Weight = 18,000 lb.
Empty Weight = 13,714 lb.

Operating Criteria	Pitch		Roll		Yaw	
	% Req.	lb-ft	% Req.	lb-ft	% Req.	lb-ft
Max. control on individual axis. Lightweight hover.	100	30350	100	11650	100	23250
Simultaneous control. Lightweight hover.	60	18210	60	6990	60	13950
Simultaneous control. Lightweight hover 1 lift engine out.	20	15740	50	8060	20	4650
Performance L/W = 1.20 min.	80	25700	50	5560	50	12500
Performance L/W = 1.09 min. 1 lift engine out.	20	17810	50	8490	20	5010

TABLE 3

NASA V/STOL RESEARCH AIRCRAFT SUMMARY OF YJ85-GE-19 ENGINE PERFORMANCE

(Installed Static Sea-Level Ratings at 80°F and Maximum Bleed Rate, $W_B/W_A = 0.10$)

		Lift Engine	L/C Engine (4)	
			Lift Mode	Cruise Mode
(1)	Engine Weight lb	420	392	392
(2)	Thrust lb	2320	2250	2680
(3)	Control Thrust, F_c lb	226	211	-
	Thrust/Weight (Engine only)	5.52	5.74	6.84
	Thrust/Weight (Eng plus F_c)	6.06	6.27	-
	Engine SFC lb/lb-hr	1.11	1.16	1.038
	Total SFC lb/lb-hr	1.012	1.06	-
	Bleed Press. at Port Exit PSIA	78.5	78.2	-
	Bleed Temp. at Port Exit °R	965	965	-
	Comp. Bleed Air Rate lb/sec	4.18	4.16	-
	Control Nozzle Specific Thrust F_c/W_B	56.9	56.4	-

(1) Includes vectoring nozzle for lift engine but not diverter valve and extended tailpipe for L/C engine

(3) Control System Losses
- A. Line press. loss, $\Delta p/p$ 0.15
- B. Bleed air noz. leakage, 0.03 W_B
- C. Nozzle velocity coeff., 0.96
- D. Bay cooling, W_c = 0.2 lb/sec
- E. Air cond. (L/C only), W = 0.2 lb/sec

(4) Bleed rate, $W_B/W_A = 0.01$

(2) Installation Losses, $\Delta F/F$

Lift Engine
- A. 0.007 (0.995 inlet recovery)
- B. 0.015 (Vector nozzle)

L/C Engine
- A. 0.014 (0.99 inlet recovery)
- B. 0.033 (Diverter and tailpipe)

Cruise Mode
- A. 0.014 (0.99 inlet recovery)
- B. 0.025 (Diverter and tailpipe)

FIGURE 1 JET-LIFT RESEARCH AIRCRAFT

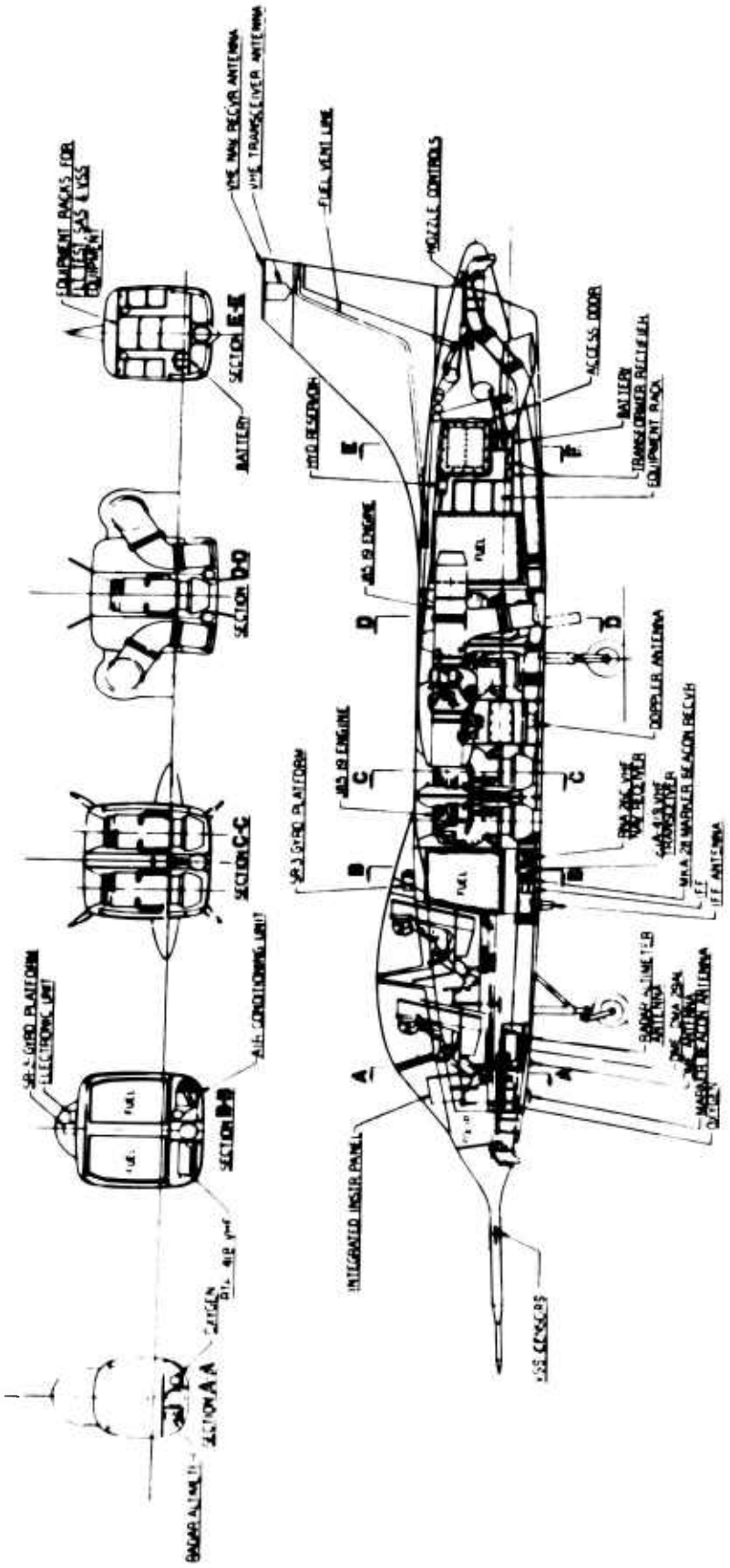

FIGURE 2. INBOARD PROFILE

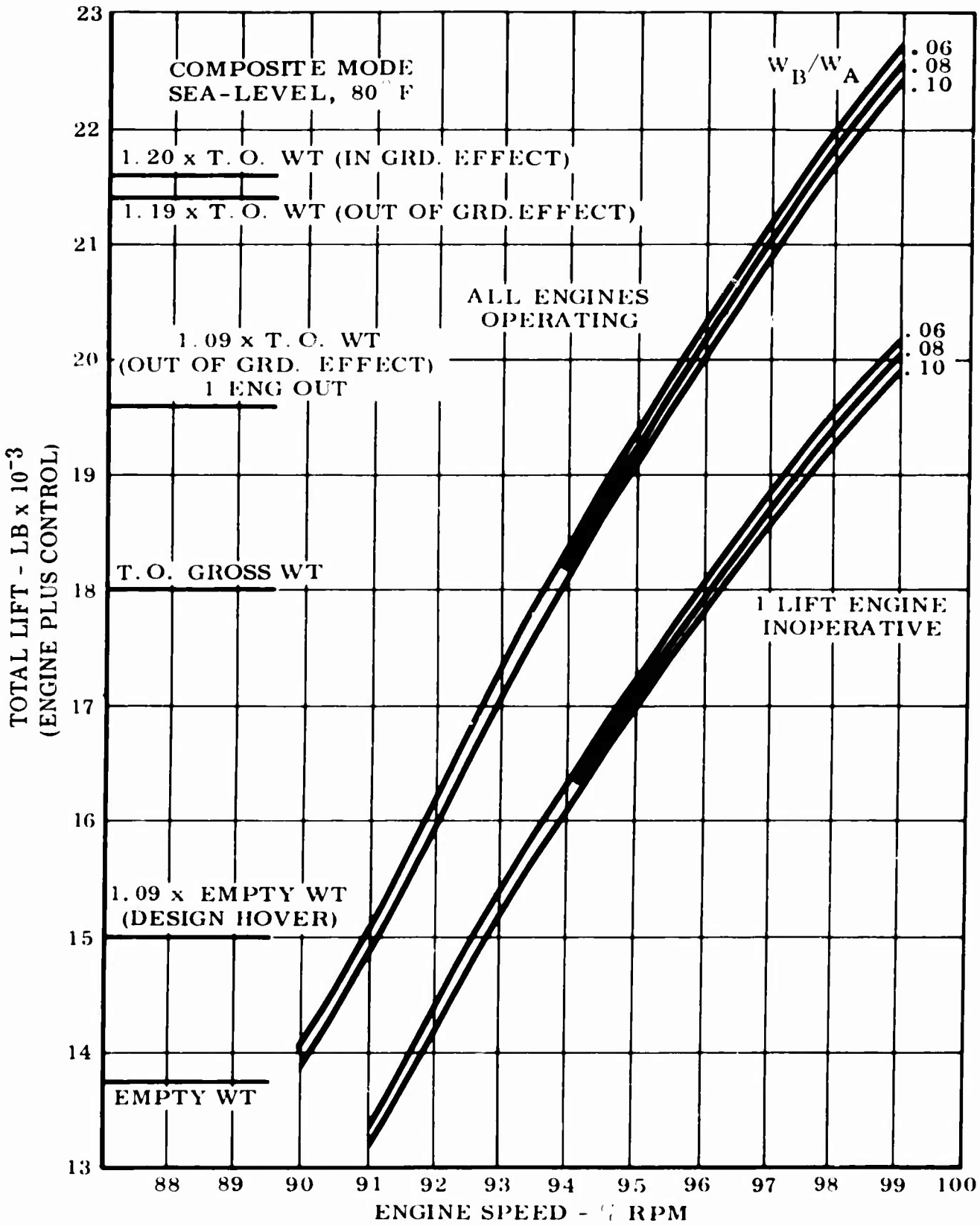

FIGURE 3. LIFT CAPABILITY

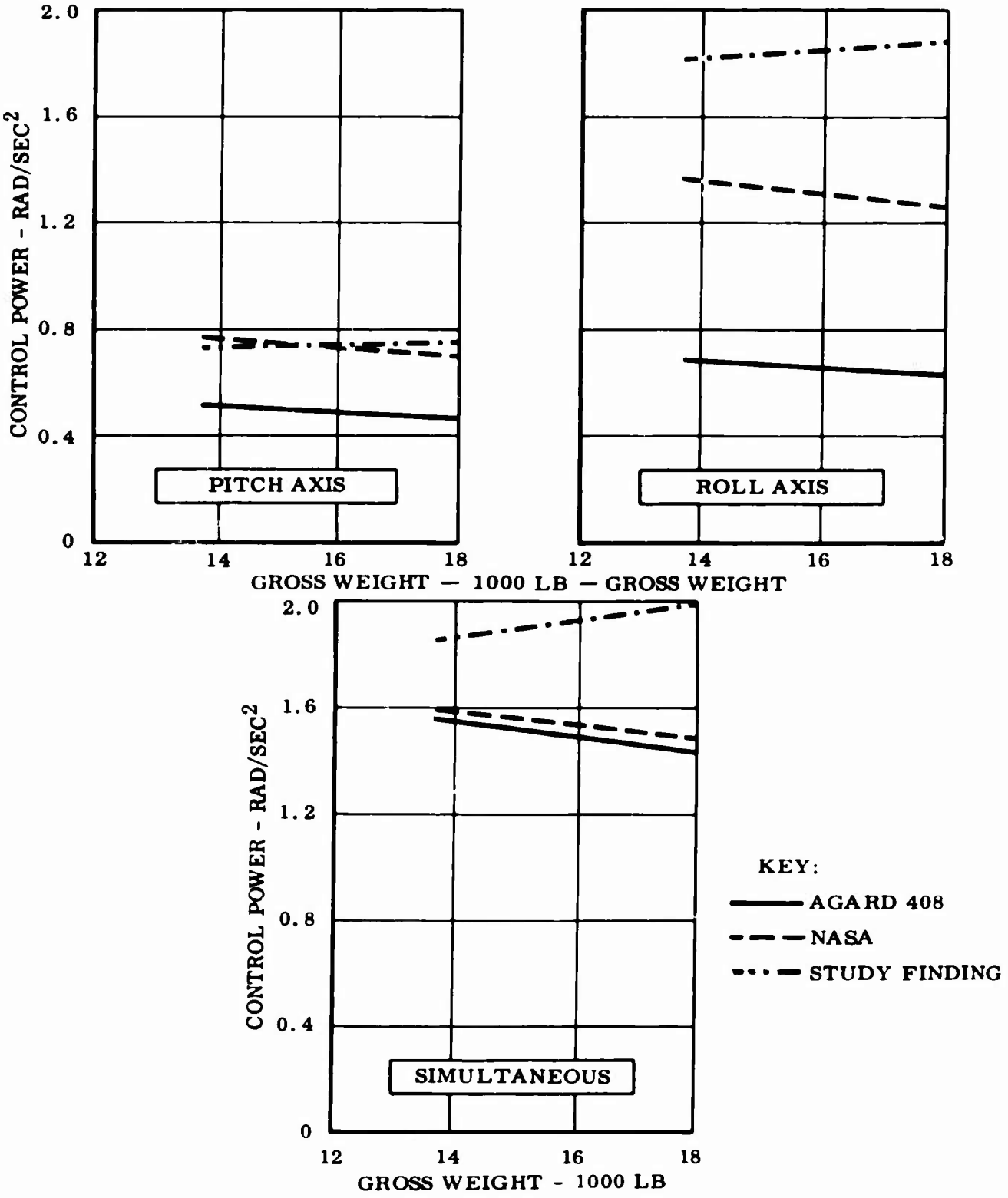

FIGURE 4. CONTROL POWER REQUIREMENTS ALL ENGINES OPERATING

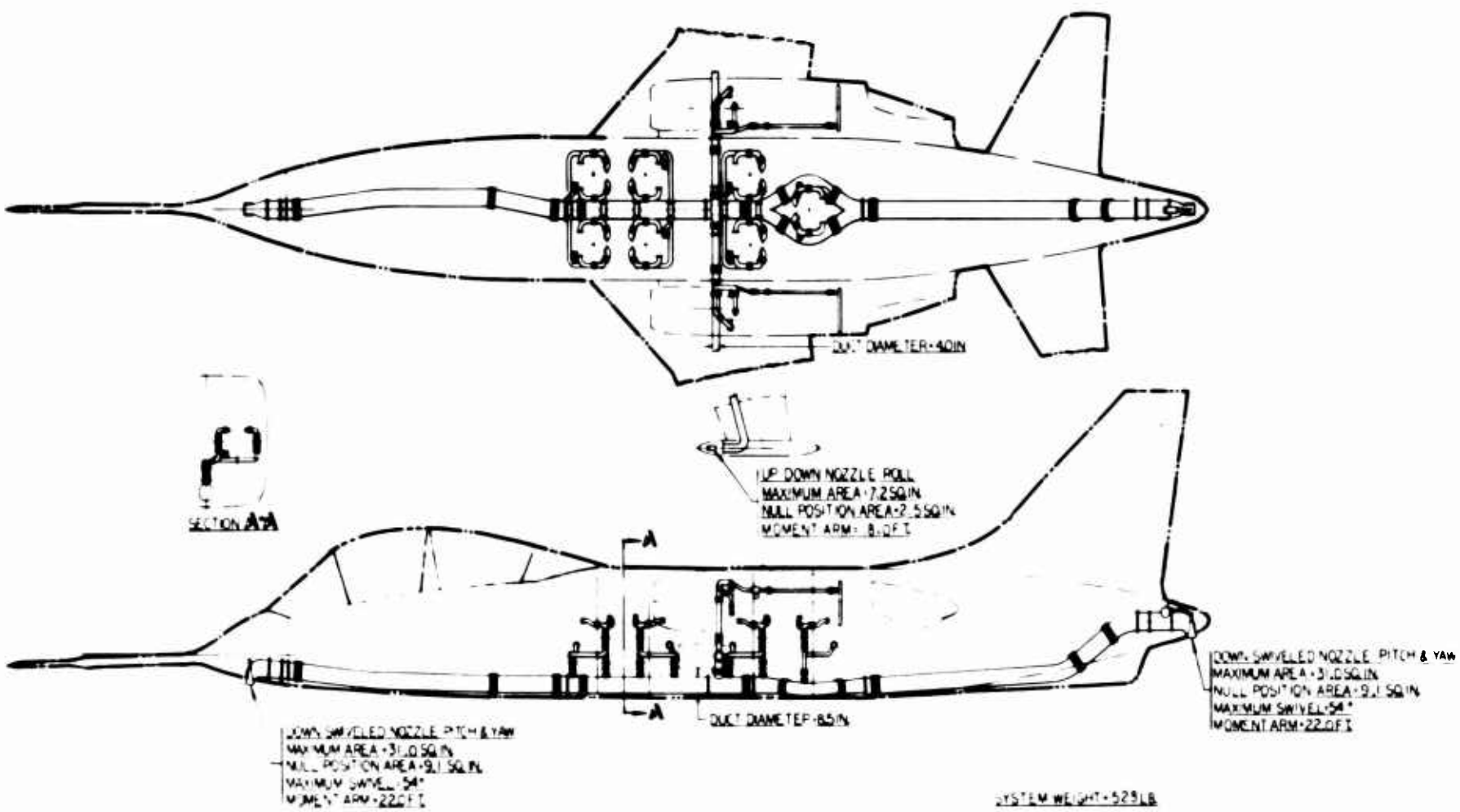

FIGURE 5. REACTION CONTROL SYSTEM

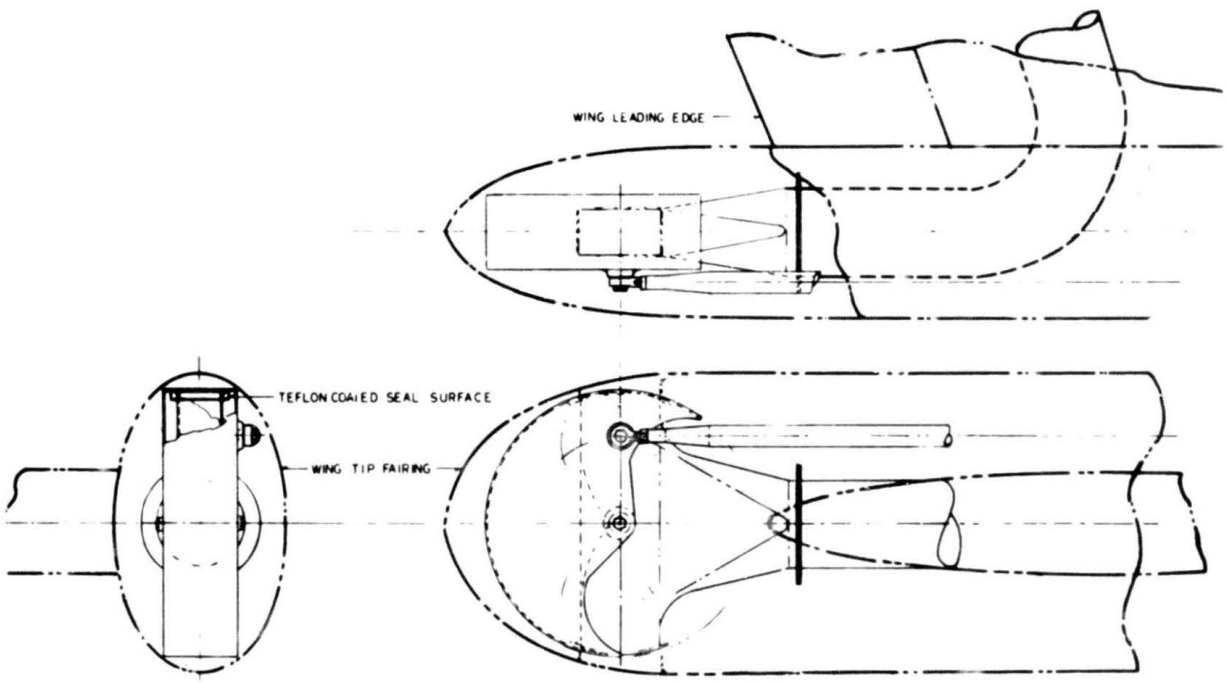

ROLL CONTROL REACTION JET NOZZLE

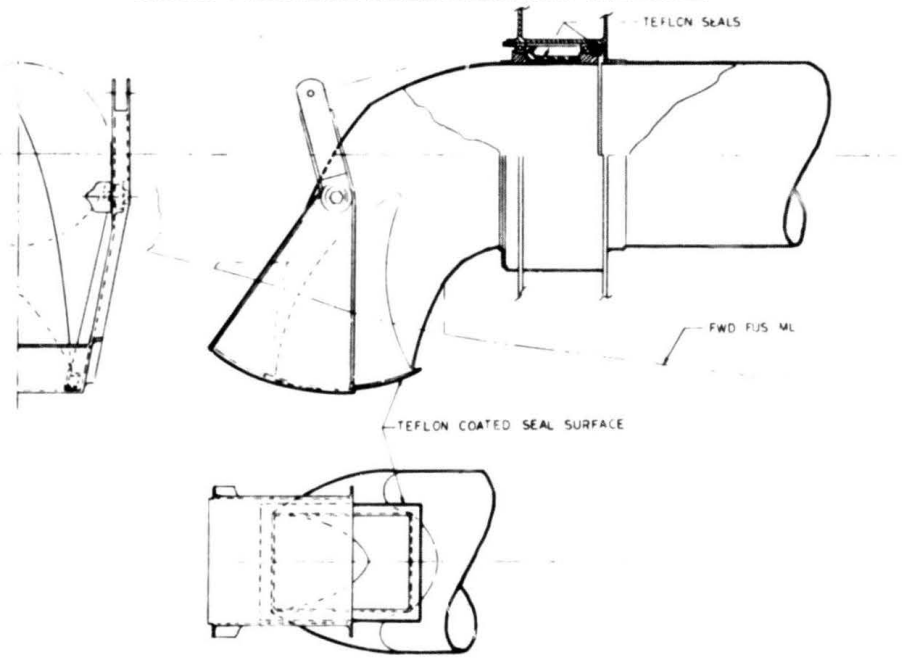

FIGURE 6. YAW-PITCH CONTROL REACTION JET NOZZLE

PITCH-YAW NOZZLE AREA SCHEDULES

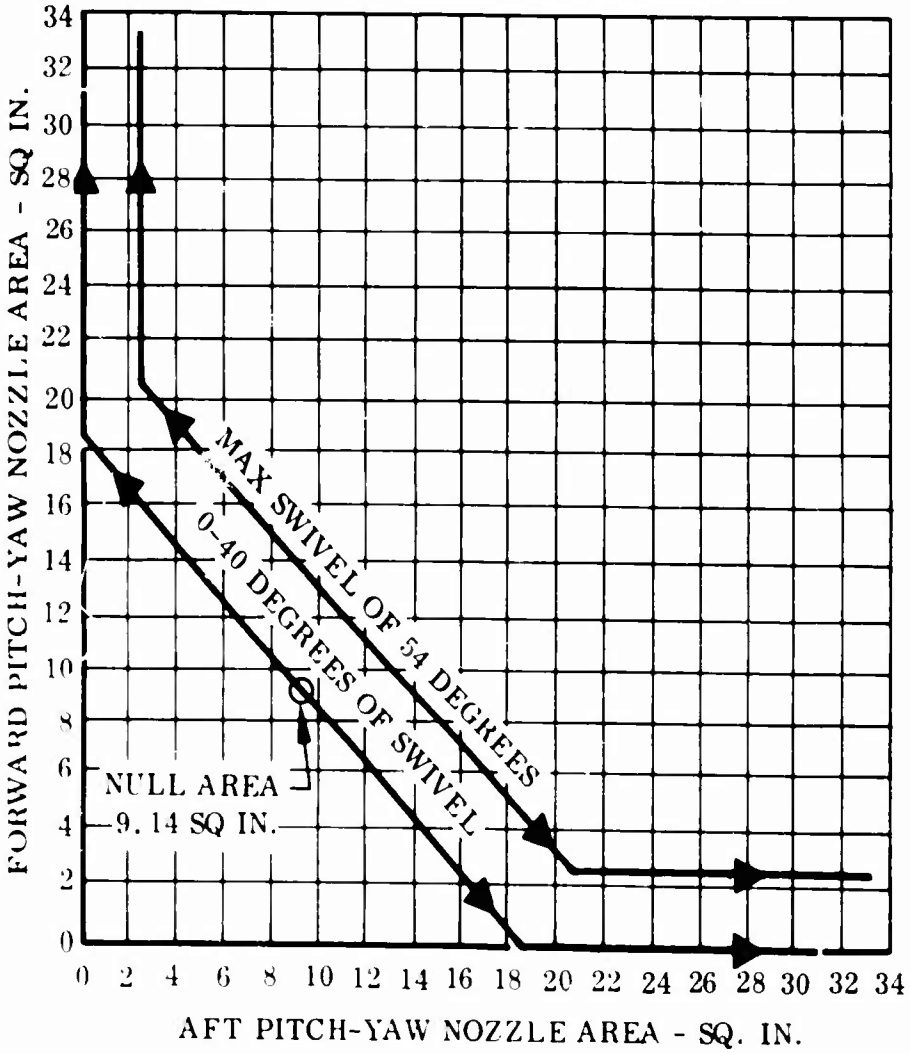

ROLL NOZZLE AREA SCHEDULES

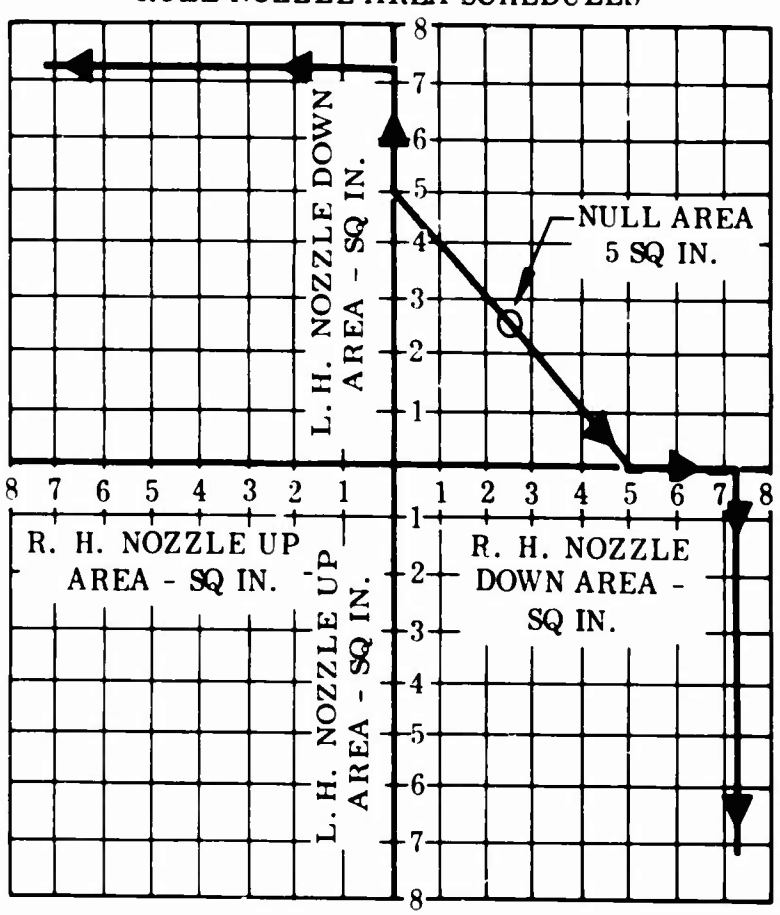

FIGURE 7. REACTION NOZZLE SCHEDULES

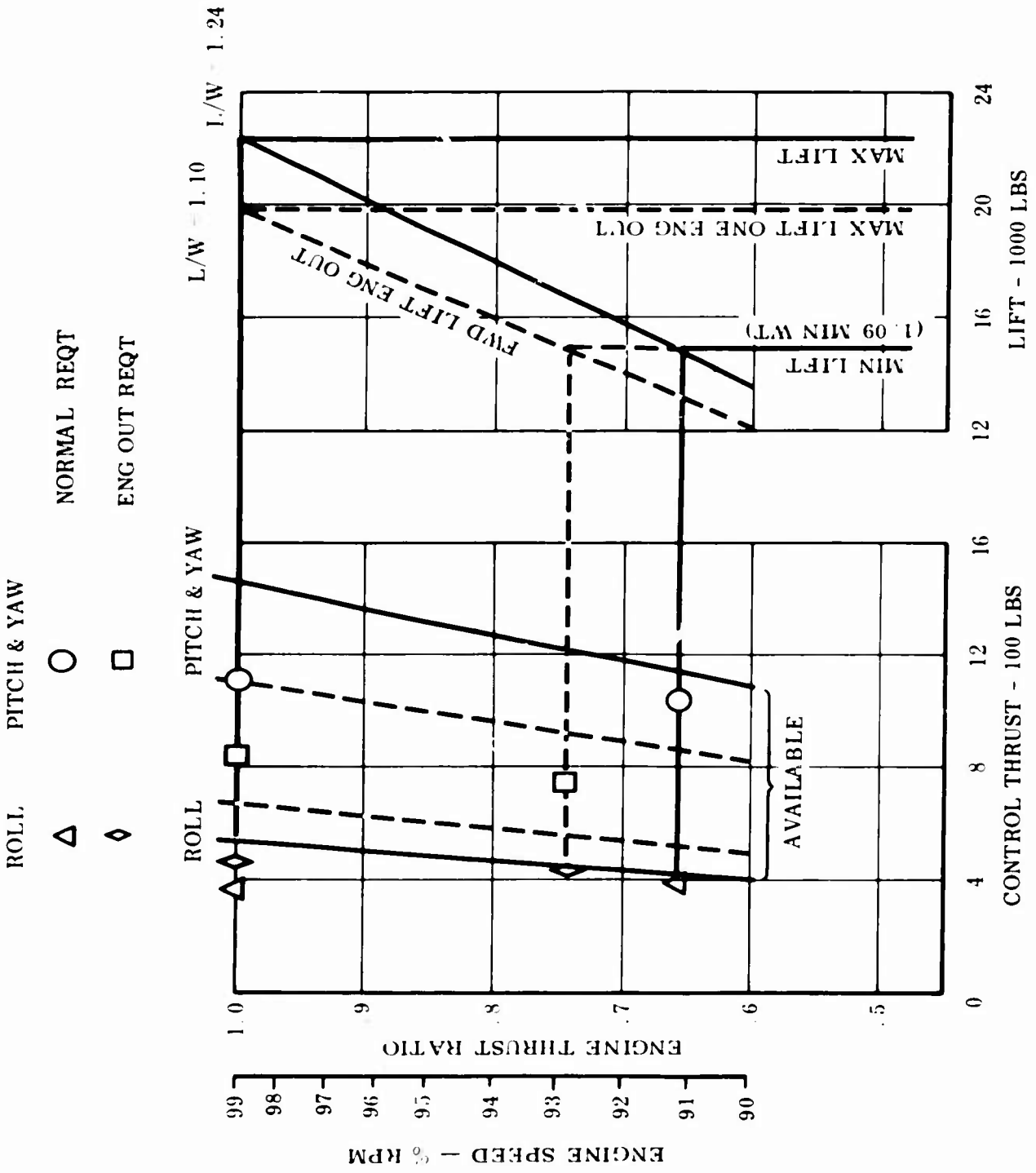

FIGURE 8. SIMULTANEOUS CONTROL THRUST AVAILABLE AND REQUIRED FOR 10% BLEED

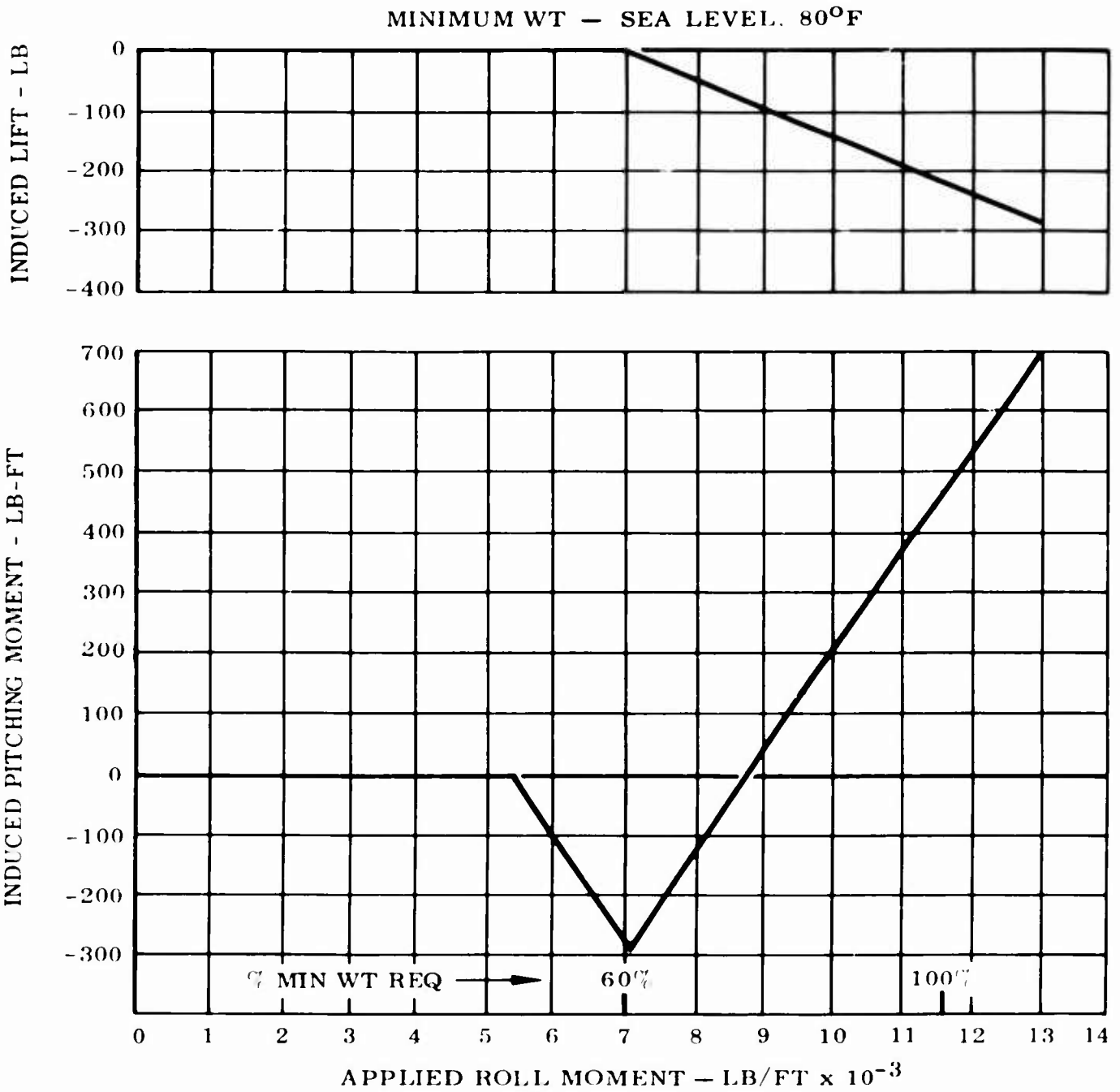

FIGURE 9. PITCH AND LIFT CROSS COUPLING RESULTING FROM APPLICATION OF ROLL CONTROL DURING HOVER

HOT-GAS INGESTION AND JET INTERFERENCE EFFECTS FOR JET V/STOL AIRCRAFT

By Alexander D. Hammond and H. Clyde McLemore

NASA Langley Research Center
Langley Station, Hampton, Va., U.S.A.

SUMMARY

Tests have been conducted in the Langley full-scale tunnel and the Langley 7- by 10-foot tunnels to investigate three of the problems that are unique with jet-powered VTOL aircraft. These problems are: (1) hot-gas ingestion, (2) aerodynamic suck-down, and (3) jet interference in transition flight. The tests concerning hot-gas ingestion were conducted on a large-scale fighter-type model which had a J85 turbojet engine mounted in the fuselage to provide the model exhaust and inlet flow during the tests. Results of the hot-gas ingestion tests showed that aircraft configuration - particularly the exhaust and inlet arrangement - and surface winds can greatly alter the ingestion problem. Deflecting the engine exhaust gases rearward and making rolling take-off to stay ahead of the hot-gas field appears to be one solution to the hot-gas ingestion problem. Another solution is to design the aircraft so that components such as wings shield the engine inlets from the direct path of the hot exhaust gases. The state of the art of hot-gas ingestion is still in an exploratory stage. It is certainly not such that one could accurately predict the inlet air temperature rise for any particular configuration or operating condition. Only gross predictions of ingestion tendencies of new configurations could be made within the scope of the present available data. At the present time, therefore, it should be considered necessary, in the development of a VTOL airplane, to make hot-gas ingestion tests of the particular configurations and operating conditions that are expected to be encountered.

Tests concerning the aerodynamic suck-down and jet interference have been conducted on a number of small-scale models. The results of these investigations have shown that the design principle that should be used to reduce the aerodynamic jet interference effects, on ground and during transition, are in conflict with the design principles that should be employed to reduce hot-gas reingestion effects. It is recommended that future test programs should be coordinated and related, in a manner such that both aerodynamic interference tests and hot-gas reingestion tests will be made on identical configurations, though not necessarily the same model.

HOT-GAS INGESTION AND JET INTERFERENCE EFFECTS FOR JET V/STOL AIRCRAFT

By Alexander D. Hammond and H. Clyde McLemore
NASA Langley Research Center

INTRODUCTION

Since the advent of the turbojet-powered VTOL aircraft several serious problems have been recognized. Three of these problems are: (1) hot-gas ingestion which occurs when the engines ingest their own exhaust or air heated by the exhaust, (2) aerodynamic suck-down, and (3) jet interference in transition flight which results from the jet efflux beneath the aircraft. The purpose of the present paper is to examine these three problem areas in some detail with a review of some recent test information relating to these problems.

The general exhaust and inlet flow patterns that cause hot-gas ingestion are shown schematically in figure 1 for still air and with surface winds. A single, fuselage mounted lift engine is illustrated for simplicity. Multiple engine configurations would complicate the flow patterns; however, this same general flow pattern will still exist. In still air the main part of the exhaust flow will be carried far away from the aircraft and probably will not get reingested into the engine. As the mainstream flows outward it entrains surrounding air, however, and slows down. The entrainment process is highly turbulent and some of the heated air is shed, and when these hot gases rise, because of buoyancy, they are close enough to the inlet to be sucked in, resulting in elevated temperature in the engine inlet. In still air, therefore, the hot-gas ingestion problem is related to the near-field flow.

The exhaust and inlet flow patterns with surface winds, however, are quite different. The exhaust flow is blown back toward the aircraft, and in some cases, very hot inlet air temperatures occur before the aircraft can accelerate up and away from the hot-gas field.

The hot-gas ingestion problem is serious because of the reasons shown in figure 1. The elevated inlet air temperatures cause a loss of engine thrust; and in some instances very rapid inlet temperature increases or large inlet temperature distortions across the engine face can result in engine stall. Some of the factors involved in the hot-gas ingestion phenomenon have been found to be (fig. 1): (1) buoyancy of the hot exhaust, (2) surface winds, and (3) aircraft configuration.

Although hot-gas ingestion is recognized as a serious problem (refs. 1 and 2), very little systematic research of a generalized nature has been done, and most of the generalized research that has been done has been at small scale. (See refs. 2 and 3.) It is not certain that

known scaling parameters are applicable in all cases, so large-scale testing needs to be done until the scaling parameters are verified. Because of this need for large-scale test information, the NASA Ames Research Center initiated an investigation utilizing the large-scale model shown in figure 2. The model was of a relatively specific airplane configuration having in-line lift engine arrangements with aft, side-by-side mounted lift-cruise engines. The results of the investigation are reported in references 4 and 5. In order to provide additional large-scale information of a more generalized nature the Langley Research Center initiated an investigation to study the problem of hot-gas ingestion of several jet VTOL fighter-type configurations. A photograph of the model is shown in figure 2. The tests were conducted outdoors (ref. 6) and in the Langley full-scale tunnel for four exhaust nozzle arrangements with test variables of model height above the ground, wing height, engine inlet position, and wind speed. The data presented herein will be limited to those that were obtained during the Langley tests which were felt to be more generalized than the Ames Research Center investigation.

NOTATION

C_T thrust coefficient, T/qS

D_e equivalent diameter; diameter of a single nozzle having the same area as the sum of several nozzles of a multijet configuration, ft

h height of model above ground, ft

ΔL increment in lift due to interference, lb

ΔL_b increment in lift due to ground proximity, lb

M_X rolling moment, ft-lb

ΔL_g increment in lift due to ground proximity, lb

ΔM increment in pitching moment due to interference, ft-lb

q free-stream dynamic pressure, lb-ft^2

S wing area, ft^2

T thrust, lb

V_j jet velocity, ft/sec

V_∞ free-stream velocity, ft/sec

δ_f flap deflection angle, deg

δ_j jet deflection angle, deg

ρ_j air density in jet, slug-ft^3

ρ_∞ free-stream air density, slug-ft^3

$(V/V_j)_e$ effective free-stream-to-jet-exit-velocity ratio, $\sqrt{\frac{\rho_\infty V_\infty^2}{\rho_j V_j^2}}$

MODEL AND TESTS DESCRIPTION

Hot-Gas Ingestion Model

The model used in the Langley investigation was approximately a 1/3-scale VTOL jet-fighter configuration. The exhaust and inlet arrangements used are shown in the sketches of figure 3. The side nozzle arrangement is somewhat similar to that of the Hawker-Sidley P.1127. Although forward-facing side inlets are illustrated, top inlets (directly over the nozzles) were also tested for all nozzle configurations except the side nozzle configuration which was tested with side inlets only. The general arrangement of the model showing the engine-inlet and exhaust relationships is shown in figure 4. The engine was mounted horizontally in the fuselage with the engine inlet attached to a plenum which allowed inlet air to be taken from either a top inlet position or forward-facing side inlets. The wing could be mounted in either a high or a low position on the fuselage.

Hot-Gas Ingestion Tests

The tests were conducted for an exhaust nozzle pressure ratio of about 1.8 and an exhaust gas temperature of 1200° F. The single nozzle diameter was 12 inches (30.48 cm) which was also the effective diameter of all the test configurations.

Since with exhaust nozzles vertical hot-gas ingestion would normally begin at the time of engine start, and since some time must be allowed for stabilizing engine conditions before recording data, some method is obviously needed to remove the hot gases from the vicinity of the model during this initial engine start and stabilization period. The method used during the subject investigation was remotely controlled exhaust nozzles capable of deflection angles of straight down and 25° rearward. In order to establish realistic time intervals, discussions were held with NASA pilots who have flown jet VTOL aircraft, and it was decided to conduct all of the Langley tests in the following manner: (1) start the

engine and stabilize at idle speed with nozzles deflected rearward 25°; (2) advance the throttle to obtain 80-percent engine rpm and then deflect the nozzles straight down; (3) pause about 3 seconds (simulating time for pilot checks), and then (4) advance the throttle to full power. After running at full power for about 10 seconds the test was terminated by shutting off the engine. This 10-second interval provided ample time to establish the operating level of the inlet air temperatures.

All the data obtained during the tests were recorded on oscillograph recorders in the form of time-history information utilizing bare-lead 0.005-inch (approximately 0.013 cm) thermocouples. Each of the side inlets had 18 thermocouples and top inlets had 9 thermocouples. A typical time history is shown in figure 5. The time histories shown are in the upper and lower portion of the left-hand inlet of the side inlet, rectangular nozzle configuration for a nozzle height of about one-nozzle diameter. The inlet air temperatures are seen to rise very quickly, following downward nozzle deflection, and are seen to vary in a very erratic manner. The inlet air temperature rise data presented herein are the average temperature increase in the inlet that occurs between the instant of downward nozzle deflection to a relatively stabilized temperature condition following the attainment of full-engine thrust. The engine thrust level is indicated by the nozzle pressure with time shown also on figure 5.

RESULTS AND DISCUSSION

Hot-Gas Ingestion

Still air.- The inlet air temperature rise in still air of all the nozzle and inlet configurations investigated is shown in figure 6 for a range of nozzle heights above the ground in effective nozzle diameters. The wing used was a high-mounted delta wing.

For convenience, the inlet air temperatures of the two forward inlets of the top, multiple inlet configurations were averaged and are presented herein. The rearmost two inlets experienced somewhat lower temperatures because of wing shielding.

With either top or side inlets the inlet air temperature rise was quite low for the single and in-line nozzle configurations, but the rectangular and side nozzle configurations resulted in very high values of inlet air temperature rise. The inlet air temperature rise is seen to be very dependent upon the nozzle and inlet position. The very large inlet air temperature rise experienced by the rectangular nozzle arrangement is believed to be the result of the fountain of hot gases that forms between the ground-impinging jets. This fountain of hot gases spreads around the fuselage and quickly arrives in the vicinity of the inlets before it has had time for much mixing with the surrounding air and is, therefore, still very hot. The side inlet, rectangular nozzle

arrangement has very high inlet air temperatures near the ground (the order of 100° F at a nominal landing gear height of about 1.5 diameters). Of particular interest, however, is that the inlet air temperature rise in general decreases very rapidly with increasing height and would probably be of little concern by the time the aircraft had risen 5 to 10 nozzle diameters above the ground.

Surface winds.- The effect of surface winds on the test configurations is shown in figure 7. It is assumed that the aircraft would be headed into the existing wind, so that data are presented for head wind conditions. The inlet air temperature rise in degrees Fahrenheit is presented as a function of wind speed in knots for a model height of about one effective nozzle diameter for a high-delta-wing configuration.

As previously stated, surface winds have been found to be cause for concern, and the reason becomes apparent here. The inlet air temperature rise, in general, is seen to increase with very low headwinds. Of particular interest, however, is that at forward speeds of the order of 30 knots, the hot-gas ingestion problem has just about disappeared. It should be pointed out that the inlet temperature for the single-jet configuration indicates a significant temperature rise even for high-speed wind conditions, particularly for the side inlets. The exact phenomena involved are not understood at this time; however, it is felt that the single-jet case is not a practical configuration and it was included in this program to provide a base of reference. The observation of smoke ejected through the exhaust nozzles shows that the exhaust gases are swept rearward and below the inlets for speeds greater than about 30 knots. This suggests a technique for eliminating the problem of hot-gas ingestion. The technique is one called a rolling vertical take-off and has frequently been proposed. For the particular configurations of the present paper, the pilot could leave the nozzles deflected rearward until forward speeds the order of 30 knots were reached and at that time could deflect the nozzles downward and take off without experiencing any hot-gas ingestion. Of course vertical take-off from a raised grating would be effective in reducing hot-gas ingestion, but the raised grating would present logistic and other problems for operational military aircraft. The rearward nozzle deflection technique cannot be used to avoid the problem of hot-gas ingestion during vertical or very low-speed landing, however, since a near vertical nozzle orientation would be required to support the aircraft in a condition of horizontal equilibrium. It appears that small rearward nozzle deflections would not eliminate the hot-gas environment near the ground. Tilting the engine nozzles apart or some other technique may be effective in reducing the hot-gas ingestion during vertical landings, however. In any case, some method other than slow forward translation speeds, must be used for the elimination of hot-gas ingestion on landing. Even though some reduced thrust could be tolerated, because landings are normally made at reduced weight, any hot-gas ingestion that could cause one or more engines to stop operating could not be tolerated during a landing maneuver.

In general, the side inlets are seen to result in higher values of inlet air temperature rise than the top inlets (fig. 7), and the various nozzle arrangements are seen to result in very different amounts of ingestion. Aircraft configuration - particularly the inlet and exhaust nozzle arrangement - is seen, therefore, to be a major factor in the hot-gas ingestion problem.

Wing position.- In addition to the obvious configuration variables of inlet and nozzle arrangement, the placement of the wing on the fuselage was also found to be an important parameter. The effect of wing height on the inlet air temperature rise of the rectangular and the in-line nozzle arrangements with top inlets for a zero wind condition is shown in figure 8. Inlet air temperature rise is shown as a function of model height above the ground in effective nozzle diameters. The wing in a low position is seen to greatly reduce the inlet air temperatures at all test heights of the rectangular nozzle configuration, but has little effect on the in-line nozzle configuration which had very low inlet air temperatures with either wing position. The reason for the low inlet air temperature, as noted by observing smoke from the exhaust nozzles, was that the low wing caused the upward-flowing hot gases to be deflected outward and away from the inlets. The in-line arrangement has a much less intense fountain than the rectangular arrangements and therefore shows little temperature rise with either a high or a low wing. The effect of fore or aft inlet location is illustrated in figure 9. The temperature rise data are for the rectangular nozzle configuration with top inlets for a range of nozzle heights and wind speeds. The temperatures of the two forward inlets and the two rear inlets were averaged. The relatively unprotected forward inlets have higher inlet temperatures than do the rear inlets. The reason for the lower rear inlet temperature is that the wing shields these inlets from the direct upward flow of hot gases.

Temperature distortion.- As stated in the outset, one of the main reasons for concern about the hot-gas ingestion problem is that very rapid inlet air temperature rises and/or very uneven temperatures across the face of the engine inlet can cause compressor stall resulting in engine flameout. Engine stall has been experienced by several investigators and, in particular, by the Ames and Langley experimenters. Of course, an engine stall cannot be tolerated in a jet VTOL aircraft so means of preventing the stall must be found. To illustrate the very rapid rise in inlet air temperatures following downward nozzle deflection and the very large temperature distortions that can occur across the face of the engine, the data of figure 5 will be reviewed. The time-history plot is for the rectangular nozzle configuration with side inlets with the model height at about one effective nozzle diameter. The two oscillograph traces represent the inlet temperature existing at two locations of the left-hand inlet for a zero wind condition. The inlet air temperature near the bottom of the inlet is seen to rise almost immediately following downward nozzle deflection to about 150° F with very rapid variations in the temperature. These rapid rises and variations are known to precipitate engine stall. The upper temperature probe location

indicates very rapid changes in temperature also, but the temperature level is of the order of 50° F. Comparison of the two traces shows the large distortions of temperatures that can occur across the face of a jet VTOL engine. Distortions of this magnitude or less (100° across the engine face) are also known to aggravate the stall problem.

Although the engines used in the Ames and Langley investigations are early versions of turbojet engines and are known to be very susceptible to stall, the newer engines of today, because of their very high performance, will probably be just as susceptible to these inlet temperature conditions. In addition to the inlet temperature problem, rapid fluctuations of inlet pressures are also known to result in engine stall on some occasions. Because the stall problem cannot be tolerated on a jet VTOL aircraft, these inlet air temperature rise and pressure fluctuation problems should continue to be given much consideration by the V/STOL engine manufacturers.

It should be reemphasized that one of the principal factors of hot-gas ingestion is aircraft configuration, that is, how the engine nozzles and inlets are arranged. The problem with multiple nozzle arrangements is that the exhaust gas tends to flow upward between the nozzles where it may reach the vicinity of the inlets very quickly while it is still very hot. The solution to this situation appears to be to group the engine nozzles in such a manner that the hot-gas fountain effects are minimized; by placing the inlets in an area removed from the direct path of the hot exhaust gases; and by designing the aircraft so that components, such as the wing, shield the inlets from the direct path of the hot gases. The other main cause of hot-gas ingestion is ground winds. In this case the problem is that winds tend to blow the far-field gases back toward the aircraft and into the inlets before these gases have had time to mix with the surrounding air and cool off. This problem of winds is difficult to assess since different configurations are affected differently by winds. One solution to the problem, and perhaps the configuration problem as well, appears to be to deflect the engine exhaust so that it is directed away from the aircraft and to make rolling takeoffs to stay ahead of the hot-gas field.

One observation that should be made from the foregoing presentation is that the state of the art of hot-gas ingestion is still in an exploratory stage. It is certainly not such that one could accurately predict the inlet air temperature rise for any particular configuration or operating condition. Only gross predictions of ingestion tendencies of new configurations could be made within the scope of the present available data. At the present time, therefore, it should be considered necessary in the development of a VTOL airplane, to make hot-gas ingestion tests of the particular configurations and operating conditions that are expected to be encountered.

Aerodynamic Interference Effects

Ground effects for hovering flight.- The hot-gas reingestion data just discussed as well as other work to date has indicated that the design principles which should be employed to minimize hot-gas reingestion are in direct conflict with those that should be used to minimize the well-known aerodynamic suck-down in ground effect. For example, the hot-gas reingestion work indicated that use of a low wing is quite powerful in reducing inlet temperature rise. However, from the aerodynamic suck-down in ground effect point of view, the high wing is preferred (ref. 7). Also the rectangular array which produces a favorable pressure region between the jets to reduce the aerodynamic suck-down (ref. 7) also produces high inlet temperatures as does spacing the jet exits further apart. As is well known, in addition to the loss of thrust from hot-gas ingestion when hovering near the ground, there is the aerodynamic lift loss resulting from the proximity of the ground during hovering flight as illustrated in figure 10. The flow characteristics are shown for a single-jet nozzle with air exhausting vertically through a flat plate at a height h above the ground. As the air from the jet impinges on the ground, it flows outward along the ground as shown. The entrainment of the surrounding air in this flow pattern creates regions of negative (suck-down) pressure. The flow pattern for multiple jet arrangements is also illustrated in figure 10. The main difference between the single and multiple jet flow patterns, of course, is the interaction of the flow between the jets of the multiple jet arrangement which results in the so-called fountain effect that creates positive pressures in the region between the jets.

Single-jet model tests.- The aerodynamic suck-down for the single-jet case is well understood and full-scale characteristics for single-jet configurations can be predicted quite well as shown by the data presented in figure 11. The increment of lift due to ground ratioed to the net thrust is plotted as a function of ground height expressed in effective nozzle diameters for full-scale flight tests and scale model tests of the X-14A airplane. L. A. Wyatt (ref. 8) has derived, from a correlation number of single-jet model tests, an empirical method to determine the effects of ground on the lift of single-jet configurations. For comparison with the model- and flight-test data, a calculated curve for the X-14A airplane, using the method of Wyatt, is also shown in figure 11. Since the jets of the X-14A are so closely spaced, it has been assumed that they act essentially like a single jet. It can be seen that the full-scale flight results are in good agreement with both the scaled model tests and the calculated results using the method of Wyatt. For this type of configuration, the hot-gas reingestion problem would be primarily due to winds.

Multijet model tests.- The serious problems of compromise between design for minimum hot-gas ingestion and aerodynamic suck-down occur for the multijet case. Although the suck-down for many multijet configurations has been investigated and many of the results have been published in the literature, the story for multijet configurations is not

as clear at this time as for single jets. However, an interesting trend can be seen in the results (fig. 12) of a systematic investigation of a wing body with several different arrangements of multiple jets made by Wilhelm Seibold (ref. 9). Since the out-of-ground lift losses were not subtracted from the data of this group of tests the combined losses due to base pressure and ground effects have been plotted as the ratio of interference lift to thrust as a function of ground height to the fuselage lower surface expressed in effective nozzle diameters (fig. 12). The basic configuration consisted of four engines arranged in a cluster near the center of the wing body. The delta-wing planform was a midwing configuration. The single-jet case was obtained by ejecting air from the right near nozzle only and the results are indicative of the general trends previously shown for the single jets. The two rear jets were tested together and since the spacing for this configuration was further apart than the X-14A model tests the data show a reversing of the lift loss due to ground at very low ground heights. As the number of jets is increased to four, the lift losses become smaller. As the spacing between the jet exits increased, as is shown by the other two four-jet configurations, the interference lift becomes favorable at ground heights above approximately two effective jet diameters. The results shown here indicate a consistent trend toward reduction of lift loss with clustering the engines exits and with spacing the engines apart so as to enlarge the model area experiencing favorable pressure regions resulting from the jet interaction on the ground under the model. The increase on spacing would, however, be expected to aggravate the hot-gas ingestion problem due to the reduction in shielding of the inlets and the probable large volumes of the fountain flow.

The hovering ground effect of a model configuration having either a single row of jets down the fuselage centerline or a rectangular array of jets in the fuselage, as indicated on the model sketch, are compared in figure 13. The model as shown in the sketch at the top of figure 13 had a low wing with an aspect ratio of 5.8, a taper ratio of 0.32, and a quarter-chord sweep of 28.2°. The data were run in a recent investigation at the Langley Research Center and the results are as yet unpublished. The incremental lift due to ground is ratioed to the thrust and plotted against ground height expressed in effective jet diameters. The beneficial effect of the rectangular array is shown by a comparison of the data for the single row of jets with the clustered jet arrangement. An additional benefit can be realized by canting the nozzles outboard from the vertical through 10°. This effect is similar to an increase in jet spacing shown in figure 12 since canting the engines increases the spacing of the jet impingement on the ground. The effect of canting the engines on the hot-gas reingestion is unknown at this time, but indications are that engine canting will have an unfavorable effect.

Although the general trends of the effects of interference of multijets in the presence of the ground have been illustrated to some extent

in figures 12 and 13, it should be emphasized that only the trends are known. The results of many different multijet investigations have been documented and have indicated that the magnitude of the lift interference due to ground effect in hovering flight is dependent on the model configuration as well as the jet-exit arrangement. Therefore, in spite of the fact that these two sets of test data seem to show consistent trends, attempts to correlate the effect of ground on the interference lift has not as yet produced the desired results.

Transition interference.- The aerodynamic interference effects experienced in the transition speed regime between hovering and conventional flight has been the subject of a number of investigations summarized in reference 10. A large part of the research effort on jet VTOL configurations has been the investigation of the forces and moments induced on the aircraft by interaction of the vertical jets with the free-stream airflow during transition flight. As is illustrated in figure 14, during transition flight, the jets issuing from an aircraft are swept rearward by the free-stream flow and are rapidly rolled up in a pair of vortices. These rolled-up vortices and the vorticity represented by the velocity change across the boundary of the jet induce suction pressures and a downwash on adjacent surfaces on the aircraft.

The results of an investigation of the aerodynamic interference effects during transition flight on this particular five-jet VTOL model (fig. 15) have been discussed briefly in reference 10. A typical set of interference data are shown in figure 15. The incremental interference lift due to forward flight ratioed to thrust is plotted as a function of the effective free stream to jet-exit velocity ratio representing flight from 0 or hovering flight to conventional flight speeds. For this configuration with all jets deflected down and operating, the expected suction pressures and downwash cause a loss in lift and a nose-up pitching moment that increase with speed during the transition from hovering to conventional flight. In an effort toward a better understanding of these transition characteristics, tests were run with the three front lift engines only operating. The results indicate that jets located in front of the wing result in an unfavorable lift loss. Similarly tests were made with the deflected cruise engines (rear jets) only operating and the results indicate that the lift interference is favorable. The results of this investigation and others which have been made recently indicate that the loss in lift due to interference during transition can be minimized with proper location of the lift jets with respect to the wing. The pitching-moment trim resulting from engine location also shows that proper engine location will minimize the interference effects.

In order to explore this effect of jet position more systematically, a generalized study of jet positions several wing-chord lengths ahead to several chord lengths behind an unswept wing was initiated at the Langley Research Center. In this investigation, an aspect-ratio-6, unswept, untapered, wing-fuselage model equipped with a 30-percent chord slotted Fowler flap was used. Two jets, one on either side of the fuselage, were positioned spanwise at about the 25 percent wing station and at the various

longitudinal and vertical positions shown by the plus marks in figure 16. The jets were mounted independently of the wing so that only the aerodynamic forces and interference effects were measured on the wing. The data show that with the exits on the wing-chord plane, considerable jet interference was experienced even with the jet as far as four chords ahead of the wing. Favorable interference effects, however, are encountered with the jets beneath and behind the 50-percent chord point of the wing and the interference effects are most favorable for positions closest to the flap. These results show general agreement then with the results for the five-jet model which have just been discussed and results reported previously by Williams in reference 11. These favorable interference increments are believed to be due to the action of the jet in helping the flap achieve its full lift potential. Another slightly different configuration with jets both in front of and behind the wing indicated an overall favorable interference lift effect, again indicating the importance of configuration geometry on the jet interference lift and moment characteristics.

CONCLUDING REMARKS

Hot-gas ingestion tests and tests concerning aerodynamic suck-down in ground effect and jet interference in transition have indicated the following:

1. The hot-gas ingestion problem depends upon the airplane configuration, particularly the position of the inlet relative to the nozzle exit arrangement and the relative position of the wing and other elements of the aircraft that could shield the inlets from the hot exhaust gases. The nozzle arrangements are an important parameter, in-line nozzles resulted in relatively low inlet temperatures whereas rectangular arrangements resulted in relatively high inlet temperatures.

2. Wind speed has a large effect on the magnitude of the inlet air temperatures. The maximum inlet air temperatures, in general, occurred for head winds between 0 and 20 knots, and the reingestion disappeared for most multijet nozzle arrangements for head winds above 30 knots.

3. Deflecting the engine's exhaust rearward and making rolling takeoff to stay ahead of the hot-gas field appeared to be one solution to the hot-gas reingestion probe.

4. The art of hot-gas ingestion is still in an exploratory stage. It is certainly not such that one could accurately predict the inlet air temperature rise for any particular configuration or operating condition. Only gross predictions of ingestion tendencies of new configurations could be made within the scope of the present available data. At the present time, therefore, it should be considered necessary in the development of a VTOL airplane, to make hot-gas ingestion tests of the particular configurations and operating conditions that are expected to be encountered.

5. The design principles that should be used to minimize aerodynamic interference effects, both in ground effect and during transition are in conflict with the design principles which should be employed to reduce the effects of hot-gas ingestion.

6. In the future, it is recommended that related and coordinated test programs, using identical configurations (not necessarily the same model) be established to investigate aerodynamic jet interference effects, both in ground effect and during transition, and the effects of hot-gas reingestion.

REFERENCES

1. McKinney, M. O., Jr.; Kuhn, R. E.; and Reeder, J. P.: Aerodynamics and Flying Qualities of Jet V/STOL Airplanes. Preprint 864A, Soc. Automotive Engrs., Apr. 1964.

2. Langfelder: Bodeneffekte bei Senkrechtstart-Flugzeugen (Ground Effects of VTOL Aircraft). EWR-Nr. 37/62, Entwicklungsring Süd (München), Mar. 1963.

3. Speth, Robert F.; and Ryan, Patrick E.: A Generalized Experimental Study of Inlet Temperature Rise of Jet V/STOL Aircraft in Ground Effect. Bell Aerosystem Co. Rept. 2099-928-003 (Contract No. N600(19)63320), April 1966.

4. Tolhurst, William H., Jr.; and Kelly, Mark W.: Characteristics of Two Large-Scale Jet-Lift Propulsion Systems. Conference on V/STOL and STOL Aircraft, NASA SP-116, 1966, pp. 205-228.

5. Lavi, Rahim: Parametric Investigation of VTOL Hot-Gas Ingestion and Induced Jet Effects in Ground Proximity. Northrop-Norair Report NOR 67-32, February 14, 1967.

6. McLemore, H. Clyde: Considerations of Hot-Gas Ingestion for Jet V/STOL Aircraft. Conference on V/STOL and STOL Aircraft, NASA SP-116, 1966, pp. 191-204.

7. Hammond, Alexander D.: Thrust Losses in Hovering for Jet VTOL Aircraft. Conference on V/STOL and STOL Aircraft, NASA SP-116, 1966, pp. 163-176.

8. Wyatt, L. A.: Static Tests of Ground Effect on Planforms Fitted With a Centrally-Located Round Lifting Jet. C. P. No. 749, Brit. A.R.C., 1964.

9. Seibold, Wilhelm: Untersuchungen Über die von Hubstrahlen an Senkrechtstartern Erzeugten Sekundärkräfte. Jahrb. 1962 WGLR.

10. Margason, Richard J.: Jet Induced Effects in Transition Flight. Conference on V/STOL and STOL Aircraft, NASA SP-116, 1966. pp. 177-189.

11. Williams, John; and Wood, Maurice N.: Aerodynamic Interference Effects With Jet Lift Schemes on V/STOL Aircraft at Forward Speeds. Aerodynamics of Power Plant Installation, Pt. II, AGARDograph 103, Oct. 1965, pp. 625-651.

STILL AIR

SURFACE WINDS

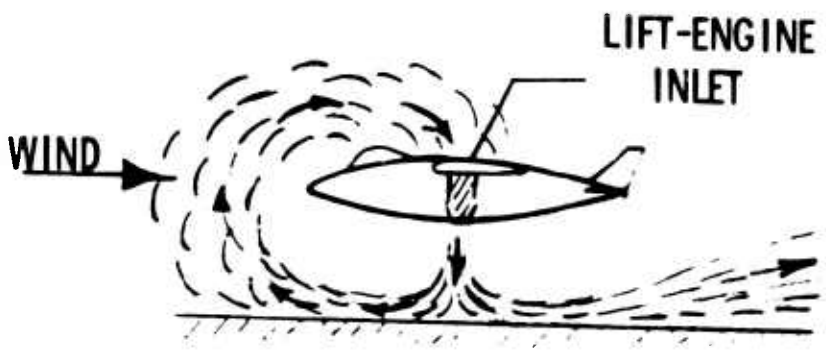

REASONS FOR CONCERN

- THRUST LOSS
  - TEMPERATURE RISE OF 40°F CAUSES 15 % LOSS OF THRUST
- COMPRESSOR STALL
  - RAPID TEMPERATURE RISE
  - TEMPERATURE DISTRIBUTION

CAUSES

- BUOYANCY OF HOT EXHAUST
- SURFACE WINDS
- CONFIGURATION
  - EXHAUST AND INLET ARRANGEMENT

Figure 1.- Hot-gas reingestion.

AMES-NORTHROP
FULL-SCALE MODEL

LANGLEY
1/3-SCALE MODEL

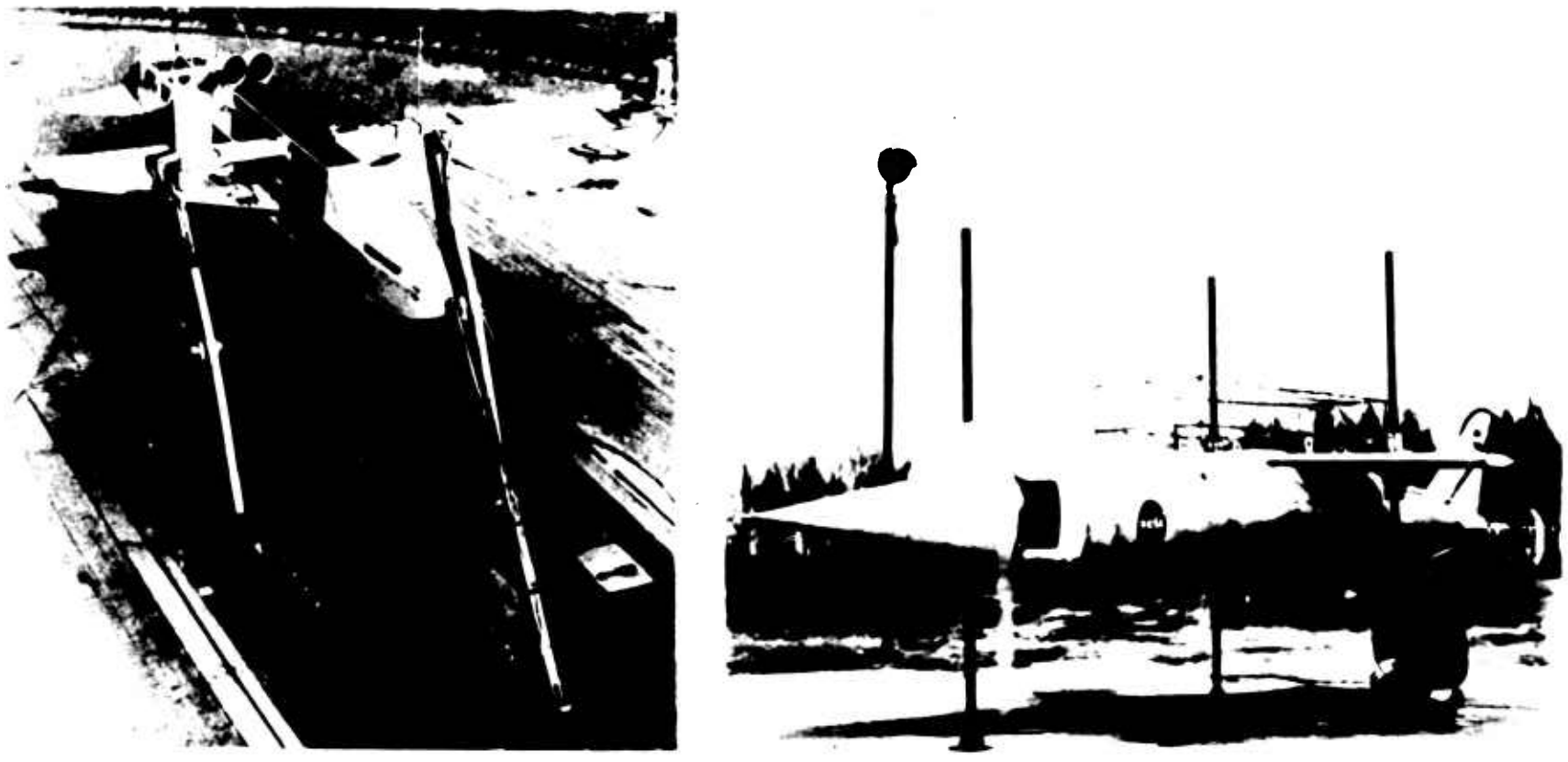

Figure 2.- Large-scale NASA models.

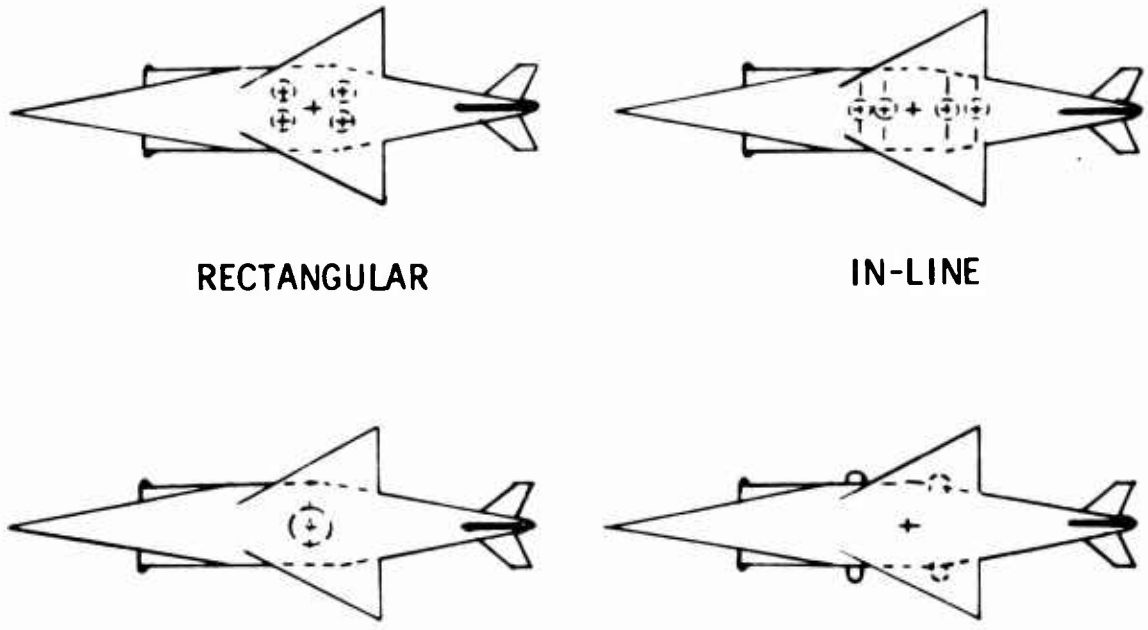

Figure 3.- Sketches of hot-gas ingestion model showing nozzle arrangement, high-delta wing, forward facing side inlets.

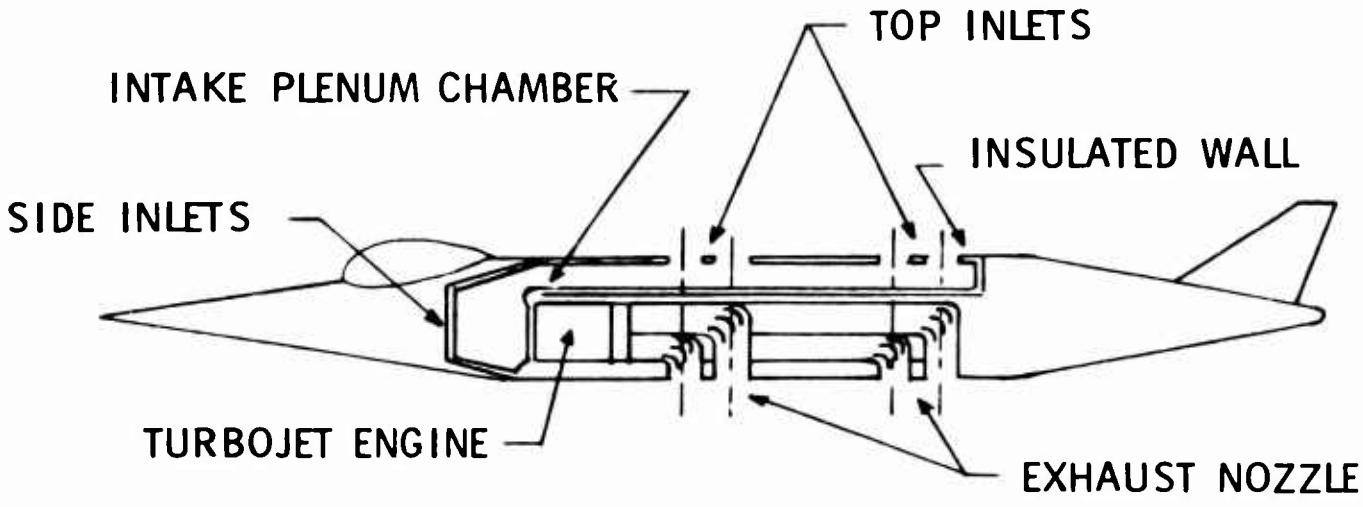

Figure 4.- Schematic arrangement of inlets, exhausts, and plenum chamber (in-line lift engine configuration illustrated).

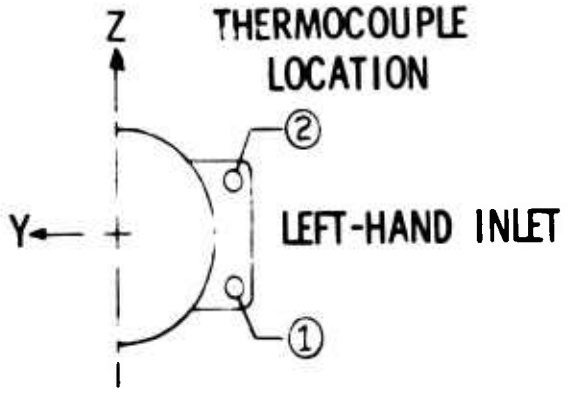

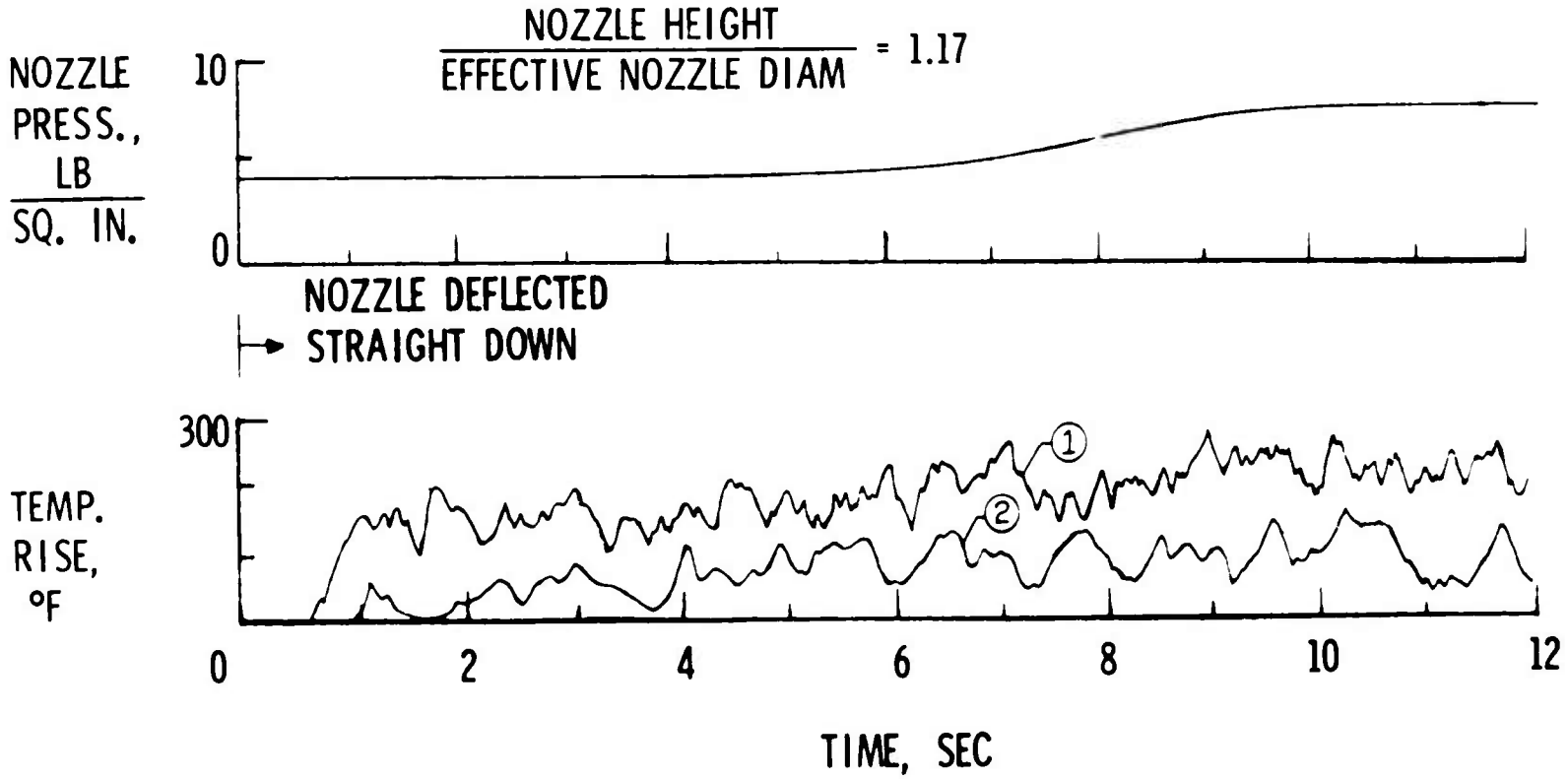

Figure 5.- Time history of inlet temperature rise and nozzle pressure, rectangular nozzle arrangement with side inlets.

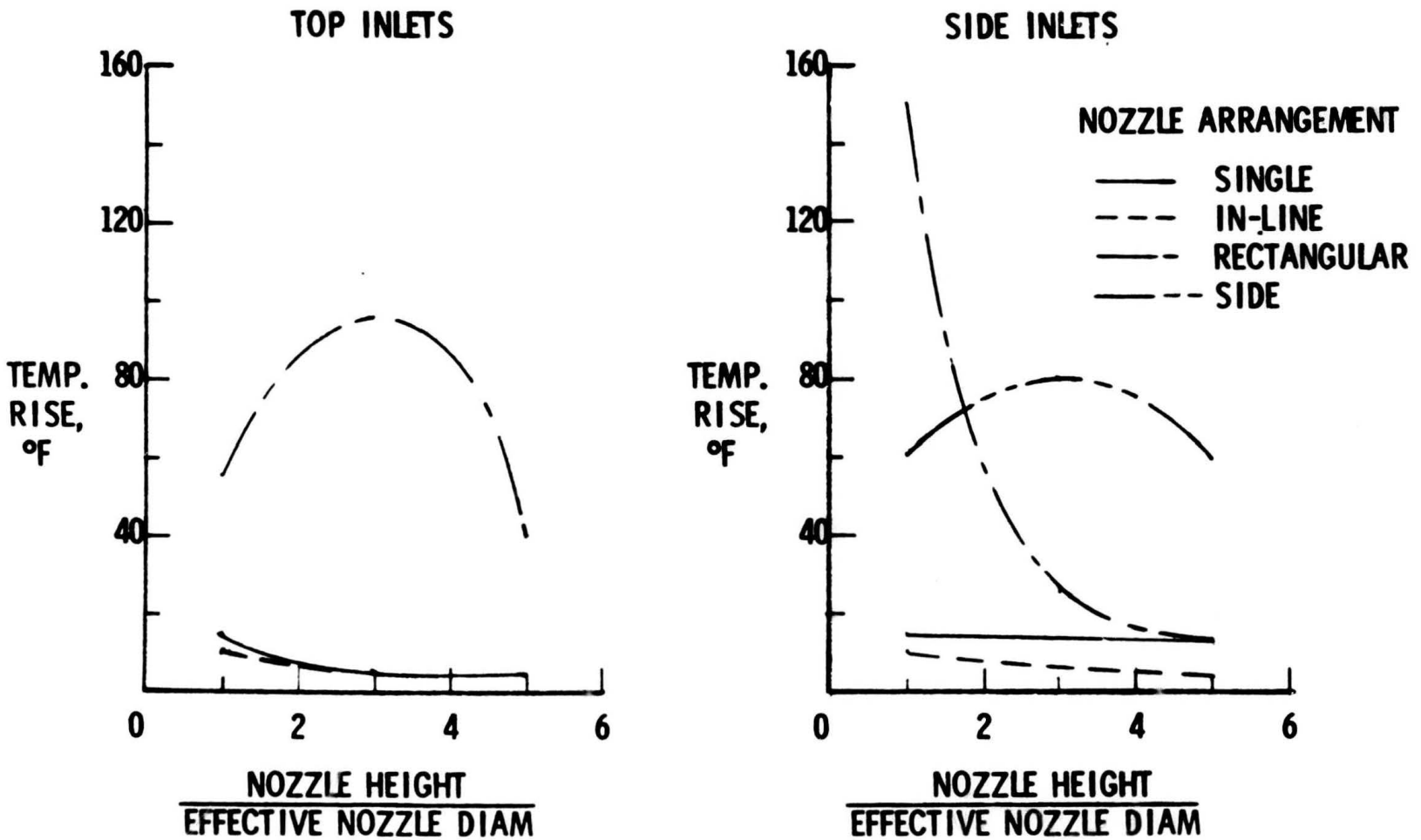

Figure 6.- Inlet air temperature rise in still air, high-delta wing.

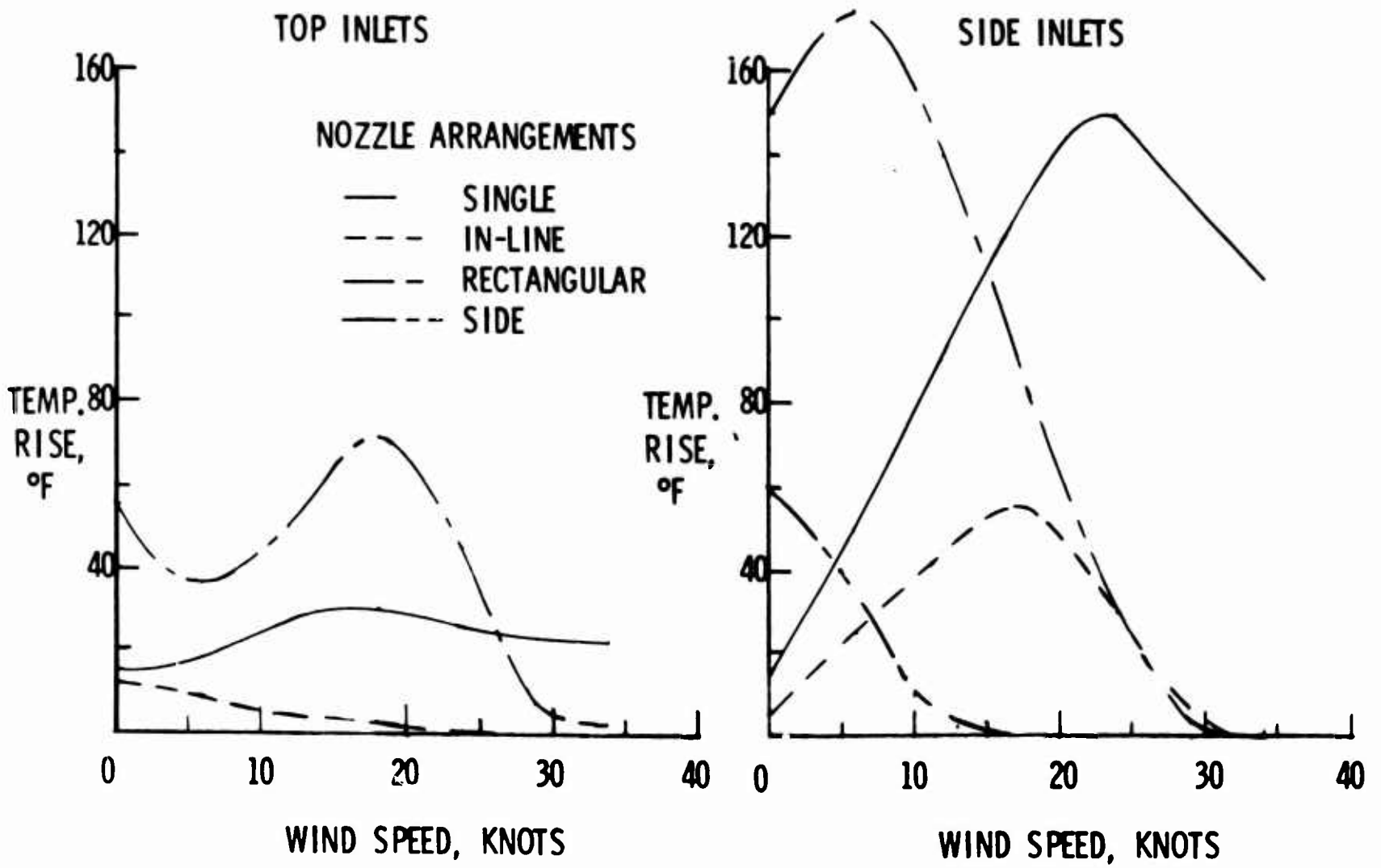

Figure 7.- Inlet temperature rise with wind; high-delta wing, $\frac{\text{Nozzle height}}{\text{Effective nozzle diam}} = 1.17$.

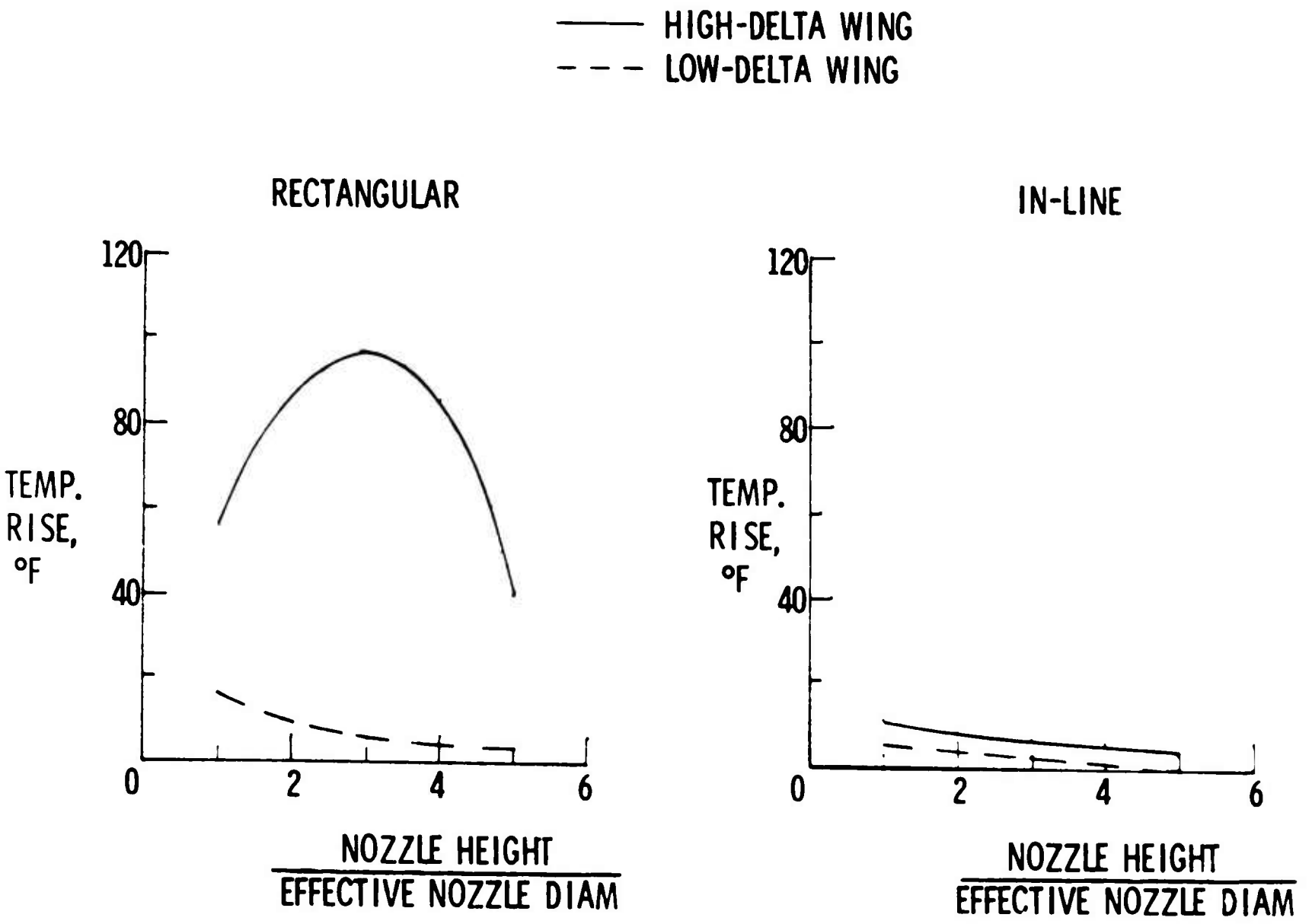

Figure 8.- Inlet air temperature rise in still air for rectangular and in-line nozzle arrangements with top inlets.

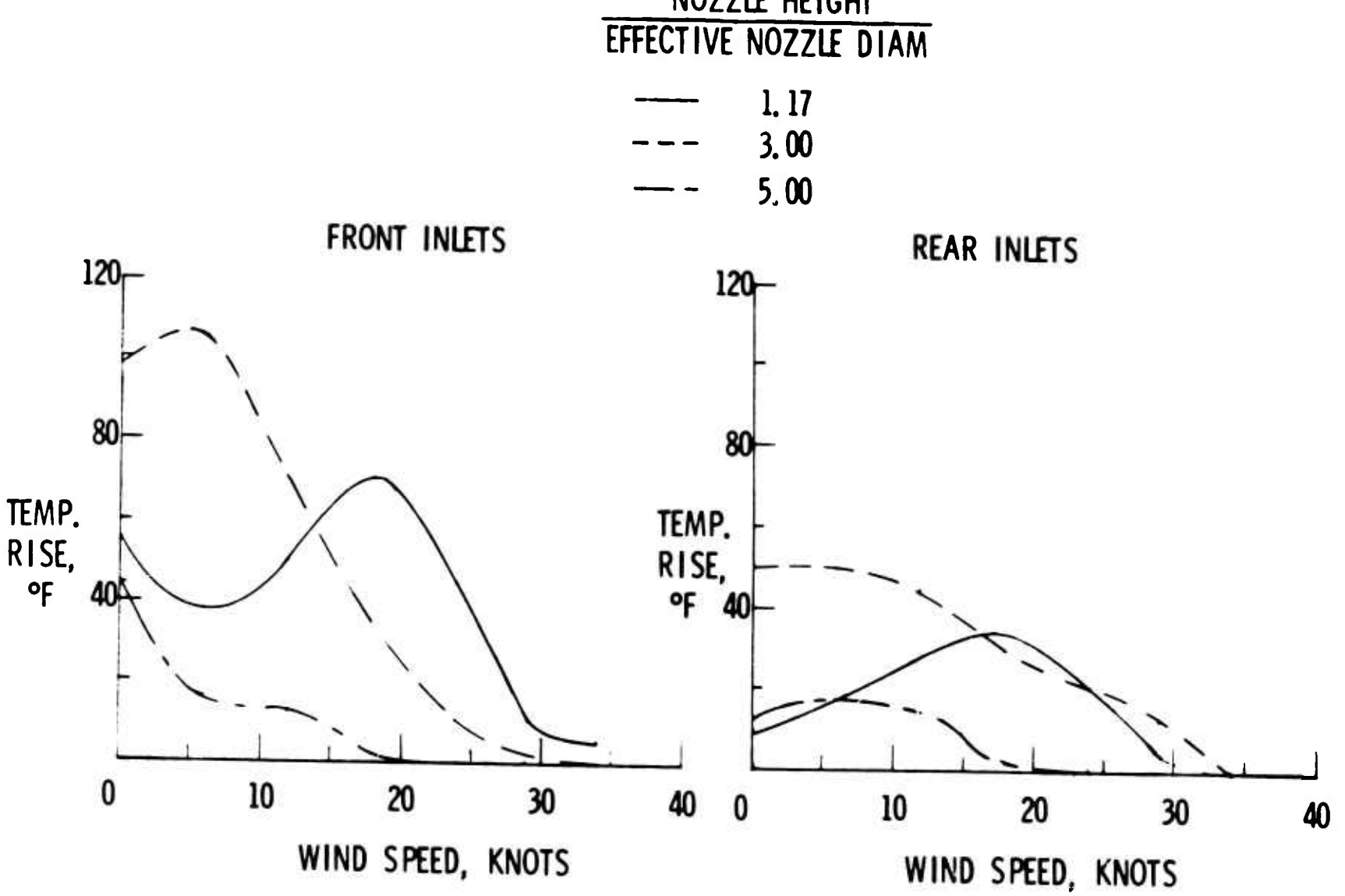

Figure 9.- Inlet air temperature rise with wind, rectangular nozzle arrangement with top inlets.

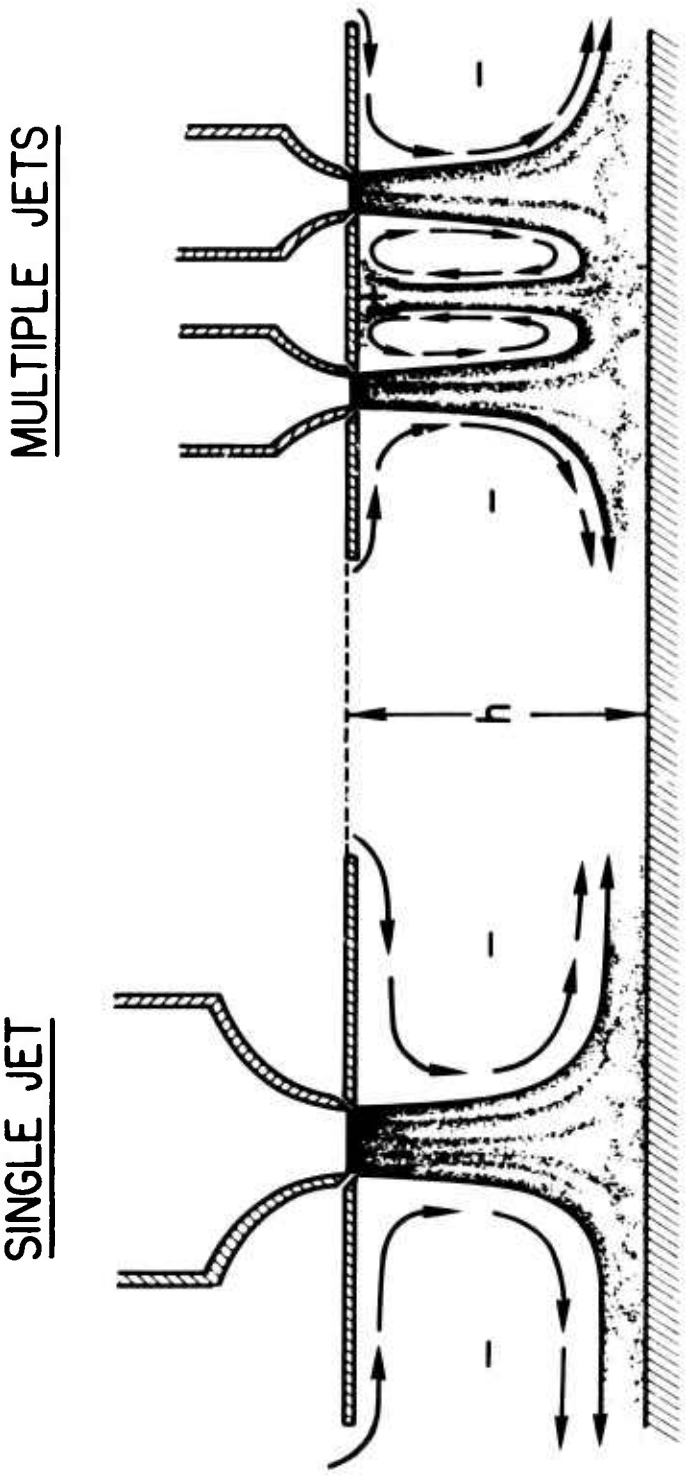

Figure 10.- Aerodynamic ground effects.

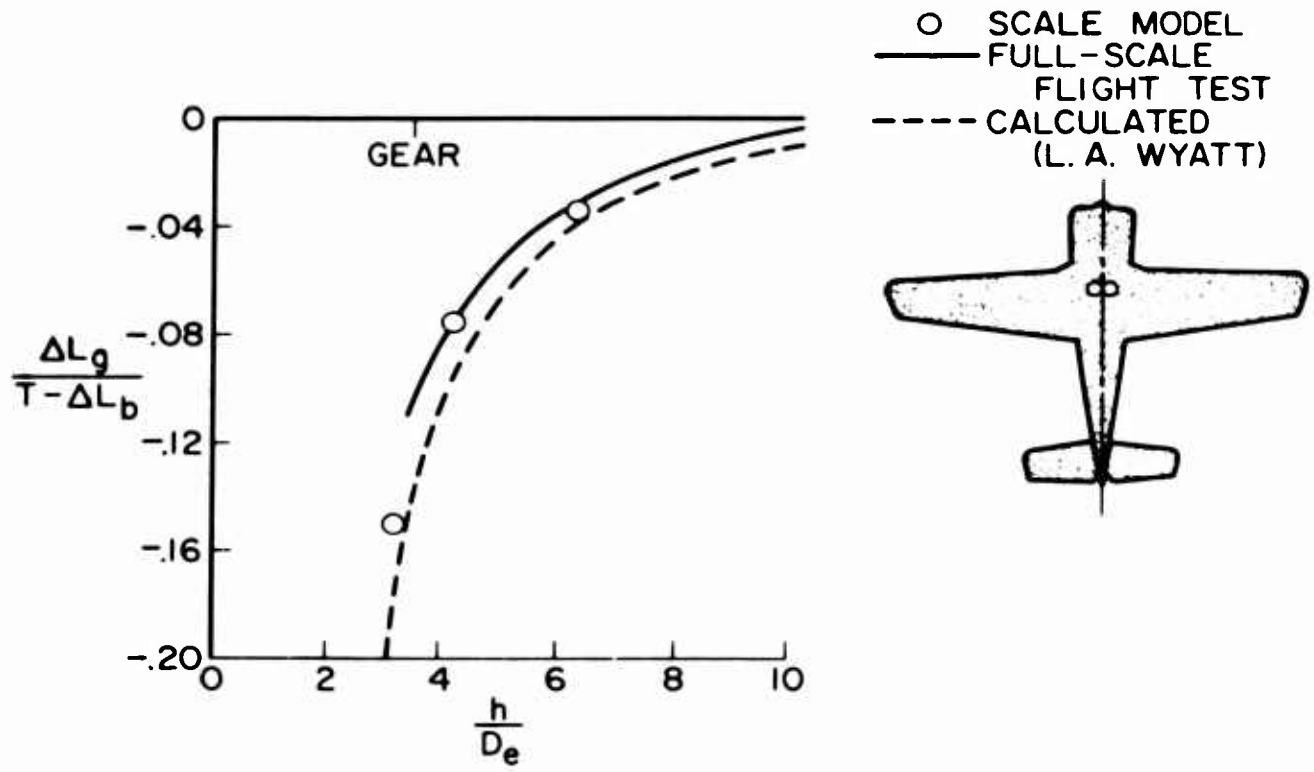

Figure 11.- Correlation of model with full-scale X-14A.

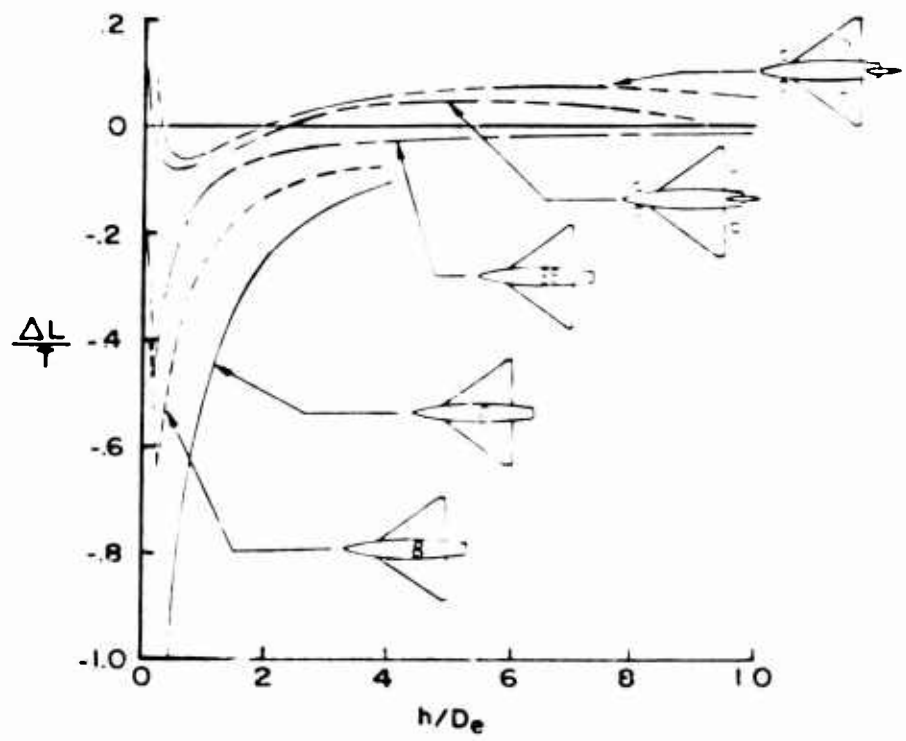

Figure 12.- Effect of multijet arrangements.

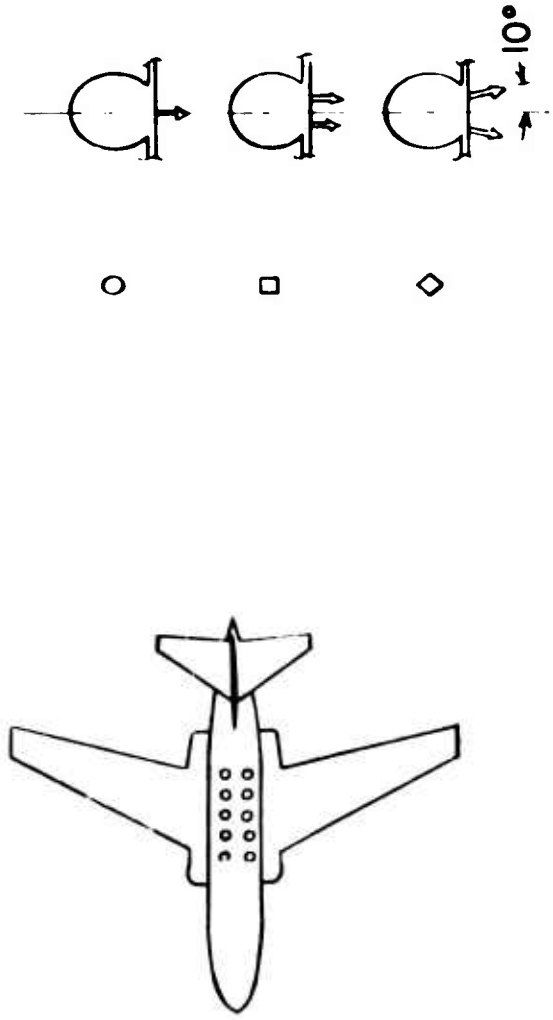

Figure 13.- Hovering ground effect.

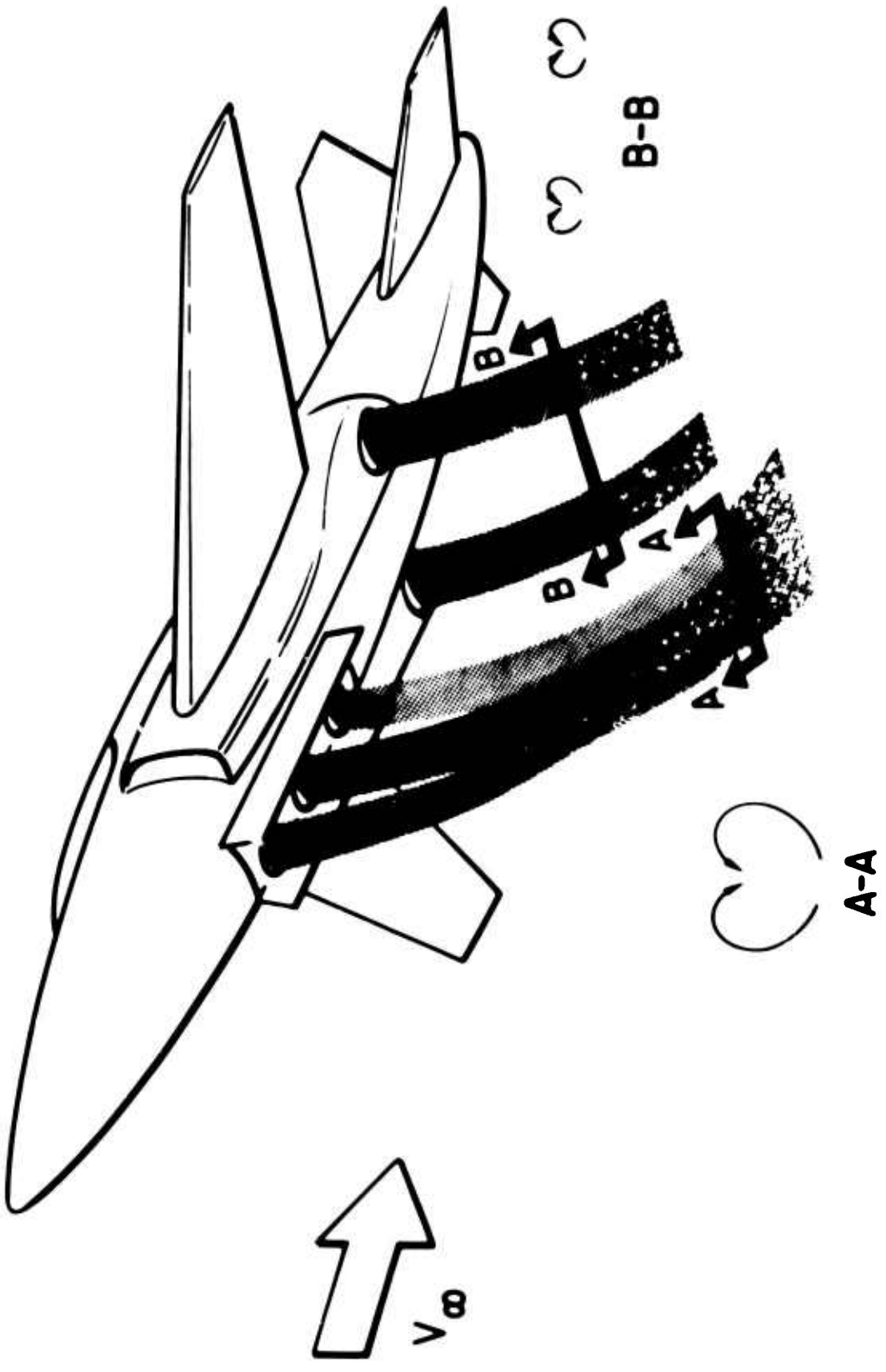

Figure 14.- Jet wakes in transition flight.

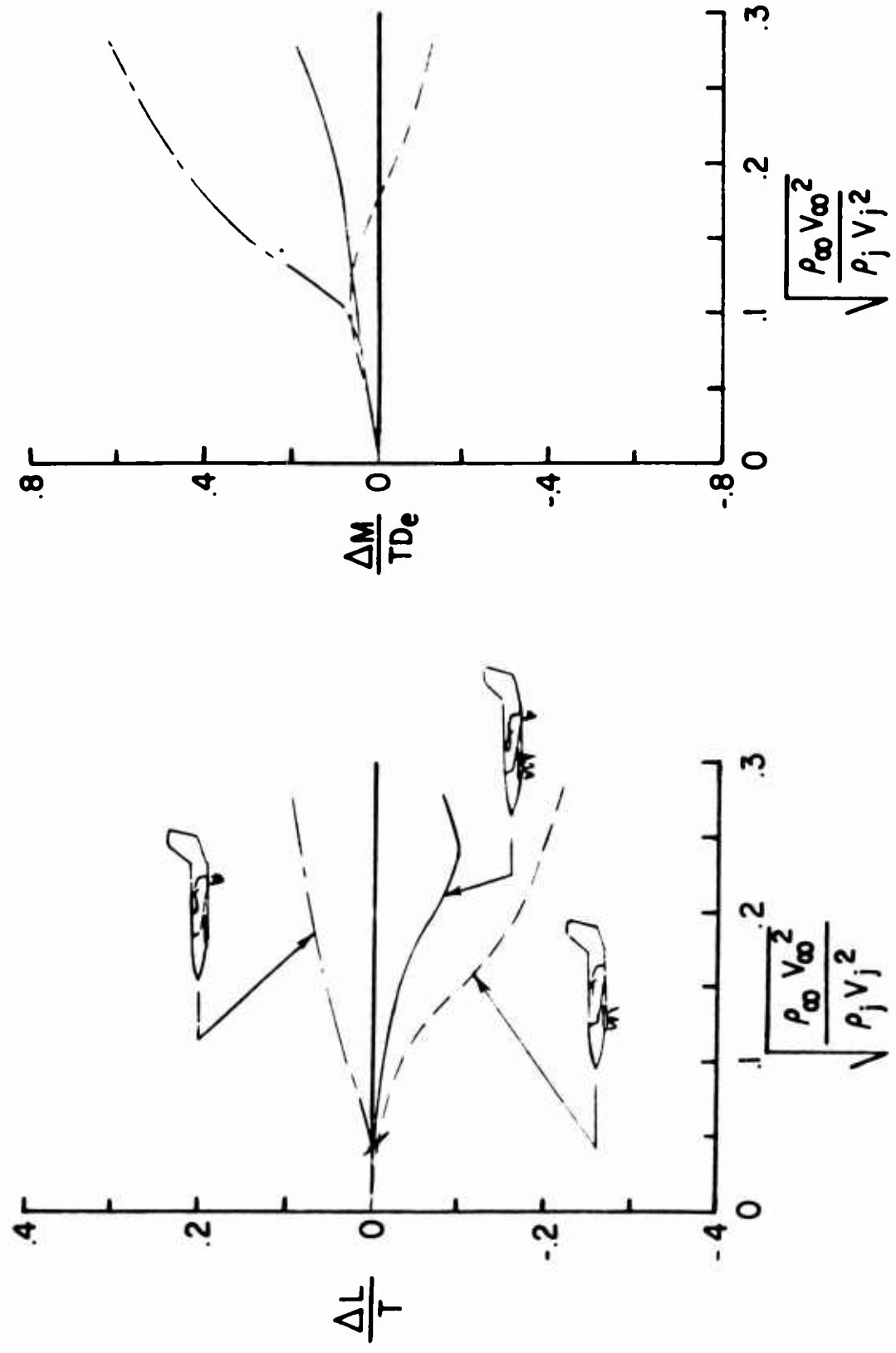

Figure 15.- Transition interference.

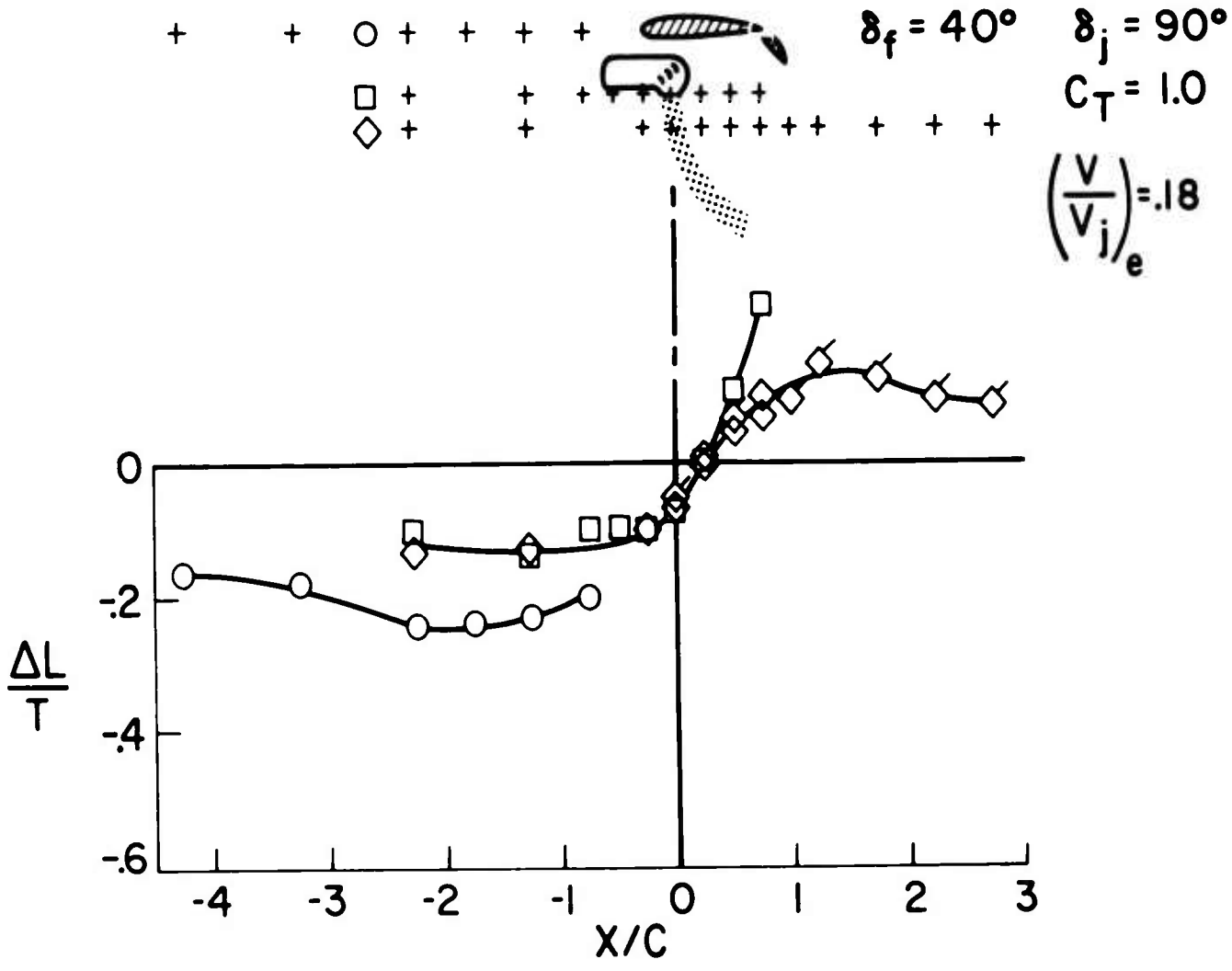

Figure 16.- Effect of jet position.

INTERACTION BETWEEN AIRFRAME-POWERPLANT INTEGRATION AND HOT GAS INGESTION FOR JET LIFT V/STOL TRANSPORT AIRCRAFT

by

U. Gittner
F. Hoffert
M. Lotz

DORNIER GMBH
Friedrichshafen
Germany

SUMMARY

The airframe-powerplant integration and the operational performance of V/STOL jet transport aircraft can be largely influenced by special VTOL problems, not easily to predict, like induced flow effects, ground erosion, hot gas reingestion etc.

The paper is concentrating on the interaction between airframe-powerplant integration and hot gas reingestion.

To predict the hot gas reingestion effects for the experimental V/STOL aircraft Do 31 corresponding model tests have been carried out. The important results have been confirmed by full-scale tests with the large hovering rig. The intake temperature rise is governed by hot gas fountains caused by opposing jet flows, meeting on the ground. The hot gas fountains are of considerable influence on the propulsion engines, but scarcely affecting the high positioned lift engine intakes. Hot gas ingestion by buoyancy effects is of minor importance.

Model tests for a proposed operational jet lift transport have shown considerably higher temperature rises at the propulsion engine intakes. However, these unfavourable results can be overcome by fairly small changes of the propulsion engine positioning.

It is concluded that operational jet lift V/STOL transport aircraft, especially of the first generation, should take advantage from a less integrated powerplant system, permitting configuration modifications without major structural changes, even in an advanced stage of development, thereby reducing the development risk.

INTERACTION BETWEEN AIRFRAME-POWERPLANT INTEGRATION AND HOT GAS INGESTION FOR JET LIFT V/STOL TRANSPORT AIRCRAFT

U. Gittner
F. Hoffert
M. Lotz

1. INTRODUCTION

Although several experimental V/STOL aircraft have already demonstrated the feasibility of high speed aircraft with vertical take-off and landing capability and promising proposals have reached fairly advanced design stages, the V/STOL concept is not yet accepted by the prospective user, neither civil nor military. This is especially true for the transport and passenger aircraft. The only production order so far has been given to Hawker Siddeley for the well known "Harrier" V/STOL combat aircraft after a successful squadron test programme. The lack of enthusiasm should not be surprising, having in mind the still confusing number of different configurations proposed. It must be fully appreciated that there are still uncertainties and problems confronting the prospective user of V/STOL aircraft. The customer can only be convinced by full-scale demonstration under operational conditions, proving the commercial and military usefulness of the whole V/STOL system.

Since more than 15 years Dornier is active in the field of V/STOL aircraft. The beginning of the Do 31 development dates back to 1959. In addition to the Do 31 experimental programme Dornier is intensively investigating the problems of high speed operational V/STOL transport. These efforts lead to a number of V/STOL proposals and feasibility studies. For a two years period, some work, especially on hot gas ingestion, has been done in collaboration with Hawker Siddely Aviation.

V/STOL aircraft and propulsion systems are interrelated to an unusual degree. The airplane powerplant integration of a transport is dictated or influenced by factors like

freight hold accessibility,
control,
engine out safety,
cruise speed,
lift loss by secondary air flow,
hot gas ingestion,
erosion etc.

The degree of integration of V/STOL transport configuration varies over a wide range. The Bell X-22A is considered as an example of relatively high airframe-engine interaction. The ducts are an integral part of the powerplant and serve as annular wings and lift generators in aerodynamic flight. The engines and propellers are not independent from each other but cross-shafted together [Fig. 1].

Dornier has done considerable work related to the V/STOL transport with a low degree of airframe powerplant integration.

The Do 31 is a rather conventional aircraft with additional lift pods for V/STOL capability. These pods can easily be removed or replaced by pods with a different number or type of engines or by extra fuel tanks. The degree of integration is low and comparable to conventional transport aircraft [Fig. 2].

An example for an operational V/STOL transport with lift pods is the Do 131, a direct derivative of the Do 31 experimental aircraft [Fig. 3].

Special advantages of this concept are:

- No major problems in the conventional flight regime,
- high development potential and flexibility; the aircraft can profit from progress in engine development without major structural changes and may be operated without lift pods in a conventional manner [Fig. 4];
- unexpected difficulties may be overcome by minor modifications even in an advanced development stage.

This paper is concentrating on the interaction of hot gas ingestion and the airframe-powerplant integration, having in mind the optimum overall solution for a V/STOL transport with lift pods. Little attention will be given to other factors affecting the configuration.

2. Do 31 RESEARCH PROGRAMME

2.1 Status of the programme

In 1962 Dornier received a contract for a comprehensive V/STOL research programme sponsored by the Federal Ministry of Defense, including design and construction of two different hovering rigs and two experimental V/STOL transport aircraft Do 31 [Fig. 5].

- The small hovering rig or control rig was equipped with four lift engines RB 108. It served as a very useful tool for the development of the VTOL control system and the attitude stabilizer. During 1964 and 1965 nine pilots have made more than 250 free flights.

- The large hovering rig is equipped with the original Do 31 powerplant, except the number of lift engines which is three per pod instead of four.

Powerplant:	2 Bristol Siddeley Pg 5-2
	6 Rolls Royce RB 162-4D
Take-off weight:	33 070 lb

The general arrangement and the overall dimensions are identical with the Do 31 aircraft. The aft fuselage is framework structure, designed only to take the control forces of the bleed air pitch nozzle. The large hovering rig is therefore well representative for the Do 31 as far as hover-

ing and ground effects like hot gas recirculation are considered. Up to September 1st 1967 the rig made 17 successful VTOL flights.

- Two experimental aircraft Do 31 have been built. Both have already flown conventionally 15 flights.

Propulsion engines:	2 Bristol Siddeley BS Pg 5-2 Nominal SLST 15 500 lb per engine
Lift engines:	8 Rolls Royce RB 162-4D Nominal SLST 4 300 lb per engine
Total thrust installed (ISA, SL):	65 400 lb
Design take-off weight:	50 000 lb

After sufficient exploration of the hovering envelope and the conventional flight envelope it is intended to perform the first transition later this year. The Do 31 research programme is an important step towards an operational V/STOL transport aircraft and the results will be of great value for all future V/STOL transport equipped with lift engines or lift fans. Valuable answers have been provided already for some of the most important problems as stability and control and hot gas ingestion.

2.2 Model test results

Recognizing the detrimental effects of hot gas ingestion on V/STOL performance corresponding tests have been carried out with a movable $1/20^{th}$ scale ingestion model of the Do 31 [Fig. 6].

At this point some remarks regarding the model scaling laws should be made.In our tests the lift engine jet temperatures were limited by technological difficulties to about 150 ^{o}C above ambient. The main engine jet temperatures and all jet velocities were determined from the conditions described by Kemp [1], i.e. equal model-to-full-scale ratio of momentum and temperature rise above ambient for all engines, and for the lift engines correct value of the similarity parameter introduced by Cox [2], which represents the ratio of inertial forces to buoyancy forces. From the theoretical point of view, similarity of flow fields can be achieved only if

(a) Boundary conditions are similar,

(b) the non-dimensionalized equations of motion are identical which leads to equal values of the various similarity parameters such as Reynolds number etc.

Condition (a) also includes similar flow conditions at the boundaries of the flow field, i.e. in our case equal density or temperature ratio of jet exit to ambient. Only after this condition has been fulfilled it is useful to investigate which of the conditions (b) are the most important and which can be released. Therefore, in our opinion the low model jet temperatures are the main shortcoming of the

current model testing technique and we would rather violate the Cox conditions than intentionally choose a lower jet temperature in order to obtain a slower model time scale. Furthermore, our experience has shown that the most important results can be obtained by steady-state tests as well. Keeping these limitations in mind, the model test results may be summarized as follows:

(1) Lift losses due to hot gas ingestion by buoyancy effects during take-off and landing are of minor importance, since the hot gas cloud surrounding the aircraft forms sufficiently slowly to accomplish the VTOL procedure before the inlet temperature rise becomes a determining factor.

(2) The real problem are the upward directed high speed hot gas fountains caused by opposing jet flows meeting on the ground [Fig. 7]. These fountains are being formed without any useful time delay. The intake temperature rise of the Pegasus propulsion engines during a simulated take-off is in good agreement with the corresponding steady-state temperature rise [Fig. 8].

(3) The lift engine inlet temperature remains relatively low. ($\Delta T = 5\ ^{o}C$). The lift engine intakes are well above the ground and are protected by the wing from the hot gas fountains.

(4) The temperature rise of the main engines is very sensitive to the nozzle position, but can be kept relatively low by adequate thrust vectoring. Fig. 9 shows the effect of Pegasus nozzle deflection under idling and max. thrust conditions. The max. temperature rise of 70 ^{o}C occurs at a nozzle angle of 110^{o} (20^{o} forward from the vertical). A favourable jet configuration for take-off is a nozzle position of 80^{o} (10^{o} aft from vertical), where 30 ^{o}C temperature rise can be expected.

(5) Fig. 10 shows the influence of height increase during take-off. The model tests indicate a fairly rapid decrease of Pegasus inlet temperature.

2.3 Flight tests of the large hovering rig

The most important result of the model tests, i.e. the strong increase of ingestion temperature with increasing forward sweep of the propulsion nozzles, was confirmed by full-scale ground tests [Fig. 11]. The nozzle angle was therefore limited to 85^{o} forward from horizontal. Together with the 15^{o} inclination of the lift engines, this results in a horizontal thrust component which leads to a forward movement of the rig just before lift-off. This movement could however be limited to less than an aircraft length by quickly performing the take-off manoeuvre.

A crosswind leads, as anticipated, to an increase of intake-temperature at the lee side which is larger than the reduction at the luff side. Furthermore, this reduction cannot be exploited from rolling moment considerations, so that crosswind leads to a reduction in available lift.

During take-off, inlet temperatures cannot be considerably reduced as compared with steady-state ground tests. Fig. 12 shows a typical flight test result. This was also predicted from model tests. Peak temperature rises from 10 take-off manoeuvres are between 25 and 70 °C with an average of 50 °C. Since the temperature is by no means constant across the inlet area, the mean ingestion temperatures, on which the thrust losses depend, are much lower.

Vertical landings were performed with sink rates between 1 and 2,5 m/sec. No consistent dependence of peak ingestion temperatures on sink rate could be established. Intake temperature rise only begins at about 3 m above ground as predicted by model tests. Therefore thrust losses lead to only moderate increase in impact velocity and no difficulties are encountered. The main consideration is to prevent engine surge. This can be achieved by shutting off the engines immediately after touch-down, since peak temperatures occur only after touch-down [Fig. 12]. Peak temperature rises from 10 vertical landings were between 25 and 70 °C with an average of 45 °C, the mean temperatures over the intake area being again much lower.

Systematic comparisons of model and full-scale results are made at the present time and will be reported at a later meeting. The limited comparisons available up to now show however, that model tests are a valuable means of predicting ingestion temperatures. In spite of the fact, that correct similarity of the flow and temperature fields cannot be achieved due to the low model jet temperatures, model tests do show whether hot gas fountains are sucked into the intakes or not and thus give an indication how this can be avoided.

3. INVESTIGATIONS TOWARDS AN OPERATIONAL V/STOL TRANSPORT

Based on the experience gained so far from the Do 31 programme, Dornier has been working on the problems of operational V/STOL transport aircraft. Considerable design and experimental work has been concentrated on the jet lift transport Do 131, a direct derivative of the Do 31. It was found that in the long term, the turbofan aircraft with additional lift engines in removable pods is a very attractive and flexible concept. It offers a straightforward solution and can take full advantage of the Do 31 experience and the progress in engine development. Fairly great modifications of the powerplant system are quite possible without major changes of the airframe structure.

3.1 Basic configuration

The basic configuration is essentially determined by the powerplant arrangement, i.e. by the number and position of the engines and by the thrust distribution between propulsion and lift engines.

The two propulsion engines are just powerful enough to meet the cruise and climb requirements. The extra thrust required for VTOL is generated by a number of light and simple lift engines.

The number of lift engines is determined by engine out safety requirements. If less than eight engines are installed, the lift loss following an engine failure becomes very high. In order to maintain hovering capability and to balance out the disturbing moments, an unnecessarily large amount of thrust would have to be installed [Fig. 13].

The Do 131 A [Fig. 14] is equipped with engines currently available:

2 Rolls Royce RB 168 with single sided switch-in cascade deflector

14 Rolls Royce RB 162-81 turbojets with air bleed for pitch control and $\pm$ 15° swivelling nozzles.

The non integrated powerplant permits a conversion to the Do 131 B with better performance by installation of advanced lift engines or lift fans and high bypass ratio propulsion engines.

Contrary to the Do 31 experimental aircraft the heavier lift pods of the Do 131 are in mid-span position. The two main engines are on pylons under the wing and positioned between the fuselage and the lift pod. With the chosen configuration we did not expect any serious recirculation effects on the lift engines. However, the position of the main engines regarding hot gas ingestion could not be justified without experimental work.

3.2 Model test results

To investigate the hot gas reingestion problems of the Do 131 and to determine the final aircraft configuration a model test programme was initiated [Fig. 15].

The experimental work shows the following results:

(1) The small intake temperature rise of the lift engines ($\Delta T \approx 10^{\circ}$) measured on the Do 31 and its relative independence from the position and jet angle of the propulsion engines is confirmed.

(2) The temperature rise at the main engine intakes is considerably higher than for the Do 31 aircraft.

The reasons are:

- A very large portion of the hot gases is concentrated in one strong fountain generated under the fuselage, whereas the Do 31 configuration is producing a number of smaller fountains [Fig. 16].
- The main engines (RB 168) are fitted with single nozzles instead of four nozzles at the Pegasus engine, where the front jets have a favourable effect on the temperature rise by jet induced downwash near the main engine inlet and because of their low temperature.

(3) The influence of the main engine thrust level and the thrust angle is a very limited one and not sufficient to prevent unacceptable high inlet temperatures.

(4) As indicated by the temperature pattern a favourable "cold" zone with an average temperature rise less than 40 °C can be found near the lift pods [Fig. 17]. These cold "corners" are far from the fuselage fountain and can be explained by the jet induced cold air downwash, decreasing the hot gas fountain effects between main and lift engines.

3.3 Effect on powerplant arrangement

It is not intended to discuss possible solutions of the reingestion problem by ground based devices, like deflectors or grids. Although such devices are not considered as practical for most military operation, they should not be fully excluded.

Realizing the unfavourable test results for the temperature rise at the main engine intakes, a number of configuration changes have been considered. Two of them shall be discussed:

The first proposal is to shift the main engines outboard to the lift pods. This is followed by two opposite effects:

- Lower intake temperature, therefore more lift thrust available [Fig. 18].
- Increased rolling moment after a main engine failure, because of greater distance of the remaining thrust vector from the aircraft centre line. This has an unfavourable effect on residual lift thrust available after a critical failure and results in a decreased safe VTOL weight [Fig. 19].

The aim should be a configuration with a considerably reduced temperature at the main engine inlets without increasing the distance of the main engine thrust vector to the centre line. Fig. 20 shows one possible solution which meets these requirements to a remarkable extent:

The lift engine pods remain unchanged. The main engines are shifted by a small amount to the outboard. In the VTOL phase the propulsion engines are swivelled upward and outboard. The air intake arrives in the "cold" corner, whilst the aft end of the pod moves inboard and down. The single sided cascade is replaced by a swing down nozzle directing the jet vertically whilst the pod remains in an inclined position. During take-off transition this pod is tilted in the horizontal position; simultanously the nozzle is moving into the cruise position.

By this means the average intake temperature rise is limited to 35 °C and does not lower the safe vertical take-off weight. This is determined by the residual thrust after the critical engine failure out of ground effect. The thrust margin necessary to cover this case is sufficient to allow simultanous intake temperature rises of 10 °C at the lift engines and 40 °C at the propulsion engines [Fig. 21].

4. CONCLUSION

- It has been proven by a considerable number of successful test flights, that the Do 31 can take off and land vertically, without any configuration modifications or change of the powerplant system.

- Hot gas reingestion by buoyancy effects is of minor importance for practical VTOL operation.

- Model tests correctly predict the position of hot gas fountains and therefore give useful information on interactions between airframe-powerplant integration and hot gas reingestion. However, model tests are not 100 % reliable and cannot replace flight testing.

- Therefore, less development risk will be taken by chosing a flexible less integrated configuration, permitting modifications of the powerplant system without major changes of the basic structure. Reingestion and other VTOL problems may so be solved more easily, even in an advanced stage of development.

- V/STOL transport aircraft like the Do 31 and its operational derivatives may profit from the progress in engine development by replacing the engines currently available by advanced by-pass jets or lift-fans, without major modifications of the airframe. Bypass lift engines would further alleviate the reingestion problem.

- Although the paper is concentrated on the military V/STOL transport, it should be mentioned that the civil VTOL aircraft from the standpoint of reingestion and ground erosion is in a better position.

  For commercial application, dependence on ground based deflection devices means no notable compromise in route structure flexibility. In this case the reingestion problem needs not to be considered at all.

REFERENCES

[1] E. D. G. Kemp — The Influence of Hot Gas Ingestion on the Choice of Configuration for Jet Lift VTOL Transport Aircraft. AGARD 27th Propulsion and Energetics Panel Meeting on Gas Turbines at NATO Headquarters, Paris, 4 - 7th April 1966.

[2] M. Cox and W. A. Abbott — Jet Recirculation Effects in V/STOL Aircraft. J. Sound Vibr. (1966) 3 (3), 393 - 406.

[3] Stanley S. Kakol Chief Experimental Test Pilot — Development Flight Tests of the First Dual Tandem Ducted Propeller V/STOL - the X-22A. Textron's Bell Aerosystems Company.

FIG.1 **BELL X 22-A, aircraft with higher degree of integration**

FIG. 2 **V/STOL-RESEARCH AIRCRAFT DO 31**

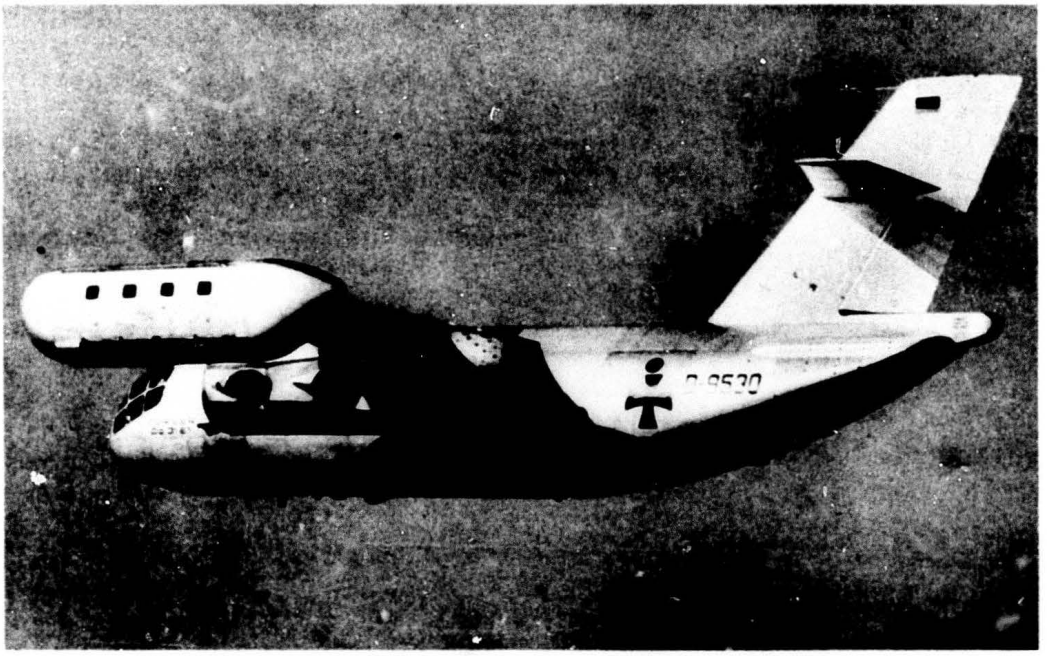

FIG. 3 **OPERATIONAL V/STOL TRANSPORT DO 131**

FIG. 4 DEVELOPMENT POTENTIAL AND FLEXIBILITY OF THE JET LIFT CONCEPT

Do 131 A

Do 131 B

CONVENTIONAL JET TRANSPORT

V/STOL - JET LIFT TRANSPORT
WITH LIFT FANS

STOL - JET TRANSPORT
WITH 8 LIFT ENGINES

FIG. 5 DO 31 EXPERIMENTAL PROGRAMME

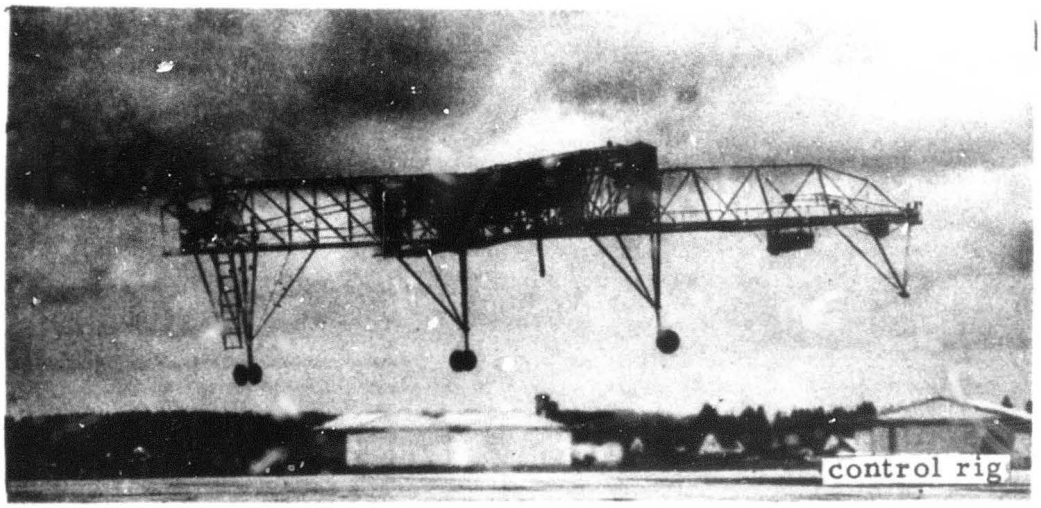

control rig

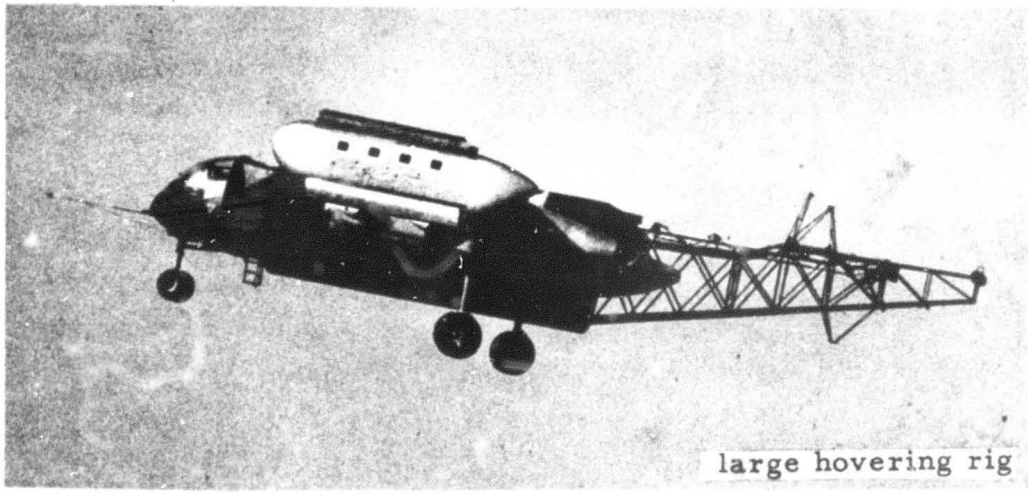

large hovering rig

Do 31 experimental aircraft

FIG. 6 **DO 31 HOT GAS INGESTION MODEL**

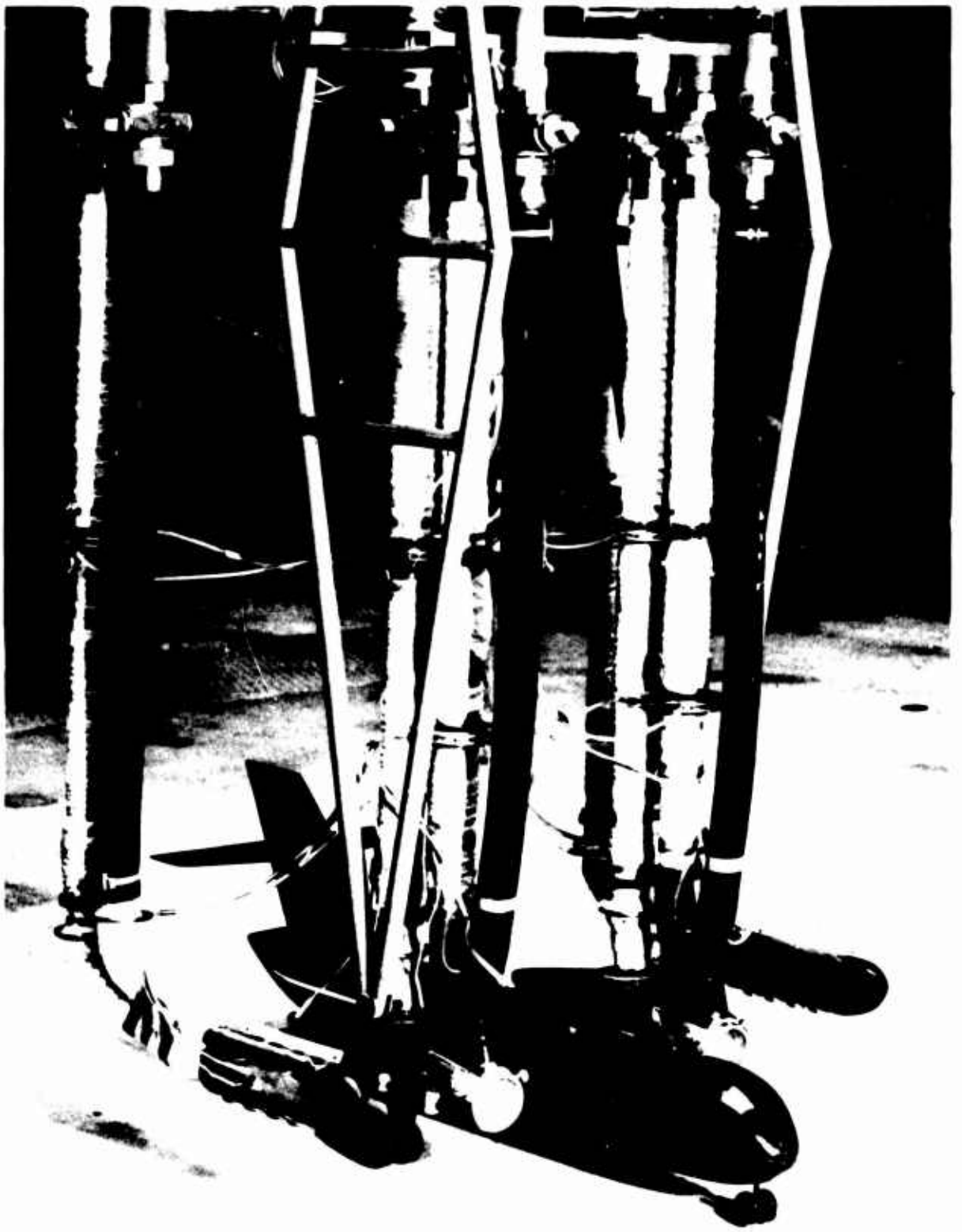

FIG. 7 DO 31 HOT GAS FLOW PATTERN AT LIFT-OFF

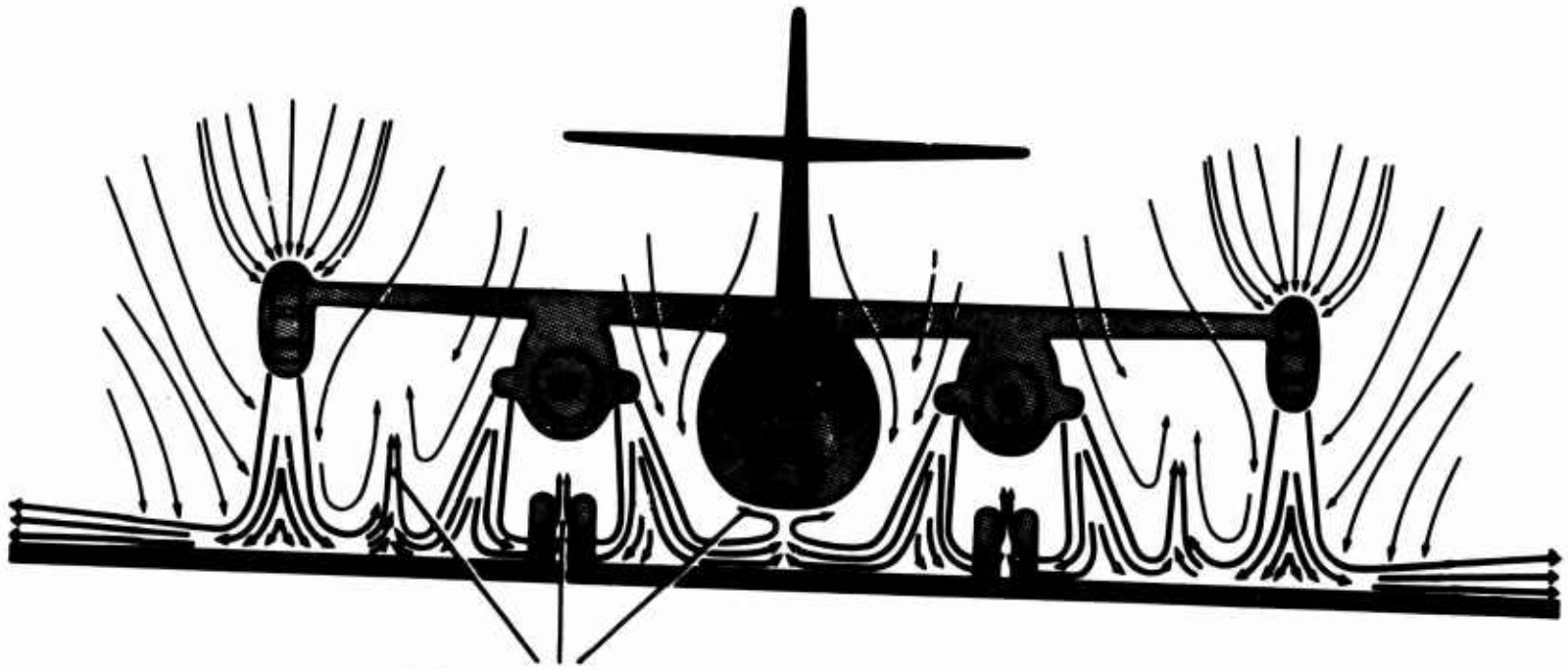

hot gas fountains

FIG. 8 **DO 31 HOT GAS INGESTION MODEL TESTS**
comparison of transient and steady-state test

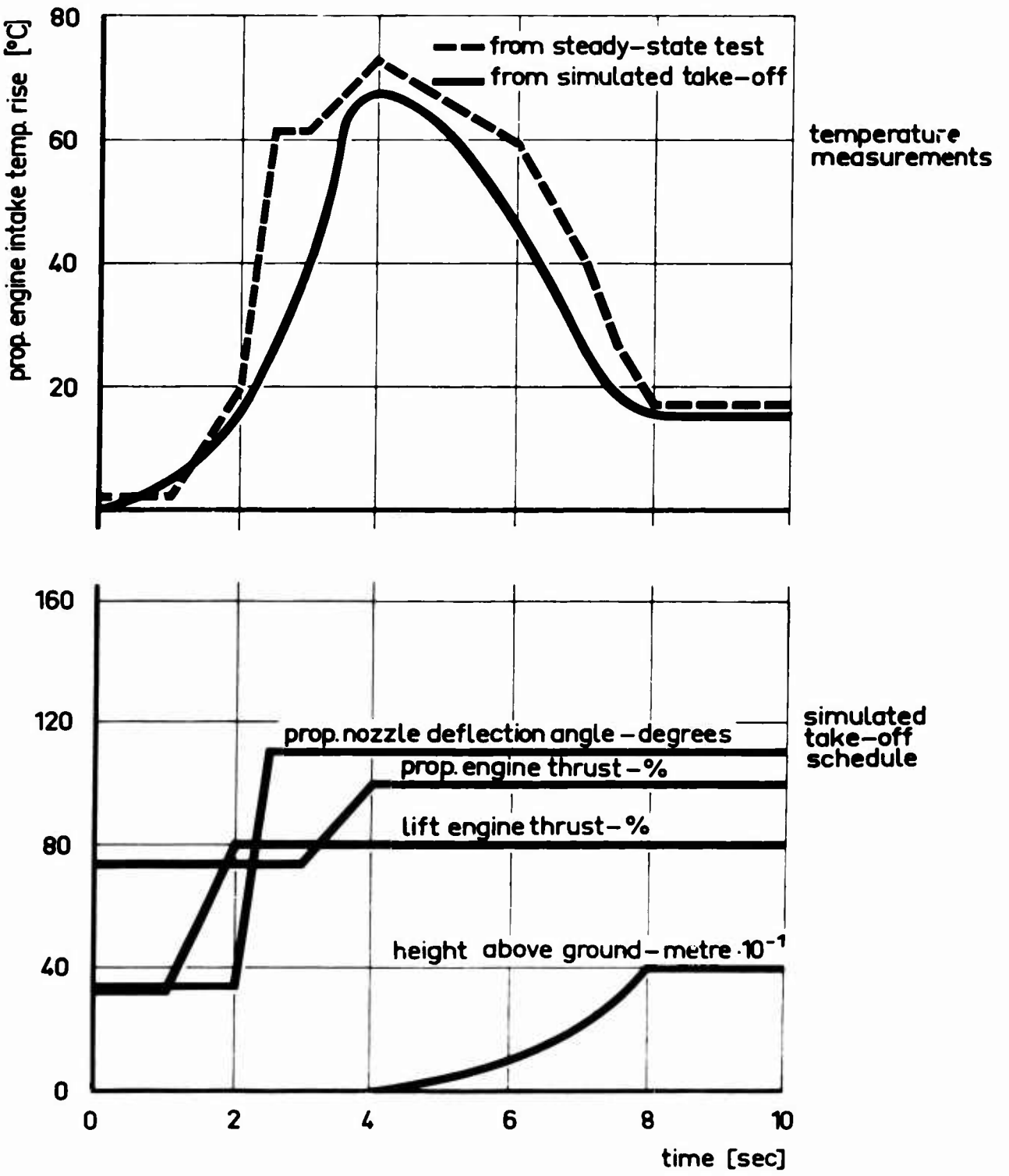

FIG. 9 **DO 31 HOT GAS INGESTION MODEL TESTS**
effect of nozzle deflection and thrust level

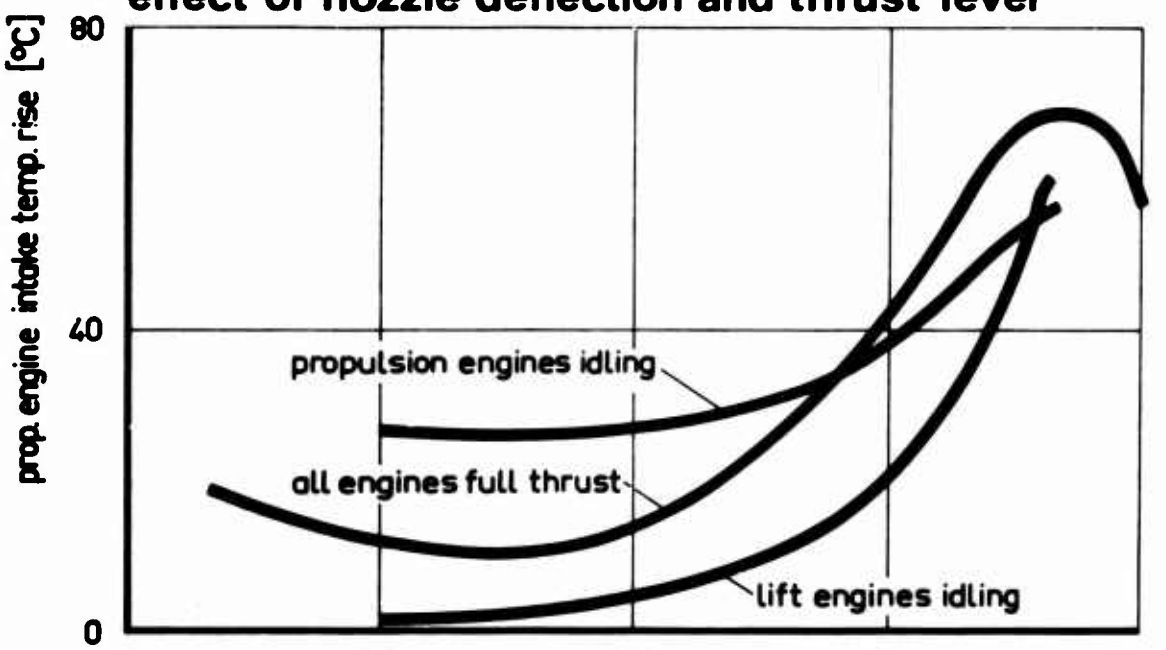

FIG. 10 **DO 31 HOT GAS INGESTION MODEL TESTS**
effect of increasing height

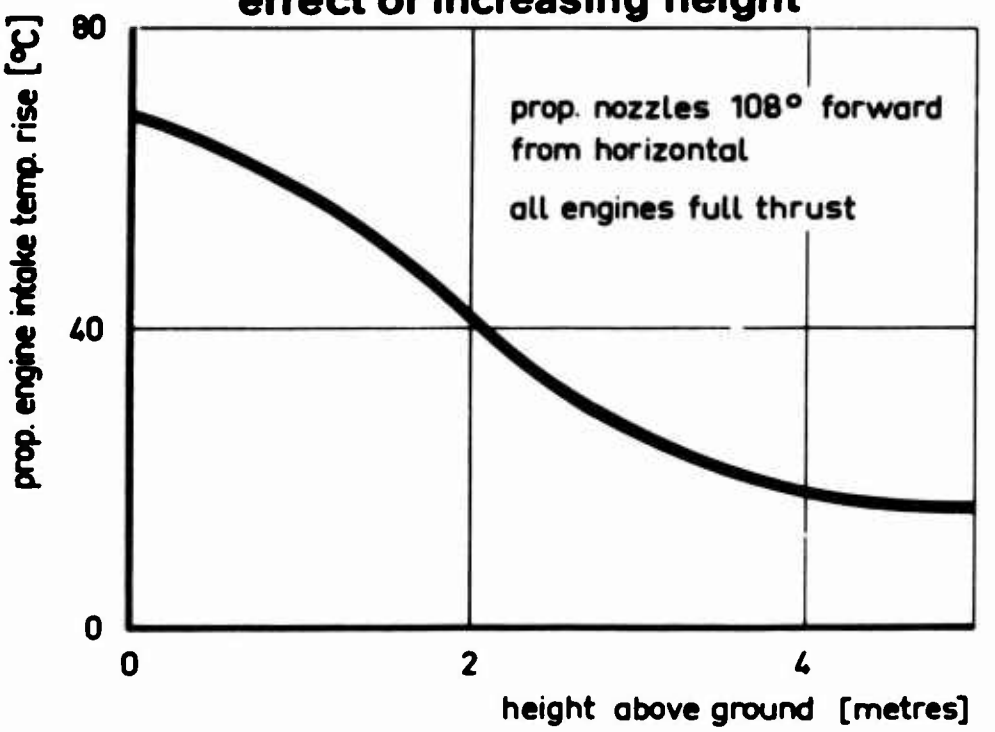

FIG.11

DO 31 HOVERING RIG HOT GAS INGESTION TESTS

effect of prop. engine nozzle deflection and thrust level

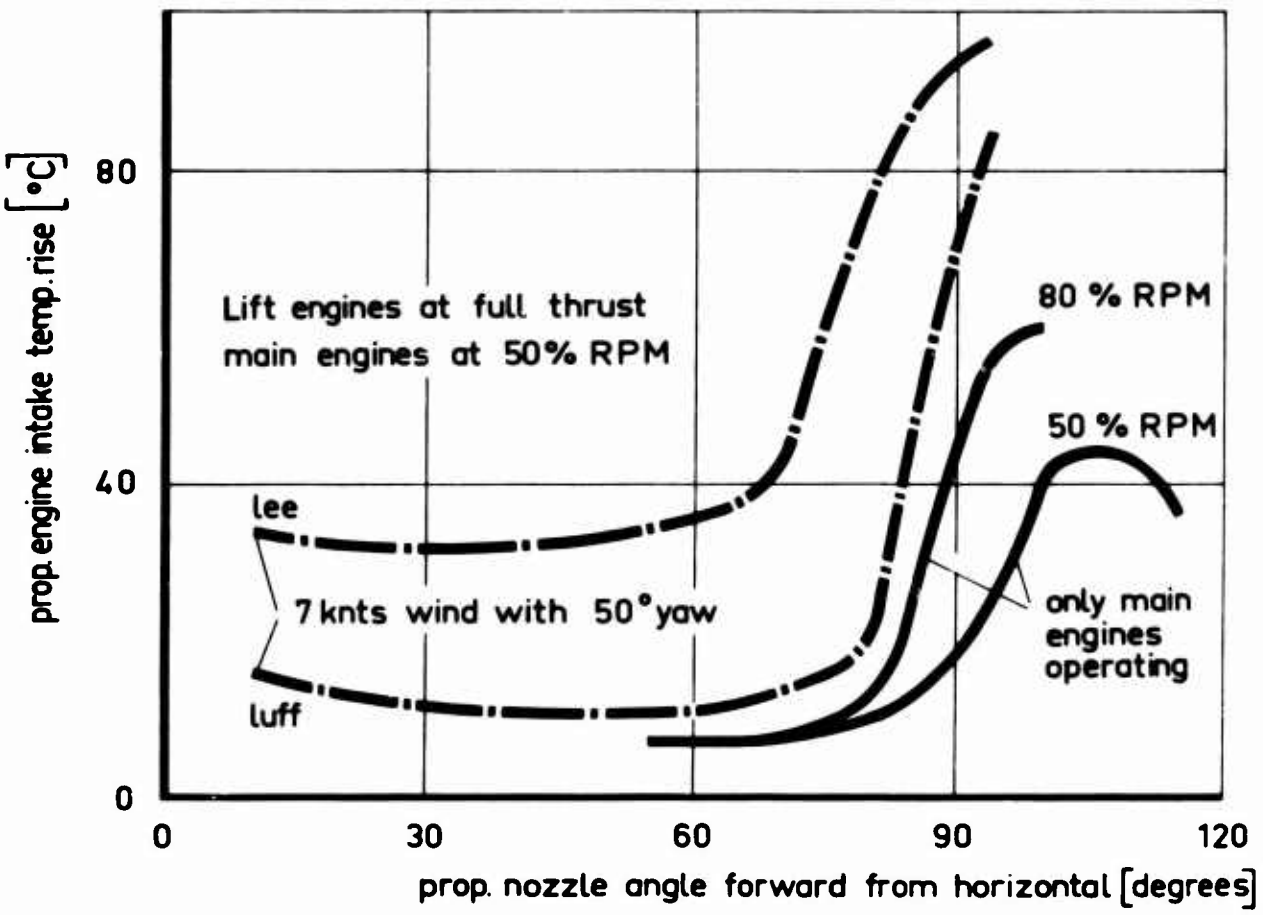

FIG. 12 **DO 31 LARGE HOVERING RIG**
typical flight test result

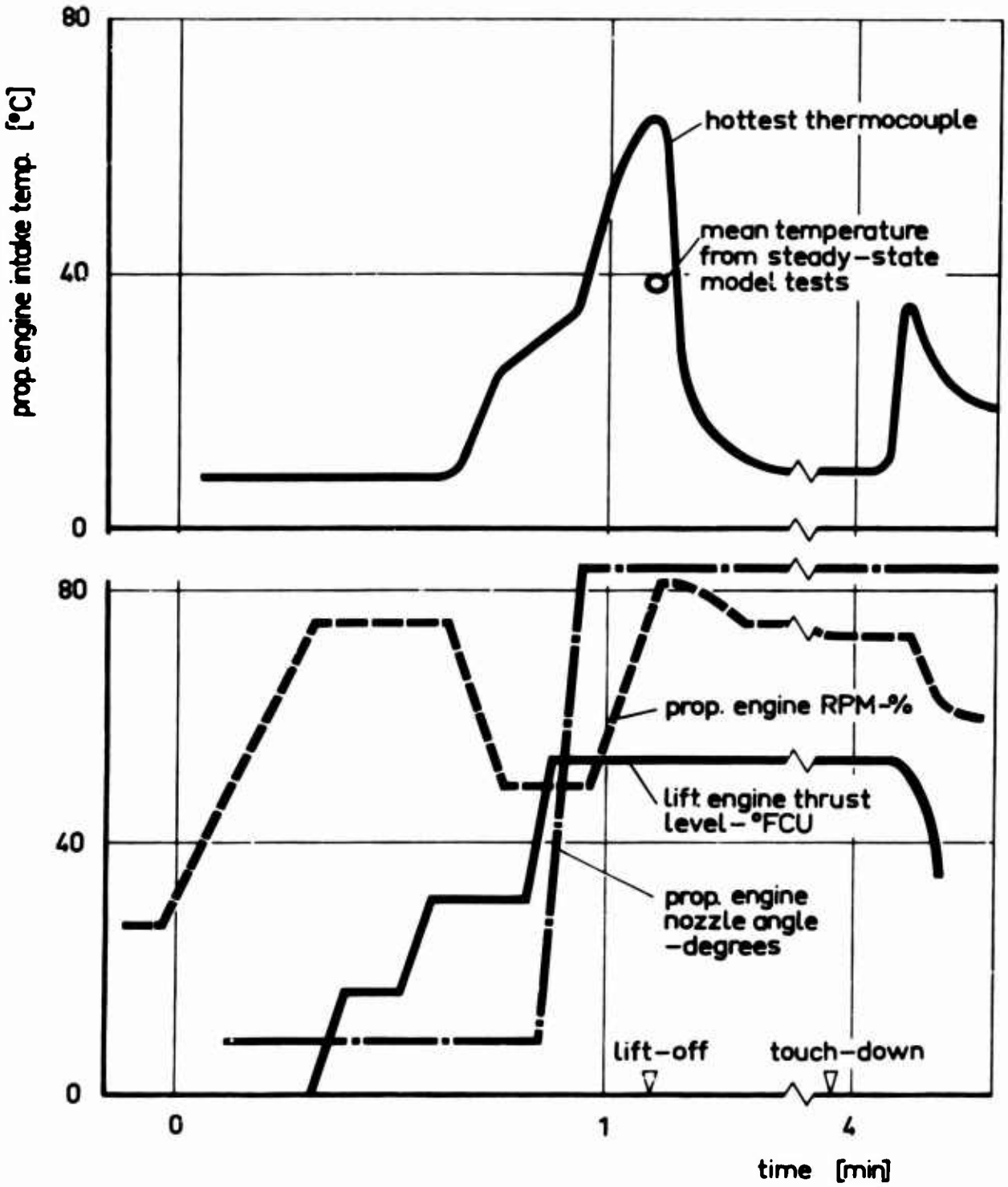

FIG. 13 DO 131 THRUST REQUIRED AND USEFUL LOAD VS NUMBER OF LIFT ENGINES

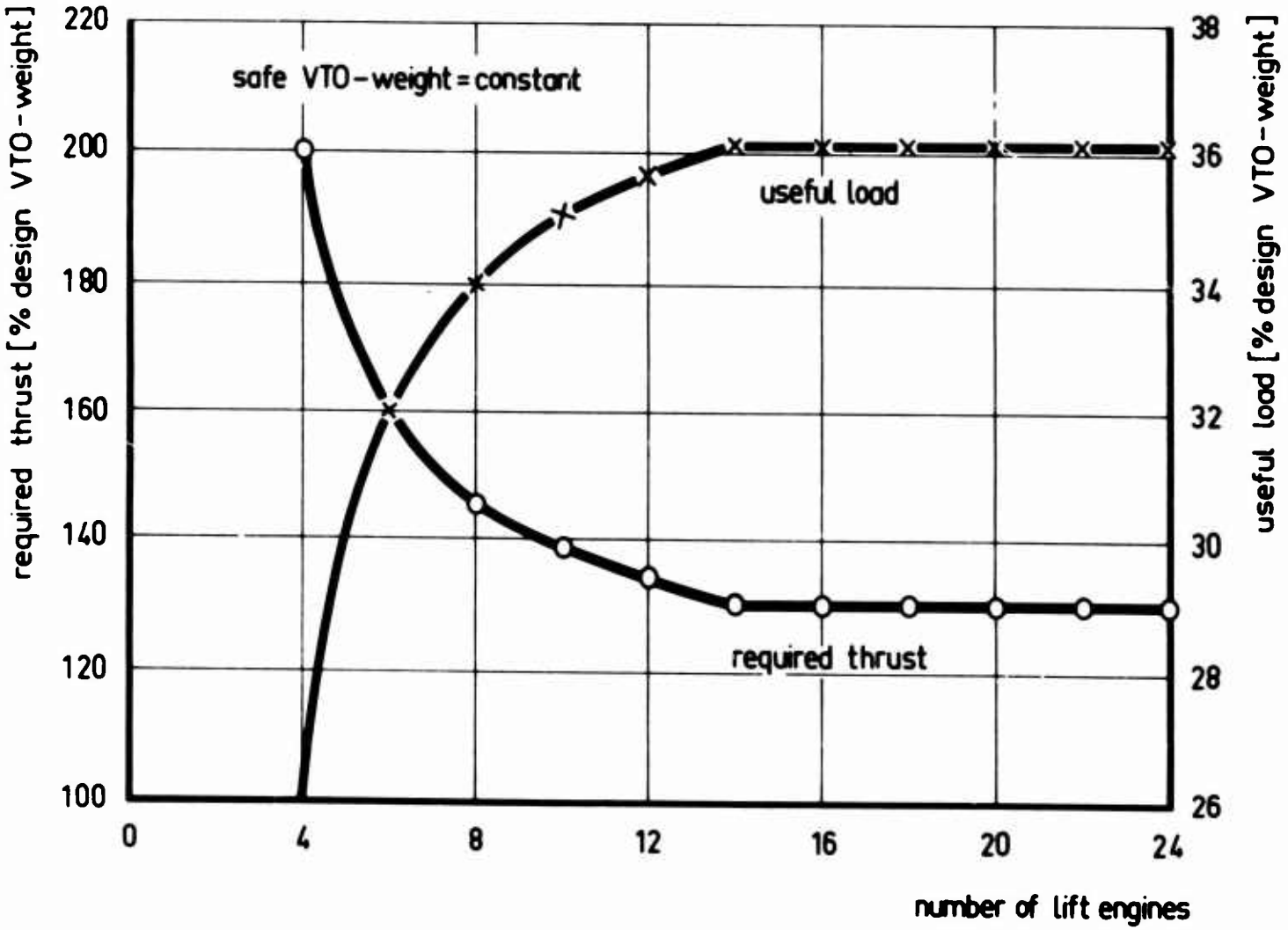

FIG. 14 **DO 131 GENERAL ARRANGEMENT**

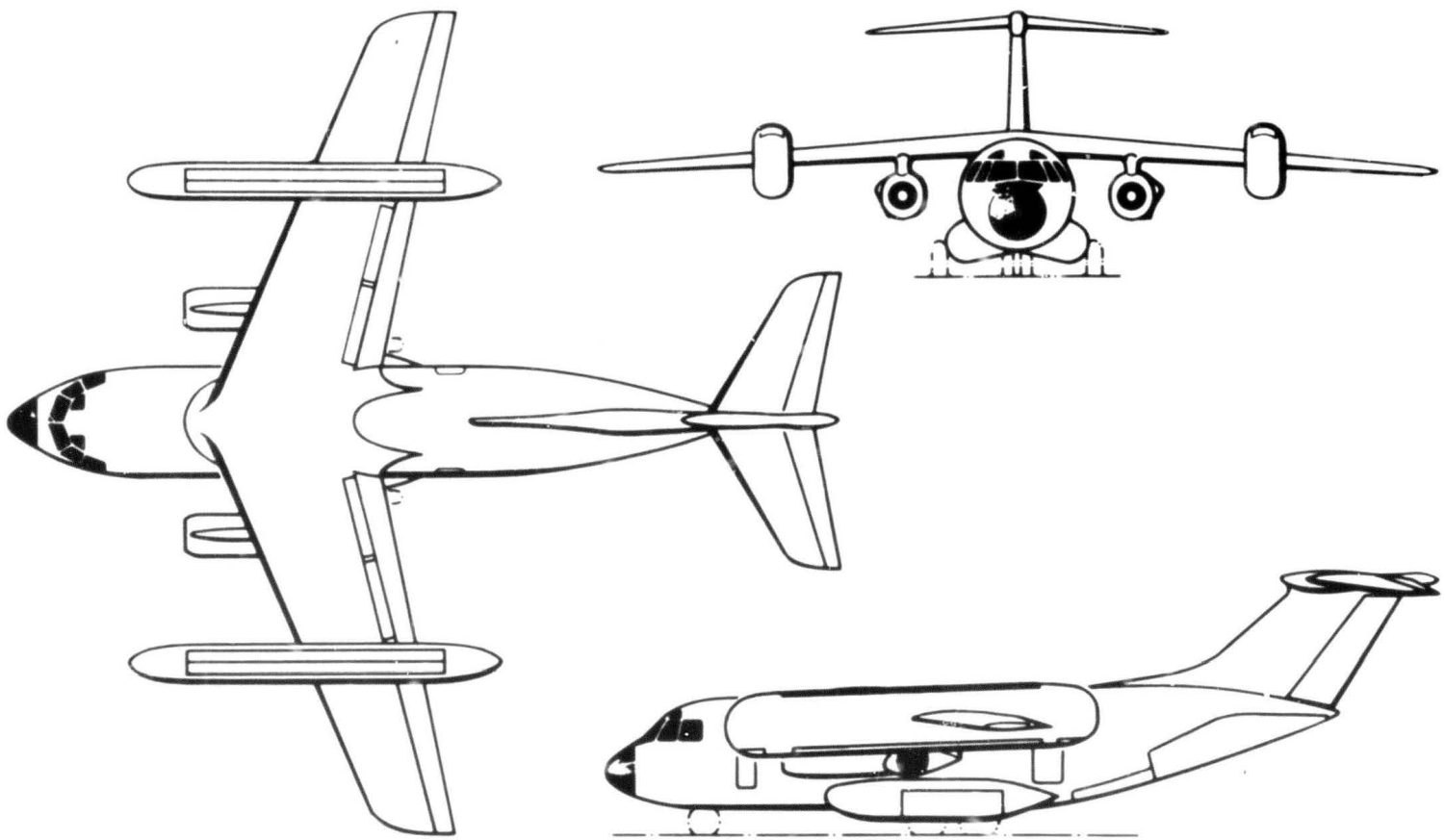

FIG. 15 **DO 131 REINGESTION MODEL**

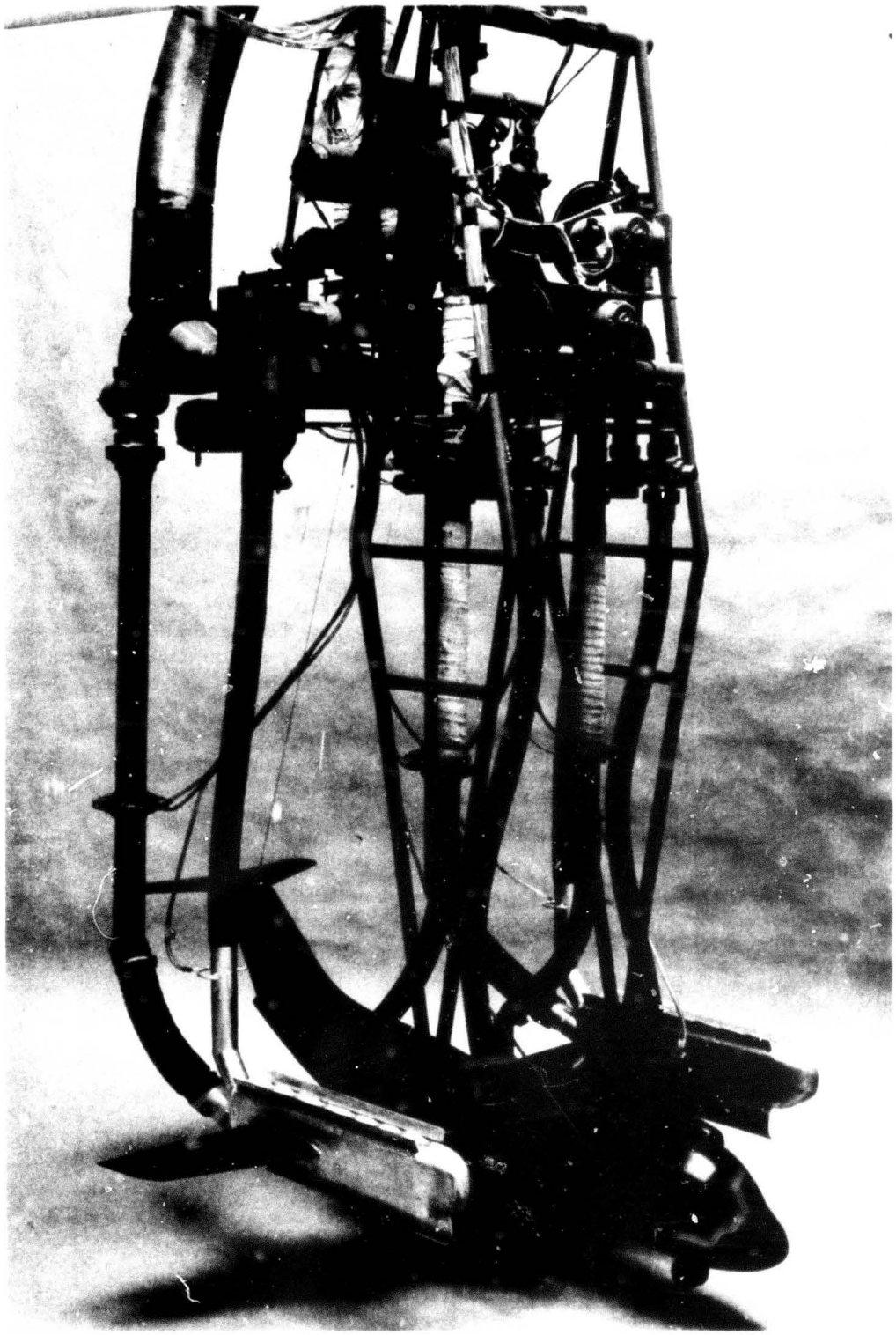

FIG. 16 **GROUND FLOW PATTERN OF DO 31 AND DO 131 A**

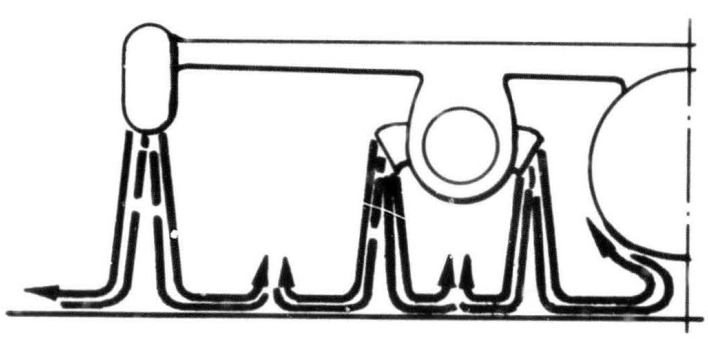

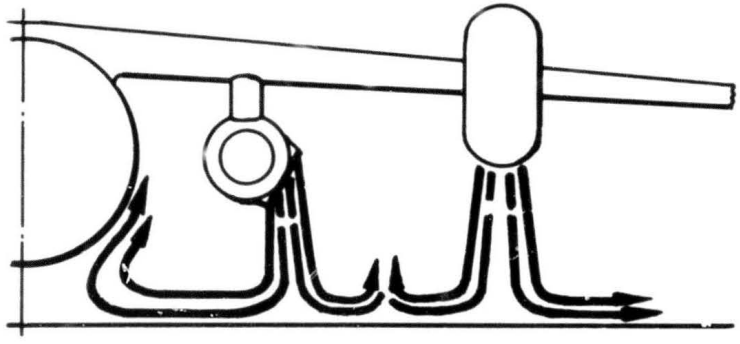

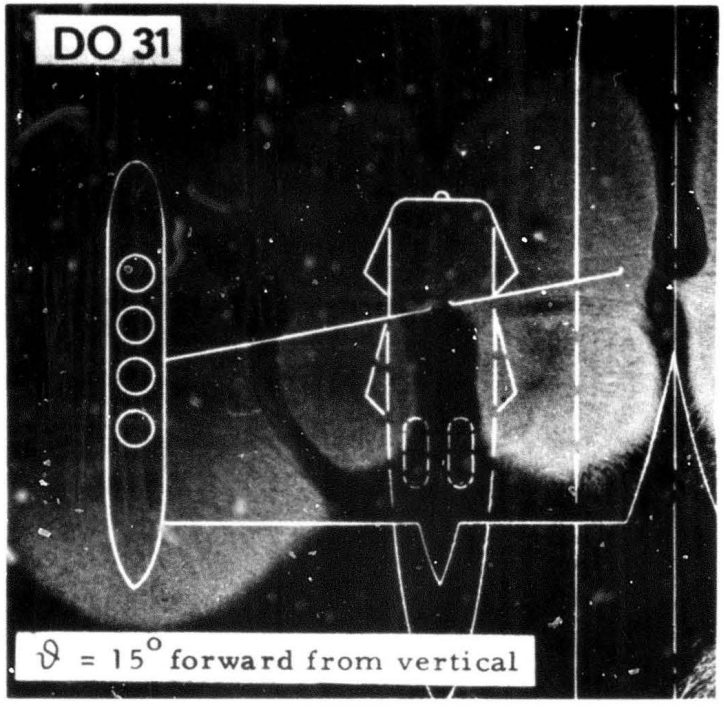

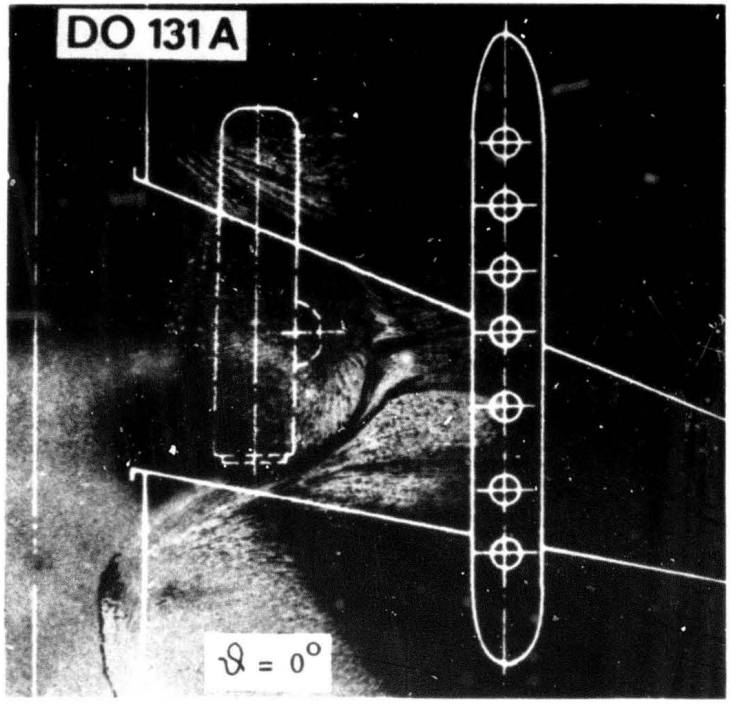

FIG. 17 DO 131 SURROUNDING AIR TEMPERATURE AT LIFT OFF

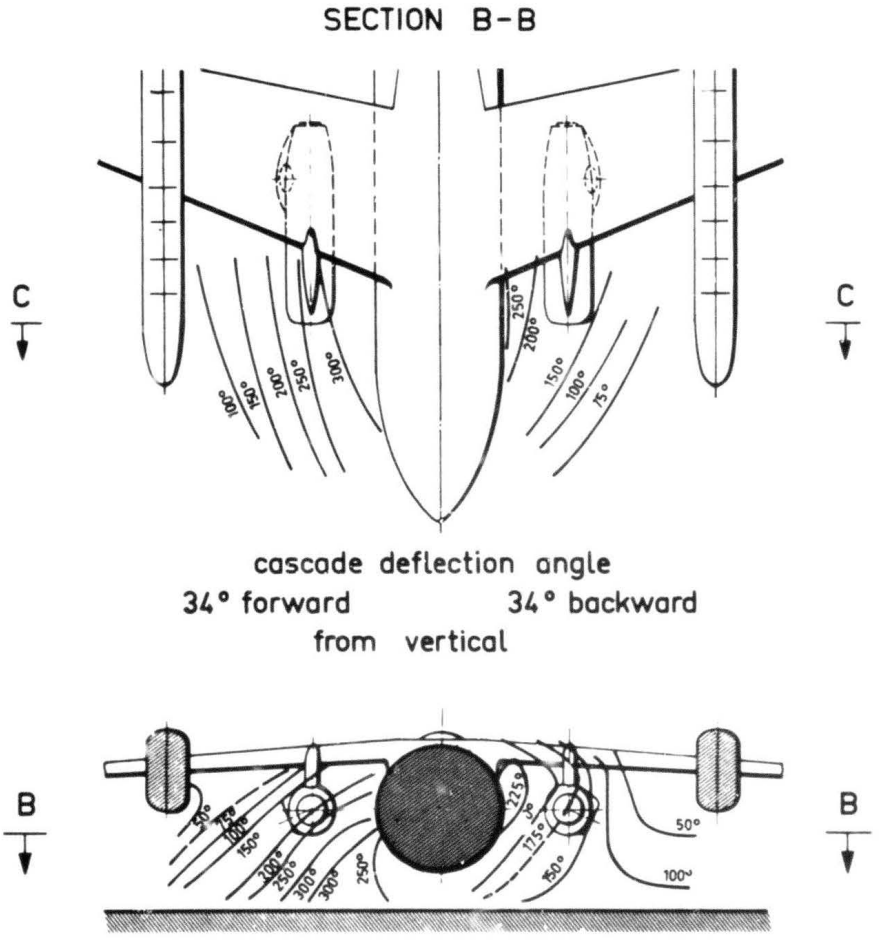

FIG.18 **TEMPERATURE RISE VS MAIN ENGINE DISTANCE FROM A/C CENTRE LINE**

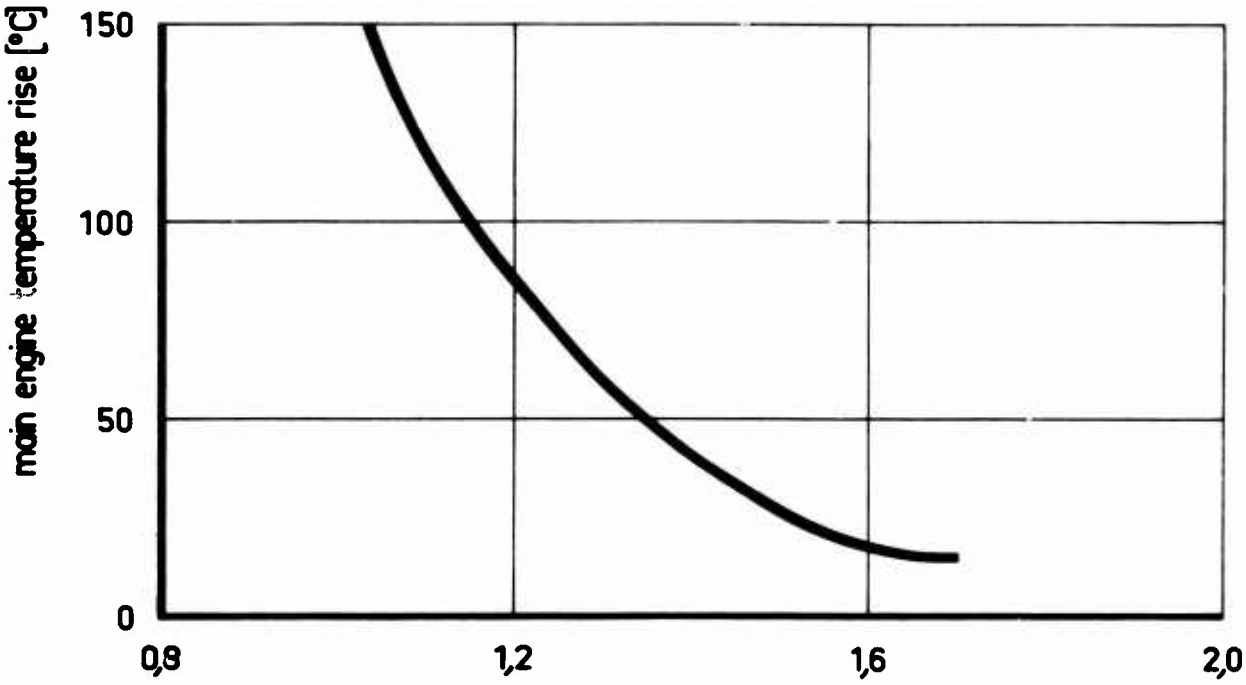

FIG. 19 **DO 131 SAFE VTO WEIGHT VS RELATIVE ENGINE POSITION**

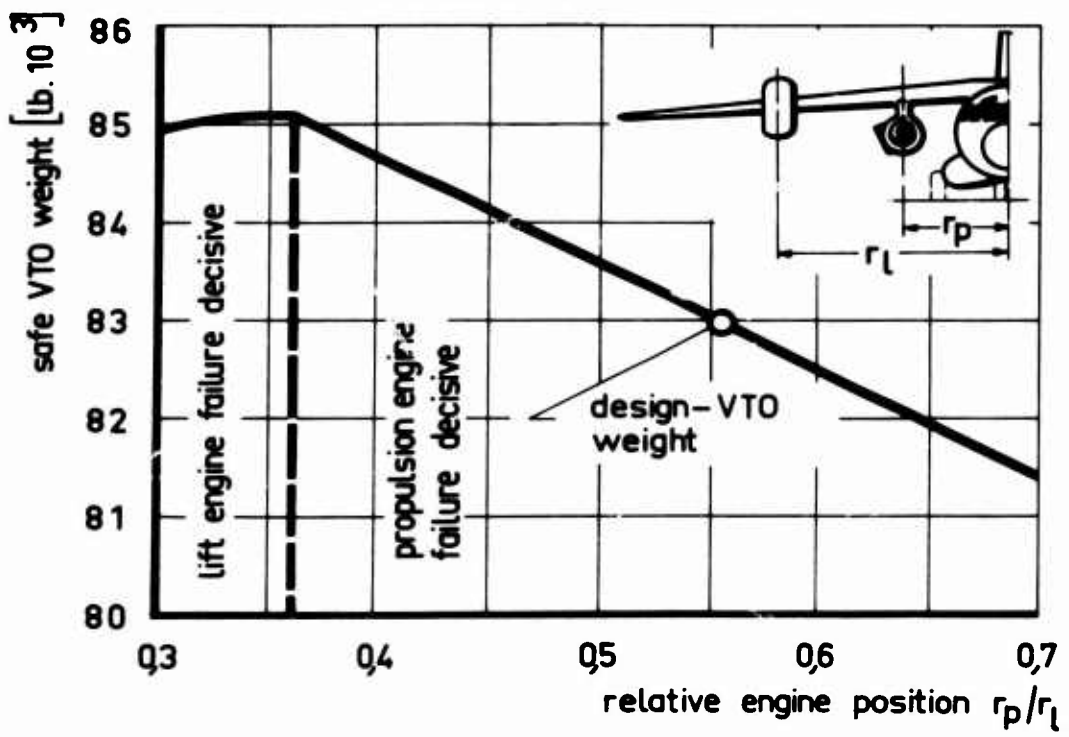

FIG. 20 **DO 131 A WITH TILTING PROPULSION ENGINE TO REDUCE HOT GAS INGESTION**

FIG. 21 INGESTION LIMITED EFFECTIVE LIFT

pitch angle $\alpha = 8°$
all jets vertical
ground proximity effects fully considered

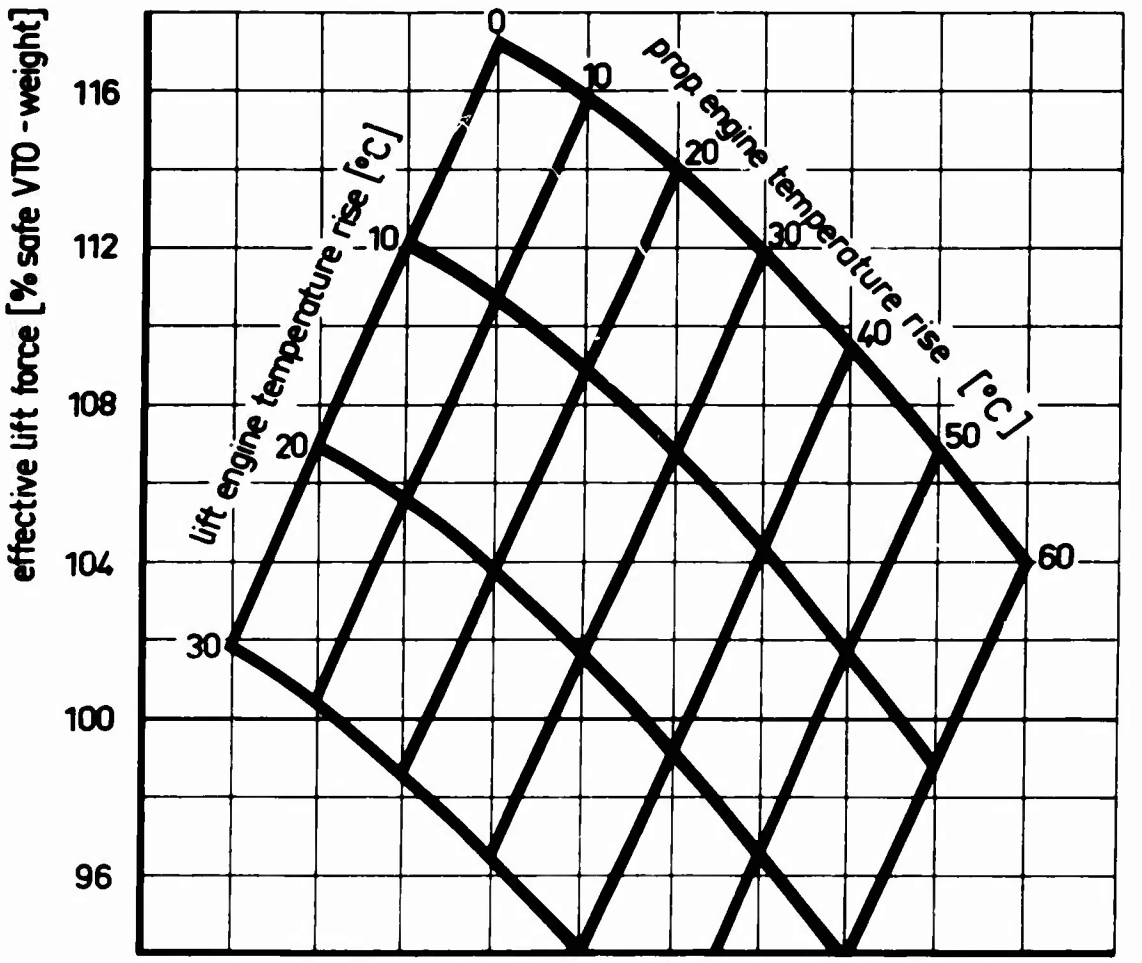

Discussion of the Paper
SOME STUDIES INTO IMPROVEMENTS IN AUTOMATIC THROTTLE CONTROL
presented by
N.H.Hughes, RAE, UK

F. Fett, *Technischen Hochschule, Aachen, Germany*

1. Over a relatively wide range of operating conditions, jet engines themselves show linear dynamic characteristics. The engines themselves also show nearly the same characteristics for increasing or decreasing fuel flow. This is also valid for the transient response of thrust.

However, to avoid compressor surging and flame-out during acceleration and deceleration, the fuel control units are normally equipped with non-linear elements. These apply limitation which are very close to the working line, especially at low thrust settings.

The thrust itself may also change during the landing phase as it is a function of changing temperature and pressure in the atmosphere and also of flight Mach number.

2. The time constants of big jet engines of about 20,000 daN (45,000 lbs) thrust are not as high as one might expect from the known behaviour of small engines. This is especially correct for two-spool engines. The time response of a modern bypass engine of the above thrust level is nearly the same as that of a single-spool engine of 4000 daN (9000 lbs) thrust built twelve years ago.

The time response of a jet engine is a function of its thermodynamic data,. the materials used and the ability of the designer. The improvements in all these parameters on modern engines lead one to expect an improvement in the direction of shorter response times.

N. H. Hughes

I am indebted to Mr Fett for his comments on the dynamic characteristics of jet engines.

While such measurements as have been made on engine response show a reasonably linear behaviour in thrust r.sponse to changes in fuel flow, this is insufficient information for the auto-throttle designer. He has to know the dynamic relationship between pilot's throttle level movement and thrust, including the effects of all non-linearities in the linkages and fuel control system. Such effects may make the response of the total engine and fuel control system very different from the response of the engine itself.

For studies of the final approach and landing, the effect on thrust of air temperature and pressure and Mach number may be neglected.

D. M. McGregor, *NRC/NA Est., Ottawa, Canada*

Why cannot the comparator to make the system non-linear operate on the forward loop gain of the airspeed error and replace entirely the requirement for the inertial system? Hence there would be an integral A/S error term and a non-linear direct term.

N. H. Hughes

In order to ensure satisfactory closed-loop speed stability of an auto-throttle system it is necessary to have a certain minimum airspeed gain. In practise, conventional auto-throttles work near this minimum in order to minimise throttle activity in turbulence.

If, with the aim of reducing throttle activity, the comparator in the modified system caused a reduction in speed gain, provided airspeed error was within certain bounds, the reduced gain would cause reduced damping of the overall speed control loop. Almost certainly in the presence of disturbances a limit cycle would occur, with airspeed oscillating between the comparator thresholds.

In the modified system described in the paper, the speed gain of the system is constant, regardless of the state of the comparator, thus ensuring closed loop stability under all conditions.

K. H. Doetsch, *DFL, Braunschweig, Germany*

Could any of the aero-engine people present help Mr Hughes to answer the very important request for data on dynamic engine response?

N. H. Hughes

This question was answered by Dipl. Ing. Fett.

Discussion of the Paper
AIRCRAFT AND PROPULSION OPERATIONAL CONSIDERATIONS RELATED TO INLET DESIGN

presented by

F. T. Rall, Jr, Aeronautical Systems Division,
Wright-Patterson Air Force Base, USA

M. Seidel, *DFL, Braunschweig, Germany*

I kindly ask the author to give the *defining equation* of the distortion parameter "D" used. Only then an interpretation of the values presented seems to be reasonable.

F. T. Rall, Jr

The distortion parameter "D" is an area weighting of the compressor face total pressures below the average total pressure. It weights the distortion on both a circumferential and radial basis.

D. J. Stewart, *BAC (Weybridge) Ltd., UK*

Has any structural damage to either engine or airframe resulted from known occurrences of intake "buzz".

If not, what is the current design philosophy to cope with this problem?

F. T. Rall, Jr

In general, no structural failures of primary structure, either airframe or engine, have occurred during inlet buzz. Basic structural design philosophy generally is predicated upon hammer shock phenomena which produces sizeable overpressures in the inlet.

P. Lecomte, *Sud-Aviation, France*

Can Mr Rall make any comment on the use of buzz detectors for flight testing aircraft inlets?

F. T. Rall, Jr

Buzz detectors have been utilized in at least three different aircraft designs that I am familiar with. The buzz detectors have worked essentially as designed.

W. Schreiber, *Entwicklungsring Süd GmbH, München, Germany*

The definition of compressor stall? Pressure gradient in Psi/sec when stall happened, absolute value of pressure decrease (compressor delivery press).

F. T. Rall, Jr

A limited amount of compressor instrumentation was utilized in these tests. These included compressor exit pressure measurements. Much more compressor instrumentation would have been desirable. The stalls in this test were quite "hard" stalls and were easily observed by noise alone. The compressor instrumentation seemed primarily to verify that stalls had occurred.

P. C. Ruffles, *Rolls-Royce Ltd., Derby, UK*

Rolls-Royce experience on engine intake pressure distortion has shown that the engine surge margin is not only dependent upon the level of distortion, but also on the distribution, particularly in the circumferential sense.

Has Mr Rall's experience shown that distribution of turbulence in the intake is important as well as its absolute level and does he consider that the effects of pressure distortion and turbulence on engine surge margin are additive?

F. T. Rall, Jr

Insufficient data are available to permit a definite conclusion regarding the importance of the spatial distribution of turbulence. There exist some indications that it is significant but a definite conclusion requires additional testing.

Turbulence and distortion are believed to be additive. But again, tests have not yet been conducted to conclusively prove this point.

Discussion of the Paper
A DISCUSSION OF THE USE OF THRUST FOR CONTROL OF VTOL AIRCRAFT
presented by
Seth B. Anderson, Ames Research Center, Moffet Field, US

X. Hafer, *Institut für Flugtechnik, Darmstadt, Germany*

In Figure 11 you show the Pilot Rating for different values of roll control lag for rate and attitude control where the latter was more effected by the control lag time. Did you optimize the attitude control system for every test with changed lag time?

Seth B Anderson

No. For these tests, which were considered to be a first look at the problem, the frequency and damping of the attitude control system were held constant as control lag was varied. It is expected that less deterioration in pilot rating would occur if the feedback loops for the attitude control system were adjusted to remove their own lag effects. The point to keep in mind is that the pilot complained about the tendency to oscillate and not the lack of response.

T. K. Szlenkier, *Hawker Siddeley Aviation, Hatfield, UK*

I would like to offer Mr Anderson our appreciation for a very interesting lecture. Mr Anderson is a well known authority in the field of VTOL control and his views are highly respected. Regarding the control of the lateral aircraft translation by means of the thrust deflector vane, it appears to offer potential performance improvement in terms of thrust to weight ratio, at least for configurations where lift engines are arranged close to the aircraft longitudinal axis. Further elaboration, by Mr Anderson, regarding this aspect would be appreciated.

Seth B. Anderson

The point to be brought out is that the lateral thrust deflector will have performance (weight reduction) benefits on configurations where adequate rolling acceleration is difficult to achieve; for example, on large VTOL transports with large roll inertia and on configurations where lift engines have a short moment arm in roll. Our limited tests on the X-14A VTOL aircraft have only indicated that the lateral acceleration control can offer a means to reduce the amount of roll acceleration required; a more detailed study must be made to adapt this type of control to a given configuration. In this regard consideration must be given to the amount of roll acceleration required for lateral upsets and landing on uneven terrain.

F. O' Hara, *RAE, Bedford, UK*

I agree that constant attitude is the natural ideal manner of low speed manoeuvres on VTOL aircraft. We have found this so also in the pitching plane. However it may be

that the pilot's assessments of handling with the side vector arrangement would be less good at low control powers in rough air conditions. It is true that lateral disturbances can be minimised by attitude stabilisation, but I think the goodness of a control arrangement can best be measured by how satisfactory it is without artificial stabilisation, and I wonder what Mr Anderson thinks about the side vector control in this respect in rough air.

The other point I should like to make is that in general it appears desirable to minimise large sideslip to develop at low speed and it is probably preferable therefore to turn the aircraft into the direction of side motion as was done by pilots with the large span simulation on the X-14A.

Seth B. Anderson

In regard to the use of the side vector control in rough air - the tests on the X-14A were purposely restricted to calm air in order to examine more clearly maneuvering requirements. In spite of this, ground effect disturbances and self-induced upsets were such that the pilot considered attitude stabilization necessary for the vane control method. Without attitude stabilization the pilot would have the *additional* task of providing wings leveling as well as sideward translation. I would emphasize that for the large aircraft, for which the vane control is more appropriate, the upset problem would be less severe.

R.P. Harper, Jr, *Cornell Aeronautical Lab., Buffalo, NY, USA*

1. Do the quoted time constants include the inherent dynamics of the thrust control system (vane, etc.)?

2. Are the stabilization inputs (rate, attitude) affected by the simulated time constants?

Seth B. Anderson

1. No, the time constants used in the simulator studies did not include the time constant of the vane system: however the effect would be small since the measured first order time constant of the vane system used in flight was less than 0.1 seconds.

2. Yes, the stabilization inputs also included a time constant. In this regard it was assumed that the time constants would be the same for increasing or decreasing values of the stabilization input.

D.M. McGregor, *NRC/NA Est., Ottawa, Canada*

1. Do you feel that a programme covering a pilot rating range of only $3 \simeq 5\frac{1}{2}$ gives the pilot enough variation to maintain his calibration?

2. Another consideration in the type of system is the characteristics (i.e. damping & control sensitivity) of the system.

3. The slope of the P.R.V.'s time lag curves being different from zero could indicate that the pilot is sensitive to the inherent time lags of the simulator.

Seth B. Anderson

1. I agree that, in general, a wide variation of pilot rating should be obtained to improve accuracy. For the case in question (Fig. 3) however, it was intended only to define an optimum value of max. lateral acceleration and not so much the limits. In defining limits, the 6° simulator obviously has the advantage over the flight vehicle (X-14A) since it is difficult to explore towards the 6½ boundary safely in flight.

2. It was recognized that in comparing the control systems, optimum values of damping and sensitivity were important considerations; and in fact, optimum values were used for the tests presented.

3. The pilot *is* sensitive to the lags of the simulator as discovered during early evaluation of the motion characteristics of the simulator itself. These simulator response lags were removed for all practical purposes by compensation to the drive mechanism of the simulator. The fact that the curves of pilot rating versus control lag are not at zero slope at zero time lag is a result of curve fairing. In reality the pilot could not detect changes in the response characteristics below 0.1 sec.

D.L. Hirsch, *Advanced Aircraft Organization, Northrop Norair, Cal., USA*

Was the control sensitivity (i.e. control power per unit of stick deflection) held constant as the control power maximums were increased during tests of handling quality requirements?

Seth B. Anderson

Control sensitivity was held approximately constant at optimized values while maximum control power was varied. In all cases maximum stick travel (±5 inches) remained constant and maximum control power for lower values was obtained at less than full stick travel.

Discussion of the Paper
REACTION CONTROL SYSTEM PRELIMINARY DESIGN CONSIDERATIONS FOR A JET-LIFT RESEARCH AIRCRAFT

presented by

D.L.Hirsch, W.W.Stark and W.B.Morris, NASA, USA

T.K.Szlenkier, *Hawker Siddeley Aviation, Hatfield, UK*

I would like to offer the authors congratulations for a very valuable study. Regarding the bleed control ducts the approach adopted by HSA and Dornier in the case of multiple lift engine installations with two banks of engines is to use two independent duct systems to provide an additional safety in the event of duct failure. It would be of interest to know why this provision was not made in the Northrop design.

D.L.Hirsch

This aircraft in its research role does not face the risk of combat damage as do the tactical aircraft named. The single duct system was overdesigned in wall thickness and number of bellows to provide a safety margin against manhandling and estimated airplane bending loads; these are expected to be less for the 300 hour research mission life than for a typical operational design life. This design approach proved lighter than including a second independent system. The J-85 bleed system in the Northrop vehicle is also a much lower pressure (and temperature) system than that associated with the Pegasus engine.

F.O'Hara, *RAE, Bedford, UK*

The question raised with Mr Hirsch was covered by the notes that Mr O'Hara gave for the question to Mr Anderson.

Discussion of the Paper
HOT-GAS INGESTION AND JET INTERFERENCE EFFECTS FOR JET V/STOL AIRCRAFT
presented by
A.D.Hammond and H.C.McLemore, Langley Research Center,
NASA, Langley Station, Hampton, Virginia 23365, USA

Remarks by Ph.Poisson-Quinton, *ONERA, France*

NOTE ON BASIC RESEARCH CONDUCTED BY ONERA IN THE FIELD OF AERODYNAMIC INTERACTION NEAR LIFTING JETS

1. Wind-tunnel and flight tests performed on two VTOL lift engine aircraft developed by the Dassault Company revealed the extreme complexity of lifting jets/wing interaction problems, in particular in transition flight, between vertical climb and forward flight.

It is difficult to investigate such problems on a small wind-tunnel model in view of the adequate miniaturization of the lifting elements (air intakes and jet exit) and the measurement of all the force and moment components which are required.

However, wind-tunnel predictions have generally been rather well corroborated by overall flight measurements[1], for the research VTOL aircraft "BALZAC", as well as for the military supersonic version, MIRAGE 3V (Fig. 2).

In both cases, a lift loss increasing with the speed has been observed; this loss is related to the aerodynamic jet interaction with the delta wing lower surface flow. This jet induced lift loss results also in the following effects:

- increase of the nose-up effect with the speed,
- interference roll torque when the aircraft is sideslipping.

The intensities of these phenomena must be known with accuracy to adjust the control jets in pitching and rolling over the whole transition range.

Figure 2 also brings out the necessity of accurately representing the shape of the lift engine nozzle: the addition of a central plug (which, for instance, exists behind the turbine disk of the RB 162 Rolls-Royce jet engine), somewhat reduces the jet induced lift loss as measured in a wind-tunnel, which is then similar to that noted in flight.

The influence of the plug on the nozzle was confirmed in the course of systematic tests on an elementary single nozzle configuration (Fig. 3).

2. In order to carry out a more fundamental investigation into the mixing process in the vicinity of a lifting jet, and particularly into the jet induced lift loss process, ONERA has developed and placed in the S1 wind-tunnels in Cannes (diameter = 3 m) and in Modane (diameter 8 m), two experimental set-ups with which a large variety of thorough tests can be conducted, in, and near, single or multiple jets.

2.1 *Figure 3* shows the diagram of the Cannes facility ($V_0 \leq 40$ m/s, V_j ranging from 0 to 600 m/s), and *Figure 4* gives a few examples of jet visualisation, obtained by injecting water on the periphery of the jets (note the difference in curvature of the two jets placed successively in line and side by side).

Figure 5 analyzes the suctions induced by this double jet on the wall: the interaction created is considerably higher in the case of side by side jets; however it is possible to reduce this interaction appreciably by making the jets converge: such a result points out how the interaction problems on a VTOL lifting jet aircraft could be improved.

2.2 Even more accurate studies can be conducted with the experimental set-up now completed in the S1 wind-tunnel in Modane (Fig.6), in view of the high scale which it is possible to achieve in this tunnel whose velocity can reach $V_0 = 300$ m/s ; its 120 mm diameter jet can reach velocities ranging from 0 to 700 m/s, with temperatures ranging from 0°C to 700°C (simulation of a real jet engine). Besides, a motorized device makes it possible to carry out a thorough analysis of the jet (Fig.8) while pressures and boundary layers are measured alone the wall.

Figure 7 illustrates the wall visualizations obtained in the presence of a jet, and *Figure 8* gives an example of the stagnation pressures measured at some distance downstream of the nozzle.

3. Analyzing the mixing area near the jet and the wall remains difficult in a wind-tunnel; this is why a simultaneous study of these problems is conducted in the Châtillon hydrodynamic tunnel[2], where flow visualizations can be performed along successive cross sections through the jet (Fig.9).

4. Conclusions

The experimental studies on lifting jet/wall interaction effects which are being conducted in various ONERA laboratories should lead to a better understanding of ver complex interaction phenomena, and to a validation of a certain number of theoretical diagrams in simple fundamental cases. Moreover, such experimental set-ups, which are very easy to modify, should enable us to find ways of minimizing parasite interactions detrimental to the development of VTOL lifting jet aircraft.

5. References

1. Poisson-Quinton, Ph. — *From wind-tunnel to flight; the role of the laboratory in aero-space design.* AIAA 30th Wright Brothers Lecture January 1967. To be published in "Journal of Aircraft".

2. Werle, H. — *Essais de soufflage au tunnel hydrodynamique à visualisation.* ONERA, NT No.61 (1960).

Discussion by A.D.Hammond and H.C.McLemore is continued on page 20.

DASSAULT "BALZAC" V.T.O.L. TRANSITION FLIGHT

Fig. 1

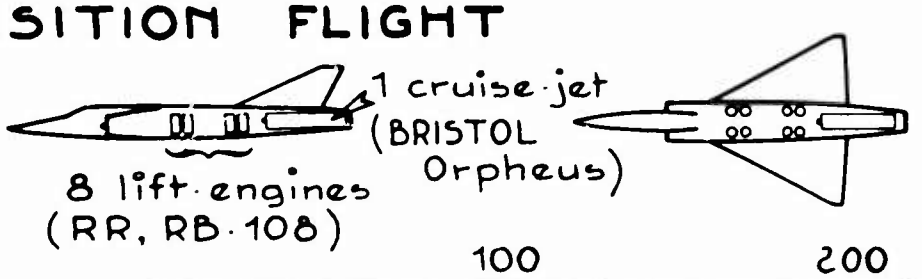

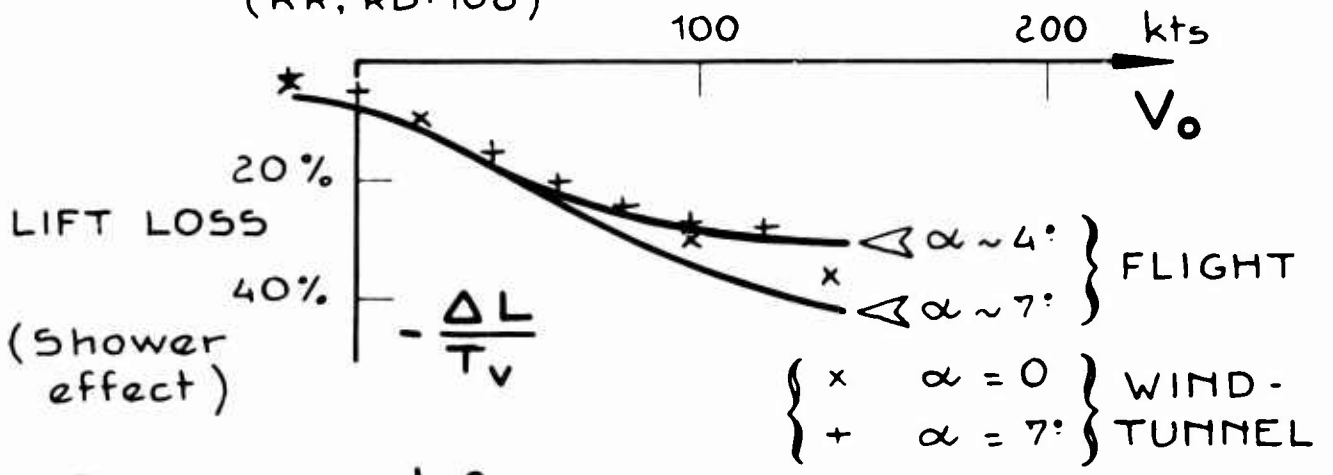

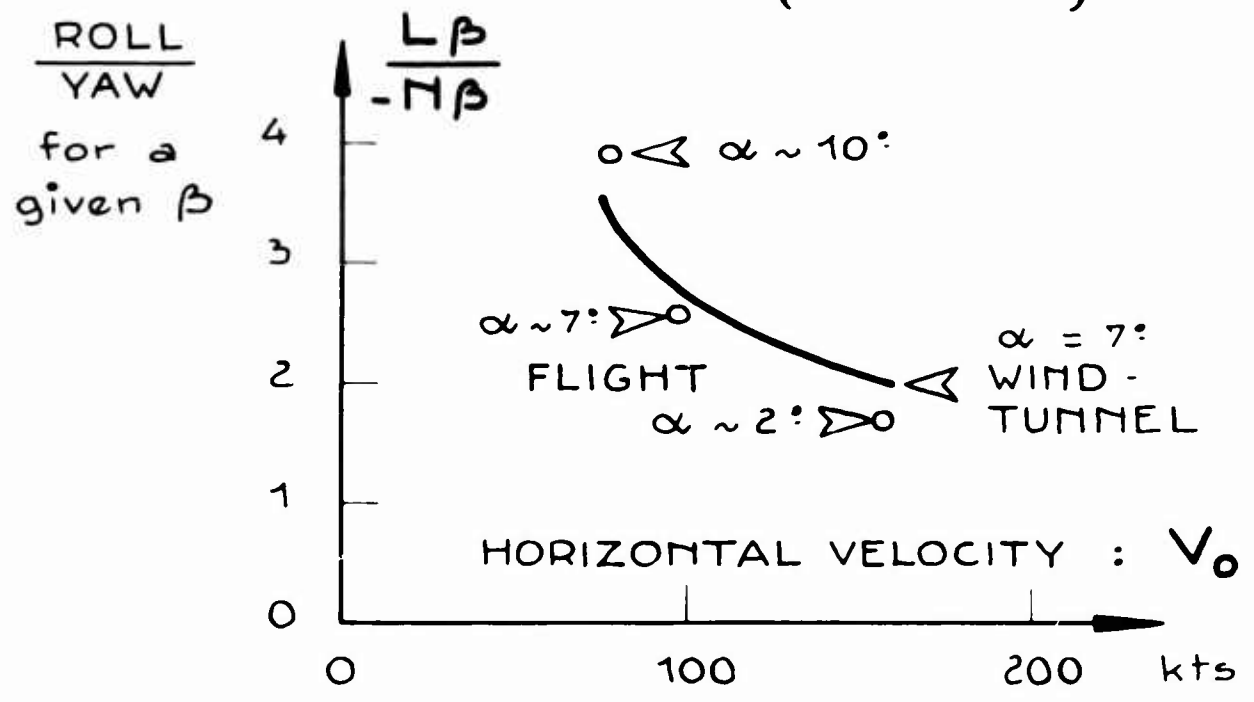

Fig. 2

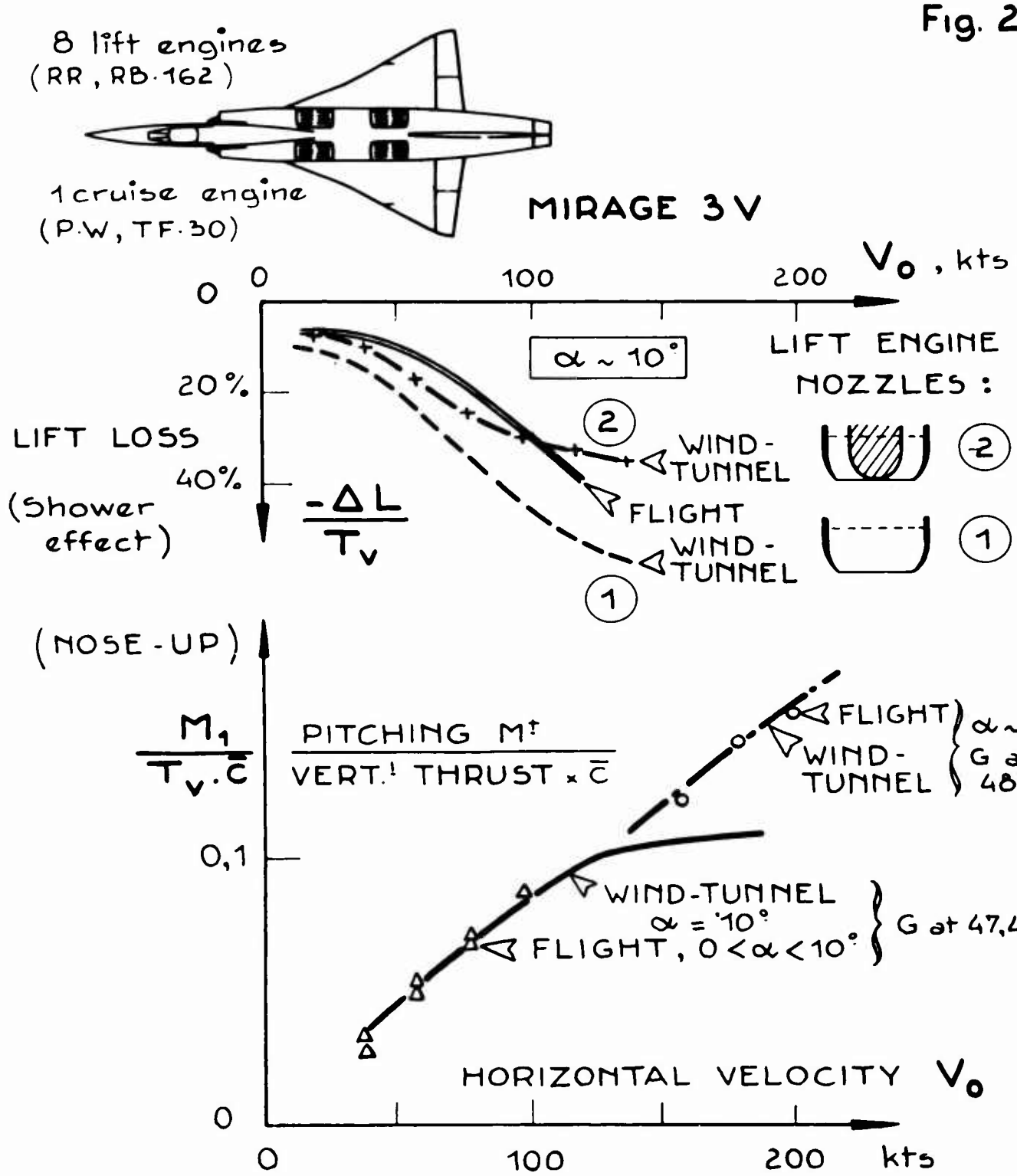
8 lift engines
(RR, RB·162)
1 cruise engine
(P.W, TF·30)
MIRAGE 3V
0
100
200
V_o, kts
α ~ 10°
LIFT ENGINE NOZZLES :
20%
40%
LIFT LOSS
(Shower effect)
$\frac{-\Delta L}{T_v}$
WIND-TUNNEL
FLIGHT
WIND-TUNNEL
2
1
(NOSE-UP)
$\frac{M_1}{T_v \cdot \bar{c}}$
PITCHING M^t / VERT.^{l} THRUST × $\bar{c}$
FLIGHT
WIND-TUNNEL
α ~ 0
G at 48%
0,1
WIND-TUNNEL
α = 10°
FLIGHT, 0 < α < 10°
G at 47,4%
HORIZONTAL VELOCITY V_o
0
0
100
200
kts

Fig. 3

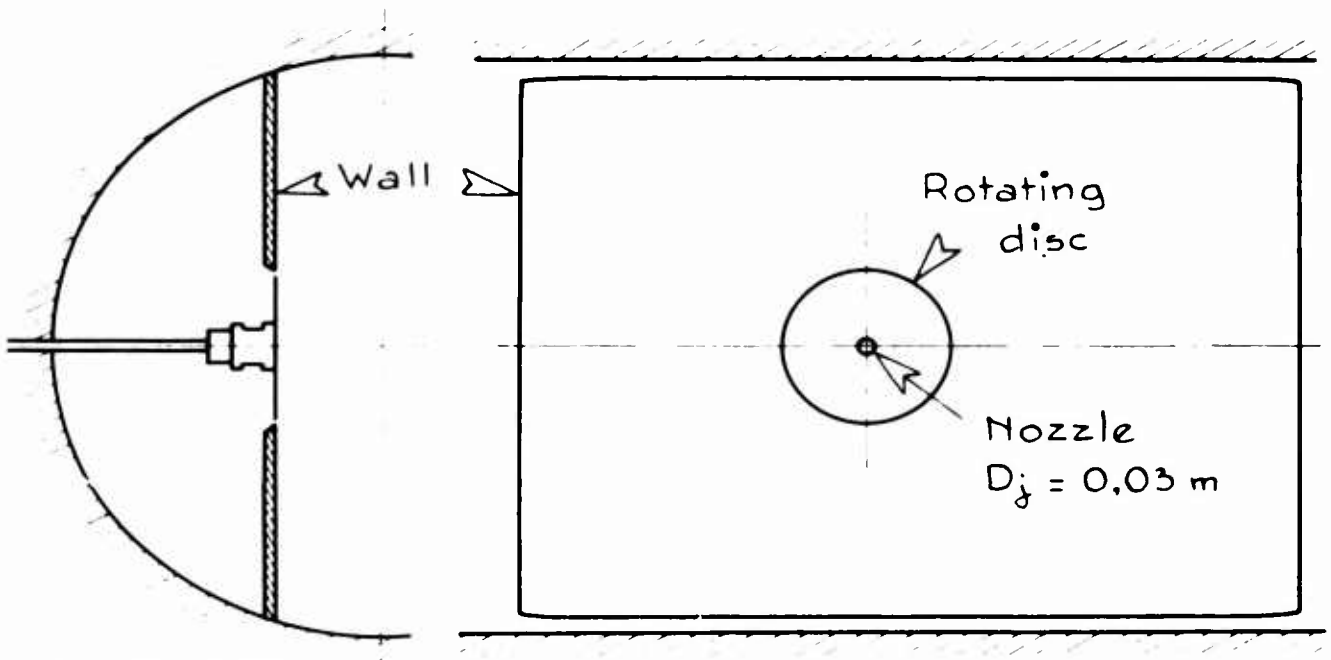

S_1 Cannes
Wind-tunnel, D = 3 m

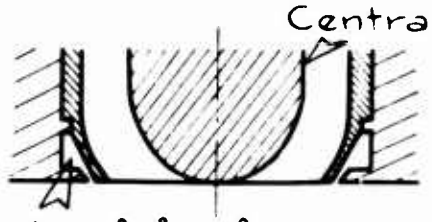

PRESSURE COEFFICIENT

iso-C_p = -0,25

$C_\mu = \frac{q_m V_j}{q_0 S_j} = 130$

V_j = 310 m/s

($M_j \sim 1$)

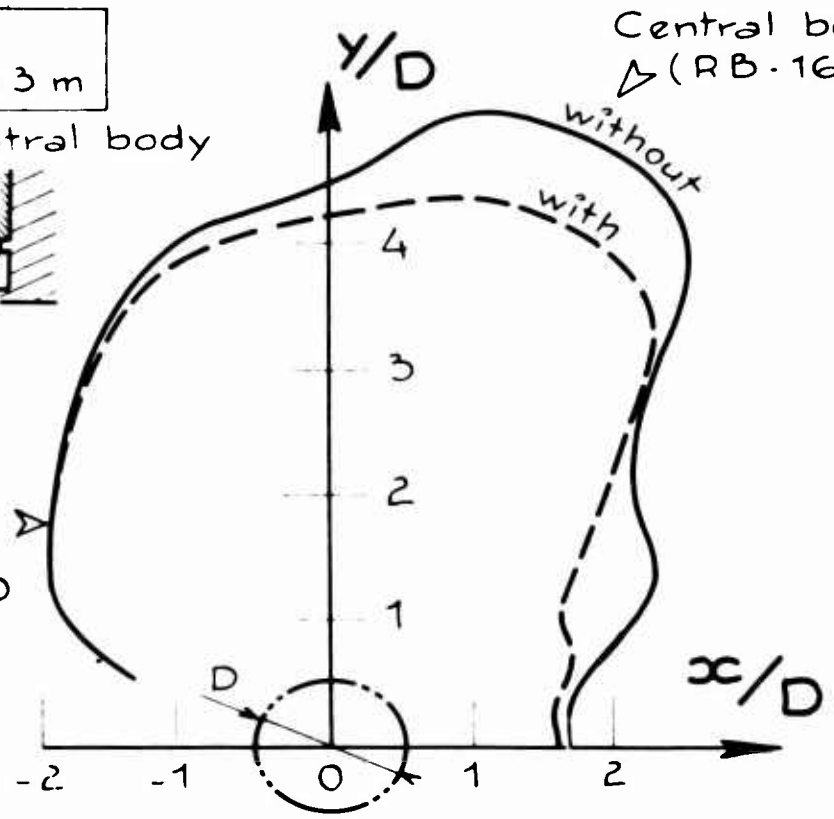

INDUCED SUCTION NEAR THE JET EXIT ON THE WALL

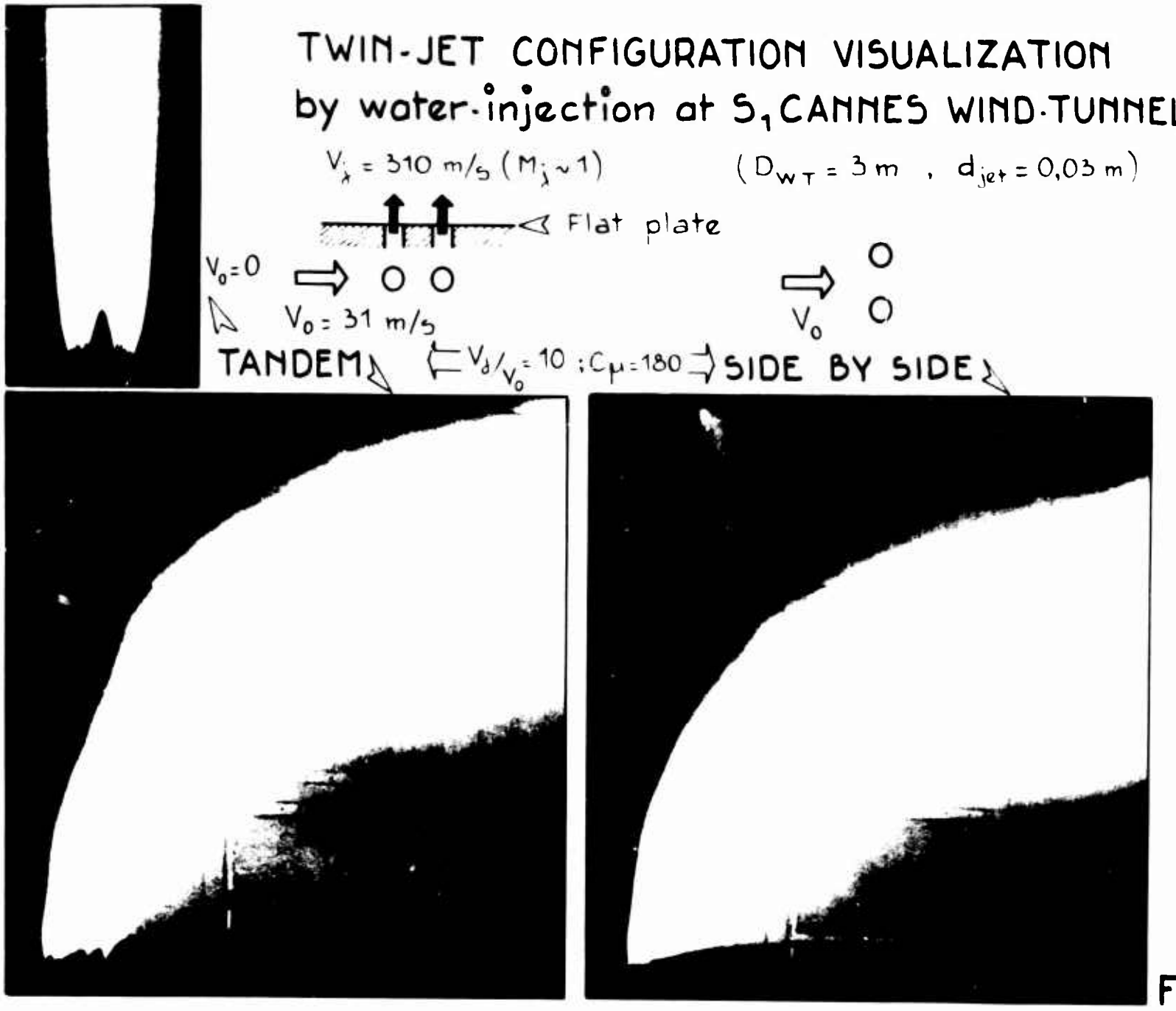
TWIN-JET CONFIGURATION VISUALIZATION
by water-injection at S1 CANNES WIND-TUNNEL
Vj = 310 m/s (Mj ~ 1)
(DWT = 3 m , djet = 0,03 m)
Flat plate
V0 = 0
V0 = 31 m/s
V0
TANDEM
Vj/V0 = 10 ; Cμ = 180
SIDE BY SIDE

Fig. 4

SUCTION EFFECT ON THE WALL WITH TWO LIFTING-JETS IN LINE OR SIDE BY SIDE

S_1 Cannes wind tunnel

$V_j = 310$ m/s ($M_j \sim 1$) , $V_j/V_0 = 10$, $C\mu = \frac{q_m V_j}{q_0 S_j} = 179$

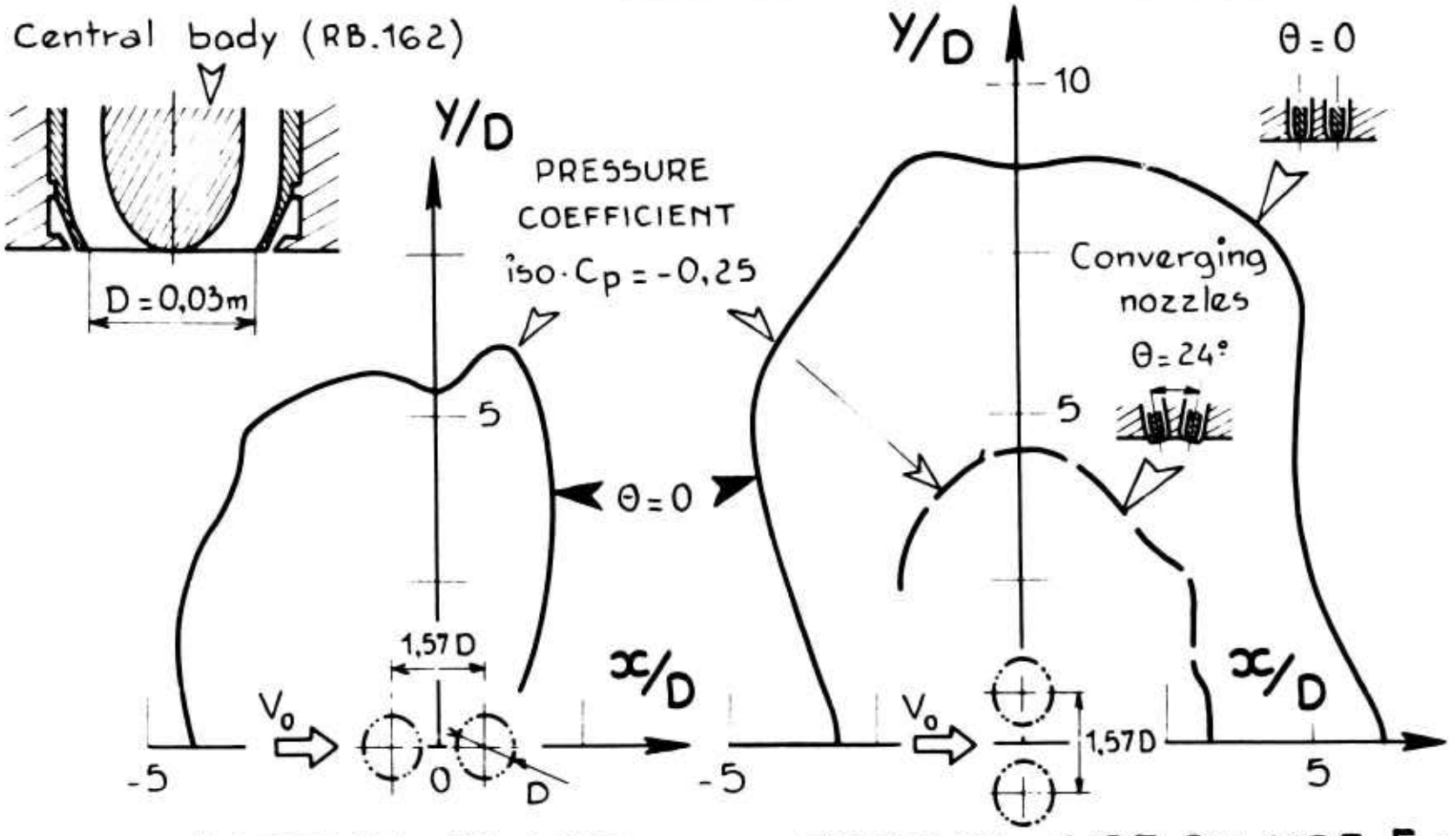

NOZZLES IN LINE

NOZZLES SIDE BY SIDE Fig. 5

ETUDE FONDAMENTALE DE L'INTERACTION JET-PAROI

$200 < V_j < 600$ m/s $20 < V_0 < 120$ m/s

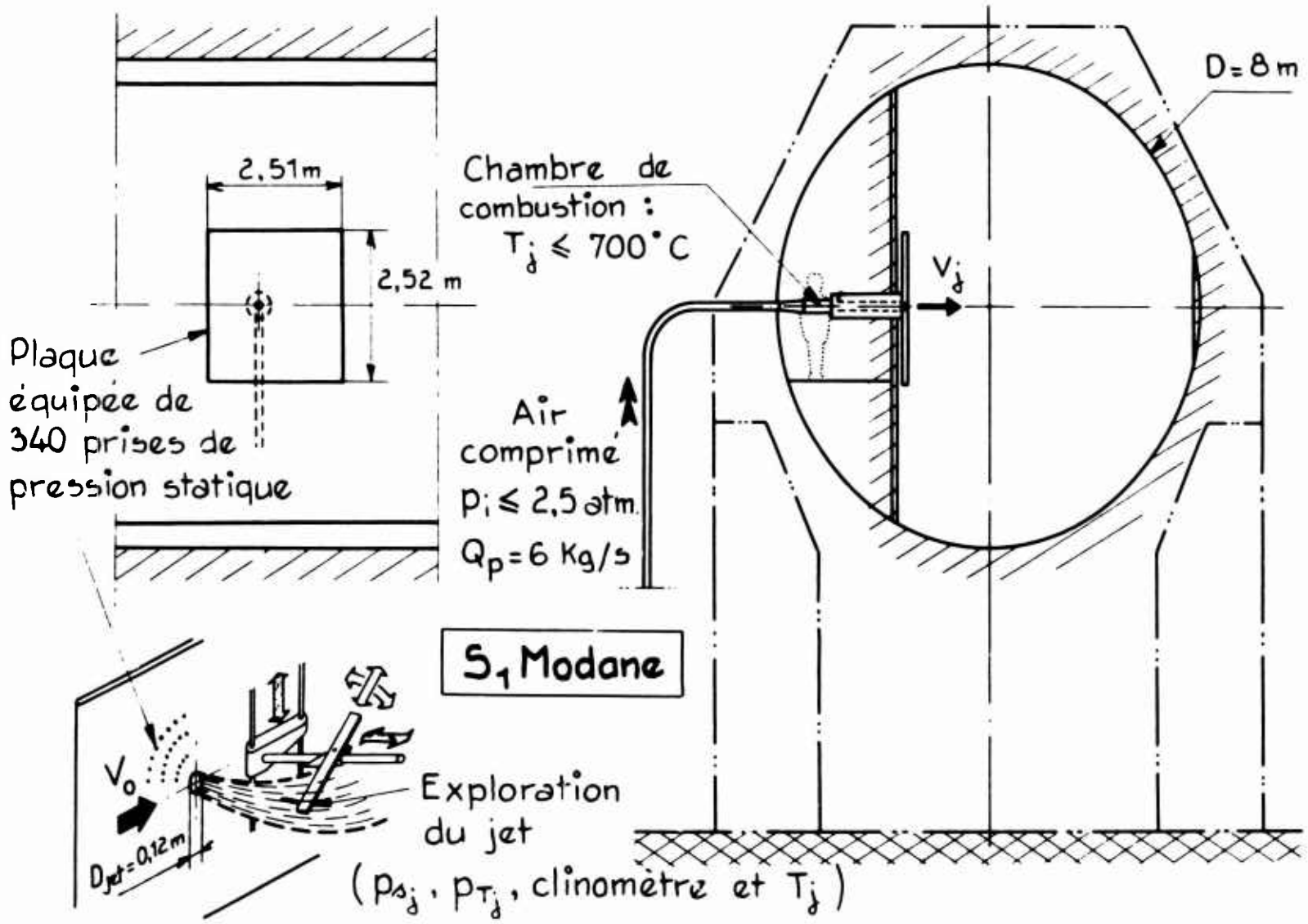

Fig.6

Fig. 7

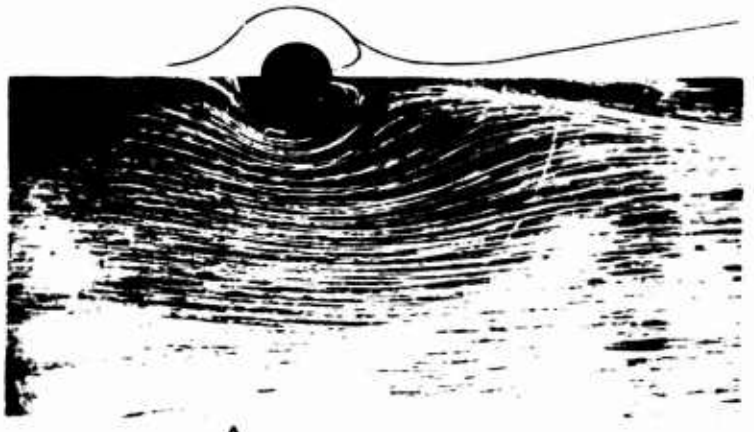

S_1 Modane

RESEARCH ON LIFTING JETS

Visualization inside the boundary-layer of the flat plate around the jet.

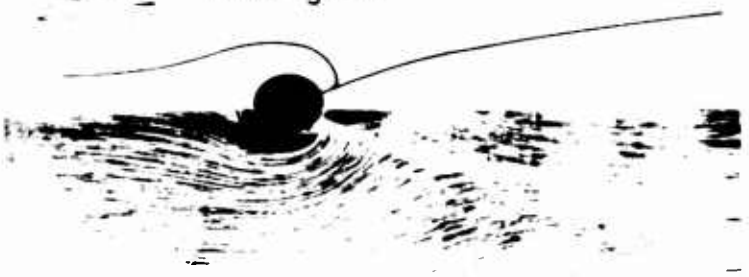

$$\frac{M_j}{M_0} = \begin{cases} \triangle \\ 2 \\ 5 \quad \triangleright \end{cases}$$

$M_0 \sim 0,18$

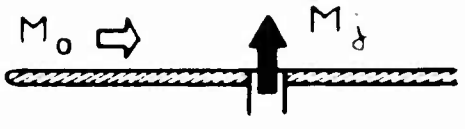

Fig. 8

PITOT ISO-PRESSURES INSIDE THE JET

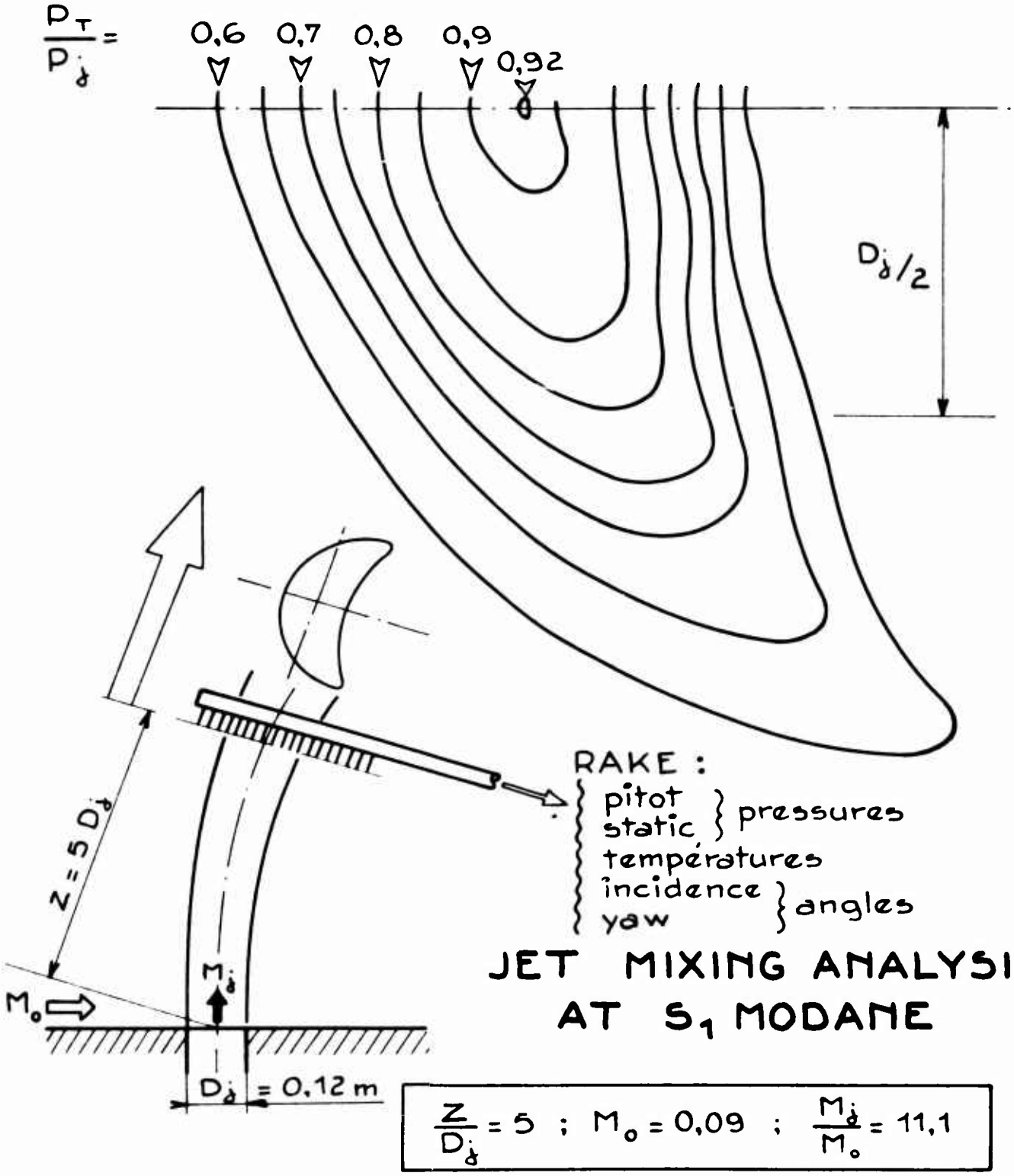

JET MIXING ANALYSIS AT S_1 MODANE

$\frac{Z}{D_j} = 5$; $M_0 = 0,09$; $\frac{M_j}{M_0} = 11,1$

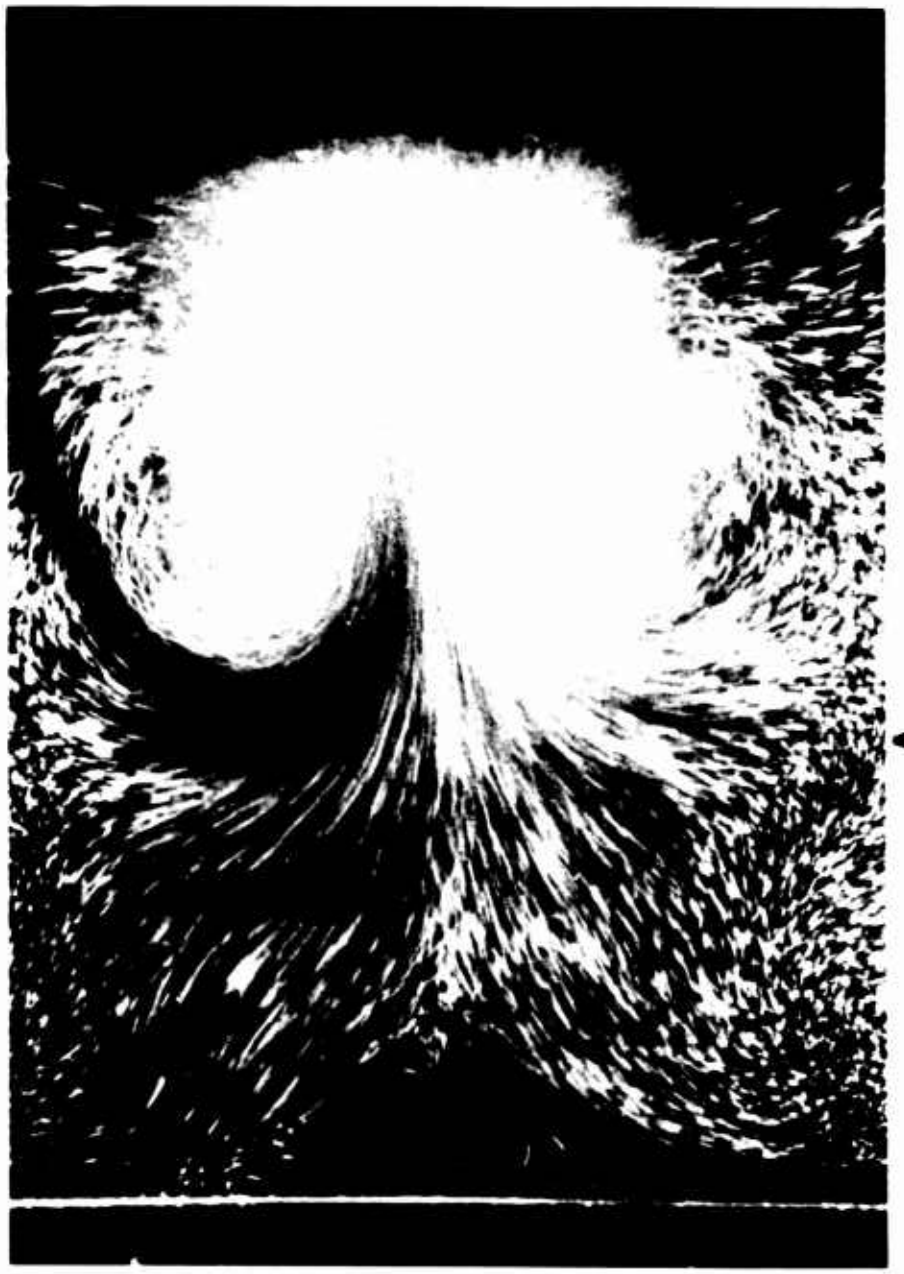

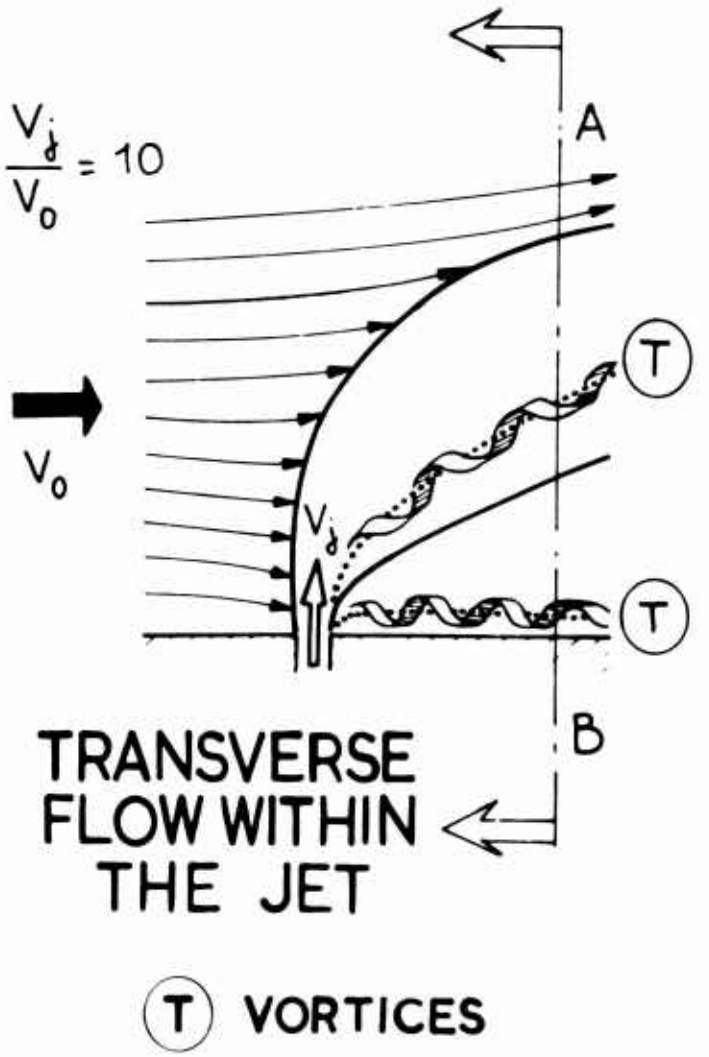

ONERA HYDRODYNAMIC
TUNNEL

Fig.9

T. S. R. Jordan, *Hawker Siddeley Aviation Ltd., Kingston-Upon-Thames, UK*

1. Figure 3 of the paper is said to represent the P.1127 configuration. On the P.1127 we have measured a temperature rise of 7% of the front jet excess total temperature. Although on the P.1127 this is low (about 80-90°C) the percentage correlates well with Mr Hammond's data if the jet nozzle is 4 to 5 diameters above the ground. (This is about the actual figure from memory.) Has Mr Hammond, however, an explanation for the sensitivity of temperature rise to height/diameter ratio of jet exit?

2. Do NASA, Langley, propose to measure intake temperature rise on the P.1127. If so, what instrumentation do they propose to use?

3. What are Mr Hammond's views on the minimum size of model, the scaling of exhaust velocities, and the representation of nozzle exhaust velocity distribution, as they affect the accuracy of results from "aerodynamic suckdown" models?

Mr Hammond

1. The side nozzle arrangement of Figure 3 is similar to the P.1127 in the mechanical arrangement of the swiveling nozzles; however, it should be pointed out that all four nozzles of the Langley model were hot jets, whereas the two forward nozzles of the P.1127 are cold jets. A direct correlation with the P.1127 in terms of temperature rise in the side inlets should not be expected because of this difference. The sensitivity of the temperature to nozzle height above the ground can be compared to the aerodynamic lift loss in the presence of the ground. As the jets get closer to the ground, the interaction of the jets, and hence the so-called fountain effects, become stronger. The hot gas is reflected quicker with less temperature loss; and, therefore, the resulting temperature rise is higher close to the ground as shown by side inlets of Figure 6.

2. The NASA Langley Research Center tests will not include hot-gas ingestion aspects; and, therefore, no inlet temperature measurements will be made.

3. The minimum size of models for aerodynamic suck-down investigations are dictated by the purpose of the tests. Static models with one-inch diameter nozzles may be sufficient for hovering ground effects, for example, where the entire aerodynamic shape may not have to be duplicated. However, the size of the wind-tunnel model is dictated more by the requirement of getting good jet simulation, that is, good nozzle flow characteristics within the confines of the required aerodynamic model shape. Ejector type jet simulators with two-inch diameters have been designed and built in the United States and used by NASA and others. Tests have indicated that the jet thrust of cold jets, as related to the inlet mass flow and the free-stream dynamic pressures, to be the important correlating parameters. Although there must be some effect of the nozzle exhaust velocity distribution, there are indications that this distribution is important only if the dynamic pressure decay downstream of the exhaust nozzle is affected. Tests have shown for example that two nozzles having entirely different nozzle velocity distributions, but having the same decay characteristics, resulted in the same aerodynamic lift loss hovering out of ground. On the other hand, two nozzles having the same nozzle velocity distribution, but different dynamic pressure decay, resulted in different aerodynamic lift loss hovering out of ground.

T. Szlenkier, *Hawker Siddeley Aviation, Hatfield, UK*

This very interesting paper by Mr Hammond and Mr McLemore ends with a set of recommendations already adopted by Hawker Siddeley Aviation. However this involves a considerable expenditure of money and effort if a variety of aircraft configurations deserving study is fully covered. A co-operative effort to spread the load is desirable. Perhaps AGARD could provide a suitable platform.

I have one specific comment on Figure 13 of the printed paper. The effect of the sideway angling of the jets is beneficial. However it was stated that the hot gas ingestion problem would become more severe. Our experience at HSA makes us think that the jet angling would reduce the strength of the central hot gas fountain and, hence, the hot gas ingestion problem would be alleviated. Could Mr Hammond explain why he expects an adverse effect?

A. D. Hammond

As stated in the text, the effects of canting the jets on the hot-gas reingestions is unknown. However, the effect of canting the engines at a given height with respect to the ground would be to increase the spacing of the jet impingement on the ground. It is felt that this would cause a larger volume of the surrounding air to be mixed with the hot gases and would also cause the fountain to be moved out from under the protective surfaces such as the body undersurface, and this in turn would allow the hot gases to rise in the vicinity of the inlets.

Discussion of the Paper
INTERACTION BETWEEN AIRFRAME-POWERPLANT INTEGRATION AND HOT GAS INGESTION FOR JET LIFT V/STOL TRANSPORT AIRCRAFT
presented by
U. Gittner, F. Hoffert and M. Lotz
Dornier GmbH, Friedrichshafen, Germany

T. K. Szlenkier, *Hawker Siddeley Aviation, Hatfield, UK*

Let me congratulate the authors on an excellent paper. I would like to stress strong personal links between HSA and Dornier forged during two years of project co-operation in 1964-65. We hope that some official support will be given to a further joint work, since both firms believe strongly about the merits of the direct lift formula for VTOL transport aircraft.

Commenting on the Dornier paper I would like to suggest that the configuration with lift pods on the wing was the most sensible choice for the first generation of the aircraft of this type because the very absence of close integration between the power-plant and airframe permitted a relatively easy resolution of such problems as hot gas ingestion, lift loss etc. However a considerable performance improvement could be achieved by engine/airframe integration. The advantages would be an extension of buffet boundary to higher Mach numbers and reduction of profile drag by some 20%. Dornier comments on these points would be welcomed.

U. Gittner

At the present time wellknown configurations with close integration between power-plant and airframe (configurations with powerplant in wing and powerplant in fuselage) are under investigation at Dornier. The corresponding best solutions can have, of course, a smaller basic drag respectively an extension of buffet boundary to higher Mach numbers. Initial studies considering all the important factors like engine weight, engine mounting weight, additional fuel weight due to powerplant fairings of changed wing induced drag etc. that means the total expense for VTOL-capability, show that with currently available lift engines the non-integrated concept seems to be very sucessful using either lift jets or lift fans.

At the present time we must help the prospective user to define specific VTOL-requirements. Dornier believe they will be able to achieve this by demonstrating solutions to specific VTOL-problems on an aircraft which looks quite conventional.

W. Schreiber, *EWR Süd GmbH, München, Germany*

1. How were the mean temperatures determined?

2. What about the scattering of test results when repeating the tests under the same conditions (repeatability)?

3. How is the quotient of model temperature rise versus temperature rise in the aircraft defined?

M. Lotz

1. The mean ingestion temperature is taken as the temperature measured in the suction tube.

2. Steady-state temperatures are taken as average values of recorded temperatures which vary in a random manner. The so determined temperatures again show differences in repeated tests. All values given in the paper are average values from a considerable number of tests. In the Do 31 model tests, the scatter was approximately 20°C full scale.

3. In the conversion of model test results to full scale, it was assumed that

$$\frac{\Delta t_{model}}{\Delta t_{jet,\ model}} = \frac{\Delta t_{full\ scale}}{\Delta t_{jet,\ full\ scale}}$$

where Δt denotes temperature rise above ambient. With our present knowledge, this is the best what can be done unless model tests are run with full scale jet temperatures. In spite of this uncertainty, model tests give correct answers to the main question, namely, whether hot gas fountains are sucked into the engine intakes or not.